

# **Investigating the mechanism of cystogenesis in TSC and ADPKD**

**Submitted for the degree of Doctor of Philosophy at  
Cardiff University**

**Mark Aldred**

**2011**



# **Investigating the mechanism of cystogenesis in TSC and ADPKD**

**Submitted for the degree of Doctor of Philosophy at  
Cardiff University**

**Mark Aldred**

**2011**

UMI Number: U585498

All rights reserved

INFORMATION TO ALL USERS

The quality of this reproduction is dependent upon the quality of the copy submitted.

In the unlikely event that the author did not send a complete manuscript and there are missing pages, these will be noted. Also, if material had to be removed, a note will indicate the deletion.



UMI U585498

Published by ProQuest LLC 2013. Copyright in the Dissertation held by the Author.  
Microform Edition © ProQuest LLC.

All rights reserved. This work is protected against  
unauthorized copying under Title 17, United States Code.



ProQuest LLC  
789 East Eisenhower Parkway  
P.O. Box 1346  
Ann Arbor, MI 48106-1346



## Summary

Tuberous sclerosis complex (TSC) is characterised by the development of benign growths across the body and is caused by mutations in *TSC1* or *TSC2*. The TSC gene products have an established role in the regulation of mammalian target of Rapamycin (mTOR) signalling. Clinical trials are underway for the treatment of TSC-associated tumours using mTOR inhibitors. Here, we show that many of the earliest renal lesions from *Tsc1*<sup>+/-</sup> and *Tsc2*<sup>+/-</sup> mice (cysts) do not exhibit mTOR activation, suggesting alternative pathways should be targeted to prevent tumour formation. Patients with TSC often develop renal cysts (derived from dilated tubules) and those with inherited co-deletions of the autosomal dominant polycystic kidney disease (ADPKD) gene 1 (*PKD1*) develop severe, early onset polycystic kidneys. Using mouse models, we have shown that the *Tsc* and *Pkd1* gene products are required for correct cell polarisation during renal tubule and bile duct elongation. When polarity is disrupted in *Tsc1*<sup>+/-</sup>, *Tsc2*<sup>+/-</sup> and *Pkd1*<sup>+/-</sup> mice, we found significant alterations in the length of primary cilia projecting from pre-cystic tubule and duct cells (consistent with the highly polar nature of this organelle). The primary cilium is proposed to facilitate many signalling events and provides a mechanosensory input into renal tubule cells. Despite widespread defects in cell polarity and primary cilia in the developing kidney of a *Tsc1*<sup>+/-</sup>, *Tsc2*<sup>+/-</sup> or *Pkd1*<sup>+/-</sup> mouse, we found no evidence of tubule dilation, occlusion or cyst formation until around 3-6 months of age. On the basis of this delay period, combined with our data showing significantly higher levels of cleaved caspase-3 in pre-cystic renal tubules from these mice, we suggest that apoptosis destroys these misaligned cells to protect against cyst formation. We found that almost all cysts without mTOR-activation failed to stain for cleaved caspase-3, and therefore sought activation of a pro-survival pathway. There was strong upregulation of Bcl2 in mTOR inactive cysts that were not undergoing apoptosis, suggesting this was the mediator of survival in our cysts. In cysts without activation of mTOR or apoptosis, we found significant activation of Jak2 and its downstream target Stat3. We finally sought gain-of-function mutations in this pathway, and found several somatic *Jak2* mutations with likely oncogenic potential in Tsc-associated cysts. These data suggest that defective cell polarity in the context of abnormal Jak2 signalling can drive Tsc-associated cystogenesis in the absence of mTOR dysregulation and targeting of this pathway may be of key therapeutic benefit.

## **Acknowledgements**

I would like to thank Prof. Jerry Cheadle and Prof. Julian Sampson for supervising my project, and providing both academic and financial support during my PhD years.

Dr Cleo Bonnet for all her technical help and guidance.

Becky Harris for being a fantastic technician.

Dr Richard Clarkson and Dr Chris von Ruhland for invaluable advice and Prof Alan Clarke for use of equipment.

Vikki, Pete, Julie, Shelley and James for their expertise and various borrowed items over the years.

The Institute and School of Medicine secretaries and staff for all their help.

Kayleigh Dodd, Hannah West, Laura Thomas, Lyndsey Seymour, Duncan Azzopardi, JP Hothi, Maria Kalogerou, Chris Lovejoy, Mark Richards, Natalie Jones, Dobril Ivanov, Chris Smith, Rachael Preston, David Hunt, Samantha Quilliam and Holly Dibble for keeping me going and being so much fun!

All my family and friends.

The Tuberous Sclerosis Association UK, the PKD foundation, the MRC and the Wales Gene Park for their funding.

## Abbreviations

3D	Three dimensional
4E-BP1	eIF4E-binding protein 1
A	Adenine
aa	Amino acid
A/B	Apical/basal
ABC	Avidin biotin complex
AC	Adenylate cyclase
ADP	Adenosine diphosphate
ADPKD	Autosomal dominant polycystic kidney disease
ADPLD	Autosomal dominant polycystic liver disease
Ala	Alanine
AML	Angiomyolipoma
AMPK	AMP-dependent protein kinase
AP-1	Activator protein 1
APC	Adenomatous Polyposis coli
Arg	Arginine
ARPKD	Autosomal recessive polycystic kidney disease
ASK1	Apoptosis signal regulating kinase 1
ATM	Ataxia telangiectasia mutated protein
ATP	Adenosine triphosphate
BAX	Bcl2-associated X protein
BBS	Bardet-Biedl syndrome
BCL2	B cell leukemia/lymphoma 2
bp	Base pair
BF	Bright field
BSA	Bovine serum albumin
C	Cytosine

CA	Cystadenoma
Ca <sup>2+</sup>	Calcium
CAD	Caspase activated DNase
CaM	Calmodulin
cAMP	Cyclic adenosine monophosphate
CDK1	Cyclin dependent kinase 1
cDNA	Complementary DNA
CICR	Calcium induced calcium release
CRR	Cysteine-rich regions
CT	Computed tomography
cyto C	Cytochrome C
DAB	3, 3'-diaminobenzidine
DAPI	4', 6-diamidino-2-phenylindole
DCT	Distal convoluted tubule
DHPLC	Denaturing high performance liquid chromatography
DISC	Death inducing signalling complex
Dkk	Dickkopf
DMSO	Dimethylsulphoxide
DNA	Deoxyribonucleic acid
DNase	Deoxyribonuclease
dNTPs	Deoxynucleotide triphosphates
ddNTPs	2', 3' di-deoxynucleotide triphosphates
DPX	Dibutyl phthalate and xylene
ds	Double stranded
Dsh	Deshevelled
Dub	Duboraya
E	Embryonic day
EDTA	Ethylenediaminetetraacetic acid
EF	E and F helices of parvalbumin

EGFR	Epidermal growth factor receptor
eIF4E	Eukaryotic translation initiation factor 4E
ER	Endoplasmic reticulum
ERK	Extracellular signal regulated kinase
ERM	Ezrin-radixin-moesin
ES	Embryonic stem
ESRD	End stage renal disease
FADD	Fas associated death domain
FasL	Fas ligand
FBS	Foetal bovine serum
FGFR	Fibroblast growth factor receptor
FITC	Fluorescein isothiocyanate
FKBP	FK506-binding protein
FLCN	Folliculin
FLIP	FLICE-like inhibitory protein
FoxO1	Forkhead box O1
Fz	Frizzled
G	Guanine
GAP	GTPase-activating protein
GDP	Guanosine diphosphate
GFR	Glomerular filtration rate
Gly	Glycine
GPS	G-protein coupled receptor proteolytic site
GSK	Glycogen synthase kinase
GTP	Guanosine triphosphate
H&E	Haematoxylin and eosin
HIF	Hypoxia-inducible factor
HMDS	Hexamethyldisilazane
Hsp	Heat shock protein

ICAD	Inhibitor of caspase activated DNase
Id	Inhibitor of DNA binding
IFT	Intraflagellar transport
IHC	Immunohistochemistry
IκB	Inhibitor of NF-κB
IKK	Inhibitory κB kinase
Inv	Inversion of embryonic turning
IRES	Internal ribosome entry site
IRI	Ischemic/reperfusion injury
IRS	Insulin receptor substrate
JAK	Janus activated kinase
Kb	Kilobase
kDa	Kilodalton
KIF3a	Kinesin family member 3a
KIP	Kinase interacting protein
LAM	Lymphangioliomyomatosis
LCM	Laser capture microdissection
LDL	Low density lipoprotein A
LH2	Lipoxygenase homology
LKB1	Liver kinase B1
LOH	Loss of heterozygosity
LRR	Leucine-rich repeats
LST8	Lethal with SEC13 protein 8
Lys	Lysine
M	Molar
MAPK	Mitogen activated protein kinase
Mb	Megabase
MDCK	Madin-Darby canine kidney
MEF	Mouse embryonic fibroblast

MEK	Mitogen extracellular kinase
MK2	MAPK activated protein kinase 2
MRI	Magnetic resonance imaging
mRNA	Messenger ribonucleic acid
mTOR	Mammalian/mechanistic target of rapamycin
mTORC	Mammalian/mechanistic target of rapamycin complex
NaCl	Sodium chloride
NF-1	Neurofibromatosis type-1
NF-κB	Nuclear factor kappa B
NF-L	Neurofilament-L
NLS	Nuclear localisation sequence
NPHP	Nephronophthisis
OCT	Optimum cutting temperature
OFD1	Oral-facial-digital syndrome type 1
OGG1	8-Oxoguanine glycosylase
ORF	Open reading frame
PATJ	PALS1-associated TJ protein
PBFG	Phosphate buffered formaldehyde glutaraldehyde
PBS	Phosphate buffered saline
PC1	Polycystin 1
PC2	Polycystin 2
PCK	Polycystic kidneys
PCNA	Proliferating cell nuclear antigen
PCP	Planar cell polarity
PCR	Polymerase chain reaction
PEN	Polyethylene naphthalate
PFGE	Pulse field gel electrophoresis
PI3K	Phosphatidyl-inositol 3-kinase
PIKK	Phosphoinositide 3-kinase-related kinase

PJS	Peutz-Jeghers syndrome
PKA	Protein kinase A
PKB	Protein kinase B
PKD	Polycystic kidney disease
PKHD	Polycystic kidney and hepatic disease
PLC	Phospholipase C
POP	Performance optimised polymer
pS6	Phosphorylated S6 ribosomal protein
PTEN	Phosphatase and tensin homologue
Puma	p53 upregulated modulator of apoptosis
Raptor	Regulatory associated protein of mTOR
Ras	Rat sarcoma
RCC	Renal cell carcinoma
REJ	Sperm receptor for egg jelly
Rheb	Ras homologue enriched in brain
Rictor	Rapamycin insensitive companion of mTOR
RNA	Ribonucleic acid
ROS	Reactive oxygen species
rpm	Revolutions per minute
RSK1	Ribosomal protein S6 kinase 1
S6K	S6 kinase
SAP	Shrimp alkaline phosphatase
SDS	Sodium dodecyl sulphate
SEGA	Subependymal giant cell astrocytoma
SEM	Scanning electron microscopy
SEN	Subependymal nodule
Ser	Serine
SNP	Single nucleotide polymorphism
ss	Single stranded



STAT	Signal transducer and activator of transcription
T	Thymine
TAE	Tris-acetate-EDTA
TBS	Tris buffered saline
TCF	T cell factor
TGF	Transforming growth factor
T <sub>m</sub>	Melting temperature
TNF	Tumour necrosis factor
TNFR	Tumour necrosis factor receptor
TOR	Target of rapamycin
TOS	TOR signalling
TRADD	TNF receptor type 1 associated death domain
TRAIL	TNF related apoptosis inducing ligand
TSC	Tuberous sclerosis complex
TUNEL	Terminal dUTP nick-end labelling
Tyr	Tyrosine
U	Uracil
UTR	Untranslated region
UV	Ultraviolet
V	Volt
Vang	Van Gogh
VEGF	Vascular endothelial growth factor
VHL	Von Hippel-Lindau
W	Watt
WSC	Cell wall integrity and stress response component
WT	Wild-type
w/v	Weigh / volume
XIAP	X linked inhibitor of apoptosis protein

## Contents

<b>CHAPTER ONE: General introduction</b>	<b>1</b>
1.1 Tuberous sclerosis complex	1
1.1.1 History of the disease	1
1.1.2 Clinical manifestations of TSC	3
1.1.3 Diagnosis of TSC	5
1.1.4 Identification of the TSC genes	7
1.1.4.1 <i>TSC1</i>	7
1.1.4.2 <i>TSC2</i>	8
1.1.5 Mutation analysis	9
1.1.6 Genotype-phenotype correlations	9
1.1.6.1 <i>A contiguous deletion syndrome involving TSC2 and PKD1</i>	9
1.1.6.2 <i>Is a TSC2 disease more severe than a TSC1 disease?</i>	10
1.1.6.3 <i>Intellectual disability in TSC1 and TSC2</i>	10
1.1.7 Knudson's two hit hypothesis	12
1.1.8 Loss of heterozygosity, haploinsufficiency and <i>TSC3</i>	12
1.1.9 Mosaicism	15
1.1.10 Biochemistry of the TSC proteins	17
1.1.10.1 <i>Hamartin</i>	17
1.1.10.2 <i>Tuberin</i>	19
1.1.10.2.1 Tuberin functions as a GTPase activating protein	19
1.1.10.3 <i>The tuberin-hamartin complex</i>	22

1.1.10.4	<i>The mTOR pathway</i>	24
1.1.10.5	<i>mTOR syndromes</i>	24
1.1.11	Treatments	27
1.1.12	TSC models	28
1.1.12.1	<i>Eker rat</i>	29
1.1.12.2	<i>Tsc1 knockout mouse</i>	30
1.1.12.3	<i>Tsc2 knockout mouse</i>	30
1.2	Autosomal dominant polycystic kidney disease	31
1.2.1	History and epidemiology of ADPKD	31
1.2.2	Clinical manifestations of ADPKD	32
1.2.2.1	<i>Renal manifestations</i>	32
1.2.2.2	<i>Hepatic manifestations</i>	32
1.2.2.3	<i>Other manifestations</i>	33
1.2.3	Diagnosis of ADPKD	34
1.2.4	Treatment options for ADPKD	34
1.2.4.1	<i>Rapamycin in ADPKD treatment</i>	35
1.2.5	Identification of the ADPKD genes	35
1.2.5.1	<i>The PKD1 gene</i>	36
1.2.5.2	<i>The PKD2 gene</i>	36
1.2.5.3	<i>A third PKD locus?</i>	36
1.2.6	Mutation analysis of ADPKD	36
1.2.7	Genotype / phenotype correlations	37
1.2.8	Loss of heterozygosity and haploinsufficiency in ADPKD	39

1.2.9 Biochemistry of the ADPKD proteins.....	40
1.2.9.1 <i>Polycystin-1 and polycystin-2 associate in vivo</i> .....	44
1.2.9.2 <i>Tissue expression patterns of the ADPKD proteins</i> .....	44
1.2.9.3 <i>Polycystin-1 and polycystin-2 signalling pathways</i> .....	45
1.2.9.3.1 Primary cilia and calcium signalling.....	47
1.2.9.3.2 JAK-STAT pathway.....	49
1.2.9.3.3 Cell cycle control.....	50
1.2.9.3.4 Canonical Wnt signalling.....	52
1.2.9.3.5 mTOR signalling.....	52
1.2.10 Mouse models of PKD.....	54
1.3 Theories of cystogenesis.....	55
1.3.1 The nature of cysts in TSC and ADPKD.....	55
1.3.2 Primary cilia theory of cystogenesis.....	58
1.3.3 Activation of mTOR.....	61
1.3.4 Polarity defects in cystogenesis.....	63
1.3.5 Ca <sup>2+</sup> homeostasis.....	66
1.3.6 Apoptotic defects in cystogenesis.....	68
1.3.6.1 <i>Apoptosis overview</i> .....	68
1.3.6.2 <i>Mouse models with aberrant apoptosis display a cystic phenotype</i> .....	68
1.3.6.3 <i>Apoptosis in ADPKD and TSC</i> .....	70
1.4 Aims.....	74

<b>CHAPTER TWO: Materials and methods</b>	<b>75</b>
2.1 Suppliers	75
2.2 Materials	76
2.2.1 Chemicals	76
2.2.2 Histology	76
2.2.3 Laser capture microdissection	76
2.2.4 DNA extraction and purification kits	76
2.2.5 Oligonucleotide primers and dNTPs	77
2.2.6 PCR	77
2.2.7 PCR purification	77
2.2.8 Electrophoresis	77
2.2.9 DNA size markers	77
2.2.10 Sequencing and DNA clean up	77
2.2.11 Antibodies	77
2.2.12 Immunohistochemistry	78
2.2.13 Immunofluorescence	78
2.2.14 Scanning electron microscopy	78
2.3 Equipment	78
2.3.1 Plastics	78
2.3.2 Histology	78
2.3.3 Immunohistochemistry and immunofluorescence	79
2.3.4 DNA quantifications and thermocycling	79
2.3.5 Electrophoresis	79

2.3.6 Scanning electron microscopy.....	79
2.3.7 Laser capture microdissection.....	79
2.3.8 Photography.....	79
2.3.9 Software.....	80
2.4 Solutions.....	80
2.5 Methods.....	80
2.5.1 Animal husbandry.....	80
2.5.2 Necrosis analysis.....	81
2.5.3 Histology.....	81
2.5.3.1 <i>Tissue fixation, embedding and sectioning</i> .....	81
2.5.3.2 <i>Snap freezing and PALM slide sectioning</i> .....	82
2.5.3.3 <i>Perfusion fixation</i> .....	82
2.5.3.4 <i>Haematoxylin and eosin staining</i> .....	83
2.5.4 Laser capture microdissection.....	83
2.5.5 Nucleic acid extraction.....	84
2.5.5.1 <i>DNA extraction from tail tips</i> .....	84
2.5.5.2 <i>DNA extraction from laser microdissected tissue</i> .....	84
2.5.6 Nucleic acid quantification.....	85
2.5.7 Oligonucleotide primer design.....	85
2.5.8 Polymerase chain reaction.....	85
2.5.9 Agarose gel electrophoresis.....	86
2.5.10 PCR purification.....	87
2.5.11 Cycle sequencing.....	87

2.5.12 Immunohistochemistry.....	88
2.5.13 Double immunofluorescence staining.....	89
2.5.14 Scanning electron microscopy.....	90
<b>CHAPTER THREE: Investigating the role of hamartin, tuberin and polycystin-1 in cystogenesis, ciliogenesis and planar cell polarity.....</b>	<b>91</b>
3.1 Introduction.....	91
3.2 Materials and methods.....	93
3.2.1 DNA extraction and genotyping.....	93
3.2.2 Animal care and husbandry.....	93
3.2.3 Immunohistochemistry.....	94
3.2.4 Scanning electron microscopy.....	94
3.2.5 Orientation of cell division.....	94
3.2.6 Statistical analyses.....	95
3.3 Results.....	95
3.3.1 Renal and hepatic pathology.....	95
3.3.1.1 <i>Renal lesion analysis</i> .....	96
3.3.1.2 <i>Hepatic lesion analysis</i> .....	97
3.3.2 Investigating the role of hamartin, tuberin and polycystin-1 in ciliogenesis.....	97
3.3.2.1 <i>Investigating the relationship between cell size and cilia length</i> .....	97
3.3.2.2 <i>Investigating the relationship between age and cilia length</i> ....	97
3.3.2.3 <i>Primary cilia in pre-cystic renal tubules</i> .....	101
3.3.2.4 <i>Primary cilia in pre-cystic liver cholangiocytes</i> .....	101

3.3.3	Primary cilia in hepatic cyst epithelia.....	104
3.3.4	Investigating the role of hamartin, tuberin and polycystin-1 in cell polarity.....	110
3.3.4.1	<i>Pre-cystic renal tubules</i> .....	110
3.3.4.2	<i>Pre-cystic hepatic bile ducts</i> .....	110
3.3.4.3	<i>Genotype and aberrant polarity</i> .....	111
3.4	Discussion.....	111
3.4.1	A genetic interaction between <i>Tsc1</i> , <i>Tsc2</i> and <i>Pkd1</i> .....	111
3.4.2	Differences between the <i>Pkd1</i> <sup>+/-</sup> mouse models and humans with ADPKD.....	115
3.4.3	Mice from <i>Tsc2</i> <sup>+/-</sup> and <i>Pkd1</i> <sup>+/-</sup> crosses occasionally experience a severe early onset kidney disease.....	116
3.4.4	Hamartin, tuberin and polycystin-1 play a role in renal and hepatic ciliogenesis.....	117
3.4.5	A physiological consequence to abnormal primary cilia?.....	119
3.4.6	Role of hamartin, tuberin and polycystin-1 in bile duct and renal tubule cell polarity.....	120
3.4.7	Planar cell polarity or apical / basal polarity.....	122
3.4.8	Wild-type misorientated cell division.....	123
<b>CHAPTER FOUR: Defective apoptosis may promote TSC-associated renal cystogenesis.....</b>		<b>124</b>
4.1	Introduction.....	124
4.2	Materials and methods.....	125
4.2.1	Animal care, genotyping and tissue preparation.....	125
4.2.2	Immunohistochemistry.....	125



4.2.3 Cell size measurement.....	126
4.2.4 Statistics.....	127
4.3 Results.....	127
4.3.1 Apoptosis in developing mouse renal tubules.....	127
4.3.2 mTOR activation in TSC-associated renal lesions.....	127
4.3.3 Caspase-3 and mTOR activation in TSC lesions.....	128
4.3.4 Cyst size investigation.....	128
4.4 Discussion.....	137
4.4.1 Latency in TSC-associated cystogenesis.....	137
4.4.2 A significant proportion of Tsc-associated simple cysts do not stain for mTOR activation.....	137
4.4.3 Advanced lesions are highly likely to be positive for mTOR activation.....	138
4.4.4 Apoptosis is elevated in developing renal tubules with defective polarity.....	138
4.4.5 Apoptosis is important in wild-type kidney development.....	139
4.4.6 Simple cysts that are negative for activation of the mTOR pathway are not likely to display apoptosis.....	139
4.4.7 Caspase and mTOR activation modulate cyst size.....	140
<b>CHAPTER FIVE: Activation of the Jak/Stat signalling pathway in Tsc-associated cystogenesis.....</b>	<b>142</b>
5.1 Introduction.....	142
5.2 Materials and methods.....	150
5.2.1 Animal care, genotyping and tissue preparation.....	150

5.2.2 Immunohistochemistry.....	150
5.2.3 Statistical analysis.....	150
5.3 Results.....	151
5.3.1 Delineating the pro-survival mechanism in mTOR-inactive simple cysts from <i>Tsc1</i> <sup>+/-</sup> and <i>Tsc2</i> <sup>+/-</sup> mice.....	151
5.4 Discussion.....	160
5.4.1 The pro-survival signalling in our simple cysts deficient in apoptosis appears to be Bcl2 mediated.....	160
5.4.2 Simple cysts that do not display apoptosis or mTOR activation are likely to have increased levels of activated Stat3 and Jak2.....	160
5.4.3 Activation of Stat3 can be mTOR-dependent or independent.....	162
5.4.4 ADPKD and JAK2 / STAT3.....	163
5.4.5 NF-κB is not activated in simple cysts from our <i>Tsc1</i> <sup>+/-</sup> and <i>Tsc2</i> <sup>+/-</sup> mice.....	164
5.4.6 HGF signalling is not activated in simple cysts from our <i>Tsc1</i> <sup>+/-</sup> and <i>Tsc2</i> <sup>+/-</sup> mice.....	165
5.4.7 Akt signalling is not activated in simple cysts from our <i>Tsc1</i> <sup>+/-</sup> and <i>Tsc2</i> <sup>+/-</sup> mice.....	166
5.4.8 p53 in cystogenesis.....	167
5.4.9 Activation of pro-survival signalling in simple cysts without mTOR dysregulation.....	168
<b>CHAPTER SIX: Oncogenic somatic Jak2 mutations may promote TSC-associated renal cystogenesis.....</b>	<b>169</b>
6.1 Introduction.....	169
6.2 Materials and methods.....	170

6.2.1 Animal care, genotyping and tissue preparation.....	170
6.2.2 DNA isolation from simple cysts.....	170
6.2.3 <i>Jak2</i> sequencing.....	171
6.2.4 Cyst progression in <i>Tsc2</i> <sup>+/-</sup> mice with and without germline <i>Jak2</i> changes.....	171
6.2.5 Cyst analysis in wild-type mice with and without germline <i>Jak2</i> changes.....	171
6.2.6 SNP severity prediction.....	172
6.2.7 Statistical analysis.....	172
6.3 Results.....	172
6.3.1 Germline <i>Jak2</i> variations are present in our <i>Tsc1</i> <sup>+/-</sup> and <i>Tsc2</i> <sup>+/-</sup> mice.....	172
6.3.2 Somatic <i>Jak2</i> mutations are present in the cysts of our <i>Tsc1</i> <sup>+/-</sup> and <i>Tsc2</i> <sup>+/-</sup> mice.....	173
6.3.3 <i>Jak2</i> mutation analysis.....	173
6.3.3.1 <i>Evolutionary analysis</i> .....	173
6.3.3.2 <i>Severity of residue change</i> .....	174
6.3.4 Germline variants in <i>Jak2</i> at K575E and G614G may modulate cyst burden in <i>Tsc2</i> <sup>+/-</sup> animals.....	174
6.3.5 Wild-type mice with germline variants in <i>Jak2</i> at K575E and G614G experience a low level of renal cystogenesis.....	178
6.4 Discussion.....	182
6.4.1 <i>Jak2</i> mutations in <i>Tsc1</i> <sup>+/-</sup> and <i>Tsc2</i> <sup>+/-</sup> simple cysts.....	182
6.4.2 Somatic <i>Jak2</i> mutations in Tsc-associated renal cysts.....	182
6.4.3 Low levels of <i>Jak2</i> mutation detection.....	184

6.4.4	Germline <i>Jak2</i> mutations.....	185
6.4.5	The effects of germline changes in <i>Jak2</i> on Tsc-associated renal cystogenesis.....	186
6.4.6	Wild-type mice with germline changes in <i>Jak2</i> experience a low level of renal cysts.....	187
<b>CHAPTER SEVEN: General discussion.....</b>		<b>189</b>
7.1	Haploinsufficiency in TSC and ADPKD.....	189
7.1.1	Haploinsufficiency in TSC and other hamartoma syndromes.....	189
7.1.2	Haploinsufficiency in ADPKD.....	192
7.2	Mechanisms of cystogenesis.....	194
7.2.1	mTOR-mediated cyst formation.....	196
7.2.2	mTOR-independent cyst formation.....	196
7.2.3	mTOR-dependent cyst progression.....	197
7.3	Implications for clinical trials.....	200
7.3.1	Inhibition of the mTOR pathway in TSC.....	200
7.3.2	JAK2 or STAT3 inhibitors in TSC?.....	201
<b>References.....</b>		<b>204</b>

## List of figures

Figure 1.1	Mutational spectrum of <i>TSC1</i> and <i>TSC2</i> .....	11
Figure 1.2	Loss of tumour suppressor gene function in cancer.....	14
Figure 1.3	Mosaicism in TSC.....	16
Figure 1.4	Hamartin, the <i>TSC1</i> protein product .....	18
Figure 1.5	Tuberin, the <i>TSC2</i> gene product.....	20
Figure 1.6	The role of the hamartin / tuberin complex in mTOR regulation.....	23
Figure 1.7	Hamartoma disease genes in mTOR signalling.....	26
Figure 1.8	Mutational analysis of <i>PKD1</i> and <i>PKD2</i> .....	38
Figure 1.9	Polycystin-1 and polycystin-2, the ADPKD proteins.....	42
Figure 1.10	Renal distribution of polycystin-1 and polycystin-2.....	46
Figure 1.11	Primary cilia, polycystins and calcium signalling .....	48
Figure 1.12	The polycystins and cell cycle control .....	51
Figure 1.13	The canonical Wnt signalling pathway .....	53
Figure 1.14	Cystogenesis in TSC and ADPKD .....	57
Figure 1.15	mTOR dysregulation in cystogenesis .....	62
Figure 1.16	Defective polarity in cystogenesis .....	65
Figure 1.17	Calcium and cAMP in cystogenesis.....	67
Figure 1.18	Apoptosis overview.....	72
Figure 1.19	Apoptosis in cystogenesis.....	73
Figure 3.1	Microscopic analyses of H&E stained renal lesions from 9-12 month old <i>Pkd1</i> <sup>+/-</sup> , <i>Tsc1</i> <sup>+/-</sup> and <i>Tsc2</i> <sup>+/-</sup> mice.....	98

Figure 3.2	Microscopic analysis of small H&E stained hepatic lesions from 15-18 month old <i>Pkd1<sup>+/-</sup></i> , <i>Tsc1<sup>+/-</sup> Pkd1<sup>+/-</sup></i> and <i>Tsc2<sup>+/-</sup> Pkd1<sup>+/-</sup></i> mice.....	99
Figure 3.3	Microscopic analysis of large H&E stained hepatic lesions from 15-18 month old <i>Pkd1<sup>+/-</sup></i> , <i>Tsc1<sup>+/-</sup> Pkd1<sup>+/-</sup></i> and <i>Tsc2<sup>+/-</sup> Pkd1<sup>+/-</sup></i> mice.....	100
Figure 3.4	Scanning electron micrographs of cholangiocyte primary cilia in pre-cystic hepatic bile ducts.....	105
Figure 3.5	Graph showing distribution of mean primary cilia lengths from pre-cystic hepatic bile ducts.....	107
Figure 3.6	Scanning electron micrograph of the luminal surface of a liver cyst from a 20 month old <i>Tsc2<sup>+/-</sup> Pkd1<sup>+/-</sup></i> mouse.....	109
Figure 3.7	Mitotic orientations of dividing pre-cystic hepatic bile duct cells from 10 day old <i>Tsc1<sup>+/-</sup></i> , <i>Tsc2<sup>+/-</sup></i> , <i>Pkd1<sup>+/-</sup></i> and wild-type mice.....	112
Figure 4.1	Apoptosis in 2 day old mouse renal tubules.....	129
Figure 4.2	mTOR activation in simple cysts and advanced lesions from 9-12 month old <i>Tsc1<sup>+/-</sup></i> and <i>Tsc2<sup>+/-</sup></i> mice.....	131
Figure 4.3	Apoptotic and mTOR status of simple cysts and advanced lesions from 9-12 month old <i>Tsc1<sup>+/-</sup></i> and <i>Tsc2<sup>+/-</sup></i> mice.....	132
Figure 4.4	The effect of mTOR activation and apoptosis on lesion size in <i>Tsc1<sup>+/-</sup></i> and <i>Tsc2<sup>+/-</sup></i> mice.....	135
Figure 5.1	Identification of key proteins within anoikis and apoptosis signalling.....	149
Figure 5.2	mTOR inactive / caspase-3 inactive simple cysts do not show activation of Akt, c-Met or p65.....	153
Figure 5.3	Activation of Jak2 in simple cysts from <i>Tsc1<sup>+/-</sup></i> and <i>Tsc2<sup>+/-</sup></i> mice.....	154
Figure 5.4	Activation of Stat3 in simple cysts from <i>Tsc1<sup>+/-</sup></i> and <i>Tsc2<sup>+/-</sup></i> mice.....	155
Figure 5.5	Upregulation of Bcl2 in simple cysts from <i>Tsc1<sup>+/-</sup></i> and <i>Tsc2<sup>+/-</sup></i> mice....	156

Figure 5.6	Upregulation of p53 in simple cysts from <i>Tsc1</i> <sup>+/-</sup> and <i>Tsc2</i> <sup>+/-</sup> mice.....	157
Figure 5.7	Serial sections of cysts stained for mTOR activation, caspase-3 activation, Bcl2, phospho-Stat3, phospho-Jak2, phospho-Akt and phospho-p65...	158
Figure 6.1	Germline changes in <i>Jak2</i> in the DNA of a collection of cysts removed from a <i>Tsc2</i> <sup>+/-</sup> mouse.....	175
Figure 6.2	Somatic changes in <i>Jak2</i> in the DNA of four separate cysts removed from <i>Tsc1</i> <sup>+/-</sup> and <i>Tsc2</i> <sup>+/-</sup> mice.....	176
Figure 6.3	Amino acid alignments of the <i>Jak2</i> variants found in our cysts.....	177
Figure 6.4	Germline changes in <i>Jak2</i> at K575E and G614G may modestly affect lesion incidence in <i>Tsc2</i> <sup>+/-</sup> mice.....	180
Figure 6.5	Germline changes in <i>Jak2</i> at K575E and G614G may cause wild-type ( <i>Tsc1</i> <sup>+/+</sup> and <i>Tsc2</i> <sup>+/+</sup> ) mice to develop renal cysts.....	181
Figure 7.1	Consequences of haploinsufficiency in <i>Tsc1</i> and <i>Tsc2</i> .....	193
Figure 7.2	mTOR-dependent and independent cystogenesis in TSC.....	195
Figure 7.3	Hamartin, tuberlin and polycystin-1 have links to A/B and planar cell polarity.....	198
Figure 7.4	Distribution of variants identified across the pseudokinase domain of <i>Jak2</i> .....	199

## List of tables

Table 1.1	Timeline of tuberous sclerosis complex .....	2
Table 1.2	The pathological findings of tuberous sclerosis complex .....	4
Table 1.3	Diagnostic criteria for tuberous sclerosis complex .....	6
Table 1.4	The domains of hamartin and tuberin.....	21
Table 1.5	Hamartoma syndromes with a proven or potential link to mTOR.....	25
Table 1.6	Domains and functions of polycystin-1 and polycystin-2.....	43
Table 1.7	Cystic kidney disease proteins located to the primary cilium .....	60
Table 3.1	The relationship between cholangiocyte cell size and primary cilium length in <i>Tsc1</i> <sup>+/-</sup> , <i>Tsc2</i> <sup>+/-</sup> , <i>Pkd1</i> <sup>+/-</sup> , <i>Tsc1</i> <sup>+/-</sup> <i>Pkd1</i> <sup>+/-</sup> and <i>Tsc2</i> <sup>+/-</sup> <i>Pkd1</i> <sup>+/-</sup> mice.....	102
Table 3.2	Primary cilium lengths from pre-cystic renal tubule cells in <i>Tsc1</i> <sup>+/-</sup> , <i>Tsc2</i> <sup>+/-</sup> , <i>Pkd1</i> <sup>+/-</sup> , <i>Tsc1</i> <sup>+/-</sup> <i>Pkd1</i> <sup>+/-</sup> , <i>Tsc2</i> <sup>+/-</sup> <i>Pkd1</i> <sup>+/-</sup> and wild-type mice.....	103
Table 3.3	Primary cilium lengths from pre-cystic hepatic bile duct cells in <i>Tsc1</i> <sup>+/-</sup> , <i>Tsc2</i> <sup>+/-</sup> , <i>Pkd1</i> <sup>+/-</sup> , <i>Tsc1</i> <sup>+/-</sup> <i>Pkd1</i> <sup>+/-</sup> , <i>Tsc2</i> <sup>+/-</sup> <i>Pkd1</i> <sup>+/-</sup> and wild-type mice.....	106
Table 3.4	Measurements of primary cilia length from epithelial cells lining liver cysts in 20 month old <i>Pkd1</i> <sup>+/-</sup> , <i>Tsc1</i> <sup>+/-</sup> <i>Pkd1</i> <sup>+/-</sup> and <i>Tsc2</i> <sup>+/-</sup> <i>Pkd1</i> <sup>+/-</sup> mice.....	108
Table 4.1	Levels of apoptosis in the developing renal tubules of <i>Tsc1</i> <sup>+/-</sup> , <i>Tsc2</i> <sup>+/-</sup> , <i>Pkd1</i> <sup>+/-</sup> and wild-type mice at 2 days of age.....	130
Table 4.2	Apoptotic and mTOR status of simple cysts in Tsc-associated renal cystogenesis.....	133
Table 4.3	Apoptotic and mTOR status of advanced lesions in Tsc-associated renal cystogenesis.....	134
Table 4.4	The effect of mTOR and apoptosis on lesion size in <i>Tsc1</i> <sup>+/-</sup> and <i>Tsc2</i> <sup>+/-</sup> mice.....	136



Table 5.1	Simple cysts staining strongly for phospho-Met, phospho-Jak2, phospho-Akt, phospho-Stat3, phospho-p65, Bcl2 and p53.....	152
Table 5.2	Patterns of activation in simple cysts, categorise by mTOR and apoptotic status.....	159
Table 6.1	Germline changes in Jak2 at K575E and G614G may modestly affect lesion incidence in <i>Tsc2</i> <sup>+/-</sup> mice.....	179

## CHAPTER ONE

### General Introduction

#### **1.1 Tuberous sclerosis complex**

Tuberous sclerosis complex (TSC) is an autosomal dominant disorder characterised by multiple hamartomatous growths across many organs.

##### **1.1.1 History of the disease**

The earliest reported case of TSC was in a neonate with cardiac rhabdomyomata (von Recklinghausen 1862), but it was not until 1879 that Désiré-Magloire Bourneville clearly documented what we now know of as the disease in a 3 year old girl with seizures, facial angiofibroma and mental handicap with the term 'sclérose tubéreuse des circonvolutions cérébrales' (Bourneville 1880). By 1905, Gaetano Perusini began to associate the cerebral, renal, cardiac and skin lesions found in TSC sufferers and in 1908 Heinrich Vogt proposed the notion of a clinical triad (Vogt 1908) of seizures, mental retardation and adenoma sebaceum (facial angiofibroma). However, only ~29% of individuals will present with the full triad (Gomez 1988), which led to an underestimate of TSC prevalence at 1:100,000 (Nevin *et al.* 1968). Technological advances such as computer tomography (CT) (1974), renal ultrasound and echocardiography (1982) and magnetic resonance imaging (MRI) (1984) provided non-invasive ways to diagnose TSC in patients not presenting with the classical triad or mental retardation (Lagos *et al.* 1967). It was a combination of these new diagnostic tools and work done by Gomez (1988) to establish a major and minor clinical feature list that helped increase the accuracy of population studies into TSC and raise the number of cases significantly. TSC is now thought to affect between one in 6,000 and one in 10,000 individuals (Sampson *et al.* 1989, Osborne 1991). The genes responsible, *TSC1* and *TSC2* (encoding hamartin and tuberin respectively) have been characterised and their roles in the repression of mTOR signalling has led to trials of Rapamycin (an mTOR inhibitor) as a TSC treatment. A timeline of key events in the history of TSC is included in Table 1.1.

**Table 1.1** Timeline of tuberous sclerosis complex, adapted from Gomez *et al.* 1999.

Date	Name	Contribution
1835	Pierre François Rayer	Publishes atlas of skin disorders including a diagram highly likely to be a facial angiofibroma.
1862	Friedrich von Recklinghausen	Documents the disease in a neonate with classic TSC cardiac rhabdomyomas and cortical tubers.
1879	Désiré-Magloire Bourneville	Gives first detailed description of TSC, and names it tuberous sclerosis of the cerebral convolutions.
1881	Hartdegen	Post-mortem study of TSC brain pathology.
1885	Balzer, Ménétrier & Pringle	Recognises and names “adenoma sebaceum”, notes the link with this and mental handicap and seizures.
1901	Pellizzi	Noted the dysplastic nature of TSC cerebral lesions.
1905	Perusini	Associated skin, renal, cardiac and cerebral lesions.
1908	Heinrich Vogt	Proposed the clinical triad in diagnosis of TSC.
1910	Kirpicznik & Berg	Both reported on the hereditary nature of TSC.
1914	Schuster	Discovered TSC patient with incomplete Vogt’s triad.
1918	Lutenbacher	Proposed the involvement of the lung in TSC.
1920	Van der Hoeve	Similarity of TSC, neurofibromatosis and von Hippel-Lindau disease, also studied TSC retinal phakomas.
1924	Marcus	Radiographic findings to aid in diagnosis.
1932	Critchley & Earl	Noted diagnostic value of hypomelanotic skin macules in TSC; detailed review of the disease.
1942	Moolten	Coins the term “Tuberous Sclerosis Complex”.
1967	Lagos & Gomez	38% of TSC group studied had normal intelligence.
1974		Invention of computed tomography for the head.
1979	Gomez	New diagnostic criteria, decline of Vogt’s triad.
1982		Renal ultrasound and echocardiography introduced.
1984		Magnetic resonance imaging—refinement of non-invasive TSC diagnosis.
1987	Fryer <i>et al.</i>	First mutated TSC gene ( <i>TSC1</i> ) linked to 9q34.3.
1992	Kandt <i>et al.</i>	Second TSC gene ( <i>TSC2</i> ) linked to 16p13.3.
1993	The European Chromosome 16 TSC Consortium	<i>TSC2</i> cloned and its product, tuberin, is identified; tuberin is found to have a region of homology to the GTPase-activating protein, GAP3.
1994	Green <i>et al.</i> & Carbonara <i>et al.</i>	Loss of heterozygosity shown in renal and cardiac TSC hamartomas; also in TSC cerebral lesions.
1997	Van Slegtenhorst <i>et al.</i>	<i>TSC1</i> is cloned and its 130 kDa protein product, hamartin, is identified.
1998	Plank <i>et al.</i>	Strong binding interaction between tuberin and hamartin demonstrated <i>in vivo</i> (1:1 stoichiometry).
2002	Tee <i>et al.</i>	Observed that tuberin and hamartin functionally interact to inhibit the mammalian target of rapamycin (mTOR) signalling pathway.
2005	Inoki <i>et al.</i>	Calls for rapamycin clinical trials on TSC lesions.
2005	Kenerson <i>et al.</i>	Size reduction in renal tumours from Eker rats (TSC model) treated with rapamycin.
2008	Davies <i>et al.</i> & Bissler <i>et al.</i>	Two year trial of rapamycin in human TSC patients reveals a size reduction in astrocytomas and renal angiomyolipomas.

### 1.1.2 Clinical manifestations of TSC

TSC primarily manifests as benign hamartomatous growths across many organs, including the brain, skin, kidneys and heart. TSC hamartomas consist of a group of dysplastic, disorganised cells that possess at least some ability for growth (Kwiatkowski 2003). Hamartomas are defined as a subtype of benign tumour, where cells will retain normal differentiation but display disorganised tissue architecture (Inoki *et al.* 2005). Table 1.2 outlines the various dermatological, neurological, renal, hepatic, pulmonary and cardiac manifestations of the disease.

After skin lesions, which are found in nearly all TSC patients, cerebral pathology is the second most common finding (~90%). It is tumours of the central nervous system (CNS) that cause the majority of morbidity and mortality in TSC (Hockenberry 2003). However, significant contributions to TSC pathology are made from renal involvement (Rosser *et al.* 2006). Liver manifestations of TSC are limited to hepatic angiomyolipomas (AMLs), which are often asymptomatic and non-progressive (Carmody *et al.* 1994). TSC-associated pulmonary defects occur exclusively in post-pubescent females, at a low incidence of 1% to 6% (Uzzo *et al.* 1994; Kwiatkowski *et al.* 1994) but can be devastating enough to require lung transplantation.

Other manifestations associated with TSC include retinal tumours (Robertson 1991), which are seen in ~50% of TSC patients (Robertson 1988). These have strong diagnostic value (Casteels 2010) but rarely affect vision (Kwiatkowski *et al.* 2010). Pathological hormone changes can be induced by AML growth on the adrenal glands (Ilgren *et al.* 1984). TSC adenomas can grow on the pancreas (Kim *et al.* 1995) or thyroid (Adhvaryu *et al.* 2004) to further subvert the endocrine system. Digestive tract involvement is divided between the mouth (nodular tumours and papillomas), and the rectum (hamartomatous colorectal polyps) (Gould 1991). These colorectal polyps have minimal malignant potential. Bender *et al.* (1981) have commented on splenic involvement, characterised as nodules of large abnormal cells throughout the parenchyma. Skeletal lesions in TSC occur as asymptomatic foci of sclerotic growth (Umeoka *et al.* 2008).

**Table 1.2** The pathological findings of tuberous sclerosis complex

System	Symptom	Manifestation
Skin	Facial Angiofibroma	Adenoma sebaceum present across the cheek bones and bridge of the nose, seen in 75% of TSC patients (Weiner <i>et al.</i> 1998). Lesion composed of abnormal vasculature and fibrous tissue.
	Hypomelanotic Macules	White patches are visible on most sufferers (Alper <i>et al.</i> 1983), although these pigmentation defects can also be present in the general population with no pathological significance.
	Ungual Fibromas, Shagreen Patches	Nail bed tumours and connective tissue hamartomas commonly appear around puberty and are relatively frequent in TSC.
Brain	Cortical Tubers	Hypomyelinated hamartomas arising from the cerebral cortex and surround white matter. Detectable as early as 20 weeks gestation (Park <i>et al.</i> 1997) and a characteristic TSC lesion.
	Sub-ependymal nodules (SEN)	Develop in the lining of cerebral ventricles and typically calcify with time (Gerard <i>et al.</i> 1987). Present in 80% of TSC patients.
	Sub-ependymal giant cell astrocytomas (SEGA)	May grow large enough to block CNS fluid flow, believed to develop from SENs and frequently calcify (Kwiatkowski 2010). Histologically, SENs and SEGAs are identical, but the two are distinguished on their ability to grow (Fujiwara <i>et al.</i> 1989).
Kidney	Angiomyolipoma (AML)	A common TSC finding (~70%) (Bernstein <i>et al.</i> 1991), but asymptomatic in many cases (O'Callaghan <i>et al.</i> 2004). AMLs are age-dependent (Gomez 1988) benign tumours formed from smooth-muscle cells, mature adipose tissue and abnormal blood vessels (Stillwell <i>et al.</i> 1987).
	Cysts	In ~35% of TSC patients (Cook <i>et al.</i> 1996), commonly multiple and bilateral, arise from all portions of the nephron (Gomez 1988), lined with hyperplastic epithelial cells derived from tubule cells. Severe renal cystic disease occurs in ~2% of patients with a contiguous deletion of both <i>TSC2</i> and the adjacent <i>PKD1</i> gene.
	Renal Cell Carcinoma (RCC)	Suggested to occur earlier (Lendvay <i>et al.</i> 2002) and more frequently in TSC patients than the general population (O'Callaghan <i>et al.</i> 2004, Kwiatkowski 2010, Washecka <i>et al.</i> 1991). Lesions most likely derive from the lining of cysts, not AMLs (Robertson <i>et al.</i> 1996). The prevalent type of RCC in TSC is clear cell carcinoma (Bjornsson <i>et al.</i> 1996).
Liver	Angiomyolipoma (AML)	Hepatic AMLs occur at a significantly lower incidence to renal manifestations (Galant <i>et al.</i> 1995). Fricke <i>et al.</i> (2003) found AMLs in 13% of TSC patients.
Lungs	Lymphangioleiomyomatosis (LAM)	Exclusively in post-pubescent females, at an incidence of 1% to 6% (Uzzo <i>et al.</i> 1994, Kwiatkowski <i>et al.</i> 1994). Characterised by hyperproliferation of smooth muscle cells throughout the lung and results in destruction of functional pulmonary tissue with multiple thin-walled cysts (Kwiatkowski <i>et al.</i> 2010).
Heart	Cardiac rhabdomyomas	Heart lesions occur in half of infant TSC sufferers (Bass <i>et al.</i> 1985; Smith <i>et al.</i> 1989), with rhabdomyomas derived from cardiac muscle cells being the only cardiac lesion directly associated with the disease (Nir <i>et al.</i> 1995). Lesions are small and commonly regress with time (Kwiatkowski <i>et al.</i> 1994).



### 1.1.3 Diagnosis of TSC

TSC has highly variable penetrance, causing a plethora of abnormalities in a variety of organs. This presents medical professionals with a diagnostic challenge that requires careful clinical evaluation (Osborne 1988). Many cases of TSC will first come to the attention of a clinician through parental concern over small raised facial tumours or spasms in early childhood. Some children may remain undiagnosed until adolescence if symptoms are phenotypically mild. Typically, minor dermatological features will lead to eventual suspicion of TSC in these cases. A new diagnosis of TSC will include a detailed family history, physical examination (skin lesions), cranial imaging (cortical tubers and SENs), renal ultrasonography (renal AMLs and cysts) and echocardiography (cardiac rhabdomyoma).

Vogt's triad of seizures, mental retardation and facial angiofibroma was the principle guide in diagnosing TSC for many years. Upon the discovery by Manuel Gomez that patients may not exhibit some or all of these clinical cornerstones (Gomez 1988), a definite need for updated and more inclusive diagnostic criteria arose. A new criterion was produced to include many more of the previously sidelined aspects of TSC (Gomez 1979) and this was later revised by a panel of experts at the Tuberous Sclerosis Complex Consensus Conference in Annapolis, Maryland (Roach *et al.* 1998). A more recent version has been released with minor changes in 2004 (Roach and Sparagana 2004). This revised consensus diagnostic criteria for TSC reflects an increased understanding of the disease and how it manifests, and is included in full in Table 1.3.

Clinical features of TSC are classified into major and minor categories, the presence of which will allow a diagnostician to give definite, probable or possible confirmation of TSC. Diagnosis can alternatively be carried out or backed up by genetic testing of the *TSC1* and *TSC2* genes. This will involve sequence analysis of the two genes followed by deletion testing if no initial mutation is detected. There are patients with a spectrum of TSC-associated manifestations in whom no mutation in *TSC1* or *TSC2* can be found (no mutation identified, or NMI), but it does not mean those individuals do not have TSC. NMI may be accounted for by mutation detection failure, a pathogenic mutation in a non-coding region, a third undiscovered TSC locus or mosaicism. These issues are discussed in more detail later on.

**Table 1.3** Diagnostic criteria for tuberous sclerosis complex.

Major Features	
<u>Location</u>	<u>Feature</u>
Head	Facial angiofibroma or forehead plaque.
Brain	Cortical tuber § Subependymal nodule Subependymal giant cell astrocytoma
Eyes	Multiple retinal nodular hamartomas
Skin	Hypomelanotic macules (>3 lesions) Shagreen patch (connective tissue nevus)
Fingers / Toes	Non-traumatic ungual fibromas
Heart	Cardiac rhabdomyoma (single or multiple)
Lungs	Lymphangiomyomatosis ¥
Kidneys	Renal angiomyolipoma ¥
Minor Features	
<u>Location</u>	<u>Feature</u>
Teeth	Multiple randomly distributed pits in dental enamel
Rectum	Hamartomatous rectal polyps (histologically confirmed)
Bones	Bone cysts (radiographically confirmed)
Brain	Cerebral white matter radial migration lines §
Gums	Gingival fibromas
Liver / Spleen	Non-renal hamartoma (histologically confirmed)
Eyes	Retinal achromic patch
Skin	"Confetti" skin lesions
Kidneys	Multiple renal cysts (histologically confirmed)
<b>Definite</b> - Either two major features or one major feature with two minor features. <b>Probable</b> - One major and one minor feature. <b>Suspect</b> - Either one major feature or two or more minor features.	

§ Cerebral cortical dysplasia and cerebral white matter migration tracts occurring together are counted as one rather than two features of TSC.

¥ When both lymphangiomyomatosis and renal angiomyolipomas are present, other features of TSC must be present in order for definite diagnosis.

#### 1.1.4 Identification of the TSC genes

The genetic aspect of TSC was fully appreciated by Kirpicznik and Pringle at the turn of the 19th century (Kirpicznik 1910, Pringle 1890). Subsequent work by Berg (1913) and Gunther *et al.* (1935) revealed a dominant inheritance pattern. In the following years, several researchers documented TSC-affected families (Dickerson 1951, Lagos *et al.* 1967), but it was not until the 1980s when progress was made in uncovering the genes responsible for TSC.

##### 1.1.4.1 *TSC1*

Fryer *et al.* (1987) conducted a linkage study in 19 multigenerational families with TSC, and found linkage between a TSC-causing gene and the ABO blood group gene on chromosome 9q34. Following this breakthrough, the locus was named *TSC1* (tuberous sclerosis complex type 1). The lack of linkage in other families led to suggestions of another TSC locus (Sampson *et al.* 1989, Haines *et al.* 1991, Northrup *et al.* 1992). Using polymorphic DNA markers, the *TSC1* candidate region was tracked to a 1.4Mb gene-rich (30-45 genes) region (Kwiatkowski *et al.* 1996). Several of these genes were good candidates based on predicted roles in signalling pathways, but no mutations were found in these genes in DNA from TSC patients (van Slegtenhorst *et al.* 1997). To find the TSC gene, predicted and confirmed exons from this region were screened for mutations using heteroduplex analysis. This was done on a set of 60 DNA samples from 20 unrelated TSC families that linked to 9q34 and 40 sporadic TSC cases. The 62<sup>nd</sup> exon screened showed shifts that indicated mutations in 10 of the 60 patient samples (Gomez *et al.* 1999). Sequencing of patient DNA from *TSC1* linked families confirmed truncating mutations in this exon, showing that it was likely to be part of the *TSC1* gene (van Slegtenhorst *et al.* 1997).

A final comparison between the genomic and cDNA clone sequences revealed the *TSC1* gene consisted of 23 exons, the last 21 of which are translated into a 130 kDa protein product, hamartin (van Slegtenhorst *et al.* 1997). *TSC1* has a 4.5kb 3' untranslated region (3'UTR), a 221bp 5' untranslated region (5'UTR) (exons 1-3) and 3492bp coding region (exons 3 through 23) (Gomez *et al.* 1999).



#### 1.1.4.2 TSC2

A genome-wide search revealed a TSC gene linking to a polymorphic marker near the autosomal dominant polycystic kidney disease type 1 (ADPKD1) locus on chromosome 16p13 (Kandt *et al.* 1992). At around the same time, a family with both TSC and autosomal dominant polycystic kidney disease (ADPKD) was found to segregate a translocation between chromosomes 16p and 22q. While the mother and daughter had a balanced translocation involving 16p13.3 and signs of PKD, the son inherited an unbalanced karyotype and displayed many of the skin and CNS symptoms of TSC in addition to renal cysts (European Chromosome 16 Tuberous Sclerosis Consortium 1994).

Identification of the *TSC2* locus was quick due to advanced mapping of 16p13.3. The distal short arm of chromosome 16 had already been of much interest due to the nearby  $\alpha$ -globin gene (Deisseroth *et al.* 1977; Simmers *et al.* 1987; Buckle *et al.* 1988) and the *PKD1* gene (Reeders *et al.* 1985). A cosmid contig of the 300kb candidate region was constructed and used to generate probes. These probes, along with pulse field gel electrophoresis (PFGE) and southern blotting were used to screen a cohort of 255 unrelated TSC patients. Deletions ranging from 30kb-100kb were observed in 5 of these patients and all mapped to the same 120kb segment, containing 4 genes (only one was disrupted in all 5 deletions). This candidate gene had 4 smaller intragenic deletions revealed under further analysis, confirming the discovery of the *TSC2* gene (European Chromosome 16 Tuberous Sclerosis Consortium 1993).

*TSC2* spans ~43kb of genomic DNA, with 41 exons and an 1807 amino acid transcript (Gomez *et al.* 1999). This is translated into a 198kDa protein product, named tuberin (European Chromosome 16 Tuberous Sclerosis Consortium 1993). Northern blotting has shown this 5.5kb transcript to be widely expressed. The gene lies proximal to the aforementioned *PKD1* gene. These are orientated 3' to 3' and the pair has polyadenylation signals separated by a mere 60bp.

### 1.1.5 Mutation analysis

Around two thirds of TSC cases are *de novo* (i.e. sporadic) (Sampson *et al.* 1989a). *TSC1* mutations are found in 10-15% of sporadic TSC cases, while *TSC2* mutations account for about 70% (Kwiatkowska *et al.* 1998, Jones *et al.* 1999, Niida *et al.* 1999), an outcome which is perhaps a result of the larger size of the *TSC2* gene (it is 1.5 times longer than *TSC1*) and the more complex genomic structure (it has twice the number of splice sites, affording an increased opportunity for various types of small mutations). However, a 4:1 ratio is higher than would be predicted from their relative genome extents and coding regions (Cheadle *et al.* 2000).

Around 700 disease causing mutations have so far been discovered in *TSC1* or *TSC2* (Au *et al.* 2007). *TSC1* mutations are mainly small deletions and insertions. The distribution of mutations in *TSC2* is quite different – many large deletions and rearrangements are detected, and missense mutations (a single base substitution leading to a single amino acid change) are far more common (Gomez *et al.* 1999) (Figure 1.1). While no 'hotspots' are apparent, 70% of *TSC1* mutations are found within exons 8, 9, 10, 15, 17 and 18. *TSC2* has a somewhat wider distribution, perhaps reflecting the larger number of exons (Au *et al.* 2007).

Six percent of *TSC2* mutations are missense and found within the GAP-domain-encoding exons 36-40 (Au *et al.* 2007). This would fit with the role of the GAP domain in regulating cellular growth through promoting the inactive GDP bound state of Rheb. A further 6% of *TSC2* mutations are contained within exon 16 on codon R611. This particular codon is known to play an important role in regulating mTOR function and a change here has been shown to lead to major conformational changes in tuberlin (Nellist *et al.* 2005).

### 1.1.6 Genotype – phenotype correlations

#### 1.1.6.1 A contiguous deletion syndrome involving *TSC2* and *PKD1*

Due to the large amount of phenotypic variability in TSC, researchers have tried to establish a link between phenotype and genotype. The most successful correlation established so far is in the event of a contiguous deletion affecting *TSC2* and the nearby *PKD1* gene, which results in a severe renal cystic phenotype (Sampson *et al.* 1997). From a cohort of 27 patients with TSC and renal cystic disease, 17 were

found to have a contiguous deletion syndrome with non-mosaic deletions of the coding regions of *TSC2* and *PKD1* and shared similar renal symptoms (Sampson *et al.* 1997). All *TSC2/PKD1* co-deletion patients had enlarged kidneys in childhood and radiographic features resembling advanced stage ADPKD.

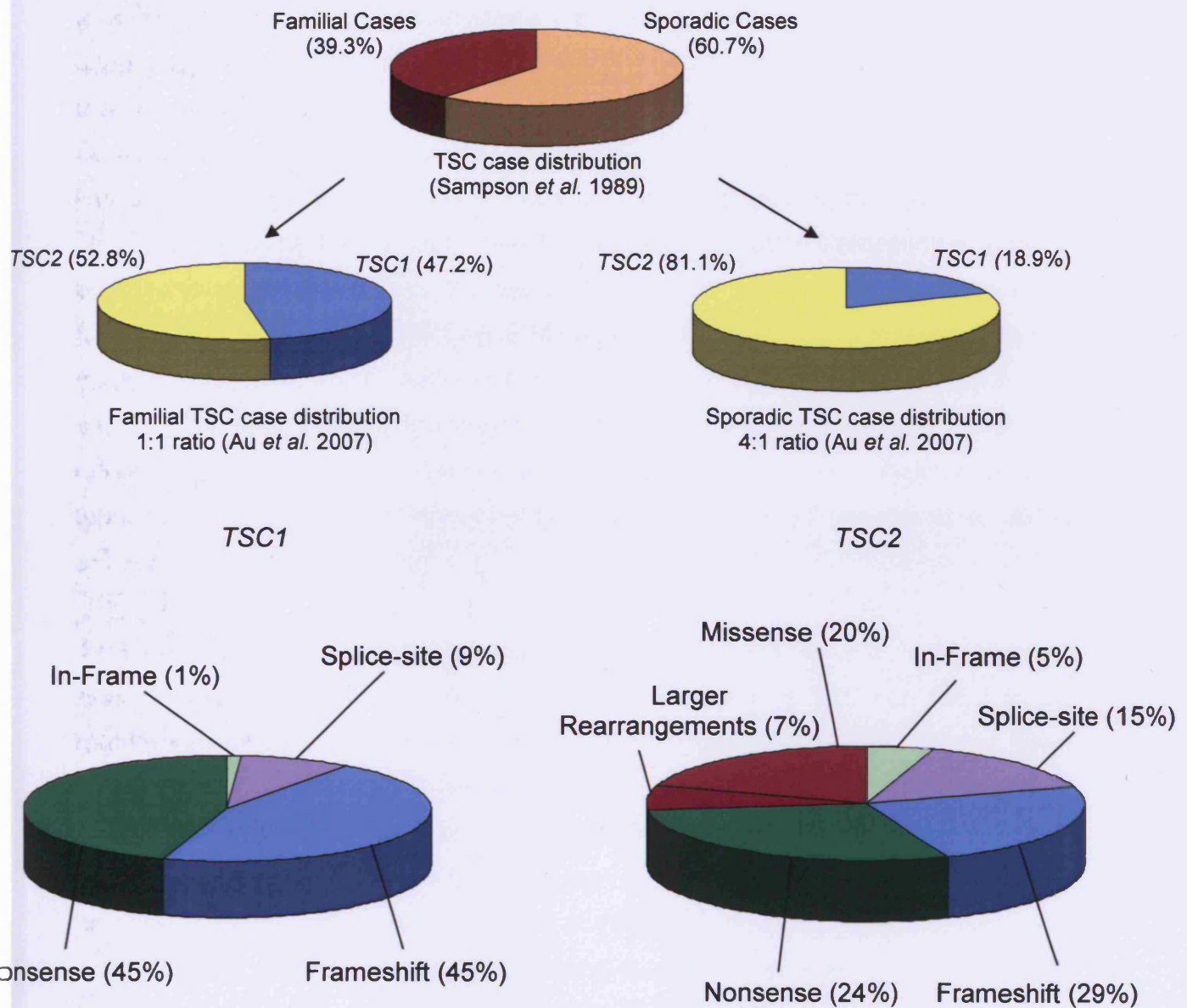
#### *1.1.6.2 Is a TSC2 disease more severe than a TSC1 disease?*

There is a clear over-representation of *TSC2* mutations in sporadic cases of TSC (a ratio of around 4:1 (Au *et al.* 2007)) when compared to familial cases (a ratio of around 1:1) (Au *et al.* 2007). This would imply that patients with sporadic *TSC1* mutations have a better chance of founding a family and are therefore less severely affected by TSC-associated symptoms than those with a *TSC2* mutation (Cheadle *et al.* 2000). In order to back such a hypothesis, large scale clinical evaluations of TSC patients are needed, and many studies have attempted to address this issue (Jones *et al.* 1999, Dabora *et al.* 2001, Sancak *et al.* 2005, Au *et al.* 2007). Sancak *et al.* (2005) noted a higher frequency of clinical features in males than females matched for age. Smalley *et al.* (1992) has also found males with TSC to be of increased risk of learning difficulties and autism compared to females. Dabora *et al.* (2001) studied 224 TSC sufferers of all ages, and showed sporadic *TSC1* mutations to be associated with a milder disease than *TSC2*, after matching for age. Studies by Au *et al.*, Dabora *et al.* and Sancak *et al.* all suggest patients with *TSC2* mutations have more severe symptoms than those with *TSC1* mutations.

#### *1.1.6.3 Intellectual disability in TSC1 and TSC2*

Intellectual disability may be more frequent among sporadic *TSC2* cases compared to *TSC1* (Jones *et al.* 1999), but others have failed to replicate this finding (Kwiatkowska *et al.* 1998, Young *et al.* 1998, van Slegtenhorst *et al.* 1999), and the issue remains a contentious one. If a difference does exist, this would go some way to explaining the difference between sporadic and familial *TSC2* cases, as a moderate to severe intellectual handicap would undoubtedly limit reproductive potential.

**Figure 1.1** Mutational spectrum of *TSC1* and *TSC2*



Types and frequencies of mutations found at the *TSC1* and *TSC2* loci (adapted from Sancak *et al.* 2005). Only data from patients with confirmed *TSC1* or *TSC2* mutations is included in the case distributions.

### 1.1.7 Knudson's two hit hypothesis

Biallelic inactivation of *TSC1* or *TSC2* is required for most of the clinical manifestations of TSC. This suggests the TSC genes are functioning as tumour suppressor genes (TSGs) (Knudson 1971). Knudson's theory states how an individual with a germline TSG mutation is more likely to acquire cancer because a single somatic event is needed to completely remove TSG function (Figure 1.2). Hence, we see lower numbers of tumours and later development of cancer in sporadic cases, as both alleles must be inactivated through independent somatic events (Knudson 1971). Loss of heterozygosity (LOH) at *TSC1* or *TSC2* has been found in up to 60% of renal AMLs (Henske *et al.* 1996). The first hit in these cells is a germline mutation which inactivates the wild-type copy of *TSC1* or *TSC2*. The second, somatic mutation inactivates the remaining wild type gene and may be detected by LOH analysis (Gomez *et al.* 1999). The complete abolition of TSC function removes any restrictive effect on cell proliferation (Tomasoni *et al.* 2011) and tumourigenesis can occur.

### 1.1.8 Loss of heterozygosity, haploinsufficiency and *TSC3*

According to Knudson's two hit hypothesis, TSGs such as *TSC1* or *TSC2* would require second hits before tumour progression (Figure 1.2). Indeed, this has been observed in TSC-associated lesions such as SEGAs, AMLs, RCCs and cardiac lesions (Green *et al.* 1994, Carbonara *et al.* 1994, Parry *et al.* 2001). However, some lesions (brain and early renal cysts) can occur without complete removal of hamartin or tuberlin. Using *Tsc1*<sup>+/-</sup> mice, Wilson *et al.* (2006) found somatic *Tsc1* mutations in ~80% of renal cystadenomas and RCCs but only 31.6% of renal cysts (P<0.0003), raising the possibility that haploinsufficiency for *Tsc1* can initiate cystogenesis. Furthermore, many cysts showed little or no staining for phosphorylated mTOR (53%) or phosphorylated S6 ribosomal protein (37%), while >90% of cystadenomas and RCCs displayed strong staining for these markers (P<0.0005). Examples outside TSC have been found where haploinsufficiency can lead to tumourigenesis (Santarosa *et al.* 2004). Haploinsufficiency occurs when a single functional allele remains after a mutagenic event, but a reduction in gene dosage is sufficient to jeopardise the tumour suppressor role played by the protein and creates tumourigenic conditions (Santarosa *et al.* 2004). Various types of TSGs have been shown to behave in this manner, such as cell cycle regulators like *p27<sup>Kip1</sup>* and *p53*;

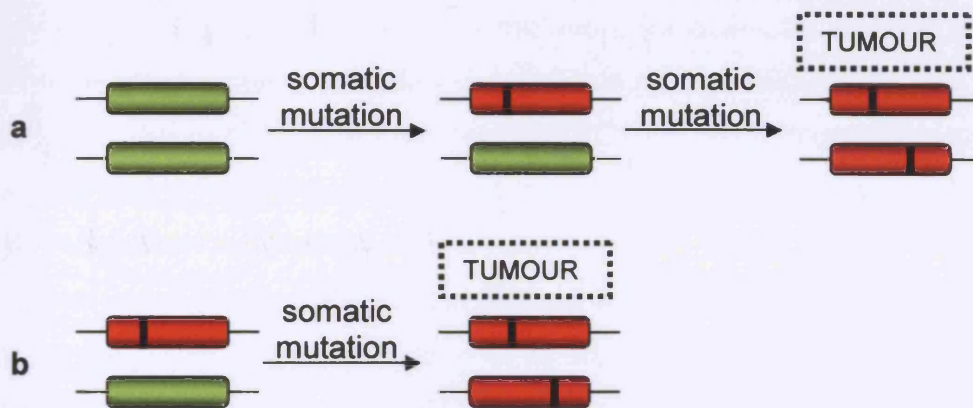
signalling molecules like *PTEN* and *LKB1*; and genome stabilisers such as *MSH2* and *MAD2*. Compound haploinsufficiency may also contribute to tumourigenesis, whereby haploinsufficiency in a gene will only manifest itself in a context of other genetic changes. Why some lesions in TSC may develop through haploinsufficiency while others require second hits is unknown. Tissue specific differences, perhaps together with compound haploinsufficiency brought on through differential gene expression may explain this.

Some groups have tentatively suggested a third TSC gene (*TSC3*), with a protein product associated with the TSC complex (Jóźwiak *et al.* 2008). Somatic mutation at this additional site may amount to a critical hit to the activity of the TSC complex and dysregulate downstream signalling, creating tumourigenic conditions. A *TSC3* locus would also account for the relatively poor mutation detection rates in TSC (Kwiatkowski 2005) although many groups stress the lack of material evidence for this additional gene.

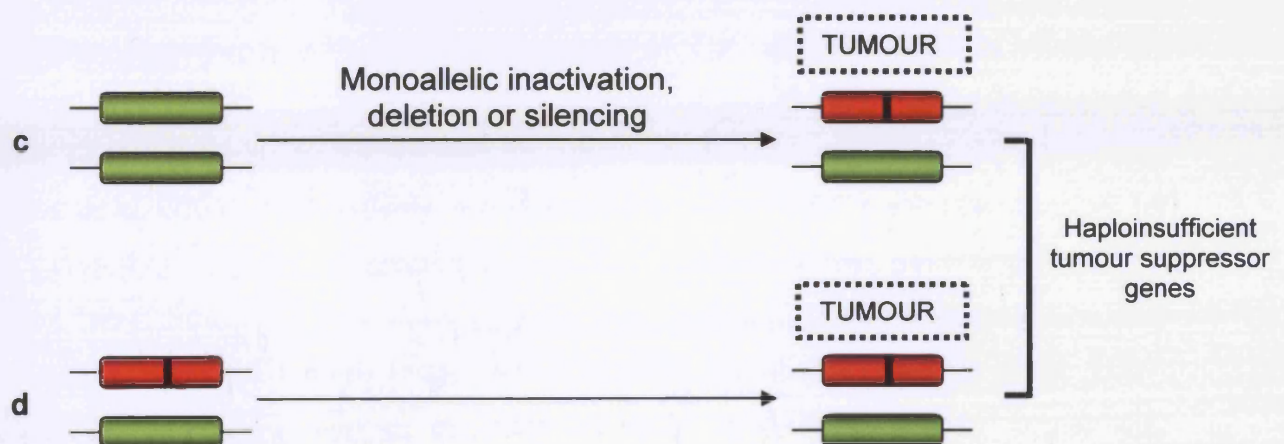
Some heterozygous TSC lesions may be developing through a combination of the loss of a single TSC allele and alternative pathogenic mechanisms (Henske *et al.* 1996, Niida *et al.* 2001). In TSC brain lesions, the presence of wild-type hamartin and tuberin is typical (Jóźwiak *et al.* 2008). Work on TSC brain lesions by Han *et al.* (2004) identified a mechanism of post-translational inactivation of tuberin to account for this discrepancy. Because abnormal activation of Akt and MAPK pathways is common in brain tumours, it has been proposed that a functional copy of *TSC2* remains in these cells, but the protein product will be inactivated through inappropriate phosphorylation (Han *et al.* 2004). It has previously been shown that Akt can phosphorylate tuberin and inhibit tuberin-hamartin function (Inoki *et al.* 2002), thereby deregulating mTOR activation without additional somatic mutations at the TSC loci. Whether a similar mechanism of TSC1/2 silencing occurs in other heterozygous lesions remains to be seen, but it is unlikely all mechanisms of disease progression in TSC can be accounted for by loss of mTOR control.



**Figure 1.2.** Loss of tumour suppressor gene function in cancer.



Classical Knudson two-hit model involves an initial mutational event in a tumour suppressor gene (TSG), which can either be an acquired somatic mutation (a) or a germline inherited mutation, present in every cell (b). This is the first hit. A second hit is then acquired through a separate mutational event to remove both copies of the TSG in specific cells (biallelic inactivation) and leads to clonal proliferation and hamartoma formation.



Haploinsufficient TSGs do not need to lose function in both alleles to confer increased risk to tumourigenesis. Loss a single gene copy may occur through a variety of means (c) and results in tumourous growth. A germline mutation in a TSG may lead to tumour development without another mutational event such as LOH (d).

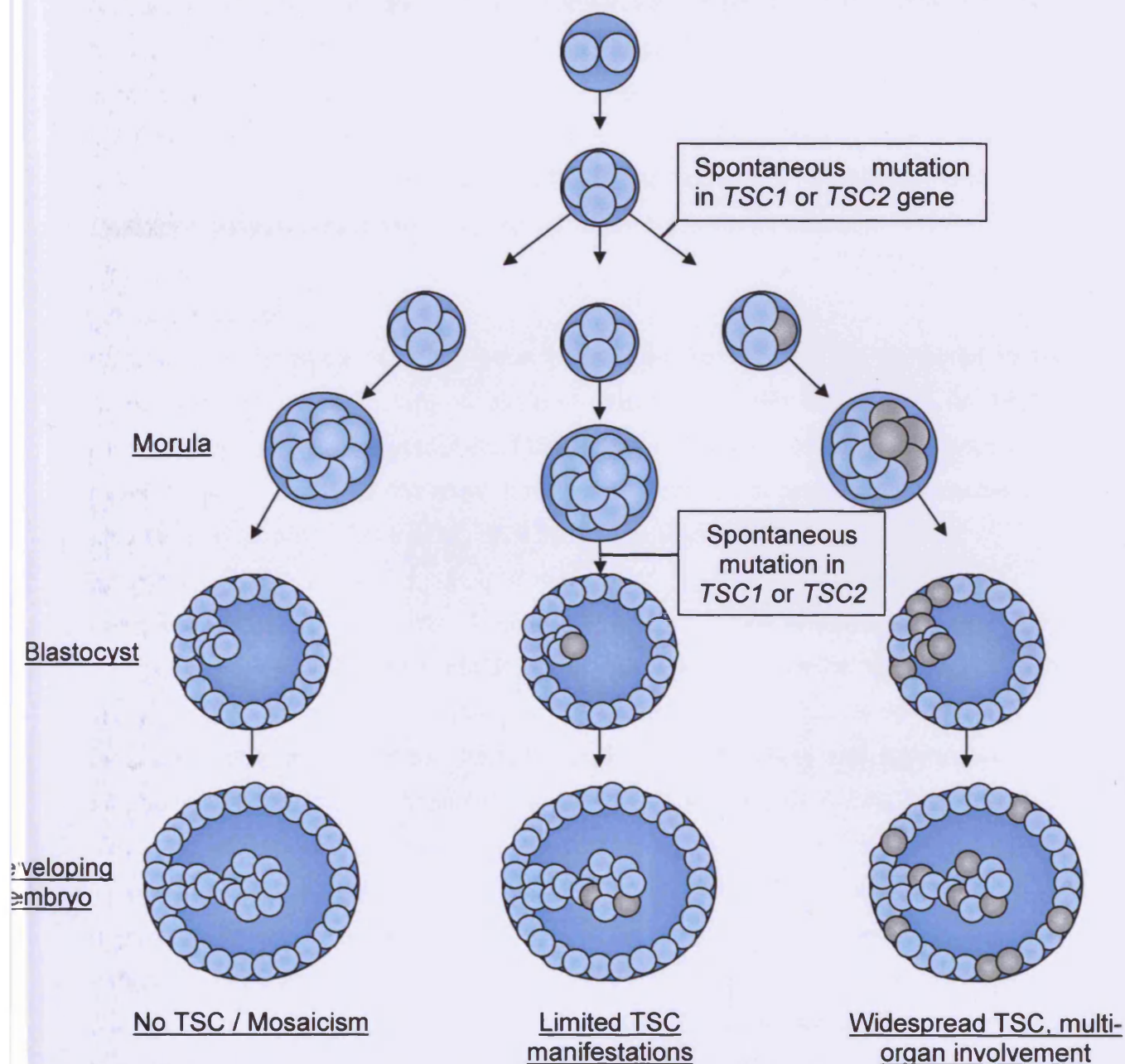
### 1.1.9 Mosaicism

Mosaicism occurs when a fraction of the cells making up an organism (rather than every cell) contain a particular DNA mutation, for example, when a mutation arises during development of a fertilised egg (Roberts *et al.* 2004). In TSC mosaicism, a fraction of the patient's cells contain a *TSC1* or *TSC2* mutation. Due to the high mutation rate in these genes (illustrated by the high levels of *de novo* mutations) TSC mosaicism is relatively likely (Gomez *et al.* 1999). The extent to which the mutation is present in cells of the patient will modify the clinical features of TSC (Figure 1.3). This will be a function of when the initial mutation occurred – if the *de novo* change arose late on in development in a small population of cells there may be little clinical manifestation (Gomez *et al.* 1999). Mild TSC clinical features have been seen in cases of 13% and 15% mosaicism (Jones *et al.* 2001). Both somatic and germline mosaicism for pathological mutations in *TSC1* and *TSC2* have been described in numerous patients (Cheadle *et al.* 2000).

Low level mosaicism may explain the poor detection rate of *TSC1* or *TSC2* mutations in patients with a clear diagnosis of TSC (around 85% in studies by Sancak *et al.* 2005, Jones *et al.* 1999, Dabora *et al.* 2001). Studies have shown some TSC mutations to be missed by direct sequence analysis of PCR products (Jones *et al.* 2001). Alternatively, the presence of a third TSC gene may account for this persistent subgroup of around 15% of TSC patients across several studies that do not have detectable mutations (Kwiatkowski 2005). This small subset invariably has milder symptoms than those with identified mutations (Dabora *et al.* 2001, Sancak *et al.* 2005). Qin *et al.* have recently used an ultradeep sequencing technique to screen a cohort of TSC patients without a confirmed mutation. They found 2/33 (6%) had *TSC2* mosaicism, and a further 5 had non-mosaic *TSC2* mutations missed the first time. The study concluded that mosaicism may not account for the majority of unidentifiable TSC mutations (Qin *et al.* 2010). However, evidence is stacked in favour of *TSC1/2* being the sole genes responsible for TSC (Kwiatkowski 2005) and it may be a failure to detect mosaicism at levels <2% in patients, or simply missing intronic mutations with splicing importance, that accounts for the majority of these unidentifiable mutations (Qin *et al.* 2010).



**Figure 1.3** Mosaicism in TSC



A sporadic mutation occurring in the *TSC1* or *TSC2* genes during the early stages of embryogenesis will result in an individual with both normal and altered cells. The distribution of these altered cells around the embryo will dictate which organs are formed from mutant and normal cell populations. The TSC-status of cell populations that comprise a mosaic individual's organs will decide the clinical manifestations of TSC. LOH is commonly seen in advanced TSC lesions, implying a classic Knudson 2-hit model of tumourigenesis, with cells derived from a mutant precursor more likely to acquire a second hit and hence form lesions. However, TSC-associated lesions in the brain, heart and early cysts in the kidneys often do not show LOH or loss of the remaining functional TSC gene (Wilson *et al.* 2006), implying tuberlin or hamartin haploinsufficiency is sufficient for TSC manifestation. In either case, a somatic mutation during early embryogenesis will lead to more compromised cells than a late event, with an increased risk of lesion formation and a wider range of organs affected.

### 1.1.10 Biochemistry of the TSC proteins

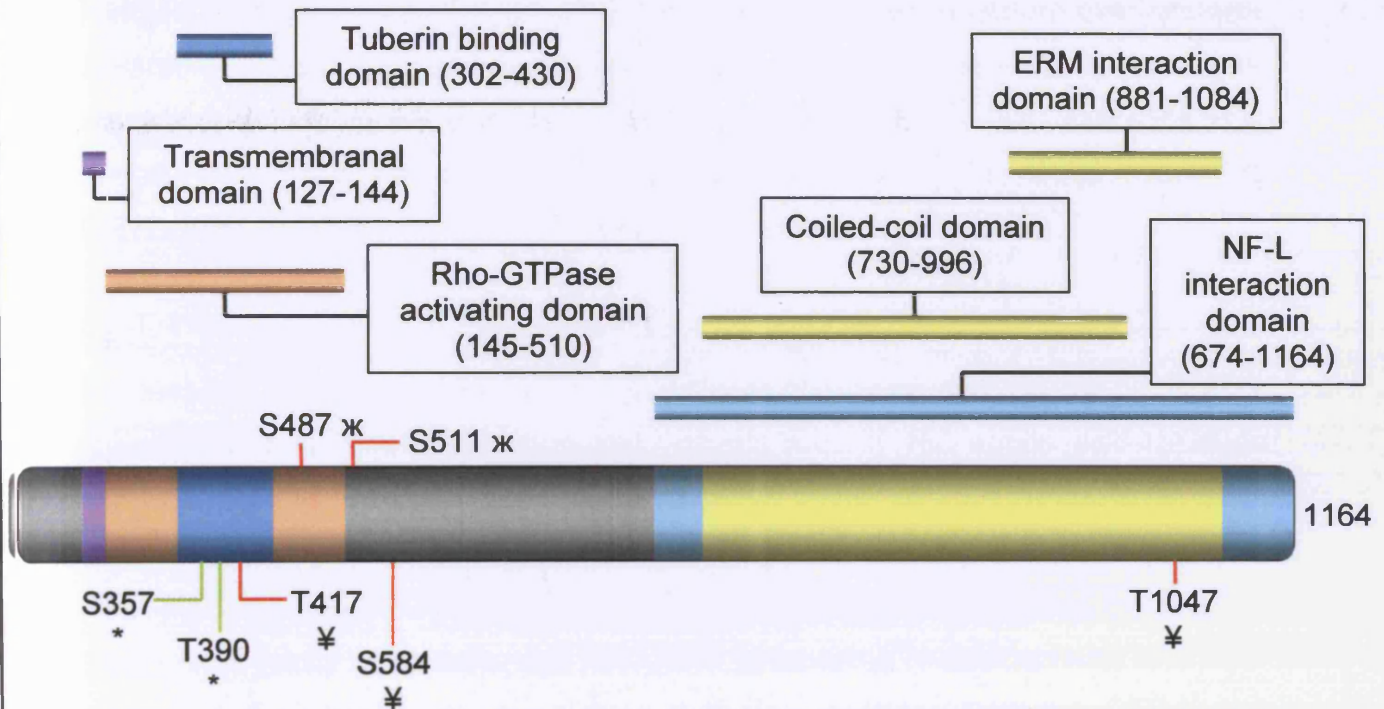
Hamartin and tuberin are evolutionarily conserved proteins that share little homology to one another or to other proteins (Huang *et al.* 2008). Much research has been conducted on the various domains of these proteins, with the rap1 GTPase-activating protein domain of *TSC2* being the best characterised to date. Early work has shown the two proteins to form a functional complex (van Slegtenhorst *et al.* 1998) of around 450kDa which is predominantly cytosolic (Nellist *et al.* 1999).

#### 1.1.10.1 Hamartin

Northern blot analysis of *TSC1* gene expression has shown the transcript to be widely expressed, particularly in skeletal muscle (van Slegtenhorst *et al.* 1997). Hamartin is a generally hydrophilic 1164 residue (130kDa) protein, with targets for several kinases and phosphatases. It has been localised to cytoplasmic vesicles and also the centrosome (Plank *et al.* 1998, Astrinidis *et al.* 2006).

Compared to tuberin, very little is known about the function of hamartin, but the fact that patients with *TSC1* and *TSC2* mutations have such similar symptoms would imply hamartin is essential to the function of tuberin (Astrinidis *et al.* 2005). A C-terminal binding domain allows hamartin to form heterodimers with tuberin and this interaction could direct subcellular localisation of tuberin, or it may have a more direct role, such as activating tuberin's functional domain (Astrinidis *et al.* 2005). Through the ezrin-radixin-moesin (ERM) family interacting domain, it is able to physically link with several actin-binding proteins, and a loss of hamartin can result in defects in cell-matrix adhesion (Lamb *et al.* 2000). Hamartin can form homodimers (Nellist *et al.* 1999) through a coiled-coil domain. This self-aggregation is inhibited through tuberin binding and may be an important level of control in mammalian target of Rapamycin (mTOR) signalling. A portion of the protein is able to interact with neurofilament-L (NF-L) (Haddad *et al.* 2002) which, along with the ERM-family interacting domain, may imply a role as a scaffolding protein in the localisation of tuberin (Astrinidis *et al.* 2005). Additional domains and functions are listed in Figure 1.4 and Table 1.4.

**Figure 1.4.** Hamartin, the *TSC1* protein product



Hamartin is an 1164 amino acid protein with a molecular mass of 130kDa. It has a number of phosphorylation sites to regulate activity – red lines indicate inhibitory phosphorylation sites, green lines show activating phosphorylation sites. A range of kinases act on hamartin and carry out these phosphorylation events: \* GSK3 $\beta$ , ¥ CDK1, ✕ IKK $\beta$ .

#### 1.1.10.2 Tuberin

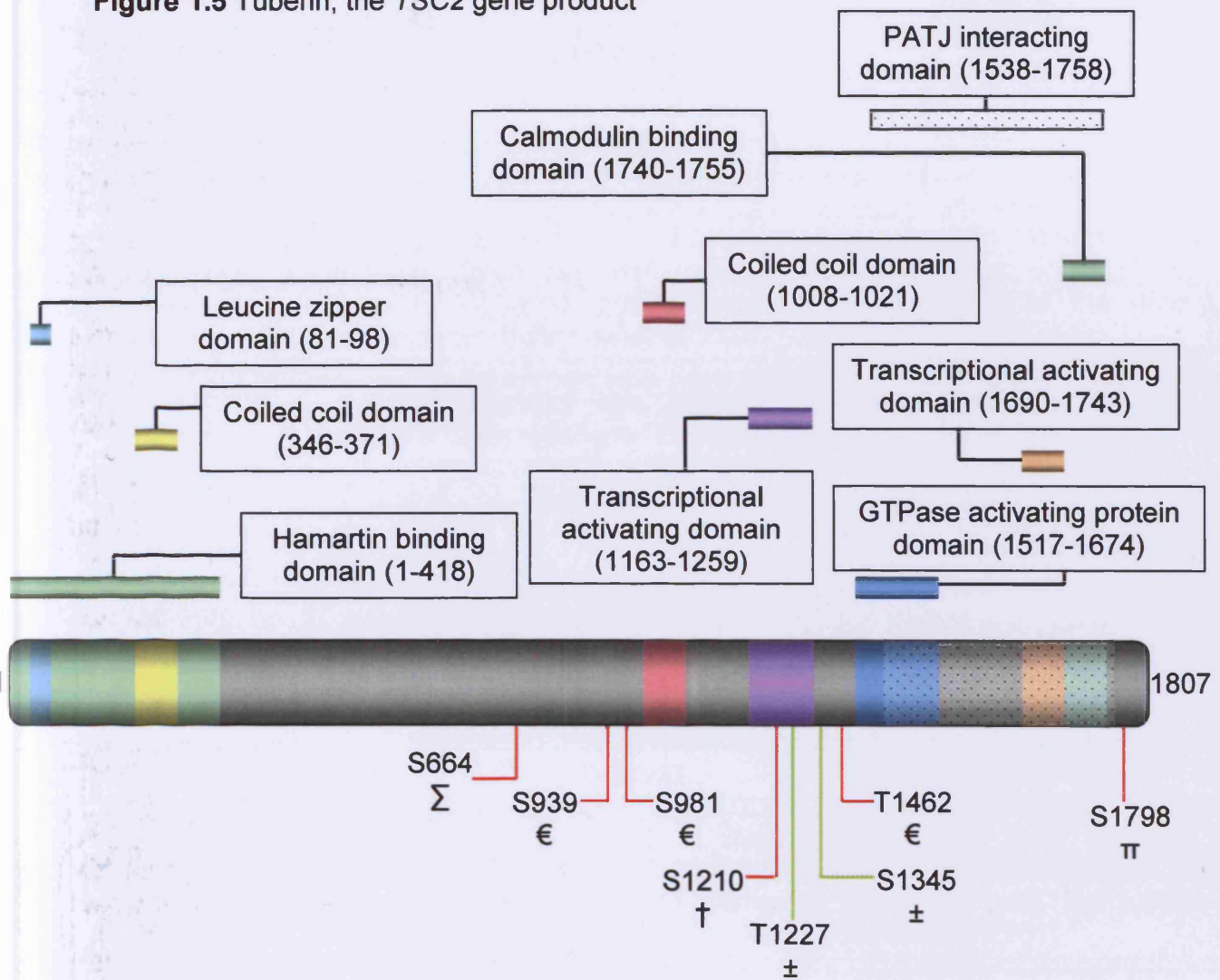
Tuberin is an 1807 residue (198kDa) protein. Northern blot data indicates expression in a wide variety of human and rodent tissues, especially the brain, heart, kidney, cerebellum and developing spinal cord (European Chromosome 16 Tuberous Sclerosis Consortium 1993, Geist *et al.* 1995). This expression pattern overlaps with hamartin (i.e. the brain, heart, lungs, liver, adrenal gland, gut, pancreas and prostate (Johnson *et al.* 2001)) but is not identical (Fukuda *et al.* 2000). Subcellular tuberin is present throughout the cytoplasm, but also localised to the Golgi apparatus (Wienecke *et al.* 1996). A subset of tuberin is nuclear (Lou *et al.* 2001).

##### 1.1.10.2.1 Tuberin functions as a GTPase activating protein

A C-terminal region of tuberin shares significant homology with the rap1 GTPase-activating protein (GAP). This homology covers around 160 amino acid residues (Maheshwar *et al.* 1997) encoded by exons 36-40 (Au *et al.* 2007). In general, GAP domains function to inhibit the signalling of Ras-related family of small G-proteins, which includes Rap1, Rab5 and Rheb (Ras homolog enriched in brain) (Inoki *et al.* 2003). This family of proteins can bind GDP (guanosine 5'-diphosphate) and GTP (guanosine 5'-triphosphate), and act as molecular switches, with the GTP-bound form being able to transduce signals. It was initially thought tuberin functioned as a GAP for rap1, but this was subsequently shown to not be the case (European Chromosome 16 Tuberous Sclerosis Consortium 1993). It is now known that tuberin's GAP domain (active only when in a heterodimer with hamartin (Rosner *et al.* 2008)) has a strong affinity for Rheb, a potent regulator of mTOR signalling (Tee *et al.* 2003). Rheb has an intrinsic GTPase domain that slowly converts GTP to GDP, but upon interaction with the tuberin/hamartin GAP domain, this process is rapidly increased, effectively switching off mTOR signalling by preventing Rheb-GTP induced formation of TORC1's active conformation (Tee *et al.* 2003, Avruch *et al.* 2006). Additional information on domains and functions are listed in Figure 1.5 and Table 1.4.



**Figure 1.5** Tuberin, the *TSC2* gene product



Tuberin is an 1807 amino acid protein with a molecular mass of 198kDa. It has a number of phosphorylation sites to regulate activity – red lines indicate inhibitory phosphorylation sites, green lines show activating phosphorylation sites. A range of kinases act on tuberlin and carry out these phosphorylation events:  $\Sigma$  ERK2,  $\epsilon$  AKT,  $\dagger$  MK2,  $\pm$  AMPK,  $\pi$  RSK1 (Rosner *et al.* 2008).

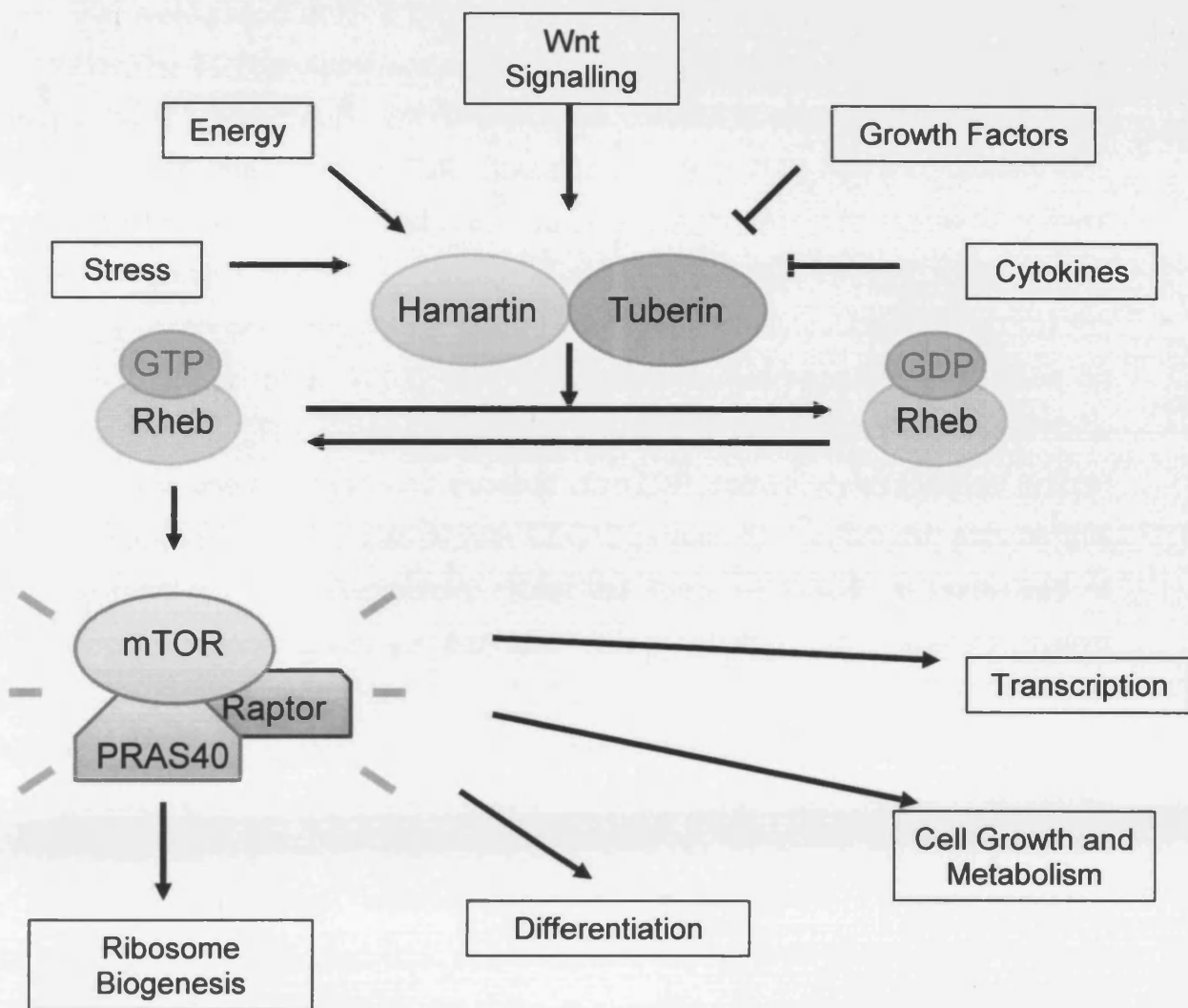
**Table 1.4** The domains of hamartin and tuberin

<b>Hamartin</b>	
<i>Protein Domain</i>	<i>Function</i>
Transmembrane (127-144)	Shown to localise hamartin to the membrane of cytoplasmic vesicles (Plank <i>et al.</i> 1998); points to a role in vesicular trafficking.
Rho GTPase activating domain (145-510)	Activates the small GTP-binding protein Rho (Lamb <i>et al.</i> 2000), thereby regulating cytokine-induced reorganisation of the actin cytoskeleton (Astrinidis <i>et al.</i> 2002)
Tuberin binding (302-430)	Heterodimerisation with hamartin to form a functional complex capable of repressing mTOR signalling (Hodges <i>et al.</i> 2001).
NF-L interaction domain (674-1164)	Capable of binding neurofilament-L and anchors neuronal intermediate filaments to the actin cytoskeleton (Haddad <i>et al.</i> 2002).
Coiled coil (730-996)	Allows homodimerisation and self aggregation with other hamartin molecules. Disrupted by tuberin interaction (Nellist <i>et al.</i> 1999).
ERM interaction domain (881-1084)	Region interacts with ERM proteins, a group of cytoskeletal anchors. Hamartin is required for cell-matrix adhesion (Lamb <i>et al.</i> 2000).
<b>Tuberin</b>	
<i>Protein Domain</i>	<i>Function</i>
Hamartin binding (1-418)	High affinity binding with hamartin, specifically with the tuberin binding domain at residues 302-430 (Hodges <i>et al.</i> 2001).
Leucine zipper (81-98)	Motif known to be involved in protein-protein interactions (European Chromosome 16 Tuberous Sclerosis Consortium 1993).
Coiled coil (346-371; 1008-1021)	Motifs outside the hamartin binding domain required for hamartin interaction (van Slegtenhorst <i>et al.</i> 1998; Hodges <i>et al.</i> 2001).
Transcriptional activation domains (1163-1259; 1690-1743)	The presence of two transcriptional activation domains, along with cellular localisation data, suggests a direct role for tuberin as a transcriptional regulator (Tsuchiya <i>et al.</i> 1996). The first domain (1163-1259) is the more potent of the two.
GTPase activating protein (1517-1674)	A key domain in the repression of mTOR signalling – able to activate the intrinsic GTPase properties of Rheb (European Chromosome 16 Tuberous Sclerosis Consortium 1993).
Calmodulin binding (1740-1755)	Interaction with the calcium-binding protein, calmodulin. A key regulator of cell signalling (Noonan <i>et al.</i> 2002).
PATJ interaction domain (1538-1758)	Creates a direct link between tuberin and the Crumbs (CRB) complex, and allows PATJ, a key polarity protein, to exert control over the mTOR signalling pathway (Massey-Harroche <i>et al.</i> 2007).

### 1.1.10.3 The tuberin-hamartin complex

Hamartin and tuberin physically interact to form a heterodimeric cytosolic complex (Nellist *et al.* 1999) that functions in a common signalling pathway as a key repressor of the mTOR complex (Orlova *et al.* 2010). This dimerisation is mediated through N-terminal specific binding motifs (Hodges *et al.* 2001). The interaction with tuberin has been previously shown to be important for the stability of hamartin and prevents self-oligomerisation (Nellist *et al.* 1999). In return, hamartin is able to prevent ubiquitination and subsequent degradation of tuberin (Benvenuto *et al.* 2000). Tuberin and hamartin also contain multiple phosphorylation sites for a range of kinases, the action of which has been shown to regulate the formation of the complex (Astrinidis *et al.* 2005). Through integration of these signals, and by funnelling them through a dichotomous event (activation or repression of Rheb and therefore mTOR), the TSC1-TSC2 complex acts as a molecular switchboard (Figure 1.6). It controls a bottleneck in the mTOR signalling pathway, where many signals converge, before the numerous targets of active mTOR lead to signal divergence and widespread downstream effects (Huang *et al.* 2008). The tuberin-hamartin complex functionality may reside within tuberin's GAP domain, but clearly the interaction with hamartin is well regulated and required for optimal function. The GAP activity of tuberin is boosted dramatically when in a complex with hamartin (Tee *et al.* 2003). Phosphorylation of hamartin by cyclin-dependent kinase-1 (CDK1) disrupts this interaction and markedly reduces tuberin GAP activity during the G<sub>2</sub>/M phase of the cell cycle (Astrinidis *et al.* 2003).

**Figure 1.6** The role of the hamartin / tuberlin complex in mTOR regulation



Hamartin and Tuberlin negatively regulate the activity of mTORC1 through modulation of Rheb GTP/GDP levels. When assembled as a complex, the GAP domain contained within tuberlin favours a GTP-to-GDP conversion of Rheb. Many signals converge on the TSC proteins, and exert control over the mTOR axis through altering the assembly or activity of the complex.



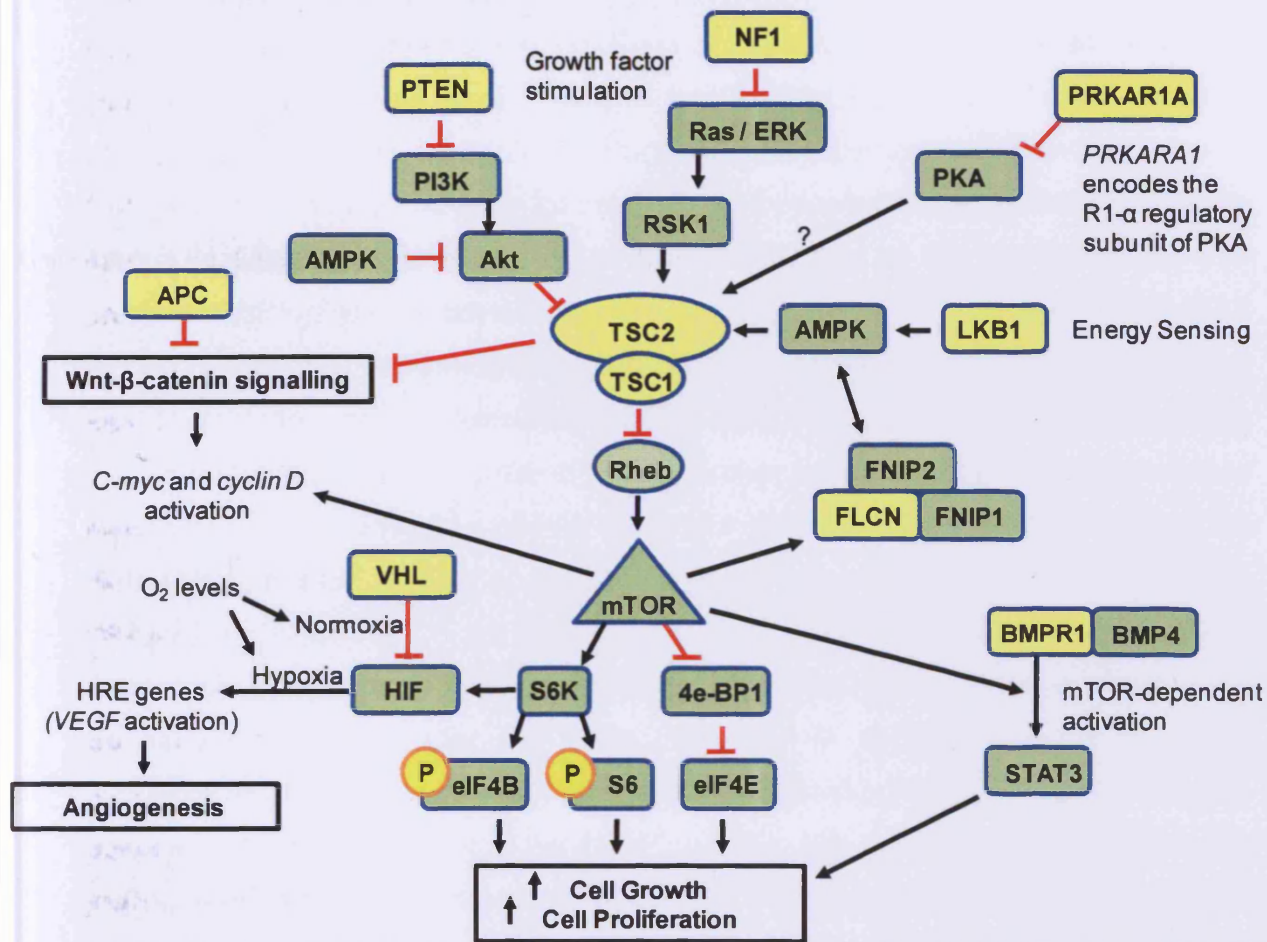
#### 1.1.10.4 The mTOR pathway

The *Tor* (target of Rapamycin) genes were originally described in yeast as a set of proteins that were responsive to the immunosuppressive drug Rapamycin (Heitman *et al.* 1991). The TOR proteins are serine/threonine kinases of the phosphoinositide 3-kinase-related kinase family, with orthologues present in all eukaryotes (Huang *et al.* 2008) including mammals (mTOR) (Inoki *et al.* 2005). TOR has a conserved role in control of cell growth, proliferation, survival and metabolism in response to nutrient and growth signals (Tee *et al.* 2005). This is carried out through regulation of translation, transcription, mRNA and protein stability, actin cytoskeleton organisation and autophagy (Inoki *et al.* 2005). mTOR functions in two separate complexes on two pathways – mTOR complex 1 (mTORC1) and mTOR complex 2 (mTORC2). mTORC1 is well characterised and consists of mTOR, regulatory associated protein of mTOR (Raptor) and LST8 (lethal with SEC13 protein 8). Rapamycin acts on this with high specificity. The Rapamycin-insensitive form, mTORC2, is composed of mTOR, Rapamycin-insensitive companion of mTOR (Rictor), SIN1 (stress activated protein kinase interacting protein 1) and LST8. Little is known about mTORC2, other than that it can regulate aspects of the actin cytoskeleton by acting upstream of Rho GTPases (Jacinto *et al.* 2004) and has Akt as a direct target (Sarbasov *et al.* 2004). mTORC1 has two classes of downstream targets- the ribosomal S6 kinases, S6K1 and S6K2, and eukaryotic initiation factor 4E (eIF4E)-binding protein (4e-BP1) (Huang *et al.* 2008). Activated S6K will phosphorylate a range of targets to promote mRNA translation and increased ribosome biogenesis (Astrinidis *et al.* 2005). Upon phosphorylation of 4e-BP1 by mTORC1, its release is triggered from eIF4E at the methyl-GTP cap of mRNAs, leading to cap-dependent translation (Gingras *et al.* 2001).

#### 1.1.10.5 mTOR syndromes

Mutation in the TSC proteins leads to mTOR dysregulation and widespread benign tumour growth. This is largely down to mTOR's central role in regulation of cell growth (Inoki *et al.* 2005). However, mutations in other genes have been linked to the mTOR pathway and Table 1.5 lists examples from the literature and Figure 1.7 illustrates the signalling networks involved.

**Figure 1.7** Hamartoma disease genes in mTOR signalling



The mTOR pathway has a central role in regulating cell growth and proliferation. Dysregulated mTOR activity is associated with several hamartoma syndromes. The TSC proteins are key regulators of mTOR through control of Rheb-GTP levels, and these are mutated in TSC. The *NF1* gene product is a GTPase activating protein for the Ras G protein (an activator of the mTOR pathway) and is mutated in Neurofibromatosis. *PTEN*, mutated in Cowden's Disease, Bannayan-Riley-Ruvalcaba Syndrome and Proteus Syndrome encodes a negative regulator of PI3K. *PTEN* deficiency leads to increased levels of activated Akt, an important regulator of TSC2. Familial Adenomatous Polyposis is caused by mutations in *APC*, a negative regulator of Wnt-β-catenin signalling. Loss of *APC* results in hyperactive β-catenin and upregulation of proto-oncogenes such as *c-myc* and *cyclin D*. mTOR has been shown to upregulate translation of these genes and TSC1/2 may interact with components of the APC complex. Juvenile Polyposis syndrome is caused by mutations in *BMPR1A* or *SMAD4*. The ligand for *BMPR1* (*BMP4*) activates *STAT3* in an mTOR-dependent manner. *SMAD 3*, a binding partner of *SMAD 4*, is able to physically interact with TSC2 and Akt (not shown on diagram). Birt-Hogg-Dube syndrome is caused by mutations in *FLCN*, and has similar clinical features to TSC, but has a higher risk of malignancy. Hartman *et al.* (2009) have suggested *FLCN* may regulate mTOR signalling. Von Hippel-Lindau syndrome is caused by mutations in *VHL*, which encodes a component of the E3 ubiquitin complex, involved in the degradation of HIF (a stimulator of angiogenesis) under normoxic levels of oxygen. **FLCN** – folliculin, **HIF** – hypoxia inducible factor, **PTEN** – phosphatase and tensin homologue, **LKB1** – liver kinase B1. Diagram constructed from Inoki *et al.* 2005, Han *et al.* 2009, Linehan *et al.* 2010, Hartman *et al.* 2009, Mak *et al.* 2003.

### 1.1.11 Treatments

Loss of *TSC1* or *TSC2* leads to dysregulated mTOR signalling, and so TSC treatment has primarily focused on Rapamycin (also called Sirolimus), a natural inhibitor of mTOR (Tee *et al.* 2003). It has antibiotic properties and anti-fungal, potent growth-inhibitory, anti-inflammatory and immunosuppressive functions. It was first used for this latter property following organ transplants. It is an analogue of the macrolide antibiotic FK506 (Abraham *et al.* 1996) and by binding to the receptor protein FKBP12, and subsequently mTOR, it is able to specifically inhibit TOR function (Inoki *et al.* 2005). Farnesyltransferase inhibitors and angiogenesis inhibitors are also under active consideration for TSC treatment (Kwiatkowski 2003). Angiogenesis inhibitors may be of clinical value as many of the TSC-associated lesions are characterised by aberrant vascular channels, likely to arise through the expression of VEGF by *Tsc1* or *Tsc2* null cells (Kwiatkowski 2003).

Rapamycin use in an Eker rat model of TSC demonstrated reductions of ribosomal S6 kinase activity, smaller cell sizes, induction of apoptosis and a promising decrease in renal tumour size (Kenerson *et al.* 2005). Although a clear effect is observed on the progression of these TSC lesions, little or no reduction was found in the number of microscopic precursor lesions. This suggests that mTOR activation may be necessary for lesion progression but other pathways drive tumourigenesis (Kenerson *et al.* 2005). A reduction in subcutaneous tumours was observed by Raukty *et al.* (2008) in a nude TSC mouse model following topical application of Rapamycin. This gives hope for the treatment of disfiguring skin lesions in TSC patients.

Human trials with Rapamycin have started to generate results. A small scale MRI study involving 5 patients that looked at the effects of Rapamycin on SEGAs found regression in all lesions (Franz *et al.* 2006). A larger study was conducted over 2 years by Bissler *et al.* (2008) with 12 months on and 12 months off Sirolimus. The study focused on AMLs from TSC patients and sporadic LAM cases, using MRI and CT scans to measure changes in tumour volumes, and pulmonary function tests to compliment the LAM findings. AMLs were found to regress under the 12 months of drug administration, but enlarged once treatment was stopped. Some of the LAM patients showed improved lung function after treatment (Bissler *et al.* 2008). Another

2 year trial by Davies *et al.* (2008) demonstrated reduction of AML volume in TSC patients treated with Sirolimus. On the basis of these promising results, randomised control trials have been initiated to test Rapamycin in a range of TSC or LAM-related clinical problems (Davies *et al.* 2010).

Several concerns have been raised with Rapamycin treatment in TSC. Long term use is undesirable because of the immunosuppressive nature of Rapamycin (Franz *et al.* 2006). Unfortunately, TSC is a long term condition, and a short Rapamycin course may not be clinically effective, with several studies showing tumour regrowth once treatment is stopped (Bissler *et al.* 2008, Franz *et al.* 2006). Side effects also include a dose dependant reduction in blood platelet count (Murgia *et al.* 1996), ulcers, diarrhoea and upper respiratory tract infections (Bissler *et al.* 2008). The discovery of the Akt feedback loop (Manning 2004) has raised further questions over the safety of Rapamycin treatment. Rapamycin-mediated mTOR inhibition induces negative feedback activation of Akt (Wan *et al.* 2007). Since Akt is one of the most frequently hyperactivated protein kinases in human cancer and associated with resistance to apoptosis and increased cell proliferation (Wan *et al.* 2007), doubts remain as to whether this is something desirable to stimulate in patients. However, clear advantages may remain from Rapamycin treatment, as it would also shut down aberrant activation of eIF4E and cap-dependant translation. Several studies have shown eIF4E to be a potent oncogene (Mamane *et al.* 2004), and possibly at the heart of tumourigenesis in mTOR overexpression syndromes (Manning 2004). In this case, Rapamycin would block the primary cellular process that drives tumour growth.

#### **1.1.12 TSC models**

The multi-systemic phenotype associated with TSC is a testament to the widespread importance of the TSC genes, and the high variability seen in the clinical manifestations demonstrate the intricate nature of signalling that surrounds the proteins. Rodent models have proved invaluable in studying human genetic disease for many reasons. They can provide an insight into mechanisms of disease, and allow the development of therapeutic targets which can be translated into human patients. Additional advantages include the ability to inbreed strains, the ease of handling and husbandry.

#### 1.1.12.1 Eker rat

The first genetic model of TSC was described in the 1950s (Eker 1954, Eker *et al.* 1961) and arose spontaneously through germline inactivation of a *TSC2* allele. It served as a model of RCC (Pan *et al.* 2004, Kobayashi *et al.* 1997) before sophisticated methods existed to recapitulate carcinogenic phenotypes with precise gene targeting. A homozygous Eker mutation is embryonically lethal at E10-12 days, indicating the importance of *TSC2* in development (Everitt *et al.* 1995). Heterozygous rats are born healthy but go on to develop kidney lesions such as cysts, branching cysts and cyst adenomas within 12 months (Eker *et al.* 1981). These lesions develop from altered renal tubules, which start to appear after around 2 months (Hino *et al.* 2002). The RCCs seen are part of a wider cancer syndrome consisting of haemangiomas of the spleen, reproductive tract leiomyomata and vascular neoplasms (Everitt *et al.* 1992). The mutation has been mapped to 10q12, and consists of a 6.3kb retrotransposon insertion into an intronic sequence of *Tsc2* (Hino *et al.* 2002) which leads to aberrant RNA expression from this gene and no stable tuberin being produced from the mutant allele (Kobayashi *et al.* 1995). The nearby *Pkd1* gene, located in a tail-to-tail orientation as in humans, is unaffected in this model (Hino *et al.* 2002).

The stages of renal carcinogenesis can be observed in the Eker rat. Initially, abnormal renal tubules will appear after 2 months and are characterised by partial replacement of the tubular epithelium with cells that are enlarged and have abnormal nuclei. These tubules develop into foci of overproliferative cells, then onto adenomas (Hino *et al.* 2002). With time, these lesions may progress to carcinomas, with a small minority becoming malignant and metastasize to the lungs, pancreas and liver (Eker *et al.* 1981).

Kobayashi *et al.* (1997) detected LOH in many neoplastic lesions from the rat model, including very early and preneoplastic renal tubules. This led them to suggest that a somatic mutation in the wild-type allele of *Tsc2* was a rate-limiting step for renal carcinogenesis in the Eker rat. In spontaneous renal carcinomas from the Eker rat, around 60% show LOH (Kubo *et al.* 1994), demonstrating consistent loss of the wild-type *Tsc2* allele.

#### 1.1.12.2 *Tsc1* knockout mouse

Several different knockout alleles in *Tsc1* have been developed, with the most recent model (Wilson *et al.* 2005) exhibiting a more severe phenotype than the two existing mouse lines (Kobayashi *et al.* 2001; Kwiatkowski *et al.* 2002).

Wilson *et al.* (2005) engineered a functionless allele of *Tsc1* by replacing part of exon 6 and all of exons 7 and 8 with a  $\beta$ -Galactosidase reporter/neomycin selection cassette. *Tsc1*<sup>-/-</sup> mice from this strain were found to be unviable past E13, as was the case with the other *Tsc1* mouse models (Kobayashi *et al.* 2001, Kwiatkowski *et al.* 2002). Examination of *Tsc1*<sup>-/-</sup> embryos revealed them to be developmentally retarded and prone to neural tube closure defects.

Strain background may have profound effects on the number and severity of renal lesions in *Tsc1*<sup>+/-</sup> mice (Wilson *et al.* 2005). When matching for age at 3-6 months, it was found that significantly more *Tsc1*<sup>+/-</sup> mice on a C3H background experienced some form of renal lesion (44%) compared to those from Balb/c (13%) or C57BL/6 (8%) strains. Interestingly, a high incidence of renal cell carcinoma (80%) in *Tsc1*<sup>+/-</sup> Balb/c mice was detected at 15-18 months, far higher than the other backgrounds. However, regardless of background, all *Tsc1*<sup>+/-</sup> mice were found to have microscopic renal lesions by 15-18 months (Wilson *et al.* 2005). Lesions found at this age range included cysts, cysts with papillae projections, branching cysts with branching papillae projections and solid carcinomas. These were noted to undergo a clear progression from small cysts to renal cell carcinomas. LOH at the wild-type *Tsc1* locus was found in 5 of 12 renal lesions (Wilson *et al.* 2005), while Kobayashi *et al.* (2001) reported LOH in 2 of 6 lesions, implying a second hit in *Tsc1* may lead to renal tumour initiation / progression.

#### 1.1.12.3 *Tsc2* knockout mouse

In 1999, two separate *Tsc2*<sup>+/-</sup> mouse lines were reported and found to display identical phenotypes (Onda *et al.* 1999, Kobayashi *et al.* 1999). Both removed germline *Tsc2* function through targeting exon 2. A third null *Tsc2* allele has since been developed through deletion of exons 2-4, and phenotypically, the resultant mice appear to be similar (Hernandez *et al.* 2007).



As in *Tsc1*<sup>-/-</sup> mice, *Tsc2*<sup>-/-</sup> mutant embryos die *in utero* between E9.5 and E12.5. Many demonstrate open neural tubes and are significantly less developed than *Tsc2*<sup>+/-</sup> littermates (Onda *et al.* 1999, Kobayashi *et al.* 1999). The primary cause of foetal death appeared to be liver hypoplasia, although cardiac hypertrophy was also seen.

Renal lesions in *Tsc2*<sup>+/-</sup> mice develop by 6-12 months (100% penetrance by 15 months) and progress as the mouse ages (Onda *et al.* 1999, Kobayashi *et al.* 1999). As in *Tsc1*<sup>+/-</sup> kidneys, examination of these lesions revealed a mix of pure cysts, cysts with papillae projections and solid adenomas. These cysts arise from the cortical region of the kidney and have similar expression profiles to collecting duct interstitial cells (Onda *et al.* 1999). Liver haemangiomas were noted in 50% of *Tsc2*<sup>+/-</sup> mice at 18 months, characterised by smooth muscle cell proliferation and large vascular spaces (Kwiatkowski *et al.* 2010). This liver phenotype appears to be strain specific, with the incidence much higher in *Tsc2*<sup>+/-</sup> 129 / SvJae mice (Kwiatkowski *et al.* 2010). LOH of *Tsc2* was noted in 9 of 37 renal cystadenomas and carcinomas, and 7 out of 14 liver haemangiomas (Onda *et al.* 1999). As with *Tsc1*, these results imply loss of remaining wild-type *Tsc2* can lead to tumour development in several organs.

## **1.2 Autosomal dominant polycystic kidney disease**

Autosomal dominant polycystic kidney disease (ADPKD) (MIM 173900) is the commonest form of inherited renal cystic disease (Torres *et al.* 2007). It is estimated to occur in around 1 in 1000 live births (Dalgaard *et al.* 1957). Primarily, it is a disease of the kidneys, but extra-renal manifestations include cysts in other organs such as the liver, seminal vesicles and pancreas.

### **1.2.1 History and epidemiology of ADPKD**

Prior to a study by Dalgaard confirming the autosomal dominant nature of inheritance (1957), ADPKD was known as adult polycystic kidney disease. Drawing from a Danish population, the incidence of ADPKD was placed by Dalgaard at 1 in 1000. A more recent study in Olmsted County, MN, USA confirmed this level of incidence (Iglesias *et al.* 1983). Thousands of people every year succumb to end stage renal disease (ESRD) as a result of ADPKD (Torres *et al.* 2007).

### 1.2.2 Clinical manifestations of ADPKD

It is possible to subdivide ADPKD into two types, depending on the mutated gene (*PKD1* or *PKD2*). In ADPKD type 1 (*PKD1*) disease progression may be more rapid but in most other ways, ADPKD type 1 and 2 share identical features (Sutters *et al.* 2003).

#### 1.2.2.1. Renal manifestations

The development and enlargement of renal cysts eventually gives rise to many of the morbidities of ADPKD (Torres *et al.* 2007). Main complications include renal failure, back pain, cyst haemorrhage and infection (Zhou *et al.* 2008). The occurrence of these cysts is age dependent and occurs in all ADPKD patients. Renal function deteriorates as cysts compress and destroy normal renal parenchyma (Sutters *et al.* 2003). Sex is known to play a role in disease progression, as men have higher rates of cystic expansion than women (Harris *et al.* 2006). Interestingly, an MRI study by Grantham *et al.* (2006) found that while *PKD1* kidneys had more cysts and were larger than those in *PKD2*, there was no difference in the rates of cystic growth over time. This suggests the disease gene may modulate cyst initiation but not progression.

Renal cyst numbers do not tend to exceed one or two in people under the age of 30, but by the age of 50, these same patients may have a cystic load of hundreds. As a result, ADPKD kidneys can reach 40cm in length (compared to 10-12cm in unaffected individuals) and be around 10 times heavier (8kg compared to 500g in unaffected individuals) (Gabow *et al.* 1993). Kidney cysts are derived from the epithelial cells lining renal tubules, and can develop in all areas of the nephron and collecting ducts (Torres *et al.* 2006). 80% of 70 year old patients with ADPKD will develop ESRD (compared to under 5% in sufferers under 40 years old) (Zhou *et al.* 2008).

#### 1.2.2.2. Hepatic manifestations

Aside from renal manifestations, ADPKD only ranks behind haemochromatosis in terms of inherited disorders involving the liver (D'Agata *et al.* 1994). As in the kidney, the number and prevalence of hepatic cysts will increase with time, and by the age of 60, 80% of ADPKD sufferers will have hepatic cysts (Gabow *et al.* 1990). Men and



women with ADPKD have similar chances of developing hepatic cysts, but women can expect greater numbers of lesions and larger sizes (Gabow *et al.* 1990, Everson *et al.* 1993, Everson *et al.* 1990). Consistent with this hormonal component, severe hepatic disease correlates both with puberty (Gabow *et al.* 1990), pregnancy and use of female steroid hormones (Qian *et al.* 2003).

Patients that develop small hepatic cysts (<2cm) will tend to remain asymptomatic, while larger cysts will commonly present with abdominal pain, early postprandial fullness or shortness of breath. Cysts have a risk of haemorrhage, infection or post-traumatic rupture (Telenti *et al.* 1990). Large scale cystic expansion can also lead to symptoms consistent with advanced liver disease, such as portal hypertension and variceal haemorrhage (Everson *et al.* 2004).

The hepatic cysts in ADPKD arise from intrahepatic cholangiocytes derived from bile ducts that have become dilated (Masyuk *et al.* 2006). Hepatic cyst epithelium is known to retain a biliary phenotype, and remains able to secrete fluid into a developing cyst lumen (Masyuk *et al.* 2006). Oestrogen receptors are also present in the epithelium lining (Alvaro *et al.* 2006), rendering the cysts sensitive to oestrogen-mediated cell proliferation.

#### 1.2.2.3. Other manifestations

The main pathology in ADPKD of progressive bilateral renal cystogenesis leads to several other morbidities. Hypertension (blood pressure over 140/90 mm Hg) is a concern in ADPKD, and is present in 50% of patients aged 20-34 years. As these patients age and develop ESRD, hypertension incidence rises to almost 100% (Kelleher *et al.* 2004). Stretching and compression of vasculature due to cyst expansion is thought to cause ischemia and lead to subsequent activation of the renin-angiotensin system, raising blood pressure (Gabow *et al.* 1990).

Pain is common in adults with ADPKD (60%) (Bajwa *et al.* 2004). Events such as cyst haemorrhage and infection are known sources of pain in ADPKD (Torres *et al.* 2007). Kidney stones occur at an increased frequency (around 20%) and these are very painful to excrete (Torres *et al.* 1993).

### 1.2.3 Diagnosis of ADPKD

With a positive family history for ADPKD, diagnosis will be based around imaging testing (Torres *et al.* 2007). Due to low cost and high safety (compared to MRI or CT), renal ultrasonography is commonly used for detecting ADPKD (Pei *et al.* 2010). An age graded ultrasound criteria for ADPKD has been established (Ravine *et al.* 1994), but in younger patients, small cysts may escape sonographic detection (especially for patients with milder *PKD2*).

Where imaging results are contentious, genetic testing (linkage analysis or direct mutation screening) for ADPKD can be used (Pei *et al.* 2010). However, the large size and complexity of *PKD1* makes molecular testing by direct DNA analysis a challenge (Torres *et al.* 2007). Linkage analysis is an option in less than 50% of cases, because it requires the consent of a reasonably sized family. Furthermore, family participants must all have a definite clinical diagnosis. It also cannot be used if the proband has a *de novo* mutation (Pei *et al.* 2010). In contrast, direct mutation analysis involves sequencing the entire coding regions of both *PKD1* and *PKD2*. While more expensive, this method does have the advantage of only requiring one blood sample. Definite disease causing mutations are only found in 40-60% of cases, with likely disease causing mutations making an additional 26-37% (Rossetti *et al.* 2007, Garcia-Gonzalez *et al.* 2007).

### 1.2.4. Treatment options for ADPKD

Treatment of ADPKD centres on reducing morbidity and mortality due to complications of the disease (Torres *et al.* 2007). Hypertension is treated with ACE inhibitors or angiotensin receptor blockers. These have a low side-effect profile, reduce blood pressure and have been shown to increase renal blood flow (Chapman *et al.* 1990, Torres *et al.* 1991, Watson *et al.* 1992).

Pain arising due to ADPKD will need further investigation before treatment, as a number of non-ADPKD related causes could be responsible (infections, tumours and stones) (Torres *et al.* 2007). Acute episodes of pain can be dealt with by narcotic analgesics, but these are not recommended for long term use. Lifestyle modification to avoid unnecessary strain may help too. If pain management fails, cyst surgery is an option (Torres *et al.* 2007, Elzinga *et al.* 1992).

Cyst haemorrhages can often be managed by bed rest, analgesics and hydration (Torres *et al.* 2007). Occasionally the resulting drop in haematocrit following rupture will require hospitalisation, transfusion and arterial embolisation. Cysts that become infected are hard to treat (Elzinga *et al.* 1996) because of poor antibiotic penetration to the lesion, but lipophilic agents can help.

ADPKD patients on dialysis for ESRD often do well due to relatively high concentrations of erythropoietin and haemoglobin (Abbott *et al.* 2002). However, transplantation is the treatment of choice for ESRD in ADPKD. This can be limited to the kidneys, or in tandem with a new liver.

No curative or preventative therapy exists for the polycystic liver disease experienced by ADPKD patients (Masyuk *et al.* 2006). Symptomatic relief is limited to surgical intervention, and includes aspiration of cyst fluid, cyst fenestration, liver resection and organ transplant (Everson *et al.* 2004, Shneider *et al.* 2005).

#### 1.2.4.1. Rapamycin in ADPKD treatment

The mTOR pathway is regulated by polycystin-1 (Shillingford *et al.* 2006) and mTOR has been shown to be aberrantly activated in ADPKD (Shillingford *et al.* 2010). Studies using mTOR inhibitors in animal models of PKD have shown promising results, with inhibition of renal cyst growth, regression of kidney size and preservation of renal function (Shillingford *et al.* 2006, Tao *et al.* 2005, Wahl *et al.* 2006). Clinical trials are underway to test the response of ADPKD-associated cysts to mTOR inhibitors in humans (Walz *et al.* 2006, Serra *et al.* 2007). Data from a clinical trial of Sirolimus has been shown to reduce polycystic liver volume in ADPKD patients (Qian *et al.* 2008), implying that mTOR inhibition may hold therapeutic options in the future.

#### 1.2.5 Identification of the ADPKD genes

ADPKD is caused by mutations in at least two genes: *PKD1* and *PKD2*. The first locus to be localised (Reeders *et al.* 1985) was *PKD1* to the short arm of chromosome 16, but families soon emerged that had no linkage to markers on chromosome 16p (Kimberling *et al.* 1988, Romeo *et al.* 1988). A second ADPKD

locus (*PKD2*) was subsequently found on chromosome 4q13-q23 (Peters *et al.* 1993, Kimberling *et al.* 1993).

#### 1.2.5.1 The *PKD1* gene

*PKD1* (chromosomal region 16p13.3) is roughly 53kb in length and split into 46 exons. Exon 15 is the largest of these and exons 1 and 2 are separated by a large intron of 15kb. The mRNA transcript is 14.5kb (The International Polycystic Kidney Disease Consortium 1995). The translational product of *PKD1* is polycystin-1 (PC1).

#### 1.2.5.2 The *PKD2* gene

*PKD2* (chromosomal region 4q13-q23) is considerable smaller than *PKD1*, being approximately 68kb in length and split into 15 exons. The mRNA transcript is 5.4kb long, which encodes a 968 amino acid product, polycystin-2 (PC2) (Mochizuki *et al.* 1996).

#### 1.2.5.3 A third PKD locus?

Several families with a clinical diagnosis of ADPKD have been discovered with no linkage to *PKD1* or *PKD2* (Daoust *et al.* 1995, de Almeida *et al.* 1995, Turco *et al.* 1996, Ariza *et al.* 1997). Although tempting to attribute such a finding to a third, unidentified ADPKD locus, other factors may explain the lack of linkage. Human error is possible – genotyping errors, sample mix ups and misdiagnosis (phenocopies and non-penetrance) (Paterson *et al.* 1998, Paterson *et al.* 1999).

### 1.2.6 Mutation analysis of ADPKD

ADPKD is genetically heterogeneous, with mutations in *PKD1* and *PKD2* making up ~85% and ~15% respectively of the pedigrees identified (European Polycystic Kidney Disease Consortium 1994, Mochizuki *et al.* 1996). A handful of rare, unlinked families have been discussed previously. The *de novo* mutation rate for *PKD1* has been estimated at  $1.8 \times 10^{-5}$  per generation (Rossetti *et al.* 2001), although other studies have placed it as high as  $6.9 \times 10^{-5}$  (Dobin *et al.* 1993). Rossetti *et al.* (2001) found no mutation hotspots, with variants spread throughout exons 1 to 46. Most of the changes were protein truncations through nonsense mutations (32%), insertions or deletions (29.6%) or splicing changes (6.2%). Large deletions are rare but result in deletion of the adjacent *TSC2* gene and severe infantile cystic kidney disease

(Brook-Carter *et al.* 1994, Laas *et al.* 2004). *PKD2* has a similar heterogeneity in mutation clusters (Rossetti *et al.* 2007), but a lower mutation rate (Rossetti *et al.* 2001). This may be because a large number of different mutations seem able to cause *PKD1*, and *PKD1* itself is a large mutational target (12,906bp coding region). Also, *PKD1* is unusually CpG rich, meaning it contains more highly mutable sequences (Rossetti *et al.* 2001). Clinical bias may exist, as *PKD1* disease is more severe than *PKD2*, it is more likely to come to clinical attention. *PKD2* is often subjected to truncating mutations (as in *PKD1*), with up to 91.5% of mutations causing a truncated protein product (Rossetti *et al.* 2007) (Figure 1.8).

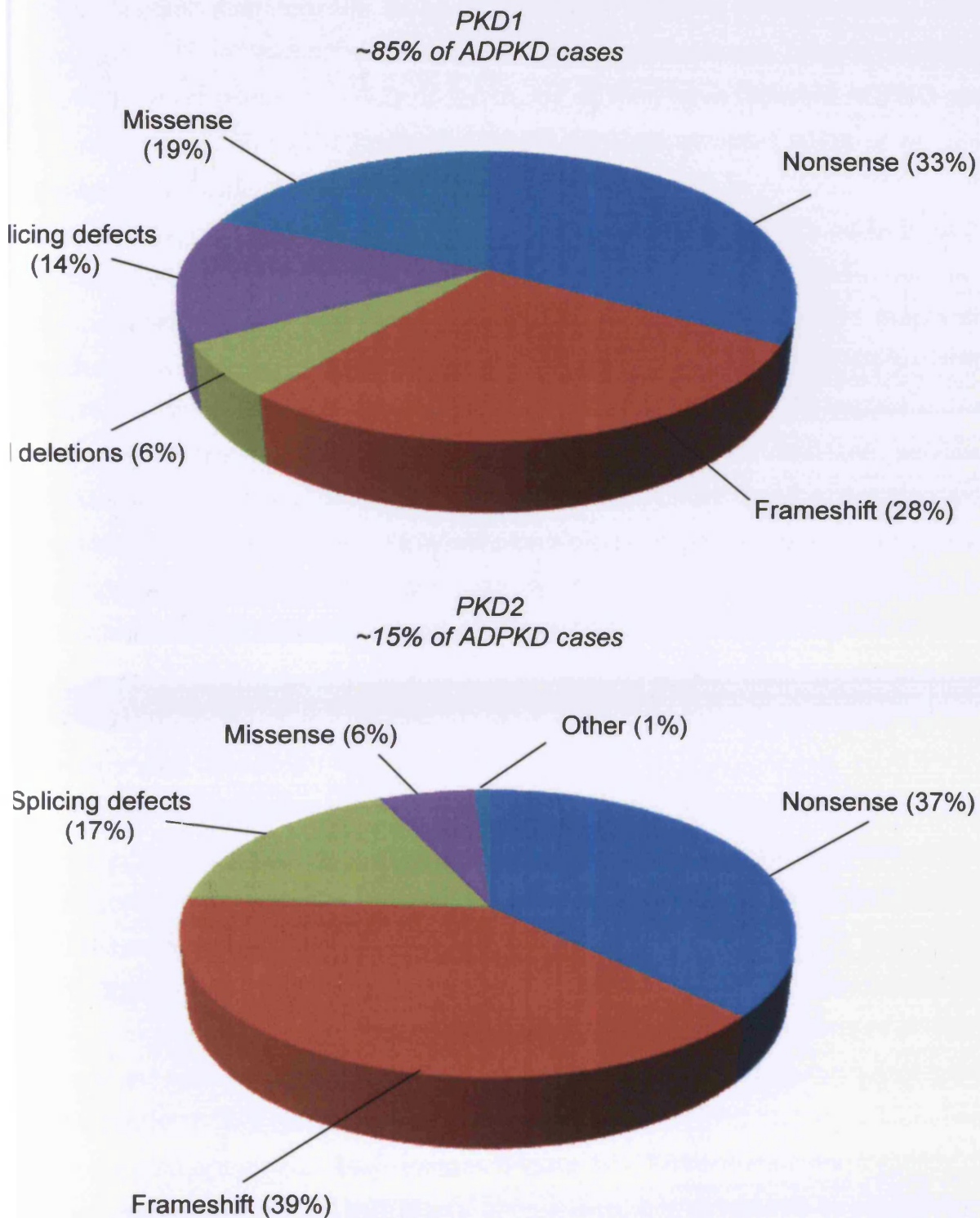
### **1.2.7 Genotype / phenotype correlations**

The phenotypes arising from ADPKD are highly variable in penetrance, both in terms of the severity of renal disease and the characteristics of any associated extra-renal lesions (Rossetti *et al.* 2007). However, *PKD1* mutations will generally result in a more severe disease than *PKD2*. This includes a younger age of clinical presentation and accelerated kidney failure, with ESRD occurring around 20 years earlier (54.3 years versus 74 years) (Hateboer *et al.* 1999, Torra *et al.* 1996).

Clinical variability, the lack of mutation hotspots and a wide range of mutations have made specific genotype / phenotype correlations hard to make in ADPKD (Gallagher *et al.* 2011). However, it appears mutations in the 5' region of *PKD1* (0-7812bp) lead to more severe disease (earlier onset of ESRD) compared to patients with 3' mutations (7812bp and on) (Qian *et al.* 2002, Rossetti *et al.* 2002, Watnick *et al.* 1999). It also appears that splice site mutations tend to result in a milder renal phenotype than other mutation types (Magistroni *et al.* 2003).

Sex also plays a significant role in ADPKD progression. Male gender has been associated with a poorer outcome in *PKD1*-linked families (Gabow *et al.* 1992). Similarly, female ADPKD2 sufferers had a later average age of ESRD compared to males (76.0 years versus 68.1 years) (Rossetti *et al.* 2007). This perhaps correlates with the data obtained from MRI studies of kidney volume and cyst size that show the rate of cystic expansion to be higher in men than women (Harris *et al.* 2006).

**Figure 1.8** Mutational analysis of *PKD1* and *PKD2*



types and frequencies of mutations found at the ADPKD loci (Rossetti *et al.* 2001, Rossetti *et al.* 2007, Magistroni *et al.* 2003). Large deletions of *PKD1* (and contiguous deletion of *TSC2*) are not included in the data, although this is thought to be a very rare occurrence. Neither *PKD1* nor *PKD2* have mutation hotspots.

### 1.2.8 Loss of heterozygosity and haploinsufficiency in ADPKD

The renal cysts associated with ADPKD are focal and sporadic (Pei *et al.* 2001). These lesions also form in an age-dependent manner (Gabow *et al.* 1991), consistent with a 'two-hit' process (analogous to Knudson's classic model for carcinogenesis) (Reeders 1992). Independent studies have reported ADPKD cysts are monoclonal, with LOH found in 17-24% of those sampled (Qian *et al.* 1996, Brasier *et al.* 1997). Up to 30% of the hepatic cysts seen in ADPKD (*PKD1*) also have second hits (Watnick *et al.* 1998). Liver cysts from ADPKD patients with a *PKD2* mutation show a similar frequency of second hits (Pei *et al.* 1999, Torra *et al.* 1999, Koptides *et al.* 1999). Interestingly, groups have noted *PKD1* inactivating mutations in cysts from patients with a *PKD2* mutation, and the converse, *PKD2* somatic mutations in cysts from patients with *PKD1* mutations. This implies a *trans*-heterozygote two-hit model of cystogenesis could operate with the polycystin proteins (Watnick *et al.* 2000, Koptides *et al.* 2000). Under these circumstances, a cyst from a *PKD1* patient with apparently functional polycystin-1 may have suffered a separate mutation in *PKD2*, changing what may be termed haploinsufficient cystogenesis to a *trans*-heterozygote two-hit model of progression.

However, a two-hit model of cystogenesis does have some inconsistencies with reported data. If second hits are indeed required for cystogenesis in ADPKD, a higher rate of somatic mutations would be expected in the cysts (Jiang *et al.* 2006). Using a highly sensitive screening method, all 15 exons and splice junctions in the *PKD2* gene were analysed and somatic hits were detected in 71% of cysts from ADPKD patients with a *PKD2* mutation (Watnick *et al.* 2000). A large proportion of cysts appear show no second hit. Another concern is the strong immunoreactivity for polycystin-1 and polycystin-2 seen in the majority of cyst epithelia (Ong *et al.* 1999a, Ong *et al.* 1999b). Mutations leading to IHC-detectable but non-functional protein may account for this discrepancy, but the vast majority of PKD mutations identified to date are stop or frame-shifting changes (Figure 1.8). While *trans*-heterozygosity may be put forward to explain both these phenomena, it is only seen in approximately 10% of ADPKD cysts and cannot account for all the instances of single-hit and/or polycystin expressing cysts (Pei 2001, Lantinga-van Leeuwen *et al.* 2004).

What may explain the failings of a two-hit model in a proportion of ADPKD cysts is haploinsufficiency, or gene dosage. Alterations in polycystin levels outside of a normal physiological range have been shown to cause renal cysts in ADPKD animal models. A reduced dosage (but not complete loss) of wild type *Pkd1* was sufficient for cystogenesis in a mouse line with a hypomorphic *Pkd1* allele (with only 15-20% normally spliced polycystin-1) (Lantinga-van Leeuwen *et al.* 2004). Jiang *et al.* (2006) found similar results in a conditional *Pkd1* knockout mouse model. The haploinsufficiency effect has also been demonstrated in *Pkd2* mice. Chang *et al.* (2006) found a highly elevated proliferative index in non-cystic tubules of *Pkd2* heterozygote mice, 5-10 times that of wild-type controls.

Taken together, these data suggest complete loss of polycystin-1 or polycystin-2 may not be strictly required for development of ADPKD (Jiang *et al.* 2006). The primary, germline mutation can, in a low but significant number of cases, lead to spontaneous cystogenesis. The focal and age-dependent nature of ADPKD cyst formation implies second hits are occurring and driving cyst formation in many lesions, but the two-hit model cannot account for all the cystogenesis seen. A reduction in gene dosage may well need additional factors, such chemical or physical renal injury and hits outside or in the polycystin-1/2 pathway to induce cystogenesis. It is important to note there may be bias when screening for second hits, which would mask haploinsufficient cyst formation. Later lesions may acquire further mutations to both the *PKD1* and *PKD2* loci as the cyst progresses. What was an initial driver mutation (and absolutely required for cystogenesis) and what was acquired as the cyst progressed (as a result of increased cell proliferation, poor cell cycle control and genetic instability) may become poorly defined.

### **1.2.9 Biochemistry of the ADPKD proteins**

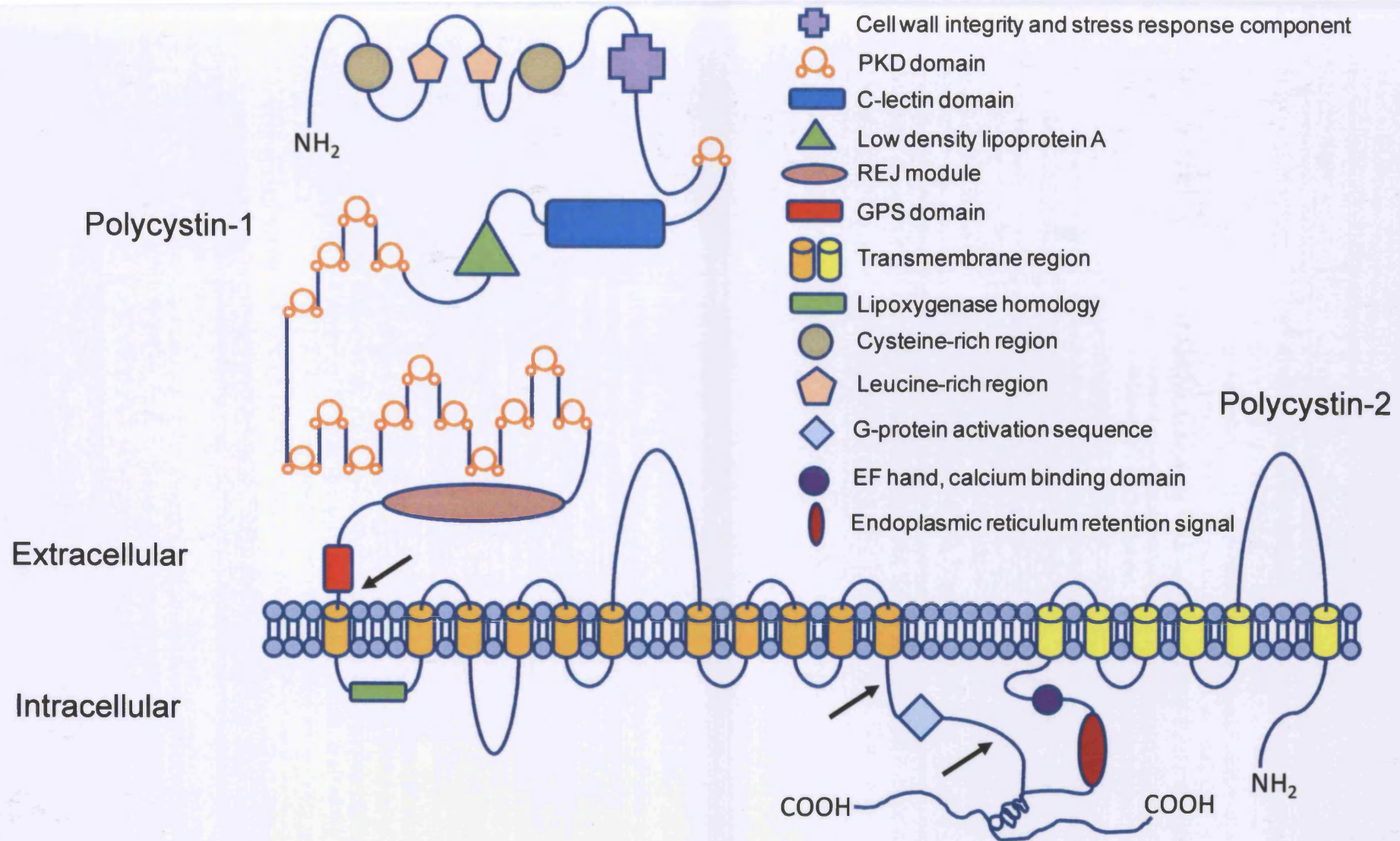
Polycystin-1 (Figure 1.9) is 4302 amino acids in length, of which, 3074 residues constitute a large extracellular domain. It has a total of 11 transmembrane spanning segments and a short, highly charged cytoplasmic tail (197 residues) (Hughes *et al.* 1995, Nims *et al.* 2003, Weston *et al.* 2003). The extracellular domain contains several motifs for protein-protein and protein-carbohydrate interactions (Hughes *et al.* 1995, Sandford *et al.* 1997), a receptor egg jelly (REJ) domain (Moy *et al.* 1996), and a G protein coupled receptor proteolytic site (GPS) (Ponting *et al.* 1999).



Following autoproteolytic cleavage at the GPS site, an extracellular NH<sub>2</sub>-terminal fragment is released. This cleavage appears to be essential for normal function (Qian *et al.* 2002). The remaining COOH-terminal fragment stays tethered to the cell membrane (Qian *et al.* 2002). Several groups have suggested that the cytoplasmic tail of polycystin-1 also undergoes cleavage. Chauvet *et al.* (2004) found the C-terminal tail to translocate to the nucleus following cleavage, where it modulates gene transcription. Low *et al.* (2006) report that a different fragment can be produced from the C-terminus that is able to interact with STAT6 and p100 to stimulate transcription. The protein is likely to play a role as a receptor for an unknown ligand (Torres *et al.* 2007), and is able to form a functional complex with polycystin-2 (Qian *et al.* 1997) through C-terminal tail interactions. Table 1.6 lists these domains and their functions in full.

The C-terminal tail of polycystin-1 can also be phosphorylated at several sites. Cyclic adenosine monophosphate (cAMP) - dependent kinase A phosphorylates polycystin-1 at S4159 and S4252, while T4237 may be phosphorylated by c-src (Parnell *et al.* 1999, Li *et al.* 1999).

Polycystin-2 (Figure 1.9) is a non-selective cation channel with a high permeability to calcium ions (Ca<sup>2+</sup>). It is a 968 amino acid protein with 6 transmembrane domains, with both C and N termini extending into the cytoplasm (Koulen *et al.* 2002). It has been localised to both the plasma membrane and the endoplasmic reticulum (Witzgall 2005), and it appears shuttling proteins such as PIGEA-14 (polycystin-2 interactor, Golgi and endoplasmic reticulum associated protein with a molecular weight of 14 kDa) may determine its final location. Polycystin-1 has also been shown to localise polycystin-2 to the plasma membrane (Hanaoka *et al.* 2000), and together, the polycystin-1- polycystin-2 complex is thought to function as a receptor-ion channel complex, in which polycystin-1 regulates the activity of polycystin-2 (Delmas *et al.* 2002, Delmas *et al.* 2004). An EF-hand domain (EF stands for the E and F helices of parvalbumin) is present on the C-terminus of polycystin-2 and is able to co-ordinate Ca<sup>2+</sup> ions. This is thought to induce conformational changes in the whole protein and may modulate polycystin-2 channel functions (Cai *et al.* 1999). Table 1.6 lists these domains and their functions in full.



PC1 and PC2 interact via their C-terminal tails. Details of domains and regions of homology are contained in the key. Domain functions are listed in table 1.5. Arrow heads indicate potential cleavage sites required for normal function. Adapted from Torres *et al.* 2007. Domains not drawn to scale

**Table 1.6** Domains and functions of polycystin-1 and polycystin-2

<b>Polycystin-1</b>	
<i>Protein domain</i>	<i>Function</i>
Cell wall integrity and stress response component (WSC)	Carbohydrate-binding domain, may be acting as a regulator of stress response pathways (Weston <i>et al.</i> 2003).
Extracellular PKD domains	Immunoglobulin-like repeats, involved in cell-cell adhesion in a calcium-independent manner (Ibraghimov-Beskrovnaya <i>et al.</i> 2000).
C-Lectin domain	Ca <sup>2+</sup> -enhanced cell adhesion through binding carbohydrate matrices and collagen I, II and IV <i>in vitro</i> (Weston <i>et al.</i> 2001).
Low density lipoprotein A (LDL-A)	Hydrophobic nature implies a ligand binding site. Studies unable to confirm its predicted presence in PC1 (Weston <i>et al.</i> 2003).
Receptor for egg jelly (REJ) domain	Module is a known regulator of ion transport, likely to support Ca <sup>2+</sup> influx (Weston <i>et al.</i> 2003, Ikeda <i>et al.</i> 2002).
G-protein coupled receptor proteolytic site (GPS)	Endogenous cleavage site, lysis is dependent on the presence of the adjacent REJ module (Ponting <i>et al.</i> 1999, Qian <i>et al.</i> 2002).
Lipoxygenase homology (LH2)	Mediates interactions with other membrane proteins and appears crucial for normal PC1 function (Bateman <i>et al.</i> 1999).
Cysteine-rich regions (CRR)	Usually flank LRRs and aid in their adhesive properties (Kobe <i>et al.</i> 1994).
Leucine-rich repeats (LRR)	Provides structural framework for the formation of protein-protein interactions, also involved in cellular adhesion (Kobe <i>et al.</i> 2001).
G-protein activation sequence	Intracellular domain that binds and activates G-proteins in a process physically regulated by PC2 (Parnell <i>et al.</i> 1998, Delmas <i>et al.</i> 2002).
<b>Polycystin-2</b>	
<i>Protein domain</i>	<i>Function</i>
EF-hand, calcium binding domain	A Ca <sup>2+</sup> binding motif, undergoes Ca <sup>2+</sup> -dependent conformational changes and regulates ion channel function (Petri <i>et al.</i> 2010).
Endoplasmic reticulum retention signal	Anchors PC2 at the endoplasmic reticulum, trafficking proteins such as PIGEA-14 deliver PC2 to plasma membrane (Witzgall 2005).
<b>Polycystin-1 and Polycystin-2</b>	
<i>Protein domain</i>	<i>Function</i>
Coiled-coil domain	Protein-protein interaction domain that binds the C-terminal tails of PC1 and PC2 (Foggensteiner <i>et al.</i> 2000, Qian <i>et al.</i> 1997).

### 1.2.9.1 Polycystin-1 and polycystin-2 associate *in vivo*

Mutations in *PKD1* or *PKD2* disrupt the same pathway and give rise to identical symptoms, suggesting a co-dependency and implying physical interaction is required for function. Polycystin-1 and polycystin-2 have been proved to associate *in vivo* and modulate their cellular location. A C-terminal endoplasmic reticulum retention signal on polycystin-2 leads to its accumulation in the ER membrane when polycystin-1 is absent (Hanaoka *et al.* 2000). Polycystin-1 expression allows polycystin-2 to localise to the plasma membrane, although polycystin-2 may have important roles to play as a  $\text{Ca}^{2+}$  channel in both these subcellular regions. Through a coiled-coil domain on their C-termini, polycystin-1 and polycystin-2 have been shown to interact and form a receptor-channel mechanosensory complex at the cell membrane (Nauli *et al.* 2003). The extent of polycystin-1 or polycystin-2 functionality outside of this complex is currently unknown. For example, polycystin-1 can be cleaved in several places and fulfil a signalling role which may be polycystin-2 -independent, but instead restricted by subcellular localisation. Polycystin-2 has been shown to localise to the cell membrane in polycystin-1 knockout mice, suggesting membrane-targeting can be polycystin-1-independent (Geng *et al.* 2006). Figure 1.9 shows polycystin-1 and polycystin-2 interacting at the cell surface membrane.

### 1.2.9.2 Tissue expression patterns of the ADPKD proteins

The ADPKD proteins have a wide expression pattern slightly at odds with their specific pathology of renal and hepatic tissue in disease. Both are expressed in the kidney, liver, brain, pancreas and vasculature (Wilson 2001). Expression of polycystin-1 is developmentally-linked, and the high levels seen during tissue development tail off to a low level in adult life (Geng *et al.* 1997, Van Adelsberg *et al.* 1997). Renal levels of polycystin-1 peak at E15 in mice and fall to a low level by two weeks post-birth (Geng *et al.* 1997). This is around the time mice with a homozygous mutation in *Pkd1* will die, suggesting a crucial role for polycystin-1 in embryogenesis at this stage. Renal polycystin-1 expression is predominantly in the collecting duct and distal convoluted tubules (Braun 2009), although Foggensteiner *et al.* (2000) found lower expression in most areas of the nephron.

Despite many theories of co-dependence, polycystin-2 has a different renal expression pattern to polycystin-1 and is present at higher levels in tubule cells

throughout adult life, especially the thick ascending Loop of Henle and the distal convoluted tubule (DCT) (Foggensteiner *et al.* 2000). This seems slightly at odds with the view that polycystin-1 and polycystin-2 function solely as a receptor-channel complex and adds weight to the idea that polycystin-2 at least, may have roles outside the polycystin complex.

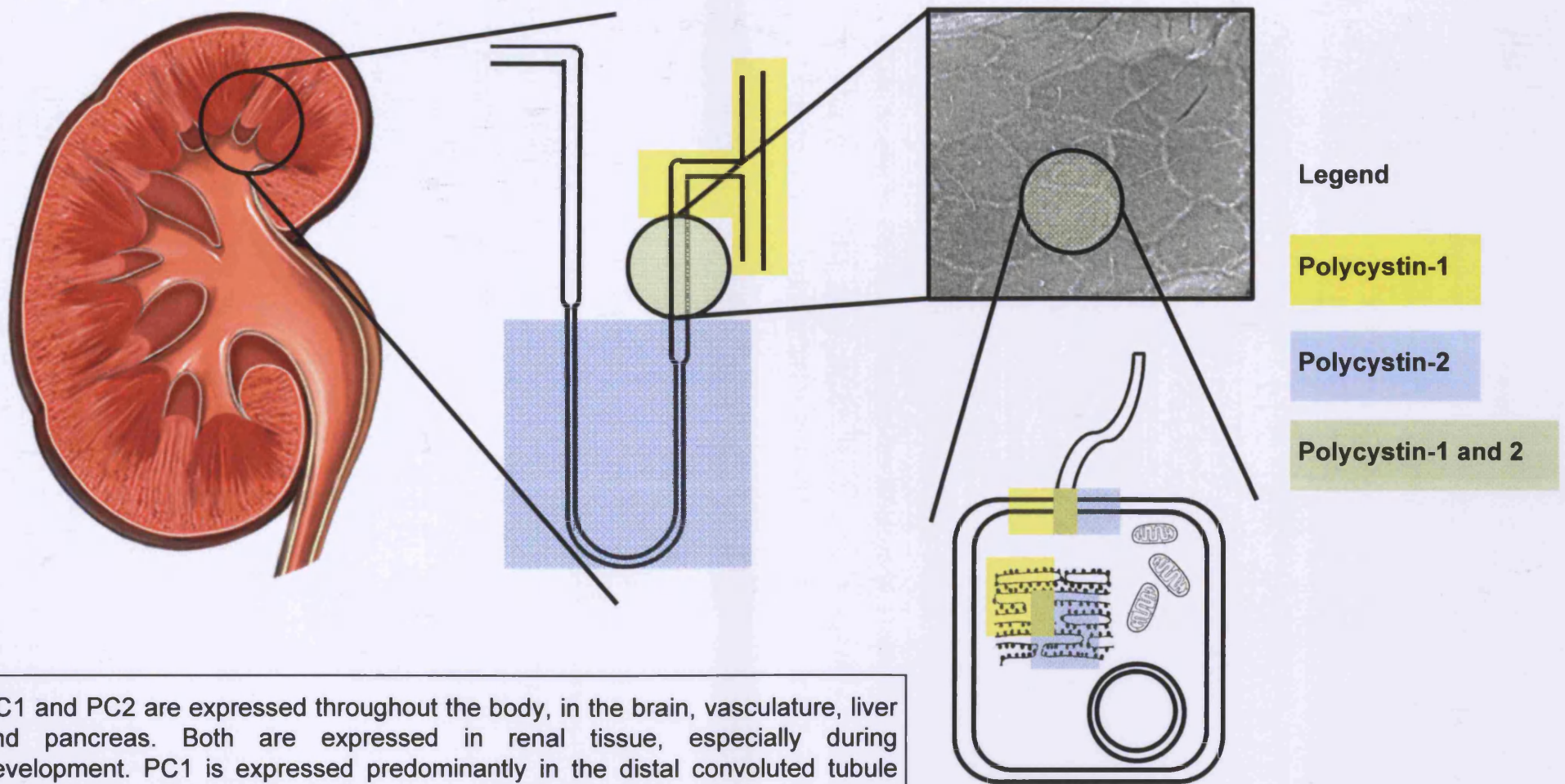
Polycystin-1 and polycystin-2 have recently been linked to the primary cilium of renal tubules *in vivo* and in cell culture, placing the mechanosensory complex at the luminal surface of collecting ducts in the kidney (Nauli *et al.* 2003, Yoder *et al.* 2002, Luo *et al.* 2003). Figure 1.10 outlines the renal and subcellular locations of polycystin-1 and polycystin-2.

*1.2.9.3 Polycystin-1 and polycystin-2 signalling pathways*

The polycystin-1 / polycystin-2 receptor-channel complex has been localised to both the ER membrane and the outer plasma membrane, at organelles called primary cilia. The most well characterised functions of the polycystin-1 / polycystin-2 complex are its roles in mechanosensatisation and cellular Ca<sup>2+</sup> modulation, but the polycystins also have links to other significant processes, such as the mTOR and Wnt pathways.



**Figure 1.10** Renal distribution of polycystin-1 and polycystin-2



PC1 and PC2 are expressed throughout the body, in the brain, vasculature, liver and pancreas. Both are expressed in renal tissue, especially during development. PC1 is expressed predominantly in the distal convoluted tubule and collecting ducts, while PC2 is expressed mainly in the distal convoluted tubule and Loop of Henle. Both transmembrane proteins are known to localise to the primary cilium, present on almost all renal tubule cells. PC1 and PC2 also co-localise to the ER membrane.

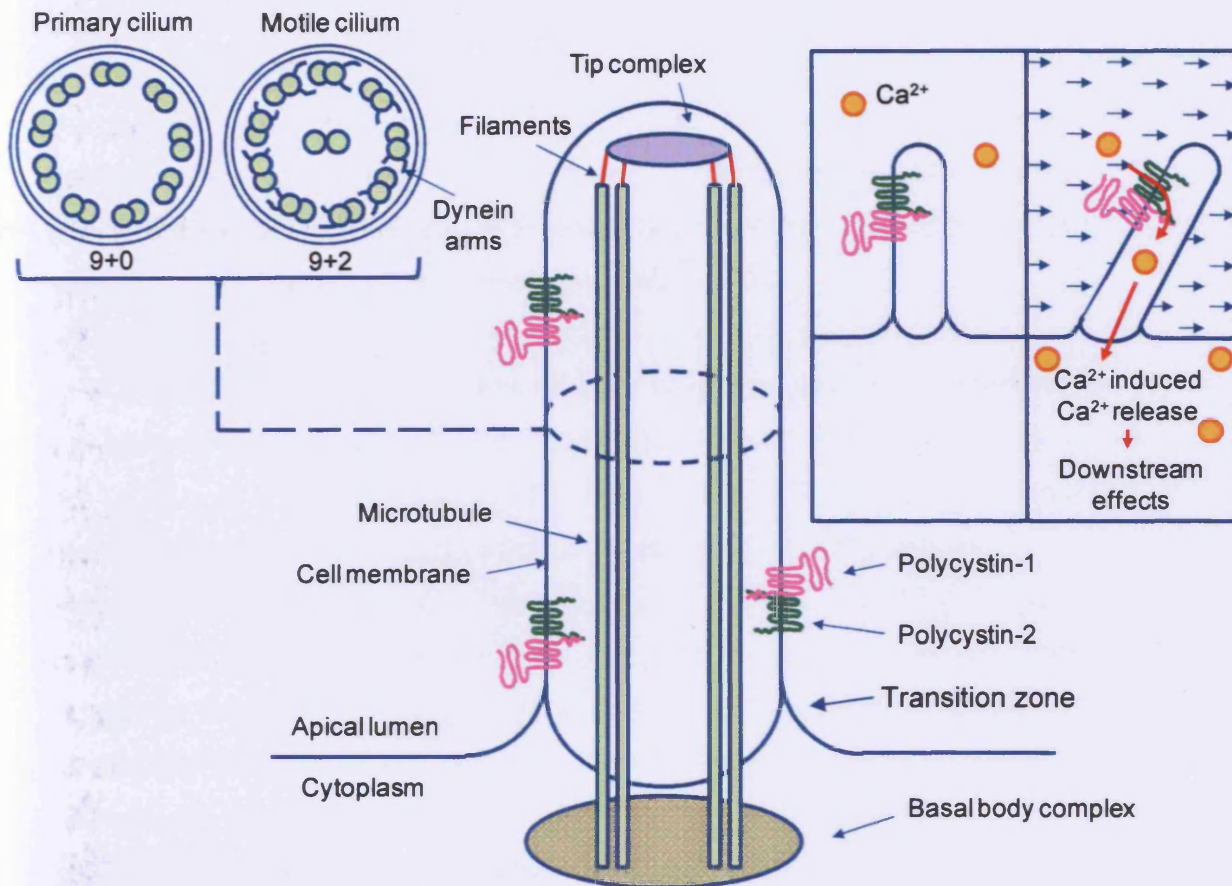
#### 1.2.9.3.1 Primary cilia and calcium signalling

Primary cilia (Figure 1.11) are single, hair-like structures that protrude from the apical surface of most eukaryotic cells, including renal tubule cells and hepatic bile duct cells (cholangiocytes). Primary cilia consist of 9 microtubule (MT) doublets (9+0 arrangement) while motile cilia generally have an extra central doublet (9+2 arrangement) (Hildebrandt *et al.* 2005). Dynein arms linking MTs are present only on motile cilia, allowing ATP-dependent conformational changes in MT structure to result in cilia movement (Fliegauf *et al.* 2007).

Primary cilia are sensory organelles that are highly conserved throughout evolution. Although it appears they can detect a wide variety of chemical and physical stimuli, the specific function they carry out depends on the cell type (Hildebrandt *et al.* 2005). Renal primary cilia extend into the tubule lumen and sense fluid flow (urine) through the nephron. Fluid flow results in cilium deflection and this is immediately followed by an influx of extracellular  $\text{Ca}^{2+}$  mediated by the polycystin proteins (Praetorius *et al.* 2001, Praetorius *et al.* 2003, Nauli *et al.* 2003). The large extracellular region of polycystin-1 may be able to sense fluid sheer stress as the cilia bends and transmit this mechanical information to associated polycystin-2. The  $\text{Ca}^{2+}$  channel properties of polycystin-2 would then be modulated to trigger an influx of  $\text{Ca}^{2+}$  across the cilium membrane. High levels of cellular  $\text{Ca}^{2+}$ , in response to adequate polycystin-1 stimulation, are proposed to trigger  $\text{Ca}^{2+}$ -induced  $\text{Ca}^{2+}$ -release. The heightened levels of intracellular  $\text{Ca}^{2+}$  can then produce downstream effects such as growth, differentiation, alter gene expression and polarity (Nauli *et al.* 2003). Cells isolated from mice lacking functional polycystin-1 showed abnormal  $\text{Ca}^{2+}$  influx in response to physiological fluid flow (Nauli *et al.* 2003).

Interestingly, lowering the levels of  $\text{Ca}^{2+}$  in wild-type renal epithelial cells reproduces the altered proliferative response of cyst-derived cells, while restoring  $\text{Ca}^{2+}$  to cyst-derived cells can dampen their responses to mitogenic stimuli (Yamaguchi *et al.* 2004, Yamaguchi *et al.* 2006). This suggests disruption of the primary cilium, or the amount of polycystin-1 /2 present in the primary cilium could disrupt  $\text{Ca}^{2+}$  homeostasis and dysregulate processes involved in cystogenesis such as proliferation.

**Figure 1.11** Primary cilia, polycystins and calcium signalling



**Main:** Primary cilia consist of 9 microtubule doublets that project from 9 triplet microtubules of the basal body complex. Motile cilia have a similar structure but an additional central couplet of microtubules. Additional dynein arms present only on motile cilia have an ATPase activity and allow movement with energy usage. Cilia are assembled through intraflagellar transport (IFT), which involves anterograde and retrograde trafficking of ciliary proteins. Although the cilia membrane may appear an extension of the cell plasma membrane, it is structurally and functionally distinct, filtered by a 'transition zone'. The distal tips of cilia are bound to microtubule capping structures (the tip complex) and this links the microtubule doublets and the ciliary membrane via structural filaments. Information from Eley *et al.* 2005. Both PC1 and PC2 have been localised to the ciliary membrane, where they are thought to function as a sensory complex and render the cell responsive to its external environment. **Inset:** In the kidney, renal tubule cell primary cilia project into the lumen, and the PC1/PC2 mechanosensory complex is able to act as an antenna, sensing fluid movement past the cell. Ciliary movement is transduced through PC1 to the Ca<sup>2+</sup> channel, PC2. The resulting activation renders the membrane permeable to extracellular Ca<sup>2+</sup> and sufficient stimulation will result in Ca<sup>2+</sup> induced Ca<sup>2+</sup> release from cellular stores. High levels of cellular Ca<sup>2+</sup> are thought to control many processes, primarily maintaining an epithelial phenotype (Deane *et al.* 2007). An absence of fluid flow, or a loss of PC1 or PC2, leads to reduced Ca<sup>2+</sup> influx. Information from Nauli *et al.* 2003.



#### 1.2.9.3.2 JAK-STAT pathway

The STAT (signal transducer and activator of transcription) proteins are phosphotyrosine activated transcription factors latent in the cytoplasm (Caló *et al.* 2003). Activation is normally transient, tightly regulated and achieved through stimulated members of the Janus Kinase (JAK) family, tyrosine kinase growth factor receptors, non-receptor tyrosine kinases and seven transmembrane pass receptors. STATs participate in normal cellular processes such as differentiation, proliferation, cell survival/apoptosis and angiogenesis (Horvath 2000).

The JAK-STAT signalling pathway has been suggested to mediate polycystin signalling (Bhunja *et al.* 2002, Low *et al.* 2006) and at least two STATs are involved – STAT6 and STAT1. Polycystin-1 is able to bind and activate JAK2 but not JAK1 (Low *et al.* 2006), providing a direct link to activation of the pathway.

Under fluid flow stress, polycystin-1 localised to renal tubule cell primary cilia is subject to C-terminal cleavage (Chauvet *et al.* 2004, Low *et al.* 2006). The resulting intracellular fragment has been shown to fulfil a signalling role by translocating to the cell nucleus and binding DNA through association with STAT6 and P100 (Low *et al.* 2006). Cells lining ADPKD cysts have elevated nuclear STAT6, P100 and C-terminal polycystin-1 fragments (Low *et al.* 2006). The researchers propose that polycystin-1 is acting as a regulator of STAT6 signalling through spatial control. Under normal conditions, STAT6 is sequestered to the cell membrane via polycystin-1, but in the absence of fluid flow (renal injury) or if reduced levels of polycystin-1 are present, STAT6 is able to constitutively initiate STAT6-dependent transcription.

Bhunja *et al.* (2002) have shown polycystin-1 to directly activate JAK-STAT signalling through physical interaction with JAK2, but not JAK1 or Tyk2. The activation of JAK2 was found to be dependent on polycystin-2, and resulted in the activation of STAT1 and STAT3. Talbot *et al.* (2011) have recently reported similar activation of STAT3 via polycystin-1 in manner dependent on the C-terminal cytoplasmic tail. Furthermore, Stat3 was found to be activated in the cysts of an ADPKD mouse model. Data now suggests polycystin-1 can differentially regulate STAT1, 3 and 6 signalling, depending on factors such as apical fluid flow, polycystin-

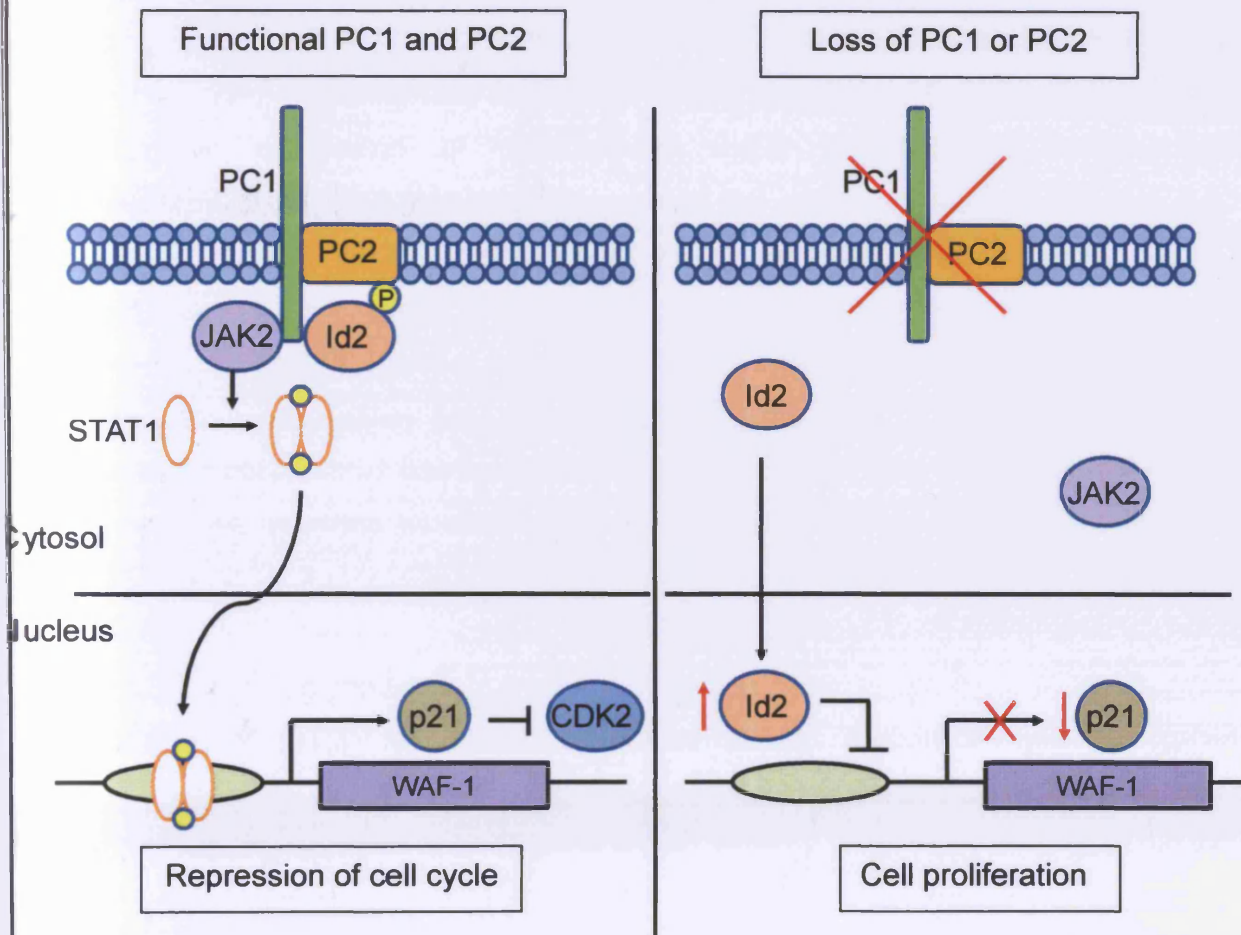
1 cleavage and cytokine/growth factor signalling environment of the cell (Talbot *et al.* 2011).

#### 1.2.9.3.3 Cell cycle control

The cysts seen in ADPKD are typically lined with a single layer of hyperproliferative epithelium (Nadasdy *et al.* 1995). Links between the polycystin proteins and cell cycle control have emerged recently (Figure 1.12). Li *et al.* (2005) have shown polycystin-2 can regulate the cell cycle through direct interaction with Id2, a member of the helix-loop-helix (HLH) protein family. Id2 is a transcription factor that promotes cellular growth and therefore requires nuclear localisation to function (Pagliuca *et al.* 2000). The *PKD2* gene transcribes a repressor of this activity, as polycystin-2 / Id2 complexes are excluded from the nucleus. While Id2 has a low level of expression in normal kidneys, in renal cysts from ADPKD patients, levels of Id2 are raised, with increased amounts of nuclear localisation (Li *et al.* 2005). The same paper showed polycystin-2 / Id2 interactions require polycystin-1-dependent Serine phosphorylation of polycystin-2, explaining why raised nuclear Id2 is found in both ADPKD1 and ADPKD2.

The CDK inhibitor, p21 is induced by polycystin-1 overexpression and is downregulated in cystic kidneys from ADPKD patients (Bhunja *et al.* 2002). Polycystin-1 is thought to control expression of p21 through the JAK-STAT signalling pathway in polycystin-2-dependent manner (discussed in 1.2.9.3.2). Interestingly, nuclear Id2 can repress transcription of p21 and promote cell cycle progression in kidney cells (Li *et al.* 2005). The full extent of polycystin control over cell cycle progression is not yet known, but clearly proliferation is perturbed in ADPKD cystogenesis.

**Figure 1.12** The polycystins and cell cycle control



PC1 and PC2 have direct links to cell cycle control through the transcription factors STAT1 and Id2. The transmembrane PC1 is able to directly interact with JAK2 (Bhunia *et al.* 2002) and activate the kinase to phosphorylate free cytosolic STAT1. The activation of JAK2 is dependent on both PC1 and PC2. Phospho-STAT dimerises in the cytosol and translocates to the nucleus, where it binds specific response elements. One target of activated STAT1 is the p21 gene, WAF-1. p21 is a cyclin dependent kinase inhibitor, and therefore a repressor of cell cycle progression. Under normal conditions, the Id2 transcription factor is bound to PC1-dependent phosphorylated PC2 and sequestered from the nucleus. Under pathologic conditions, with a mutation in PC1 or PC2, Id2 is free to translocate to the nucleus, where it can promote cell proliferation through modulation of several genes. This includes repression of the p21 CDK inhibitor. Information from Bhunia *et al.* 2002, Li *et al.* 2005.

#### 1.2.9.3.4 Canonical Wnt signalling

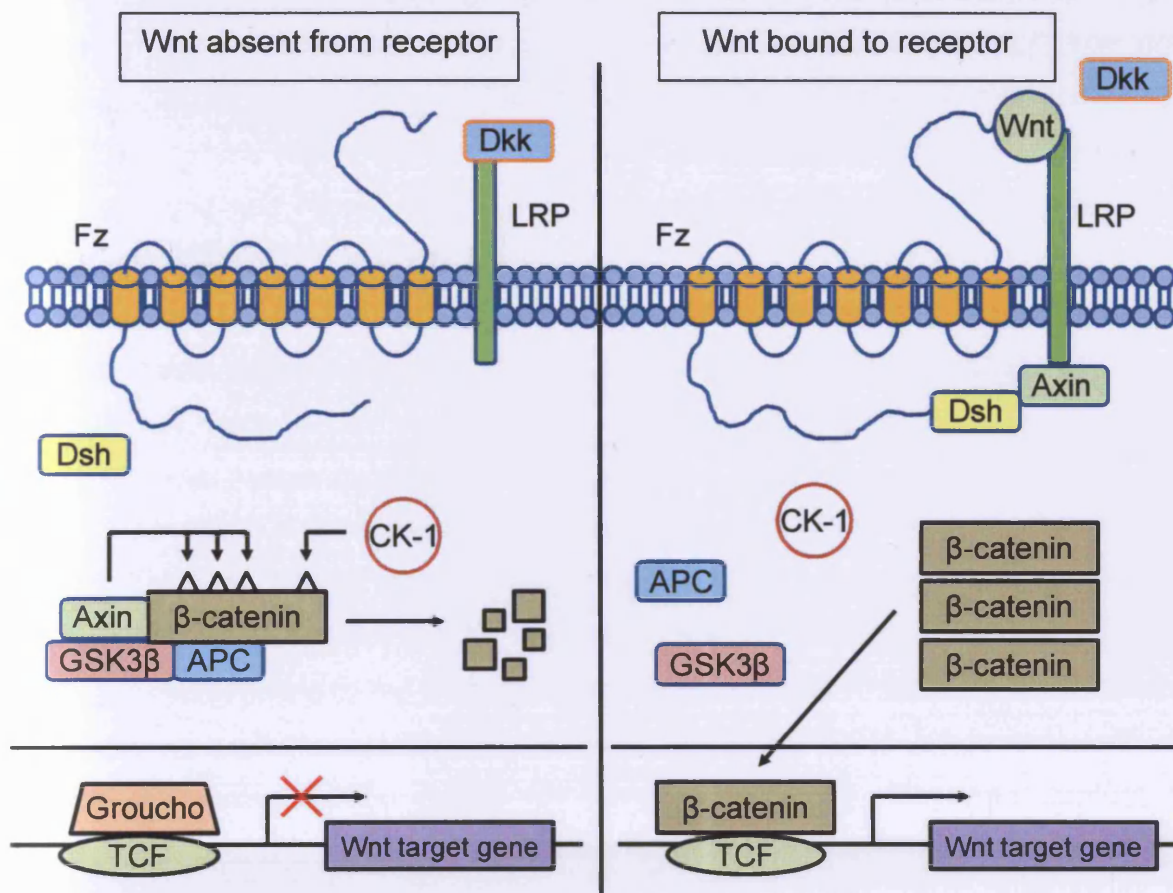
Canonical Wnt signalling (Figure 1.13) functions through altering levels of active and nuclear-localised  $\beta$ -catenin. In doing so, it controls cell proliferation and differentiation during development (Moon *et al.* 2005). The first clues that PKD and canonical Wnt signalling may have a link came through phenocopy mouse models. Transgenic expression of constitutively active  $\beta$ -catenin or kidney-specific inactivation of APC (a crucial component of the pathway) leads to a renal cystic phenotype (Karner *et al.* 2009, Qian *et al.* 2005, Saadi-Kheddouci *et al.* 2001). A direct connection between polycystin-1, polycystin-2 and Wnt signalling remains contentious. The C-terminus of polycystin-1 may activate  $\beta$ -catenin transcription in human embryonic kidney cells (Kim *et al.* 1999), but other more recent studies have suggested polycystin-1 has no such role (Le *et al.* 2004, Low *et al.* 2006) or is doing the opposite, in acting as an inhibitor of  $\beta$ -catenin-mediated transcription (Lal *et al.* 2008).

#### 1.2.9.3.5 mTOR signalling

Activation of mTOR results in increased protein translation and cell growth (Gallagher *et al.* 2011). While the pathway is known to be stimulated by a variety of inputs, feeding through the TSC proteins, several links have emerged between polycystin-1, polycystin-2 and mTOR. Studies have demonstrated that downstream targets of the mTOR pathway are inappropriately activated in ADPKD cysts (Shillingford *et al.* 2006). Additionally, repression of the mTOR pathway through Rapamycin treatment reduces cystogenesis in rodent models of PKD (Shillingford *et al.* 2006, Wahl *et al.* 2006, Tao *et al.* 2005). A trial by Qian *et al.* (2008) also highlighted a use for Rapamycin in reducing polycystic liver volume in ADPKD patients. Distefano *et al.* (2009) have since suggested polycystin-1 inhibits the mTOR pathway in a TSC2 dependant manner, while Shillingford *et al.* (2006) have previously shown the C-terminal cytoplasmic tail of polycystin-1 to interact with tuberin. It has been suggested that a function of the polycystin-1 tail may be to assemble a repressive complex with tuberin and mTOR. In a disease state where *PKD1* is mutated, the tuberin-mTOR complex cannot form correctly, leading to aberrant mTOR activation (Shillingford *et al.* 2006, Mostov *et al.* 2006).



**Figure 1.13** The canonical Wnt signalling pathway



**Left panel:** When the Wnt receptor complex is not bound to a Wnt ligand, the intracellular  $\beta$ -catenin turnover complex (consisting of APC, axin and GSK3 $\beta$ ) sequesters available  $\beta$ -catenin. Following CK-1 phosphorylation of  $\beta$ -catenin on Ser 45, GSK3 $\beta$  further phosphorylates  $\beta$ -catenin at specific residues Thr 41, Ser 37 and Ser 33. This hyperphosphorylated form of  $\beta$ -catenin is recognised by a ubiquitin ligase and removed for ubiquitination and degradation. Through this continual turnover, levels of  $\beta$ -catenin are kept low in the absence of a Wnt signal. In the nucleus, under low levels of  $\beta$ -catenin, Groucho binds TCF (T-cell factor) elements and inhibits transcription of Wnt target genes. Dkk is able to further inhibit Wnt signalling through binding the LRP portion of the co-receptor complex.

**Right panel:** Following the binding of a Wnt ligand to the Fz/LRP co-receptor complex, Dkk is displaced and the canonical Wnt signalling pathway is activated. Binding of ligand to receptor induces a conformational change in the cytosolic region of Fz, allowing Dsh to be recruited to the membrane and phosphorylated. Activated Dsh can in turn recruit Axin to the cell surface membrane and this leads to the dissociation of the  $\beta$ -catenin turnover complex. With no turnover complex to target  $\beta$ -catenin for degradation, levels of this protein accumulate and translocate to the nucleus. Groucho is displaced by  $\beta$ -catenin from TCF regions and transcription of Wnt target genes is initiated. Information from Eisenmann 2005.

### 1.2.10 Mouse models of PKD

Mouse models have been generated from spontaneous mutations, random mutagenesis and targeted transgenic approaches. Several models (*cpk*, *bpk*, *orpk*, *pcy*, and *Pkd2*<sup>WS25/-</sup>) have been used to test potential therapies (Torres *et al.* 2007). The ideal mouse model will carry a mutation in an orthologous gene to the human disease gene and reproduce the phenotypic effects faithfully (Torres *et al.* 2007). Few, if any, of the PKD mice meet this specification. An animal may capture the renal phenotype nicely (the *cpk* line for example (Preminger *et al.* 1982)) but the disease-causing gene (*Cys1*, in this case) is not associated with renal pathology in humans.

*Pkd1* and *Pkd2* mutant mice have been generated, but the renal phenotype in heterozygous animals is often normal or mild, with late onset cystogenesis (Torres *et al.* 2007, Guay-Woodford 2003). Homozygous mutations are embryonically lethal. There are exceptions to the mild cystogenesis (*Pkd1*<sup>nl</sup> and *Pkd2*<sup>WS25/-</sup>) but phenotypic variability is a problem in these animals (Torres *et al.* 2007). While mice with mild phenotypes may not be useful for therapeutic testing, they can capture the processes behind a cyst forming. Boulter *et al.* (2001) have produced a *Pkd1*<sup>del17-21 $\beta$ geo</sup> mouse with a truncating mutation in the *Pkd1* gene, replacing exons 17-21 with a *lacZ-neomycin* fusion gene ( $\beta$ geo) downstream of a splice acceptor site and an internal ribosome entry site. The mutant *Pkd1* transcript encodes a truncated form of polycystin-1 that only includes the extracellular domains of the protein. Homozygous *Pkd1*<sup>del17-21 $\beta$ geo</sup> mice die *in utero* at E13.5-E14.5 due to severe developmental defects involving the heart and skeletal tissue (Boulter *et al.* 2001).

By 9 months, approximately 50% of *Pkd1*<sup>del17-21 $\beta$ geo</sup> mice will have developed renal cysts, with some forming as early as 3 months. These are similar to human ADPKD lesions (cysts lined with hyperplastic or apoptotic cells), and arose throughout the nephron. Liver cysts are occasionally found in heterozygous *Pkd1*<sup>del17-21 $\beta$ geo</sup> mice later in life (Boulter *et al.* 2001).

### **1.3 Theories of cystogenesis in TSC and ADPKD**

It is unclear why renal tubules and hepatic bile ducts form cysts in TSC and ADPKD. Many theories exist, with plenty of scope for cross-talk between them. Interestingly, Torres *et al.* (1999) have suggested multiple causes can all lead to a remarkably similar cystic phenotype.

#### **1.3.1 The nature of cysts in TSC and ADPKD**

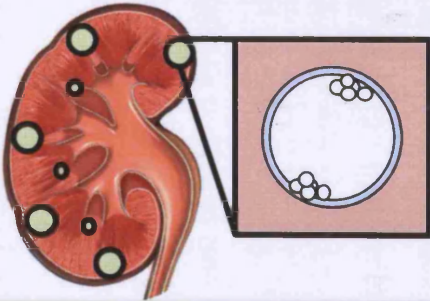
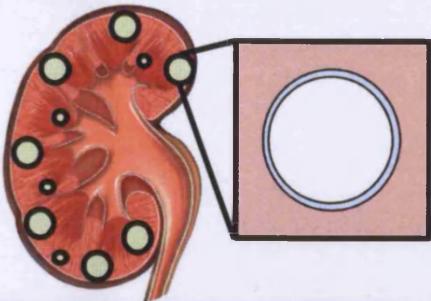
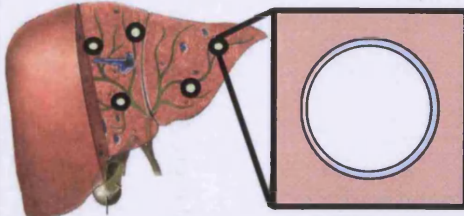
TSC renal cysts can be unilateral or bilateral, diffuse or localised. They are found in the cortical region of the kidney, often in the most superficial areas and then later extend into the medulla. Large cuboidal cells resembling the tubule epithelium line these cysts, often in a monolayer, with an eosinophilic cytoplasm and hyperchromatic nucleus. Cells may pile up and protrude into the centre of the cysts, forming a multicellular projection and eventually, a branch. This 'piling-up' distinguishes a TSC cyst from an ADPKD cyst (Cook *et al.* 1996). Lesions arise through clonal expansion of a single cell (Kwiatkowski *et al.* 2002). Some lesions in TSC are thought to be hormone driven (such LAM) but renal cysts do not appear to be influenced in this manner (Cook *et al.* 1996). Whether cyst incidence increases with age is a contentious issue - conflicting studies have found both positive (cohort of 167, Rakowski *et al.* 2006) and no association (cohort of 139, Cook *et al.* 1996).

ADPKD renal cysts have a similar medulla-cortical distribution as TSC cysts and are lined by a proliferating layer of epithelial cells. They show characteristic mislocalisation of proteins such as Na<sup>+</sup>K<sup>+</sup>-ATPase (sodium pump) (Wilson *et al.* 1991). Cysts develop after gradual tubule dilation (commonly the proximal and distal tubules) following abnormal periods of proliferation, apoptosis and fluid accumulation. ADPKD cysts that started as a tubule diverticulum will eventually separate from parent tubules and become sac-like structures reaching up to 10cm (Boletta *et al.* 2003). Most ADPKD cysts develop from clonal expansion of single cells (Qian *et al.* 1996), and are able to secrete a rich cocktail of cytokines and growth factors. These can act in a paracrine, endocrine or autocrine fashion to promote, cell proliferation, vasculistion or matrix remodelling (Ye *et al.* 1992, Munemura *et al.* 1994). Figure 1.14 illustrates the similarities between cysts in TSC and ADPKD.

ADPKD hepatic cysts arise from dilation of biliary microhamartomas, which in turn result from an overgrowth of the biliary epithelium of the intralobular ductules (Qian *et al.* 2003). The liver cyst epithelium retains characteristics of the biliary epithelium and is able to secrete fluid in response to secretin stimulation (Everson *et al.* 1990). As in the ADPKD kidney, hepatic cyst development is clonal (Nichols *et al.* 2004) and may be hormonally augmented, with lesions rarely observed before puberty (Everson *et al.* 2004) and enlarged livers reported in women with ADPKD undergoing oestrogen therapy (Sherstha *et al.* 1997). However, cyst initiation may not be hormone dependent, as men and women share an equal lifetime risk of ADPKD hepatic cysts (Everson *et al.* 1993). Liver cyst epithelium shares the ability of renal cysts to secrete a rich but distinct profile of cytokines and growth factors (Nichols *et al.* 2004). As in the kidney, hepatic cyst incidence increases with age (Masyuk *et al.* 2006). As in TSC and ADPKD renal lesions, hepatic cysts demonstrate dysregulated mTOR and are Rapamycin sensitive (Spirli *et al.* 2010).



**Figure 1.14** Cystogenesis in TSC and ADPKD

TSC renal cysts	ADPKD renal cysts	ADPKD hepatic cysts
		
Tubule derived	Tubule derived	Duct derived
Possibly age independent	Increase with age	Increase with age
Dysregulated mTOR	Dysregulated mTOR	Dysregulated mTOR
Hormone insensitive	Hormone stimulated	Hormone stimulated
Clonal expansion	Clonal expansion	Clonal expansion
Excess proliferation	Excess proliferation	Excess proliferation
Multicellular projections	Single cell lining	Single cell lining
Lesion progression	No lesion progression	No lesion progression

### 1.3.2 Primary cilia theory of cystogenesis

Defects in primary cilia have been implicated in many forms of cystic disease and can have profound consequences for cellular homeostasis (Boletta *et al.* 2003, Hildebrandt *et al.* 2005). Table 1.7 lists some of the major cystic kidney diseases and their associated genes. Evidence for a link between dysfunctional primary cilia and renal cystogenesis is provided by the fact that nearly all genes mutated in cystic kidney disease are expressed in the primary cilia, basal body or centrosome proximal to the primary cilium (Watnick *et al.* 2003). Both the TSC (Hartman *et al.* 2009) and ADPKD (Yoder *et al.* 2002) proteins have been localised to the primary cilia. The cilium is a focal point for many signalling pathways, and as such, a ciliary theory of cystogenesis is a collection of hypotheses.

As previously discussed, primary cilia are able to bend under fluid flow in renal tubules to trigger a rise in intracellular  $\text{Ca}^{2+}$ . This is suggested to help maintain an epithelial phenotype and suppress growth (Boletta *et al.* 2003). In the absence of this signalling input, epithelial cells dedifferentiate and undergo changes that promote the formation and enlargement of cysts, including an elevated level of cAMP (discussed in section 1.3.6) (Deane *et al.* 2007).

Aside from modulation of cellular  $\text{Ca}^{2+}$  and cAMP levels, cilia have been implicated in other flow-sensitive signalling pathways (Deane *et al.* 2007). The C-terminal domain of polycystin-1 is subject to cleavage in a flow dependent manner. The resulting polycystin-1 fragment can translocate to the nucleus in a complex with STAT6 and P100 and activate the AP-1 pathway (Chauvet *et al.* 2004). Loss of control over this particular aspect of cell signalling, through renal injury or a lack of functional ciliary localised polycystin-1, may give rise to cystic changes.

Furthermore, under fluid flow primary cilia are able to act as a switch between canonical and non-canonical Wnt signalling by increasing levels of the cilium-localised protein Inversin (Simons *et al.* 2005). During early embryonic development, canonical Wnt signalling is important for metanephric mesenchyme induction and cell proliferation during branching morphogenesis (Perantoni 2003). Later in development, signalling switches to non-canonical Wnt, or planar cell polarity (PCP) pathway (Park *et al.* 2005, Veeman *et al.* 2003, Wallingford *et al.* 2005), which is

required to align mitotic orientations occurring within renal tubules. In this manner, tubules can lengthen without increasing their diameter (Fischer *et al.* 2006). Defective switching between canonical and non-canonical Wnt signalling may have pathogenic effects in renal tubules. Cyst formation is associated with increased numbers of cells in the tubule circumference (Bisgrove *et al.* 2006), and this may well be a result of aberrant polarity signalling and increased cell proliferation.

The cilium itself may also have direct role in cell cycle regulation (Pan *et al.* 2007). During G0 phase, the cilium is assembled and projects from the basal body. Before a cell can re-enter the cell cycle, the primary cilium must first be disassembled and reabsorbed. At this point, the basal body converts back to a centriole and duplicates to form two centrosomes that will eventually form the poles of the mitotic spindle apparatus. Upon completion of mitosis, the centriole returns to a basal body complex and cilia assembly is resumed. Because the primary cilia and cell cycle are so closely linked, researchers have suggested a regulatory role for the cilium itself in this process. The presence of a primary cilium (regardless of the numerous other signalling roles it may be fulfilling) could be enough to block cell cycle progression. Therefore, defects in cilium structure may reduce the control of the primary cilium over this cycle and lead to aberrant proliferation and misaligned centrioles.

Despite the large body of evidence accumulating in favour of a ciliary hypothesis, it is important to note the distinction between passenger and driver causes of cystogenesis. Due to the highly polar nature of the primary cilium, it may be disrupted as a consequence of other, more fundamental changes in cell physiology caused by reduced levels of the TSC or ADPKD proteins. There is no doubt that once perturbed, the cilium can disrupt cell homeostasis and bring about a cystic phenotype, but it remains to be proved that a ciliary defect is the very first event in cystogenesis.

**Table 1.7** Cystic kidney disease proteins located to the primary cilium

Cystic Kidney Disease	Gene	Protein	Subcellular location
TSC	<i>TSC1</i>	Hamartin	Basal body, cytosol
	<i>TSC2</i>	Tuberin	Cilia, cytosol
ADPKD	<i>PKD1</i>	Polycystin-1	Cilia, cell membrane, ER
	<i>PKD2</i>	Polycystin-2	Cilia, cell membrane, ER
ARPKD	<i>PKHD1</i>	Fibrocystin	Cilia, basal body
NPHP1 (juvenile)	<i>NPHP1</i>	Nephrocystin 1	Cilia, basal body, centrosome
NPHP2 (infantile)	<i>INVS</i>	Inversin	Cilia, basal body, centrosome
NPHP3 (adolescent)	<i>NPHP3</i>	Nephrocystin 3	Cilia, retinal connecting cilia
NPHP4 (juvenile)	<i>NPHP4</i>	Nephroretinin	Cilia, basal body
Senior-Locken	<i>NPHP5</i>	Nephrocystin 5	Cilia, retinal connecting cilia
Oral-facial-digital	<i>OFD1</i>	OFD1	Cilia, basal body, centrosome
Bardet-Biedl	<i>BBS1-8</i>	BBS1-8	Cilia, basal body

**ARPKD** – Autosomal recessive polycystic kidney disease, **BBS** – Bardet-Biedl syndrome, **NPHP** – Nephronophthisis, **OFD1** – Oral-facial-digital syndrome type 1, **PKHD1** – polycystic kidney and hepatic disease 1. Information for table was taken from Hildebrandt *et al.* 2005, Bisgrove *et al.* 2006.

### 1.3.3 Activation of mTOR

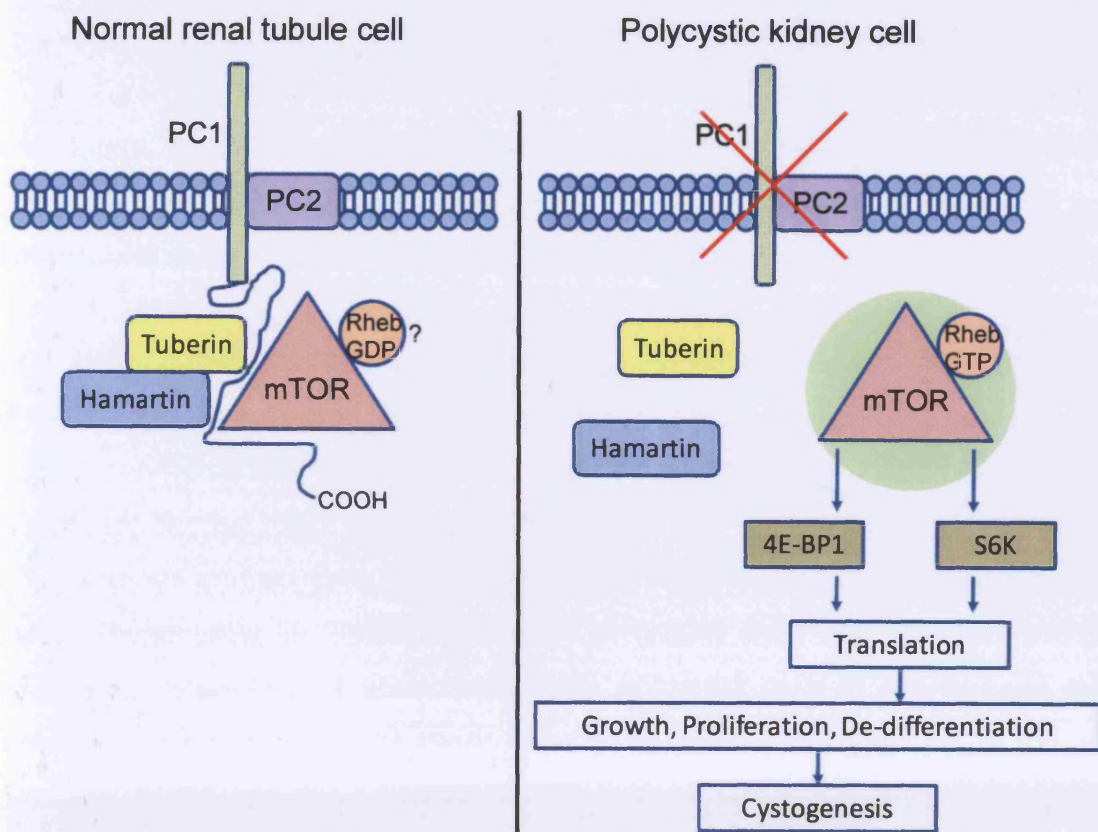
Dysregulation of the mTOR pathway, as indicated by positive staining of phospho-S6-kinase and phospho-mTOR, is frequently seen in cysts arising from the kidneys of TSC and ADPKD patients (Bissler *et al.* 2008, Boletta 2009, Shillingford *et al.* 2006). Additionally, Rapamycin (a potent inhibitor of the mTOR complex) treatment has been shown in a number of cystic mouse models to reduce lesion size significantly, and trials in humans with TSC and ADPKD have yielded similar results (Bissler *et al.* 2008, Davies *et al.* 2008, Qian *et al.* 2008). Figure 1.15 outlines a model for the interaction of mTOR, the TSC proteins and the polycystins. The end results of constitutive mTOR stimulation (cell growth, proliferation and de-differentiation) coincide with many features of a TSC or ADPKD lesion, and can clearly be a strong driver in an early cell to divert towards cystogenesis.

Another feature of the model outlined in Figure 1.15 is that polycystin-1 may be able to sequester tuberlin so that it is unavailable as a substrate for inactivating kinases such as Akt and RSK1. In ADPKD, defects in this complex formation may expose tuberlin to GF stimulated kinases, in effect hypersensatising the mutant cell to GF signalling, inhibiting tuberlin through Akt or ERK-RSK1 phosphorylation and leading to activation of mTOR. Since many ADPKD and TSC cysts have been shown to secrete a cocktail of cytokines and GFs, this may be a significant in cystogenesis (Weimbs 2006).

Interestingly, *Tsc1*<sup>+/-</sup> mouse data suggests not all early cysts have loss of control over the mTOR pathway. However, many of the later lesions do, implying mTOR dysregulation certainly has a hand in cyst progression but questioning its absolute role in cyst formation (Wilson *et al.* 2006). A proportion of cysts were found with second hits in the *Tsc1*<sup>+/-</sup> gene, suggesting a two hit hypothesis can account for some of the cystogenesis seen in TSC, with the subsequent mTOR dependent proliferation leading to renal tubule dilation and cystic changes (Wilson *et al.* 2006). Similarly, mTOR upregulation is not observed in all ADPKD-associated cysts either, but rather in a subset of the cystic epithelia (Hartman *et al.* 2009).



**Figure 1.15** mTOR dysregulation in cystogenesis



**Left panel:** Staining data suggests that mTOR is inactive in both normal human and mouse adult kidney epithelial cells, indicated by a lack of phospho-mTOR or phospho-S6-kinase (S6K). Additionally, Rapamycin, an mTOR inhibitor, has no effect in normal kidney. Although the TSC proteins are the major negative regulators of mTOR, this repression may be mediated by PC1. Interaction data has suggested a function of PC1 cytoplasmic tail may be to assemble tuberin and mTOR into a complex at the cell membrane. Because tuberin-mediated mTOR repression is known to occur through its GAP action on Rheb, this is also proposed to be a part of this complex. PC1 is facilitating mTOR repression in this model through bringing the various components into close proximity. **Right panel:** Following mutation of tuberin, hamartin or the polycystin proteins, the TSC-Rheb-mTOR complex does not form, leading to mTOR activation. Via downstream targets 4E-BP1 and S6K, mTOR is able to constitutively stimulate cell growth, proliferation and de-differentiation, all features seen in the cysts associated with TSC and ADPKD. Adapted from Mostov 2006.

### 1.3.4 Polarity defects in cystogenesis

The non-canonical Wnt (PCP) pathway is well conserved in evolution and examples in vertebrates include coordination of inner ear hair cells, organisation of fur growth and perhaps most importantly, during development, in convergent extension. It is through convergent extension that tissues are lengthened and narrowed during development, and it is errors in this process that can lead to neural tube closure defects (Bacallao *et al.* 2009). PCP is a common feature of many epithelia and is perpendicular to the apical/basal (A/B) polarity axis.

One of the first indications of a link between cystic kidney disease and PCP was that one of the genes mutated in NPHP, *inversin* (see Table 1.7), acts as a switch between canonical and non-canonical (PCP) Wnt signalling (Simons *et al.* 2005). More recent studies have shown how PCP signalling is required for development of normal kidneys and suggest how defective PCP can lead to cystic changes in renal tubules (Bacallao *et al.* 2009). Fischer *et al.* (2006) used cell lineage tracing and precise measurements to show that when epithelial cells in the straight tubular segments of the outer medulla divide, 95% of divisions occur with 34° of the axis of the tubule. In the emerging model of PCP in kidney tubulogenesis, orientated cell division is thought to be essential for producing the precisely structured nephron (Figure 1.16). Examination of several cystic kidney mouse models by the authors lead to the further discovery that orientated cell division was disrupted in these animals, in changes that predate cyst formation.

Links between the ADPKD proteins and PCP have emerged, as Lal *et al.* (2008) have demonstrated that the C-terminal tail of polycystin-1 can associate with  $\beta$ -catenin and inhibit canonical Wnt signalling (by inhibiting TCF-dependent gene transcription). In this manner, functional polycystin-1 is acting as a switch to 'turn on' PCP and in human *PKD1* cysts, strong evidence suggests canonical signalling pathway is aberrantly activated (Lal *et al.* 2008). While  $\beta$ -catenin association may not be directly dependent on the presence of polycystin-2, correct localisation of polycystin-1 to the ciliary membrane for cleavage in response to fluid flow is, providing a role for both polycystins in this process.

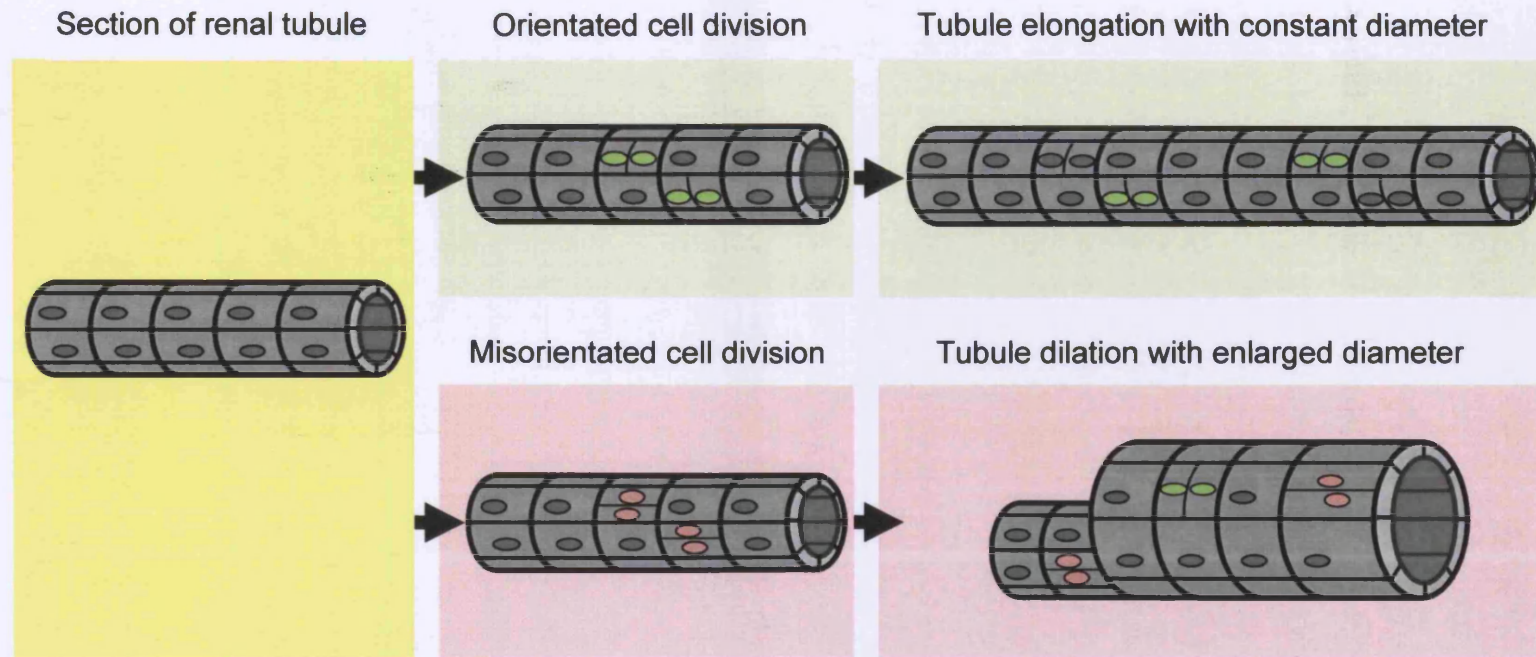
Work in the MDCK renal epithelial cell line has shown overexpression of Crumbs3 (CRB3) (part of a complex that includes Pals1 and PATJ) induces A/B polarity defects (Roh *et al.* 2003, Lemmers *et al.* 2004). PATJ, a key scaffold member of the CRB3 complex was able to directly interact with the C-terminus of TSC2 in a two-hybrid yeast study, verified through co-localisation and co-immunoprecipitation assays (Massey-Harroche *et al.* 2007). Interestingly, dPatj (the *drosophila* analogue of PATJ) has been shown to bind the cytoplasmic tail of Fz1 (the *drosophila* analogue of Fz) and inhibit its function as a canonical Wnt receptor (Djiane *et al.* 2005). In this manner, dPatj is acting as a switch between A/B and PCP polarity, with tuberin placed at its side. It is therefore possible that animal models and humans deficient in hamartin or tuberin may experience defects in polarity.

The ciliary connection to PCP and cystogenesis is a contentious one. The ciliary protein Inversin acts as a molecular switch between canonical and PCP signalling by targeting dishevelled (Dsh) for destruction (Simons *et al.* 2005). Additionally, the PCP proteins Fat4 and Vangl2 (Saburi *et al.* 2008, Ross *et al.* 2005) localise to the primary cilium and this has led to the suggestion that the primary cilium is the mediator of PCP in renal tubules and other epithelial cells (Bacallo *et al.* 2009). Defective cilia, therefore, would lead to defective PCP and subsequent cystogenesis. However, given the highly polar and apical nature of the primary cilium, it may be possible that defects in its length or structure are secondary consequences of perturbed polarity. Consistent with this hypothesis, loss of the PCP effector genes *fuzzy* and *inturned*, leads to disruption of ciliogenesis (Park *et al.* 2006).

Regardless of its origins, evidence suggests that defective PCP may not be enough to trigger cystogenesis alone. In zebrafish, most of the defects associated with a loss of PCP signalling can be ameliorated through blocking cell proliferation (Ciruna *et al.* 2006). It now appears defective cilia / PCP does not lead to formation of cysts unless new proliferation is induced (Bacallao *et al.* 2009, Patel *et al.* 2008).



**Figure 1.16** Defective polarity in cystogenesis



The lengthening of developing renal tubules is associated with the mitotic orientation of cells along the tubule axis and demonstrates intrinsic planar cell polarity. This orientated cell division is thought to ensure a constant tubule diameter is maintained during tubular lengthening, thereby preventing cyst formation (Germino 2005).

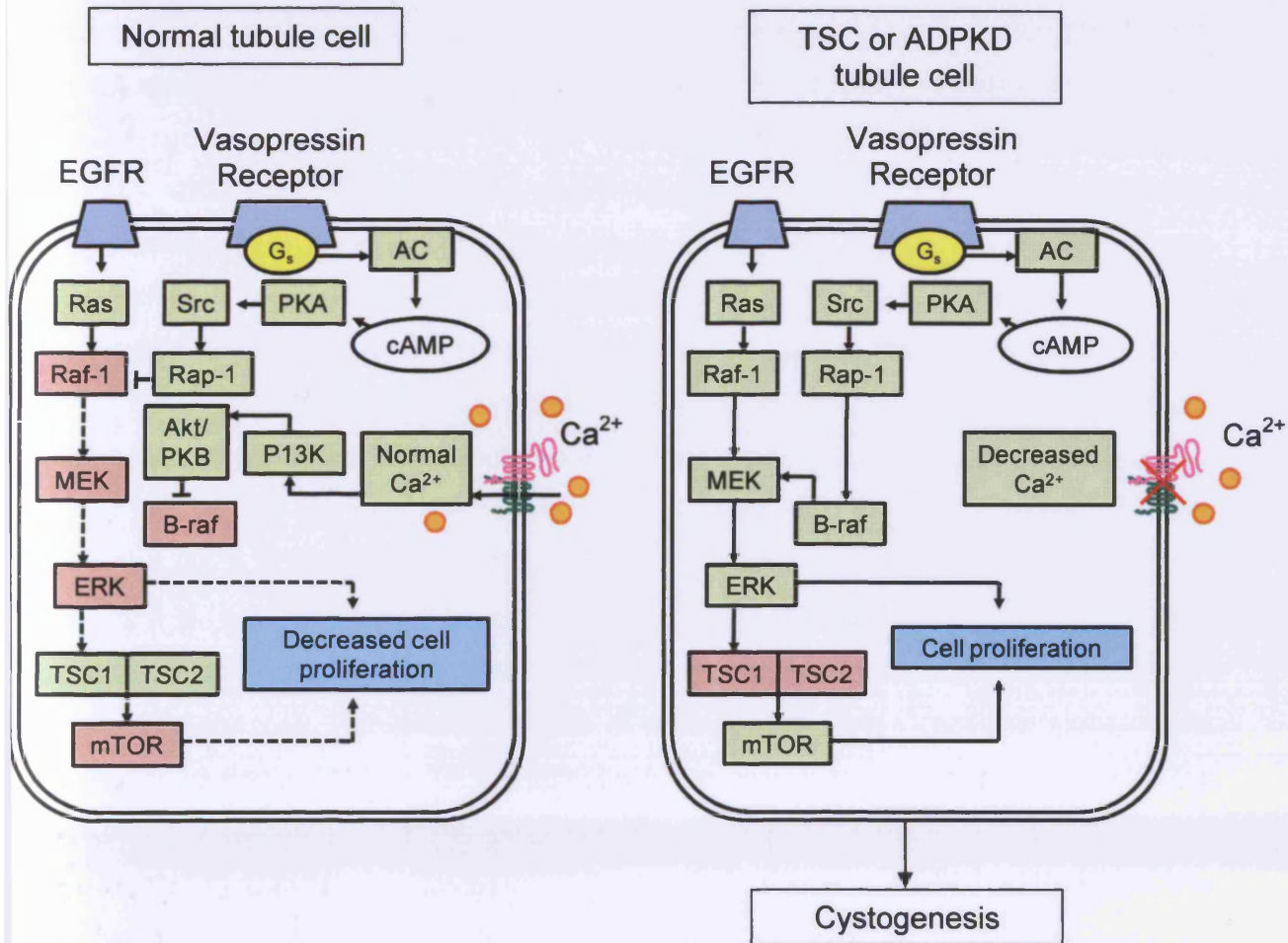
### 1.3.5 Ca<sup>2+</sup> homeostasis

In normal cells, epidermal growth factor (EGF) is mitogenic but cAMP is not. This is because normal Ca<sup>2+</sup> influx can inhibit B-raf activation (via PI3K and Akt) (Grantham 2003). In renal cells with defective primary cilia, there may be an inability to respond to flow-induced Ca<sup>2+</sup> influx. This lack of Ca<sup>2+</sup> entry could change cAMP from an anti-mitogenic to a pro-mitogenic compound and the subsequent activation of MEK and ERK would lead to strong cell proliferation. cAMP-mediated Raf-1 repression is also lost under low cell Ca<sup>2+</sup> levels, leading to co-ordinated mitogenic stimulation (Grantham 2003). Similar conditions may arise under renal injury, when fluid flow across the epithelium is disrupted. Cyst epithelia may contain many times more than the normal amount of vasopressin receptors, leading to a rise in the level of cyst cell cAMP through inappropriate activation of Adenylate cyclase (Torres *et al.* 2007). Figure 1.17 illustrates the roles of Ca<sup>2+</sup> and cAMP in renal cystogenesis.

Through mitogenic stimulation, Ca<sup>2+</sup> is an important factor to be considered in cystogenesis. It may also have role to play in cyst progression. As a cyst develops and occludes tubule fluid flow, mechanical stimulation of polycystin-1/2 may drop and promote further cyst expansion. Similarly, cyst formation is often accompanied by increased secretion of cytokines and growth factors (Munemura *et al.* 1994), and these may feed back to a growing cyst with defective Ca<sup>2+</sup> levels and stimulate proliferation via EGFR and Vasopressin receptors.

Further links may exist between cystogenesis and Ca<sup>2+</sup> homeostasis. Tuberin contains a calmodulin-binding domain (Noonan *et al.* 2002), rendering the TSC complex sensitive to Ca<sup>2+</sup> levels. Mutations in this calmodulin-binding region, and a subsequent inability to respond to differential Ca<sup>2+</sup> levels, have been linked to TSC disease pathology (Noonan *et al.* 2002). Additionally, raised cAMP levels have been linked to elevated mTOR signalling, another key feature of cystogenesis (Blancquaert *et al.* 2010).

**Figure 1.17** Calcium and cAMP in cystogenesis



**Left panel:** In response to mechanical stimulation, the PC1/PC2 complex mediates Ca<sup>2+</sup> influx and this inhibits B-raf activation via PI3K and Akt. This in turn, causes EGF signalling to be mitogenic and cAMP to be anti-proliferative. A functional TSC complex acts further downstream to reduce mTOR activity, providing additional breaks on cell proliferation. **Right panel:** Cells lacking functional polycystins or primary cilia do not show the normal Ca<sup>2+</sup> influx in response to fluid flow. The result is a proliferative response to cAMP (which may be elevated due to increased expression of vasopressin receptors on the cell surface). EGFR activation (due to cytokine stimulation) is no longer repressed and leads to Ras/ERK signalling augmented with B-raf activity. This proliferation stimulation can be reversed with Ca<sup>2+</sup> ionophores or channel activators. The TSC complex downstream is repressed by ERK signalling, leading to mTOR activation and cell proliferation. Faulty TSC genes lead to the same result.

**EGFR** – Epidermal growth factor receptor, **cAMP** – cyclic adenosine monophosphate, **AC** – Adenylate cyclase, **PKA** – activated protein kinase A, **PI3K** – phosphatidylinositol 3 kinase. Illustration adapted from Grantham 2003 and Torres *et al.* 2007.

### 1.3.6 Apoptotic defects in cystogenesis

#### 1.3.6.1 Apoptosis overview

Apoptosis (programmed cell death) is vital in normal embryonic development and morphogenesis (Woo 1995) but may be perturbed in disease – either with too much (neurodegenerative disorders) or too little (neoplasia) taking place. During the process, an apoptotic cell shrinks and becomes denser as its chromatin becomes condensed and packed against the nuclear membrane. The whole cell becomes rounded and retracts from its surroundings (Majno *et al.* 1995). In the nucleus DNA is fragmented, and a period of membrane blebbing occurs, resulting in the ‘pinching off’ of many of these blebs as small vesicles termed apoptotic bodies (Taylor *et al.* 2008). Apoptosis is brought about in a variety of ways, but can be separated into two broad pathways – intrinsic (mitochondrial stimulated) and extrinsic (binding of death receptors), which both lead to activation of caspases (Fulda *et al.* 2006). The intrinsic pathway is activated in response to cell stress, such as injury, DNA damage, elevated  $\text{Ca}^{2+}$  or hypoxia, or when there is a lack of external survival signals stimulating the cell. Extrinsic apoptosis is reserved for death receptor signalling in response to FasL, TNF or TRAIL stimulation of cell surface receptors. Pro-survival signals may also feed into the pathway, in the form of cytokine and GF signalling (Figure 1.18). Caspases (Cysteine proteases that cleave aspartic residues) are the mediators of controlled cell death, and are typically expressed as latent pro-enzymes which are activated in response to pro-apoptotic stimuli (Creagh *et al.* 2003). The enzyme family is divided into two - initiators (caspase-8, -9, -10) and effectors (caspase-3, -6, -7). Initiator caspases are often activated through auto-proteolysis and will propagate death signals by direct proteolytic activation of downstream effector caspases. It is these effectors that will dismantle cellular structures, disrupt cell metabolism, inactivate cell death inhibitory proteins and activate additional destructive enzymes.

#### 1.3.6.2 Mouse models with aberrant apoptosis display a cystic phenotype

Evidence for apoptotic defects in cystic disease has come from several sources, including phenocopy data. Mice with a knockout of the *AP-2 $\beta$*  gene die after 2 days due to polycystic kidney disease. Researchers found downregulation of *bcl2* coordinated with apoptosis in the collecting ducts and distal tubular epithelia. Other organs appeared normal but the kidneys were smaller than wild type littermates and

contained numerous small cysts. Proximal tubuli were unaffected. Cell line work by the authors has shown an *in vitro* ability of AP-2 to suppress *c-myc* induced apoptosis, suggesting AP-2 $\beta$  plays a role in renal epithelium cell survival (Moser *et al.* 1997).

The transcription factor p53 is able to prevent tumourigenesis through its capacity to regulate the cell cycle, apoptosis and DNA repair genes (Vousden *et al.* 2000). By binding DNA directly, at specific consensus sequences, p53 can repress transcription of proliferative genes (PCNA) and stimulate pro-apoptotic genes (Bax) (Saifudeen *et al.* 2002). Interestingly, a p53<sup>-/-</sup> rat model was found to acquire renal cysts shortly after birth (5 days old), along with enlarged renal tubules and aberrant nephron structure. Cyst epithelia frequently stained positive for PCNA, and the cysts themselves appear indistinguishable from those in ADPKD or TSC.

Overexpression of *c-myc* specifically in renal tissue was found to precipitate a polycystic kidney phenotype by Trudel *et al.* (1997). *C-myc* has previously been shown to stimulate cell growth and proliferation, while elevated expression is known to lead to apoptosis and cell cycle arrest (Schmidt 1999). Mice overexpressing *c-myc* developed cysts at E16.5 and progressed to ESRD by 3-6 months. Cyst number and size was found to increase with age, as in ADPKD. Cysts had a proliferation index ten times that of non-transgenic controls, while the apoptotic index was ten to one hundred times elevated; leading the authors to suggest the cystogenesis seen was a result of imbalanced proliferation and apoptosis.

Veis *et al.* (1993) have reported *Bcl2* deficient mice (*Bcl2*<sup>-/-</sup>) complete embryonic development but are growth retarded and have polycystic kidneys. Renal failure in these mice was found to result from severe polycystic kidney disease arising from dilated distal and proximal tubules. No linear relationship was found between age and cyst size, although evidence of lesion progression was seen. Earliest lesions appeared around 10 days, with hyperproliferation and 'piling-up' around some of the cysts, as seen in TSC. An earlier study by Kamada *et al.* (1995) into *Bcl2*<sup>-/-</sup> mice found similar results to Veis *et al.*, but also described an additional phenotype of poor epithelial cell alignment in the small intestine (a possible polarity defect). The



authors suggest apoptosis is a crucial part of a developing kidney, and perturbing this process (through *Bcl2* removal) will lead to a devastating renal phenotype.

#### 1.3.6.3 Apoptosis in ADPKD and TSC

Markers of proliferation and apoptosis share a similar distribution in ADPKD cysts, and there appears to be a positive correlation between the degree of proliferation and amount of apoptosis (Lanoix *et al.* 1996). As highly proliferative cells are known to stimulate apoptosis (Vermeulen *et al.* 2003), this is perhaps not a surprising observation. A tilt in this balance can also produce a renal cystic phenotype – either with apoptosis reduced and proliferation proceeding unchecked or with apoptosis and proliferation present in excess amounts (see section 1.3.5.2) (Figure 1.19).

A theory as to how too much apoptosis might lead to cystogenesis was put forward by Lin *et al.* (1999). Madin Darby canine kidney (MDCK) cells in a collagen-type 1 matrix require apoptosis for cyst formation through a process of cavitation. Cystogenesis in this system can be blocked by overexpression of *Bcl2*, a pro-survival gene. The idea that excess apoptosis may contribute to cystogenesis in TSC and ADPKD is borne out by observations of a very low incidence of renal cell carcinoma despite high levels of cell proliferation (Torres 1999). However, cystogenesis through cavitation is not supported by pathological studies of TSC and ADPKD cysts. These are known to form from existing tubules and eventually bud off. Cavitation would require a mass of cells undergoing central apoptosis to produce a cyst.

Ali *et al.* (2000) used *cpk* mice (ADPKD) to confirm high levels of apoptosis in the cystic kidneys from these mice. The apoptosis was localised solely to the interstitium, with no evidence of cell death in the actual cyst epithelium. This led the authors to suggest accumulation of interstitial mononuclear cells attracted to the dying cells, and the resulting induction of interstitial scarring may contribute to cystic progression through loss of functional renal mesenchyme. Similarly, Winyard *et al.* (1996) found elevated apoptosis in the interstitium around undilated tubules in polycystic kidneys, and suggested that dysregulation of cell survival leads to spontaneous involution of renal tubules and contributes to incomplete tissue maturation. Nishio *et al.* (2005) have suggested why apoptosis can promote cyst

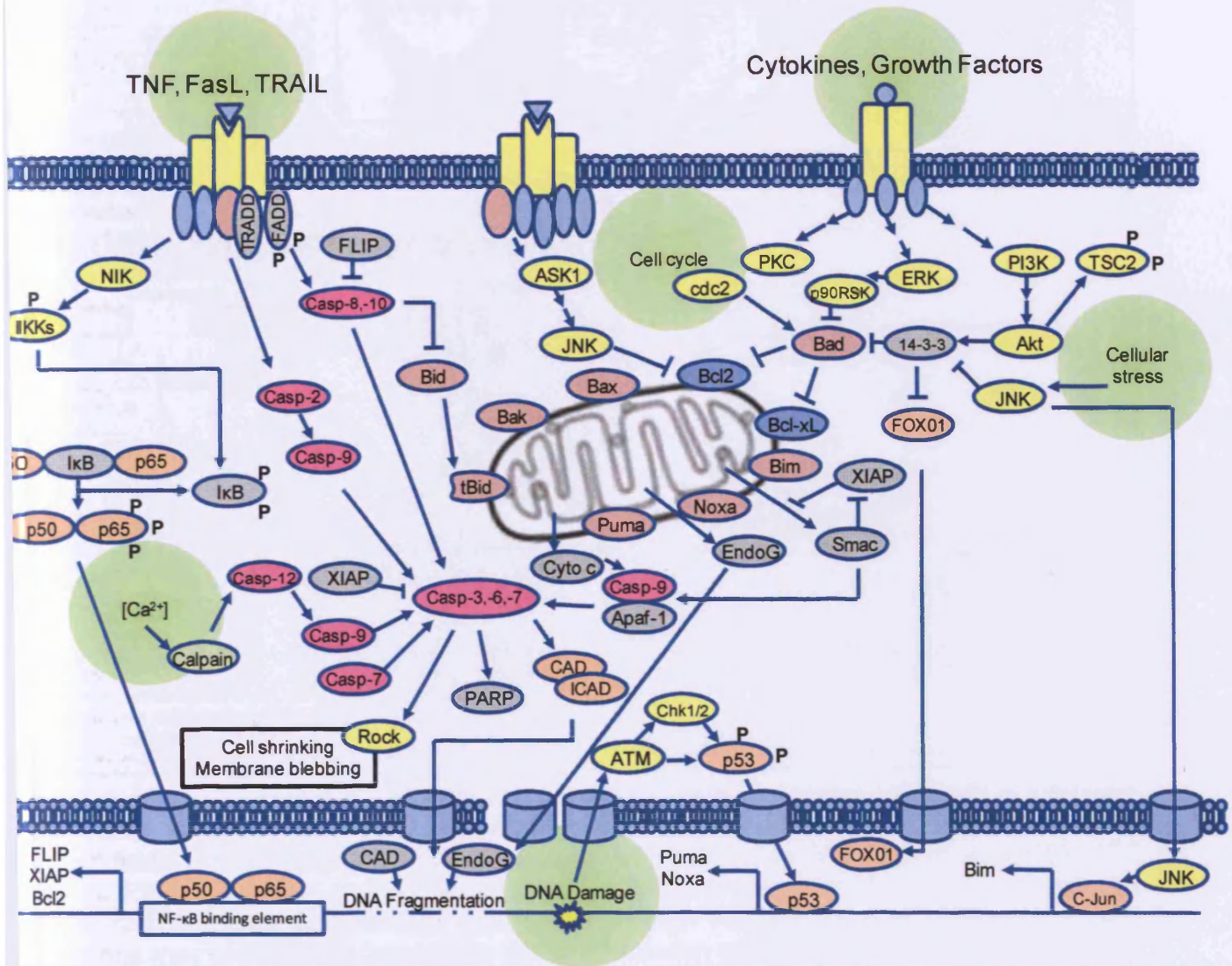
formation. Using a *Pkd1* mouse model, early cyst epithelia were found to be composed of both *Pkd1*<sup>-/-</sup> and *Pkd1*<sup>+/-</sup> renal tubule cells. With time, the *Pkd1*<sup>-/-</sup> cells replaced *Pkd1*<sup>+/-</sup> cyst epithelial cells lost to JNK-mediated apoptosis. Late-stage cysts from this model were lined with *Pkd1*<sup>-/-</sup> and had downregulated p53. In this instance, apoptosis is selectively killing off non-mutant cells and leading to cyst progression.

Conversely, increased apoptosis in tubule cells may decrease cyst formation (Ostrom *et al.* 2000). *Pax2*-deficient mice (with increased apoptosis) were bred onto *cpk* mouse lines (with a renal cystic phenotype). The resultant mice had elevated renal apoptosis and less cystic disease than controls. Battini *et al.* (2006) produced a knockdown of polycystin-1 expression in MDCK cells to stop tubulogenesis and induce formation of cysts under hepatocyte growth factor stimulation. These polycystin-1 deficient cells were significantly less susceptible to anoikis (apoptotic cell death through loss of contact with the extracellular matrix). These effects were seen under polycystin-1 haploinsufficiency.

Hamartin may have a role in negatively regulating apoptosis. Inoue *et al.* (2009) have found hamartin can be phosphorylated (at T417) and bind to Hsp70 (heat shock protein). The hamartin-Hsp70 complex was found to localise to the outer membrane of mitochondria, where it was able to inhibit cell death *via* intrinsic apoptosis. This process may be tuberin-independent, as hamartin and Hsp70 localised in the absence of *TSC2*.

Shillingford *et al.* (2006) have treated polycystic mouse models with Rapamycin and found startling cyst regression and an overall reduction in kidney size. This result was attributed to induction of apoptosis specifically in the cyst lining epithelial cells (Shillingford *et al.* 2006).

**Figure 1.18 Apoptosis overview**

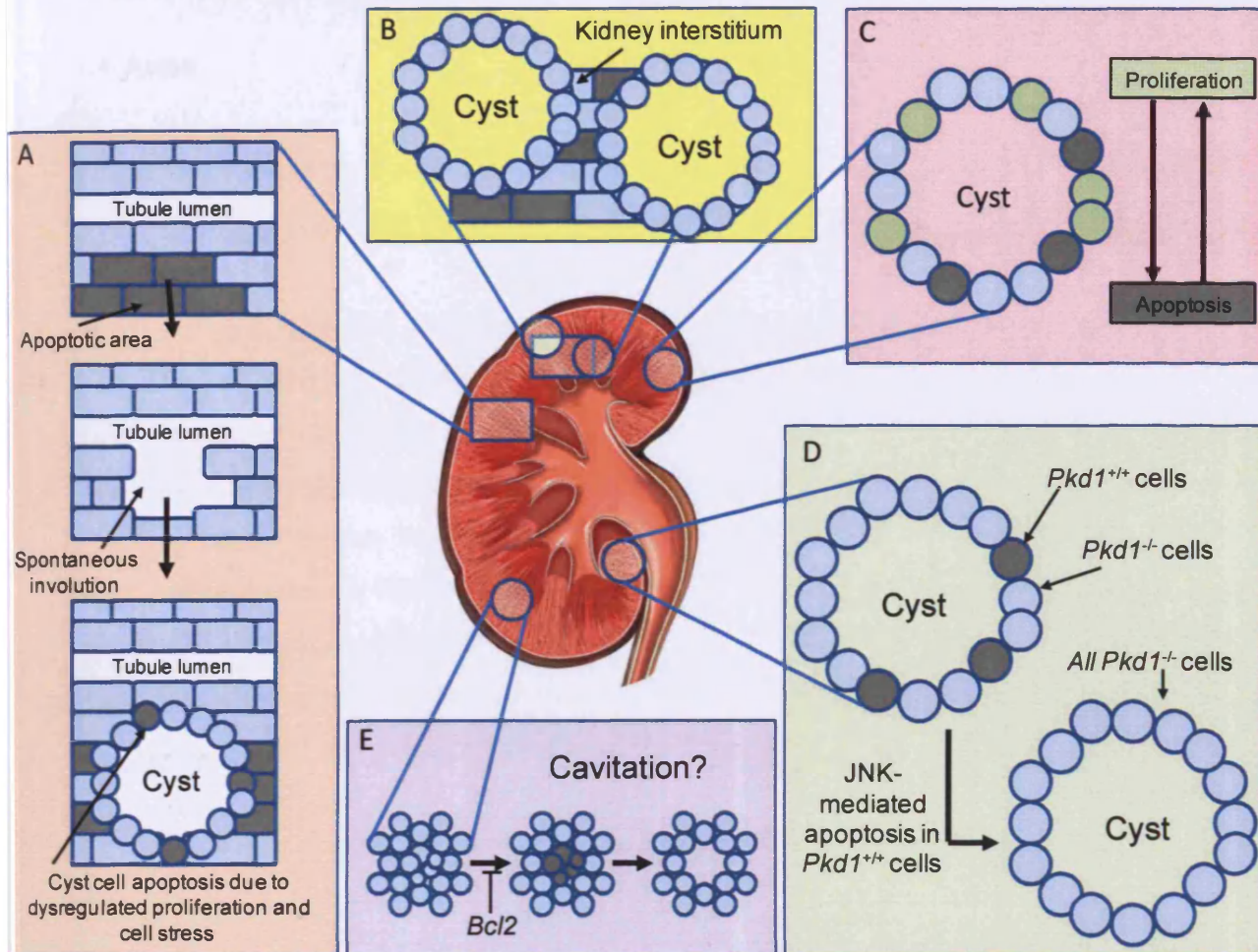


Apoptosis can be modulated in a variety of manners (green areas), including death receptor ligand signalling (such as TNF, FasL or TRAIL), DNA damage (via ATM), excessive mitogenic stimulation (via cdc2) and fluctuations in intracellular calcium levels (due to ER stress). Extrinsic cell death results from triggering cell surface death receptors, leading to transmembrane signalling and activation of initiator caspases. Intrinsic apoptosis is activated in response to DNA injury, or stresses (high calcium levels, DNA damage, hypoxia) or lack of survival signals. It is mitochondrial dependent and is a balance between pro-survival (Bcl2) and pro-apoptotic (Bim) factors. Ultimately, a tip in this balance towards cell death will result in release of mitochondrial Cytochrome c and activation of caspase-9 (an initiator caspase). Regardless of the route, once initiator caspases (-8,-9,-10) are activated, the death signal is propagated through proteolytic activation of downstream effector caspases (-3,-6,-7). These will then dismantle cellular structures, disrupt cellular metabolism and activate additional destructive enzymes (CAD) to bring about the controlled death of a cell.

**Yellow** indicates a kinase, **Orange** indicates a transcription factor, **Pink** indicates a caspase, **Crimson** indicates a protein (pro-apoptotic), **Blue** indicates a pro-survival protein. **TNF** – tumour necrosis factor, **FasL** – Fas ligand, **TRAIL** – TNF related apoptosis inducing ligand, **XIAP** – X linked inhibitor of apoptosis protein, **Smac** – second mitochondrial derived activator of caspase, **CAD** – caspase activated DNase, **ICAD** – inhibitor of caspase activated DNase, **FADD** – Fas associated death domain, **TRADD** – TNF receptor type 1 associated death domain, **FLIP** – FLICE like inhibitory protein, **NIK** – NF-κB inducing kinase, **NF-κB** – nuclear factor kappa B, **IKK** – inhibitor of NF-κB, **IκB** – inhibitor of NF-κB, **ASK1** – apoptosis signal regulating kinase 1, **JNK** – c-Jun N terminal kinase, **FOXO1** – Forkhead box O1, **PKC** – protein kinase C, **PI3K** – phosphatidylinositol 3 kinase, **Endo G** – endonuclease G, **PARP** – poly ADP ribose polymerase, **Bcl2** – b cell lymphoma 2, **ATM** – ataxia telangiectasia mutated protein, **Chk1/2** – checkpoint kinase 1/2, **ERK** – extracellular signal regulated kinase, **Apaf1** – apoptotic protease activating factor 1, **Puma** – p53 upregulated modulator of apoptosis, **Noxa** – (Latin for damage), **p90RSK** – p90 ribosomal S6 kinase, **cdc2** – cell division control 2 (CDK1), **Bax** – Bcl associated X protein, **cyto C** – Cytochrome c.



**Figure 1.19** Apoptosis in cystogenesis



**Panel A:** While apoptosis is a normal part of development, excessive cell death in interstitial cells surrounding tubules is a feature of both early and late cystic kidneys. This is suspected to contribute to cyst progression by destruction of renal tissue (Winyard *et al.* 1996). TSC and ADPKD cysts are hostile environments that promote cell death through excess proliferation, hypoxia and nutrient deprivation. A high turnover of cyst cells under these conditions may promote the incomplete tissue maturation seen in cyst epithelial cells.

**Panel B:** Ali *et al.* (2000) found a *cpk* mouse model of ADPKD had high levels of renal apoptosis but very little of this was localised to cyst epithelium. The kidney interstitium was severely apoptotic in these mice, and accumulation of mononuclear cells (attracted to the dying cells) could cause interstitial scarring and contribute to cystic progression.

**Panel C:** One of the key features of TSC and ADPKD renal cysts is the hyperproliferative nature of the cells lining the lesion and the excessive amounts of apoptosis taking place. These two processes are thought to be intrinsically linked processes. The ability of cyst cells to retain a link between these two processes may explain the low rate of oncogenesis seen in TSC and ADPKD and with such a high turnover, the immature phenotype of cystic cells.

**Panel D:** Nishi *et al.* (2005) found a line of chimeric ADPKD mice to have cysts composed of both PC1 positive ( $Pkd1^{+/+}$ ) and PC1 negative ( $Pkd1^{-/-}$ ) renal tubules epithelial cells. Normal cells are recruited to the cyst in an effort to maintain tubule diameter. However, as the cysts developed from early to late-stage lesions,  $Pkd1^{-/-}$  cells were found to replace  $Pkd1^{+/+}$  cells lost by JNK-mediated apoptosis in intermediate stages. Elevated apoptosis in this setting would contribute to cyst development and select for abnormal cells.

**Panel E:** Cavitation is seen in MDCK cells during cystogenesis. Excessive apoptosis leads to a central vacuation forming inside a polarised epithelial lining. The process is known to be inhibited by *Bcl2* but it is unlikely this occurs in TSC or ADPKD kidneys. This is because histological evidence has clearly demonstrated cysts form from dilations of renal tubules that slowly separate from the parent tubule to become a separate sac-like structure.

## 1.4 Aims

The aims of the project were:

- to investigate the renal and hepatic phenotype of *Tsc1*<sup>+/-</sup>, *Tsc2*<sup>+/-</sup> and *Pkd1*<sup>+/-</sup> mice.
- to examine the structure of primary cilia in pre-cystic renal tubules and hepatic bile ducts in *Tsc1*<sup>+/-</sup> and *Tsc2*<sup>+/-</sup> mice.
- to measure PCP in our *Tsc1*<sup>+/-</sup>, *Tsc2*<sup>+/-</sup> and *Pkd1*<sup>+/-</sup> mouse livers and kidneys to assess the role of cell polarity in the pathogenesis of TSC.
- to characterise the role of mTOR activation in early cystogenesis and lesion progression in *Tsc1*<sup>+/-</sup> and *Tsc2*<sup>+/-</sup> mice.
- to further investigate the possibility of an mTOR-independent route of cyst initiation, involving defects in renal tubule apoptosis.

## **CHAPTER TWO**

### **Materials and methods**

#### **2.1 Suppliers**

The suppliers of products used in this study are listed below;

Abcam (Cambridgeshire, UK)

ABGene (Surrey, UK)

Anachem (Bedfordshire, UK)

Applied Biosystems (Cheshire, UK)

Bibby Sterling (Staffordshire, UK)

BioGenex (San Ramen, CA, USA)

Bioquote (Yorkshire, UK)

Bio-Rad Laboratories Ltd (Hertfordshire, UK)

Bright Instrument Co Ltd (Cambridgeshire, UK)

Carl Zeiss MicroImaging GmbH (Jena, Germany)

Cell Signalling Technologies (Danvers, MA, USA)

DAKO (Cambridgeshire, UK)

EMScope (Kent, UK)

Eurofins MWG Operon (Ebersberg, Germany)

Eurogentec (Hampshire, UK)

Fresenius Kabi AG (Homburg, Germany)

GE Healthcare (Buckinghamshire, UK)

InterFocus Ltd (Cambridgeshire, UK)

Invitrogen Life Technologies (Paisley, UK)

JEOL (Tokyo, Japan)

Labtech International Ltd (East Sussex, UK)

Leica Microsystems (Heidelberg, Germany)

Millipore (Hertfordshire, UK)

New England Biolabs (Hertfordshire, UK)

Olympus Optical (London, UK)

Qiagen (West Sussex, UK)

Raymond A Lamb (East Sussex, UK)

Roche Diagnostics (West Sussex, UK)

Santa Cruz Biotechnology Inc (Santa Cruz, CA, USA)

Sigma-Aldrich (Dorset, UK)

Soft Imaging System GmbH (Münster, Germany)

Starlabs (Buckinghamshire, UK)

TAAB Laboratory and Microscopy (Berkshire, UK)

Thermo Fisher Scientific (Surrey, UK)

Vector Laboratories (Peterborough, UK)

VWR International Ltd (Dorset, UK)

## **2.2 Materials**

### **2.2.1 Chemicals**

General chemicals were supplied by Sigma-Aldrich or Thermo Fisher Scientific unless stated otherwise.

### **2.2.2 Histology**

Plastic processing cassettes, accu-edge low profile microtome blades, paraffin wax and cork discs were all supplied by Raymond A Lamb Ltd. VWR International Ltd provided Superfrost slides, 22x50mm cover slips, xylene, optimum cutting temperature (OCT) embedding compound, dibutyl phthalate and xylene (DPX) mountant, formaldehyde, ethanol, haematoxylin and eosin (H&E) stain, isopentane and hydrogen peroxide. Poly-L-lysine and mineral oil were purchased from Sigma-Aldrich.

### **2.2.3 Laser capture microdissection**

PALM slides with a 1.0 PEN (polyethylene naphthalate) membrane were supplied by Carl Zeiss Microscopy and mounted tissue was stained with toluidine blue dye from Sigma-Aldrich.

### **2.2.4 DNA extraction and purification kits**

Proteinase K, QIAamp DNA mini kits and QIAamp DNA microkits were supplied by Qiagen. Isopropanol was obtained from VWR International Ltd.

**2.2.5 Oligonucleotide primers and dNTPs**

Deoxynucleotidetriphosphates (dATP, dTTP, dCTP and dGTP) were obtained from GE Healthcare. High purity salt free oligonucleotide primers were purchased from either Eurofins MWG Operon or Eurogentec. Primer stock solutions were made by dilution to 100pM in sterile water, produced by Fresenius Kabi AG.

**2.2.6 PCR**

Applied Biosystems provided AmpliTaq Gold DNA polymerase and 10x PCR buffer.

**2.2.7 PCR Purification**

New England Biolabs supplied restriction enzyme Exonuclease I and GE Healthcare provided the Shrimp Alkaline Phosphatase.

**2.2.8 Electrophoresis**

Agarose powder was obtained from Roche Biochemicals.

**2.2.9 DNA size markers**

1Kb DNA ladder was purchased from Invitrogen Life Technologies.

**2.2.10 Sequencing and DNA clean up**

POP6 polymer, BigDye® Terminator v3.1 and v1.1 Cycle sequencing kits were obtained from Applied Biosystems. Montage SEQ<sub>96</sub> sequencing reaction clean-up kits were purchased from Millipore.

**2.2.11 Antibodies**

Cell Signalling Technologies supplied the anti-phospho-histone H3 (Ser<sup>10</sup>) (#9701), the anti-phospho-Stat3 (Tyr<sup>705</sup>) (#9131), the anti-phospho-p65 (Ser<sup>276</sup>) (#3037), the anti-phospho-Akt (Ser<sup>473</sup>) (#4060) the anti-phospho-Met (Tyr<sup>1234/1235</sup>) (#3077), the anti-cleaved Caspase-3 (Asp<sup>175</sup>) (#9661) and the anti-phospho-S6 ribosomal protein (Ser<sup>240/244</sup>) (#2211) antibodies. Anti-Cytokeratin 19 (N-13) (sc-33111-R) antibody was purchased from Santa Cruz Biotechnology Inc, along with anti-phospho-Jak2 (Tyr<sup>1007/1008</sup>) (sc-16566-R). Anti-Bcl2 antibody (ab7973) was purchased from Abcam. BioGenex supplied an anti-p53 antibody. Fluorescein conjugated chicken anti-goat IgG and rhodamine conjugated goat anti-rabbit IgG were obtained from Millipore.

### **2.2.12 Immunohistochemistry**

Vector Laboratories supplied the rabbit Vectastain Elite ABC horseradish peroxidase kit and the 3, 3'-diaminobenzidine (DAB) peroxidase substrate kit. Cytomation wax pens were supplied by DAKO.

### **2.2.13 Immunofluorescence**

Sigma-Aldrich provided the Triton X-100. Goat serum was purchased from Vector Laboratories and Invitrogen Life Technologies supplied the ProLong® Gold anti-fade reagent with DAPI.

### **2.2.14 Scanning electron microscopy**

Phosphate buffered saline for use during perfusion fixation was supplied by Sigma-Aldrich. Hexamethyldisilazane (HMDS), carbon paint, aluminium stubs, 70% vacuum distilled glutaraldehyde and 16% methanol-free formaldehyde were all provided by TAAB Laboratory and Microscopy.

## **2.3 Equipment**

### **2.3.1 Plastics**

Sterile pipette tips (all sizes) provided by Starlabs. Plastic eppendorf tubes (0.6ml, 1.5ml and 2.0ml) purchased from Bioquote. Anachem provided 96-well plastic plates, while ABGene produced the adhesive PCR film. Bibby Sterling supplied the sterile universal tubes.

### **2.3.2 Histology**

InterFocus Ltd provided tweezers and scissors used in mouse dissection. Fixed tissue processing was facilitated by a Thermo Shandon Citadel 2000 tissue processor and embedded with a Raymond A Lamb Ltd wax embedder. A Leica RM2235 microtome was used to cut paraffin sections and slides were stained with H&E on a Thermo Shandon Varistain Gemini machine. Frozen tissue was cut on a cryostat, and a sledge microtome with freezing stage (Bright Instrument Co Ltd) was used to cut un-embedded fixed tissue. An Olympus BX51 BF light microscope was used to analyse H&E and immunohistochemistry samples. Slides for paraffin embedded tissue were obtained from Superfrost and for frozen tissue destined for laser capture microdissection, special PALM slides with 1.0 PEN membrane were



purchased from Carl Zeiss MicroImaging GmbH. Both types of slide were pre-treated with UV light for 30 minutes and then with Poly-L-Lysine solution for 5 minutes. Drying took place overnight in a 40°C oven.

### **2.3.3 Immunohistochemistry and immunofluorescence**

Plastic slide racks and cardboard slide holders were supplied by Raymond A Lamb Ltd. An Olympus BX51 BF microscope fitted with a mercury lamp was used to analyse the immunofluorescent samples.

### **2.3.4 DNA quantifications and thermocycling**

A NanoDrop 8-Sample Spectrophotometer supplied by Labtech International was used to measure DNA concentration. Thermocycling was carried out in a DNA thermal cycler 480 from Applied Biosystems. Ninety-six well plates were thermocycled on a PTC-225 Peltier thermal cycler from GRI.

### **2.3.5 Electrophoresis**

Invitrogen Life Technologies provided the Horizon 11.14 gel tanks used for agarose gel electrophoresis. Power packs were obtained from Bio-Rad Laboratories Ltd.

### **2.3.6 Scanning electron microscopy**

Dehydrated samples mounted on aluminium stubs with carbon paint were sputter coated with gold using an EMScope vacuum coater. Samples were then viewed in a JEOL 840A scanning electron microscope.

### **2.3.7 Laser capture microdissection**

Samples were viewed and dissected on a PALM Microlaser system and visualised using the associated PALM Robo software.

### **2.3.8 Photography**

Agarose gels were photographed using a Gel Doc 2000 ultraviolet Transluminator from Bio-Rad Laboratories Ltd and printed via a Mitsubishi P91 video processor stocked with high-density thermal paper. A Carl Zeiss Axiocam digital camera was used to capture micrographs.

### **2.3.9 Software**

AxioVision software from Carl Zeiss Vision was used for fluorescent image analysis. Soft Imaging System GmbH provided the AnalySIS software used to measure cilia in scanning electron micrographs. Minitab 15, SPSS 16 and Microsoft Excel were used to facilitate statistical analysis and graph construction. Sequencer 4.6 was used to analyse sequencing data.

## **2.4 Solutions**

- 1xTAE (0.4M Tris-acetate, 10mM EDTA, pH 8.0)
- 1xTBS (0.15M NaCl, 0.005M Tris, pH 7.6)
- Tail Buffer (50mM Tris, 100mM EDTA, 100mM NaCl, 1% SDS, pH 8.0)
- 1xTBS/0.3% Triton X-100 (to produce 1 litre solution: 100ml 10xTBS, 900ml dH<sub>2</sub>O, 3ml Triton X-100)
- 1xTBS/4% BSA (to produce 50ml solution: 2g BSA in 5ml 10xTBS, 45ml dH<sub>2</sub>O)
- 10mM sodium citrate buffer (to produce 1 litre solution: 2.94g sodium citrate trisodium salt dehydrate, 1L dH<sub>2</sub>O, pH 6.0)
- 10% formal saline (to produce 1 litre solution: 100ml 38% w/w formaldehyde, 900ml dH<sub>2</sub>O, 9g NaCl)
- 0.3% H<sub>2</sub>O<sub>2</sub> solution (for 300ml: 300ml dH<sub>2</sub>O, 3ml 30% w/v H<sub>2</sub>O<sub>2</sub>)
- Phosphate buffered 4% formaldehyde/0.2% glutaraldehyde (PBFG)
  - Buffer solution of 3.35% sucrose and 0.167M Na<sub>2</sub>HPO<sub>4</sub> (pH 7.4).
  - Add 40% formaldehyde (produced from 16% methanol-free formaldehyde stock) in a 40:60 ratio with the buffer solution to produce a 4% formaldehyde in 100mM buffer + 2% sucrose solution.
  - Filter the cloudy solution through fine filter paper.
  - Glutaraldehyde (70% vacuum distilled) is added to 0.2% (2.857ml/L) to produce PBFG, which can be transferred into smaller containers and stored at -30°C.

## **2.5 Methods**

### **2.5.1 Animal husbandry**

All procedures with animals were carried out in accordance with Home Office guidelines. Mice used in this study were kept in filter top cages and supplied with



filtered food and water. These cages were maintained on a 12 hour light, 12 hour dark cycle (7:30 to 19:30 each day) and kept at a constant 22°C temperature. *Tsc1*<sup>+/-</sup> mice on a Balb/c background (Wilson *et al.* 2005) were crossed with *Tsc2*<sup>+/-</sup> mice on a Balb/c background (Onda *et al.* 1999) and *Pkd1*<sup>+/-</sup> mice on a 129/Sv background (Boulter *et al.* 2001) to produce *Tsc1*<sup>+/-</sup>, *Tsc2*<sup>+/-</sup>, *Pkd1*<sup>+/-</sup>, *Tsc1*<sup>+/-</sup>*Pkd1*<sup>+/-</sup> and *Tsc2*<sup>+/-</sup>*Pkd1*<sup>+/-</sup> mice, as well as wild-type littermates. Identification of mice was facilitated through microchip implantation and tail tip samples were removed for genotyping under a local anaesthetic. Mice were killed by cervical dislocation.

## **2.5.2 Necropsy analysis**

Brain, lungs, heart, kidneys, spleen, uterus (in females) and liver underwent macroscopic analysis upon dissection. Once removed from the body, organs were longitudinally bisected with a scalpel blade, with half fixed and processed to paraffin wax for sectioning and the other half being snap frozen. Bisected kidneys and liver tissue removed for SEM analysis were fixed overnight in PBFG and transferred to 1xTBS for longer storage. Large hepatic cysts from 20 month old mice were removed, fixed overnight in PBFG and set aside for SEM processing.

## **2.5.3 Histology**

### **2.5.3.1 Tissue fixation, embedding and sectioning**

Formaldehyde based solutions are able to penetrate deep into tissue due to its small molecular size. Once immersed, CH<sub>2</sub> cross-links form between protein amino groups in the tissue, thus preserving tissue morphology and integrity. Formaldehyde is also an effective disinfectant, ensuring no fungal or bacterial contamination of the tissue at this early stage in processing.

Dissected tissue was transferred to a universal tube containing 10% formal saline solution and left on the bench top at room temperature overnight. The sample was then drained and moved to a solution of 1xTBS for long term storage of fixed tissue at 6°C. Fixed tissue was placed on to the processor in solutions of 70%, 90% and 100% ethanol for an hour each. This was followed by two sets of 2 hour immersions in 100% ethanol solution and 1 hour in xylene. Finally, the tissue was transferred to a fresh solution of xylene for 1.5 hours, a step which was repeated, and then moved to

paraffin wax for 3 hours, twice. During the final embedding stage, tissues were placed into paraffin cut side down and at stored at room temperature.

Paraffin embedded livers and kidneys were sectioned at 4µm, placed in a 60°C water bath and floated onto poly-L-lysine treated Superfrost slides. Slides were moved to a 45°C oven for drying overnight and stored at room temperature the following morning.

#### *2.5.3.2 Snap freezing and PALM slide sectioning*

Following dissection, tissue was placed cut side down onto cork disks and coated with OCT embedding medium. The sample was transferred to a 1-litre glass beaker containing liquid nitrogen cooled isopentane and left until the OCT became opaque and the tissue was deemed frozen. The frozen tissue was removed using forceps and stored in cryotubes at -80°C. A medium was used to snap freeze the samples as direct freezing with liquid nitrogen is less efficient in terms of heat transfer and can lead to ice crystal formation.

Frozen kidney samples were sectioned at 10µm on a freezing stage cryostat (set to -20°C) and transferred onto PALM slides. This thicker sectioning increased tissue integrity during slide mounting and allowed more tissue depth to obtain genetic material from during microdissection. Once cut, these slides were dried at room temperature and stored long term at -20°C.

#### *2.5.3.3 Perfusion fixation*

In order to maintain the fine morphological detail needed during SEM analysis of primary cilia in hepatic bile ducts, a mixture of formaldehyde and glutaraldehyde (PBFG) was used to quickly and efficiently cross-link mouse livers following cervical dislocation. Due to the small molecular size of formaldehyde, quick tissue infiltration was possible. This initial cross-linking was then complimented by the slower penetrating but more stabilising glutaraldehyde. Through the action of PBFG, hepatic bile ducts and the associated primary cilia were fixed in their physiological positions and able to withstand the chemically harsh processing needed for SEM analysis.

Following animal sacrifice, the rib cage was opened up and clamped to expose the heart and lungs. Dissection scissors were used to cut the right oracle and provide a drainage point for blood, saline and fixative pumped around the body during the procedure. A second incision of around 2-3mm was made on the left ventricle, providing an entry point for a blunted syringe needle. This was clamped in place to ensure a water-tight seal. A syringe with 50ml PBS was attached to the needle and gentle pressure was applied to flush the mouse of blood. A second syringe with 50ml PBFG was then pumped through the bloodstream and correct fixation was indicated by blanching of liver and muscle contractions of the deceased mouse. The liver was then removed and placed into a universal tube containing more PBFG. Following 24 hour immersion, samples were transferred into 2.3M sucrose in TBS solution for long term storage at 6°C.

#### *2.5.3.4 Haematoxylin and eosin staining*

To expose often subtle kidney and liver lesions such as cysts, H&E staining was used. The haematoxylin colours the nuclei of cells blue, while a counterstain of eosin colours eosinophilic structures (including the majority of the cytoplasm) pink. Paraffin embedded sections were H&E stained using the following protocol: xylene (1 minute) x3, 100% ethanol (1 minute) x2, 70% ethanol (1 minute), Meyer's haematoxylin (5 minutes), running water (1 minute), eosin (2 minutes), running water (1 minute), 70% ethanol (1 minute), 100% ethanol (1 minute) x2, xylene (1 minute) x2. Cover slips and DPX were used to mount the sections and these were left to air dry in a fume-hood.

#### **2.5.4 Laser capture microdissection**

Laser capture microdissection allows highly selective excision of user-defined areas of tissue, perfect for cutting around the cysts present in our mice. Frozen tissue was sectioned onto poly-L-lysine and UV treated PEN membrane covered slides. Following a 5 minute wash in tap water, samples were treated with toluidine blue stain for 2 seconds and rewashed under tap water. Sections were then passed through 50%, 70% and 100% ethanol solutions for 15 seconds and dried on the bench top overnight. Slides placed under the PALM Microlaser system were cut with a pulsed UV laser. The focused laser beam dissects tissue without heating adjacent

material, and leaves a defined gap between the newly isolated cyst and surroundings. Samples are then automatically ejected from the plane and captured in the oil coated cap of a microfuge tube (positioned above the slide). Through analysis of serial sections, cysts can be followed over several slides and multiple samples collected to increase the amount of genetic material obtained. Microfuge tubes containing sample cystic tissue were transferred to a -80°C freezer for long term storage.

## **2.5.5 Nucleic acid extraction**

### *2.5.5.1 DNA extraction from tail tips*

Routine DNA analysis was conducted on our mice in order to ascertain genotype for breeding and experimental purposes. The top 3mm of each mouse tail was removed and frozen prior to DNA extraction. After thawing, tail tips were placed in 2ml eppendorf tubes together with 500µl tail buffer and 20µl proteinase K (20mg/ml) and incubated in a 65°C water bath overnight. The following morning, the samples were agitated in a bench top vortex and assessed for digestion. An extra 20µl proteinase K was added and vortexed if the tail was not fully digested. The resulting lysate was added to 250µl of 6M supersaturated NaCl (causing precipitation of proteins and carbohydrates but leaving DNA in solution) and vortexed until a cloudy colour was produced. This was centrifuged at 13,000 rpm for 10 minutes to produce a salt pellet and clear supernatant. The supernatant was transferred into a 1.5ml eppendorf along with 150µl of isopropanol and manually inverted to precipitate DNA. If a DNA precipitate could not be seen, tubes were left overnight at -20°C to aid the process. DNA was separated from the remaining solution with centrifugation at 13,000 rpm for 5 minutes, removed and washed with 150µl of 70% ethanol. The final stage required the pellet to be air-dried for 15 minutes to ensure complete removal of residual ethanol. DNA pellets were resuspended in 30-50µl of DNase-free water overnight at 35°C before storage at -20°C.

### *2.5.5.2 DNA extraction from laser microdissected tissue*

DNA was extracted from microdissected frozen tissue (see section 2.5.4) using QIAamp DNA mini kits and following the manufacturers' instructions. DNA from the tissue is bound to a silica-gel membrane in a salt medium and through repeated

washing with various buffers impurities are gradually removed, leaving just the DNA. Microdissected cysts in microfuge tube lids were left overnight at 65°C with 180µl of Buffer ATL and 20µl of proteinase K prior to incubation. The lysed tissue was added to 200µl of Buffer AL and incubated for 10 minutes at 70°C. This solution was combined with 200µl of 100% ethanol and transferred to a QIAamp silica gel based Spin Column and centrifuged for 1 minute at 8,000 rpm. The filtrate in the collecting tube was discarded and the Spin Column was transferred to a fresh collection tube where 500µl of Buffer AW1 was added and the solution re-centrifuged for 1 minute at 8,000 rpm. The filtrate was discarded and a second wash was performed using 500µl of Buffer AW2 and spinning for 3 minutes at 13,000 rpm. This was followed by an extra 1 minute of centrifugation to remove residual buffer from the washes. Finally, DNA was eluted in a variable amount of DNase free water (ranging from 20µl to 200µl for concentrated samples) by incubating the membrane at room temperature for 5 minutes and centrifuging at 13,000 rpm for 1 minute. The resulting samples were stored at -20°C.

### **2.5.6 Nucleic acid quantification**

DNA concentrations were determined using UV spectrophotometry at wavelengths of 260nm and 280nm. A ratio of 1.8 at 260nm:280nm implies high sample purity.

### **2.5.7 Oligonucleotide primer design**

Web-based program Primer 3 (Rozen *et al.* 2000) was used to design primers between 18 and 23 nucleotides in length. Primers deemed to have repetitive motifs, a high likelihood to dimerise or form secondary structures were selected against. Attempts were made to represent the four bases in equal amounts, and to ensure melting temperatures of the primer pairs used were within 2°C of each other.

### **2.5.8 Polymerase chain reaction**

The polymerase chain reaction, or PCR, allows selective amplification of DNA sequences. The procedure relies on the repetition of 20-40 thermal cycles, with each cycle consisting of 3 discrete stages (denaturation, annealing and elongation). The initial denaturation step occurs at a high temperature to separate the double helix template DNA into single strands. A cooler annealing step follows that allows primers

to bind to complimentary DNA sequences and direct new DNA synthesis. During elongation, DNA polymerase synthesises a new DNA strand complementary to the primer bound DNA template strand by adding dNTPs.

PCR conditions for genotyping of mouse DNA were set as follows: 25ng of template DNA, 2µl 10x reaction buffer (100mM TrisHCl, pH8.3, 500mM KCl, 15mM MgCl<sub>2</sub>, 0.01% w/v gelatin), 0.25mM dNTPs, 25pmol of each primer, 0.5 Units (U) of AmpliTaq Gold DNA Polymerase in a total reaction volume of 20µl. These amounts were then scaled up to a 50µl total volume and covered in a layer of mineral oil to insulate the reaction mixture against evaporation. Cycling temperature conditions were set as follows: initial denaturation at 94°C for 10-12 minutes, 35 cycles of 52°C-60°C (denaturation) for 1 minute, 72°C for 1-2 minutes (annealing) and 94°C for 1 minute (extension). The PCR ends with a final elongation step for 12 minutes at 72°C, and is then held at 4°C until the products are removed from the machine.

### **2.5.9 Agarose gel electrophoresis**

Small and large DNA fragments will travel different distances when passing through an agarose gel under an electrical current. Due to the negatively-charged phosphate groups, DNA will migrate from the negative electrode to the positive electrode when in an ion solution. Agarose acts as a molecular sieve, restricting the passage of DNA in a size and shape dependent manner. By increasing the concentration of agarose present in the gel mixture, gel pore size decreases and better separation can be achieved in terms of small DNA fragments.

Agarose gels of 2% w/v concentration were prepared using 1x TAE buffer. To this, 0.05µg/ml ethidium bromide was added. This dye combines with any DNA present on the gel and subsequently makes the nucleic acid visible under ultra-violet (UV) light. A plastic comb was used to create wells in the gel, and to these, 10µl of PCR sample mixed with 2µl of loading dye (15% w/v ficol, 10mM Tris pH 8, 1mM EDTA, 0.2% orange G dye) was added. Fragment sizes were determined through comparison with a 1kb DNA fragment ladder run on the same gel in a separate well. Once loaded, gels were submerged in 1x TAE buffer and run at 100 volts for approximately an hour. Following sufficient migration of the loading dye down the

gel, DNA was visualised through UV exposure at 300nm wavelength and images captured on a Gel Doc 2000 system.

### **2.5.10 PCR purification**

PCR products destined for cyclic sequencing require purification to remove non-incorporated dNTPs and primers from the reaction mixtures. To do this, the hydrolytic enzymes Exonuclease I (Exo) and Shrimp Alkaline Phosphatase (SAP) were used to degrade any single stranded primers and hydrolyse dNTPs respectively. To 15µl PCR product, 5µl Exo I and 0.5µl SAP were added and incubated at 37°C for 1 hour. This was followed by an 80°C denaturation step for 15 minutes.

### **2.5.11 Cycle sequencing**

The chain termination method of DNA sequencing was first envisaged by Sanger (1977), and relies on 2', 3' di-deoxynucleotide triphosphates (ddNTPs). These molecules lack the 3' OH group found on dNTPs and cannot form phosphodiester bonds once incorporated into a DNA chain, leading to termination. During the specialised PCR reaction, DNA strands are produced by a polymerase using normal dNTPs and terminating ddNTPs. As the cyclic amplification continues, single stranded DNA fragments are formed, differing in length by one base. Since the 4 types of ddNTP (ddATP, ddCTP, ddGTP and ddTTP) are fluorescently labelled with identifying colours, the sequencing reaction can take place in one tube. The ABI sequencer can identify the position of the labelled base by passing the DNA through a capillary gel. The smaller fragments in the mixture will migrate faster across the gel and reach the laser beam for analysis in a size dependent order. The emitted wavelength is detected and related to the specific ddNTP incorporated in the chain.

The BigDye® Terminator Cycle Sequencing kit (Version 3.1 or 1.1) was used during sequencing reactions. To make up a total reaction volume of 10µl, 5µl of purified PCR product (see section 2.5.10) was added, along with 0.16µl of primers, 0.25µl of terminator ready reaction mix (which contained A, C, T and G dye terminators, dNTPs, AmpliTaq DNA polymerase FS, MgCl<sub>2</sub> and Tris-HCl buffer, pH 9.0), 2µl BigDye® terminator sequencing 5x buffer and 2.59µl purified water. Conditions for sequencing were set as follows: 96°C for 1 minute followed by 25 cycles of 96°C for

10 seconds, 50°C for 5 seconds and 60°C for 210 seconds. Montage SEQ<sub>96</sub> sequencing reaction clean up kits were then used to purify the cycle sequencing products. Twenty micro litres of injection fluid was added to the sequencing reactions and transferred to a micro well filter plate. The samples were drawn through the plate using a vacuum pump (20 inches Hg). This step was repeated with two additional washes of injection fluid (25µl). The purified sequencing products were re-suspended in 20µl of injection fluid by shaking on an orbital mixer for 10 minutes. Ten micro litres of sample were run on an ABI 3100 Genetic Analyser and the resulting sequence data viewed on Sequencher version 4.6.

### **2.5.12 Immunohistochemistry**

Immunohistochemistry (IHC) refers to the process of localising antigens in cells of a tissue section through specific binding to complimentary antibodies. An avidin-biotin complex (ABC) method was used that exploits the very high affinity between the large glycoprotein avidin and the vitamin biotin. Biotin can be conjugated on to antibodies whilst avidin can be labelled with peroxidase or fluorescein. The ABC IHC method involves application of the unlabeled primary antibody, addition of a biotin-conjugated secondary antibody and the application of avidin-biotin peroxidase. The antigen-localised peroxidase is then developed using DAB to produce a colour change. As avidin has 4 binding sites for biotin, the signal produced is amplified significantly.

Slides containing paraffin embedded 5 micron thick sections of kidneys and livers were deparaffinised and rehydrated by immersing in xylene x2, 100% ethanol x2, 70% ethanol, 50% ethanol and water for 5 minutes per wash. For antigen retrieval, sections were placed in a plastic slide rack and boiled in 10mM citrate buffer (pH 6.0) for 10 minutes. Slides were cooled under running tap water for 5 minutes then transferred to a solution of hydrogen peroxide (0.3%) for 20 minutes to block endogenous peroxidase activity. Following another 5 minute wash under running tap water, slides were placed in 1xTBS solution for 5 minutes. The rabbit VECTASTAIN ELITE ABC horseradish peroxidase kit was used to immunostain paraffin sections. This kit contains the goat serum, rabbit secondary antibody and avidin-biotin complex components. A wax pen was used to circle the sections and 100µl blocking solution was added to each slide (7.5µl goat serum and 500µl dH<sub>2</sub>O). This was



incubated in a humidified chamber for 20 minutes. Primary antibodies were diluted to optimal concentrations in 1x TBS or 1x TBS/4% BSA (depending on manufactures' recommendations), applied and left overnight at 6°C. The following morning, slides were washed in 1xTBS for 5 minutes x2 and exposed to the biotinylated secondary antibody (2.5µl secondary antibody, 7.5µl goat serum, 500µl dH<sub>2</sub>O) for 30 minutes. After another two 5 minute washes in 1xTBS, 100µl of avidin-biotin complex was added to each slide and incubated for 30 minutes. After another two 5 minute washes in 1xTBS, sections were developed using DAB, counterstained in Gills haematoxylin for 1 minute and blued in tap water. The final dehydration stage required 5 minute immersions in 50% ethanol, 70% ethanol, 100% ethanol x2 and xylene x2. DPX was used to mount the slides with cover slips and these were left to air dry in a fume hood. An Olympus BX51 microscope was used to view the results.

#### **2.5.13 Double immunofluorescence staining**

Double immunofluorescence staining is similar to the previous protocol in section 2.5.12. However, in order to visualise a pair of antigens in a sample, such as a biomarker for a specific tissue type (e.g. anti-Cytokeratin 19 for cholangiocytes) and a marker for a specific event (e.g. anti-phospho-histone H3 for dividing cells), certain modifications must be made to the standard IHC protocol. By choosing antibodies derived from different animals (but not mouse, as this is the target tissue), the reagents can be incubated as a single cocktail. Secondary antibodies are selected to specifically recognise these antibodies and will have conjugated fluorescent molecules for detection. There is no need for ABC peroxidase to visualise the staining, so steps involving hydrogen peroxide, ABC application and DAB can be omitted. However, because of the sensitive nature of the fluorescent molecules used, care must be taken to shield the sections from exposure to natural light. Overexposure during the protocol will lead to a reduction in signal intensity when the slides are analysed, so tin foil is used to prevent this.

Slides containing paraffin embedded 5 micron thick sections of kidneys and livers were deparaffinised and rehydrated by immersing in xylene x2, 100% ethanol x2, 70% ethanol, 50% ethanol and water for 5 minutes per wash. For antigen retrieval, sections were placed in a plastic slide rack and boiled in 10mM citrate buffer (pH 6.0) for 10 minutes. Slides were cooled under running tap water for 5 minutes then

transferred to a solution of hydrogen peroxide (0.3%) for 20 minutes to block endogenous peroxidase activity. Following another 5 minute wash under running tap water, slides were placed in 1xTBS solution for 5 minutes. Blocking was carried out in 2x 5 minute washes in 1xTBS/0.6% bovine serum albumin (BSA). Through-out the protocol, immunofluorescent staining was carried out in a humidified chamber, covered in tin foil and placed in a dark cupboard. This was to minimise evaporation from the sections, keep out light and preserve fluorescence. A wax pen was used to circle the sections and 100µl of antibody solution (consisting of an optimal concentration of antibody diluted in 1x TBS) was applied prior to overnight incubation at 6°C. The following morning, slides were washed twice in 1xTBS/0.6% BSA for 5 minutes and immersed for 1 hour in fluorescent secondary antibody. A further two 5 minute washes in 1xTBS/0.6% bovine serum albumin followed this, and then sections were mounted using ProLong<sup>®</sup> Gold antifade reagent with DAPI and allowed to cure overnight in the dark. Slides were sealed with clear nail varnish and examined immediately on an Olympus BX51 microscope. Slides transported in the light were covered with tin foil to minimise loss of fluorescent signal. For storage, slides were kept at 6°C in a light-proof container.

#### **2.5.14 Scanning electron microscopy**

Samples were prepared for SEM analysis according to the hexamethyldisilazane (HMDS) method (Nation 1983), which progressively lowers the water content of the tissue without shrinkage or distortion of the surface.

Tissues underwent two 10 minute washes in dH<sub>2</sub>O, followed by successive washes for 15 minutes in 50%, 70%, 90% and twice in 100% ethanol. The samples were fully dehydrated by three 10 minute immersions in HMDS and transferred to a perspex cabinet with silica gel crystals to prevent re-hydration of the desiccated tissue during the final air drying stage. Carbon paint was used to mount the specimens onto aluminium stubs, which were transferred to an EMScope vacuum coater and sputter coated with gold. Sample analysis was carried out at 5kV using a JEOL 840A scanning electron microscope.

## **CHAPTER THREE: Investigating the role of hamartin, tuberin and polycystin-1 in cystogenesis, ciliogenesis and planar cell polarity.**

### **3.1 Introduction**

Patients with TSC often develop renal cysts and those with contiguous germline deletions of *TSC2* and *PKD1* develop severe infantile polycystic kidney disease (Brook-Carter *et al.* 1994), suggesting a functional co-operation between their gene products (Chapter 1, Section 1.1.10). Hamartin and tuberin function as a complex within the PI3K-Akt-mTOR pathway and regulate nutrient and growth factor signalling to mTOR (Chapter 1, Section 1.1.10). Many lesions from patients with TSC exhibit activation of mTOR and clinical trials are underway for the treatment of these tumours using mTOR inhibitors (Bissler *et al.* 2008, Davies *et al.* 2008).

The primary cilium is a microtubule based sensory organelle that receives both mechanical and chemical signals from other cells and the environment, and transmits these signals to the nucleus to elicit a cellular response (Chapter 1, Section 1.2.9.3.1). Primary cilia are anchored to the cell via the basal body. Hamartin has been localised to the basal body (Hartman *et al.* 2009) and tuberin interacts with the *ADPKD1* gene product, polycystin-1 (Shillingford *et al.* 2006), which has been localised to the primary cilium (Yoder *et al.* 2002). Numerous other proteins associated with cystic kidney disease have also been localised to the renal cilium or basal body including the ADPKD2 protein polycystin-2 (Yoder *et al.* 2002, Pazour *et al.* 2002), the product of the human autosomal recessive polycystic kidney disease gene (*PKHD1*), fibrocystin (Ward *et al.* 2003), and polaris and cystin, which are mutated in two mouse models of polycystic kidney disease (Yoder *et al.* 2002). Mice with mutant polaris develop shortened cilia or no cilia in kidney epithelia (Pazour *et al.* 2000) and PCK rats (an orthologous model for *PKHD1*) (Ward *et al.* 2002) have cilia that are abnormal and shortened (Masyuk *et al.* 2003).

Renal primary cilia monitor urinary flow through kidney tubules via the mechanotransduction properties of polycystin-1 and polycystin-2 (Nauli *et al.* 2003), and the ciliary protein inversin acts as a molecular switch from the canonical to the noncanonical/planar cell polarity (PCP) Wnt signalling pathways by targeting cytoplasmic dishevelled (Dsh) for degradation (Simons *et al.* 2005) (Chapter 1,

Section 1.3.2). Furthermore, mutations in *Kif3a*, *Ift88* and *Odf1*, that disrupt ciliogenesis, restricts the activity of the canonical Wnt pathway with loss of *Kif3a* causing constitutive phosphorylation of Dsh (Corbit *et al.* 2008). Interestingly, hamartin and tuberin associate with the GSK3/axin complex to promote  $\beta$ -catenin degradation and inhibit canonical Wnt-signalling (Mak *et al.* 2003) and tuberin also interacts with Dsh upon Wnt stimulation (Mak *et al.* 2005). The lengthening of developing renal tubules is associated with the mitotic orientation of cells along the tubule axis demonstrating intrinsic PCP (Fischer *et al.* 2006) and this oriented cell division is thought to dictate the maintenance of constant tubule diameter during tubular lengthening, thereby preventing renal cyst formation (Germino 2005) (Chapter 1, Section 1.3.4). Defects in this process have been found in mice with a renal-specific inactivation of *Tcf2*, a transcription factor essential for the expression of genes involved in polycystic kidney disease (Fischer *et al.* 2006), the PCK rat (Fischer *et al.* 2006) and *Kif3a* mutant mice (Patel *et al.* 2008).

While hepatic involvement in TSC sufferers is limited to AMLs, patients with ADPKD will experience progressive renal and hepatic cyst formation (Lu *et al.* 1999). The liver is analogous to the kidney in several ways (Alpini *et al.* 1997) that make it an attractive target for research. The entire organ is perfused by bile ducts, lined with simple epithelia or cholangiocytes that modify through a series of absorptive and secretory events, bile of canalicular origin before it reaches the bowel (Alpini *et al.* 1997). These ducts develop in a similar manner to kidney tubules, carrying bile instead of urine, and are lined with primary ciliated epithelial cells as found in renal tissue (Huang *et al.* 2006). Just as renal cysts are known to arise from kidney tubules, the hepatic cysts seen in *Pkd1* mice have been shown to develop from these bile ducts (Lu *et al.* 1999). Renal tubules demonstrate high levels of intrinsic cell polarity that allows intense cell proliferation during kidney development to lead to tubule elongation with a constant diameter (Fischer *et al.* 2006, Simons *et al.* 2006). Hepatic tissue must meet a similar challenge when forming the complex biliary tree and it is likely precise orientation of cell division is required for this process.

Here, we investigate the relationship between hamartin, tuberin and polycystin-1 through examining *Tsc1*<sup>+/-</sup>, *Tsc2*<sup>+/-</sup> and *Pkd1*<sup>+/-</sup> mice, and their compound heterozygous littermates. To understand the role these proteins play in primary cilia formation and cell polarity, we sought defects in these processes in our mice.

### 3.2 Materials and methods

#### 3.2.1 DNA extraction and genotyping

Following the method outlined in Chapter 2, Section 2.5.5, DNA was extracted from scalpel-dissected tail tips using NaCl/isopropanol. PCR amplification of wild-type or mutant alleles for *Tsc1*, *Tsc2* and *Pkd1* was performed using the following primers in a 35 cycle reaction with AmpliTaq gold DNA polymerase (Applied Biosystems): *Tsc1* wild-type, Ex8F 5'-TGCCTGGAAGCCCAGGAAGGT-3' and Ex8R 5'-CTGCAGGGCCCATGGTGGTT-3' (183bp product), *Tsc1* mutant, TSC1HETF2 5'-CGTTGGCTACCCGTGATATT-3' and TSC1HETR 5'-CCAATGGGCTCATTACTCTCA-3' (268bp product), *Tsc2* wild-type, genF 5'-AATCGCATCCGAATGATAGG-3' and TSC2WTR 5'-GTTTAATGGGCCCTGGATCT-3' (~900bp product), *Tsc2* mutant, genF and TSC2HETR 5'-GGATGATCTGGACGAAGAGC-3' (658bp product), *Pkd1* wild-type, PKD1WTF 5'-GCTCGCACTTTCAGCAATAAGAC-3' and PKDWTR 5'-CAGGATTTCCACTGGGTTCT-3' (661bp product), *Pkd1* mutant, PKDNEOF 5'-AGCGTTGGCTACCCGTGATATTG-3' and PKDEXON21R 5'-GTCTCCGTGATGTTCTTACGCATT-3' (731bp product). Products were analysed on 2% agarose gels.

#### 3.2.2 Animal care and husbandry

All procedures with our mice were carried out under Home Office guidelines outlined in Chapter 2, Section 2.5.1. *Tsc1*<sup>+/-</sup> (Wilson *et al.* 2005) and *Tsc2*<sup>+/-</sup> mice on a Balb/c background (Onda *et al.* 1999) were crossed with *Pkd1*<sup>+/-</sup> mice on a 129/Sv background (Boulter *et al.* 2001) to produce *Tsc1*<sup>+/-</sup>, *Tsc2*<sup>+/-</sup>, *Pkd1*<sup>+/-</sup>, *Tsc1*<sup>+/-</sup>*Pkd1*<sup>+/-</sup> and *Tsc2*<sup>+/-</sup>*Pkd1*<sup>+/-</sup> mice, as well as wild-type littermates. Livers from 10 day old mice, and kidneys from 48 hour and 10 day old mice, were removed following cervical dislocation and processed into paraffin wax for sectioning at 4µm. Livers and kidneys from 3 month old mice were removed, fixed in PBFG overnight and set aside for examination by SEM. Livers and kidneys from 15-18 month old mice were processed into paraffin wax for sectioning and lesion analysis. 20 month old mice were investigated for large hepatic cysts, and these were taken for SEM processing.

### 3.2.3 Immunohistochemistry

Five 4µm thick sections of paraffin embedded renal and hepatic tissue were cut from 9-12 month (kidney) or 15-18 month (liver) old wild-type, *Tsc1*<sup>+/-</sup>, *Tsc2*<sup>+/-</sup>, *Pkd1*<sup>+/-</sup>, *Tsc1*<sup>+/-</sup>*Pkd1*<sup>+/-</sup> and *Tsc2*<sup>+/-</sup>*Pkd1*<sup>+/-</sup> mice as described in Chapter 2, Section 2.5.12. A section was taken every 200µm from the samples to provide a representation of the respective organ. Slides were H&E stained to reveal lesions and evaluated under blind conditions. Analyses of hepatic tissues were led by myself and analyses of renal tissue were led by Dr. Cleo Bonnet in our laboratory.

### 3.2.4 Scanning electron microscopy

At least five mice of each genotype were culled and perfused transcardially with 40ml of phosphate buffered saline (PBS) at pH 7.4 followed by 50ml of phosphate buffered 4% formaldehyde / 0.2% glutaraldehyde (PBFG). The kidneys and liver were removed, bisected longitudinally, post-fixed for 24hrs in PBFG and infiltrated with 2.3M sucrose in tris buffered saline (TBS). Kidneys and livers were frozen and the tubule lumens and bile ducts exposed by sectioning with a freezing stage sledge microtome. All specimens were then dehydrated using the hexamethyldisilazane method (Nation 1983), mounted on aluminium stubs using carbon paint, sputter coated with gold using an EMscope vacuum coater and viewed at 5kV in a JEOL 840A SEM. Primary cilia lengths were measured using analySIS software by an observer blinded to genotype and exported as Microsoft excel tables.

### 3.2.5 Orientation of cell division

Kidney sections from mice at 48 hrs and 10 days of age and liver sections from mice at 10 days of age were stained with anti-phospho-histone H3 (Ser<sup>10</sup>) antibody (anti-H3pS10) (1:50 dilution) to label the chromosomes of dividing cells in late anaphase and telophase. Rehydrated 4µm kidney and liver sections were boiled in 10mM citrate buffer (pH 6.0) for 10 minutes and incubated overnight at 4°C with anti-H3pS10 and further incubated for 30 minutes at room temperature (RT) in the dark with tetramethyl rhodamine isothiocyanate (TRITC) conjugated goat anti-rabbit IgG (H+L) (1:300 dilution). Sections were counterstained with either fluorescein

isothiocyanate (FITC) *Lotus tetragonolobus* lectin (LTL) (1:100 dilution) for the proximal kidney tubule, FITC *Dolichos biflorus* agglutinin (DBA) (1:100 dilution) for the collecting duct or immune-stained overnight at 4°C with Tamm-Horsfall glycoprotein (THP) (1:150 dilution) for the thick limb of the loop of Henle/distal convoluted tubule or cytokeratin 19 (CK19) (1:100 dilution) for cholangiocytes lining the bile duct, followed by FITC conjugated chicken anti-goat IgG (H+L) (1:200 dilution). All staining with fluorescent labelled reagents was performed in the dark for 30 minutes at RT. Slides were mounted with ProLong® Gold antifade reagent with DAPI and examined using an Olympus BX51 microscope. Images were acquired using a Zeiss AxioCam digital camera and analysed with AxioVision software. The orientation of cell division was determined by measuring the angle between the mitotic spindles of dividing cells and the longitudinal axis of the kidney tubules or bile ducts, using five mice per genotype for the kidneys and 8 mice per genotype for the livers. Metaphase chromosomes were ignored to avoid the measurement of spindles that had not yet reached their definitive orientation. Image acquisition and angle measurement were carried out by an observer blinded to genotype.

### **3.2.6 Statistical analyses**

Lesion counts were compared using the Mann-Whitney U test. Primary cilia lengths were compared using the 2-sample T-test for parametrically distributed measurements, and the Mann-Whitney U test for non-parametric data. The chi-squared test was used to compare distributions of mitotic angles between genotypes.

## **3.3 Results**

### **3.3.1 Renal and hepatic pathology**

Several groups have previously published studies of the renal pathology seen in *Tsc1*<sup>+/-</sup> (Wilson *et al.* 2005, Wilson *et al.* 2006), *Tsc2*<sup>+/-</sup> (Onda *et al.* 1999) and *Pkd1*<sup>+/-</sup> (Boulter *et al.* 2001) mice. *Tsc1*<sup>+/-</sup> and *Tsc2*<sup>+/-</sup> mice experience a renal cystic phenotype in an age-dependent manner. By the age of 15-18 months, the majority of *Tsc1*<sup>+/-</sup> animals will have developed some form of renal lesion (Wilson *et al.* 2005),



while all *Tsc2*<sup>+/-</sup> mice will display renal cysts and cystadenomas by 15 months of age (Onda *et al.* 1999). *Tsc1*<sup>+/-</sup> mice occasionally develop small renal cysts by the age of 3 months. Renal lesions in these *Tsc1*<sup>+/-</sup> and *Tsc2*<sup>+/-</sup> animals ranged from simple cysts, with a single epithelial cell lining, branching cysts, cystadenomas (cysts with papillae projections into the lumen) and renal cell carcinomas (Figure 3.1). Simple cysts are smaller and more numerous than cystadenomas and RCCs, suggesting these lesions progress from cysts to cystadenomas to RCCs (Wilson *et al.* 2006). *Pkd1*<sup>+/-</sup> mice experience a milder renal phenotype, with microscopic cysts observed in approximately half of mice analysed at 9 months of age (Boulter *et al.* 2001). These cysts were noted to arise throughout the nephron and be present in mice as young as 3 months old. All three mouse models (*Tsc1*<sup>+/-</sup>, *Tsc2*<sup>+/-</sup> and *Pkd1*<sup>+/-</sup>) have been observed to die *in utero* with a homozygous genotype.

#### 3.3.1.1 Renal lesion analysis

Here, we examined the functional relationship between hamartin, tuberin and polycystin-1 by crossing *Tsc1*<sup>+/-</sup> and *Tsc2*<sup>+/-</sup> mice with *Pkd1*<sup>+/-</sup> mice to produce compound heterozygotes. We found that *Tsc1*<sup>+/-</sup>*Pkd1*<sup>+/-</sup> mice had significantly more renal lesions (an average of 33.2 microscopic lesions per mouse) as compared to either *Pkd1*<sup>+/-</sup> (5.2 lesions per mouse, *P*=0.01) or *Tsc1*<sup>+/-</sup> (10 lesions per mouse, *P*=0.01) mice at 9-12 months. In terms of the type of lesion, *Tsc1*<sup>+/-</sup>*Pkd1*<sup>+/-</sup> mice had significantly more cysts and cystadenomas as compared to either *Pkd1*<sup>+/-</sup> (*P*=0.02 and *P*<0.01, respectively) or *Tsc1*<sup>+/-</sup> (*P*=0.01 and *P*=0.009, respectively) mice. We also found that *Tsc2*<sup>+/-</sup>*Pkd1*<sup>+/-</sup> mice had more renal lesions (228.8 lesions per mouse), that were more advanced, as compared to *Tsc2*<sup>+/-</sup> mice (152 lesions per mouse) at 15-18 months (*P*=0.03). While lesions from our *Tsc1*<sup>+/-</sup> and *Tsc2*<sup>+/-</sup> mice became more advanced with time, our *Pkd1*<sup>+/-</sup> mice showed no evidence of lesion progression towards cystadenomas or RCCs at 9-12 months of age. No renal cysts or dilated renal tubules were found in wild-type littermates at the age of 18 months.

### 3.3.1.2 Hepatic lesion analysis

Under H&E analysis, no hepatic cysts were observed in our *Tsc1*<sup>+/-</sup> or *Tsc2*<sup>+/-</sup> mice at 15-18 months of age (N=5), nor were any hepatic cysts or dilated bile ducts found in wild-type littermates up to 15 months (N=12). In the *Pkd1*<sup>+/-</sup> mice, hepatic cysts were rare, occurring in 27% (2/7) of 15-18 month old animals, with an average of 2.7 hepatic cysts per mouse. *Tsc1*<sup>+/-</sup>*Pkd1*<sup>+/-</sup> mice more frequently developed more hepatic cysts, occurring in 75% (3/4) of animals at 15-18 months, with an average of 2.25 cysts per mouse. *Tsc2*<sup>+/-</sup>*Pkd1*<sup>+/-</sup> mice developed hepatic cysts in 50% (3/6) of animals studied at 15-18 months, with an average of 1.7 cysts per mouse. Cysts ranged in size from under a millimetre (Figure 3.2), several millimetres (Figure 3.3) and up to 2-3cm, and had a similar appearance – a single epithelial cell lining with no papillary projections. These lesions were commonly found in clusters or foci. The majority of the very large cysts were recovered from the livers of >20 month old mice. Haemangiomas were not identified on any of the sections analysed. Neither liver cyst incidence nor liver cyst number was significantly different between genotypes.

### 3.3.2 Investigating the role of hamartin, tuberin and polycystin-1 in ciliogenesis

#### 3.3.2.1 Investigating the relationship between cell size and cilia length

To ensure that cilia measurements taken from cholangiocytes were not related to the size of the cell analysed, cell size (largest diameter of the ciliated cell) and their projecting cilia were measured from SEM micrographs and tested for correlation. Table 3.1 provides a summary of the data and reveals no significant association across the genotypes between cell size and cilium length. These results imply cell size is not a factor that needs to be considered when assessing cilium length.

#### 3.3.2.2 Investigating the relationship between age and cilia length

To test the effect of age on cilia length, bile duct primary cilia from 3 month and 11 month old mice were measured. Cholangiocyte cilia from 3 month old wild-type mice had a mean length of 7.34µm (SD=1.4) (72 measurements, median=6.98µm, 4 mice), while those from 11 month old mice had a mean of 6.99µm (SD=1.3) (120

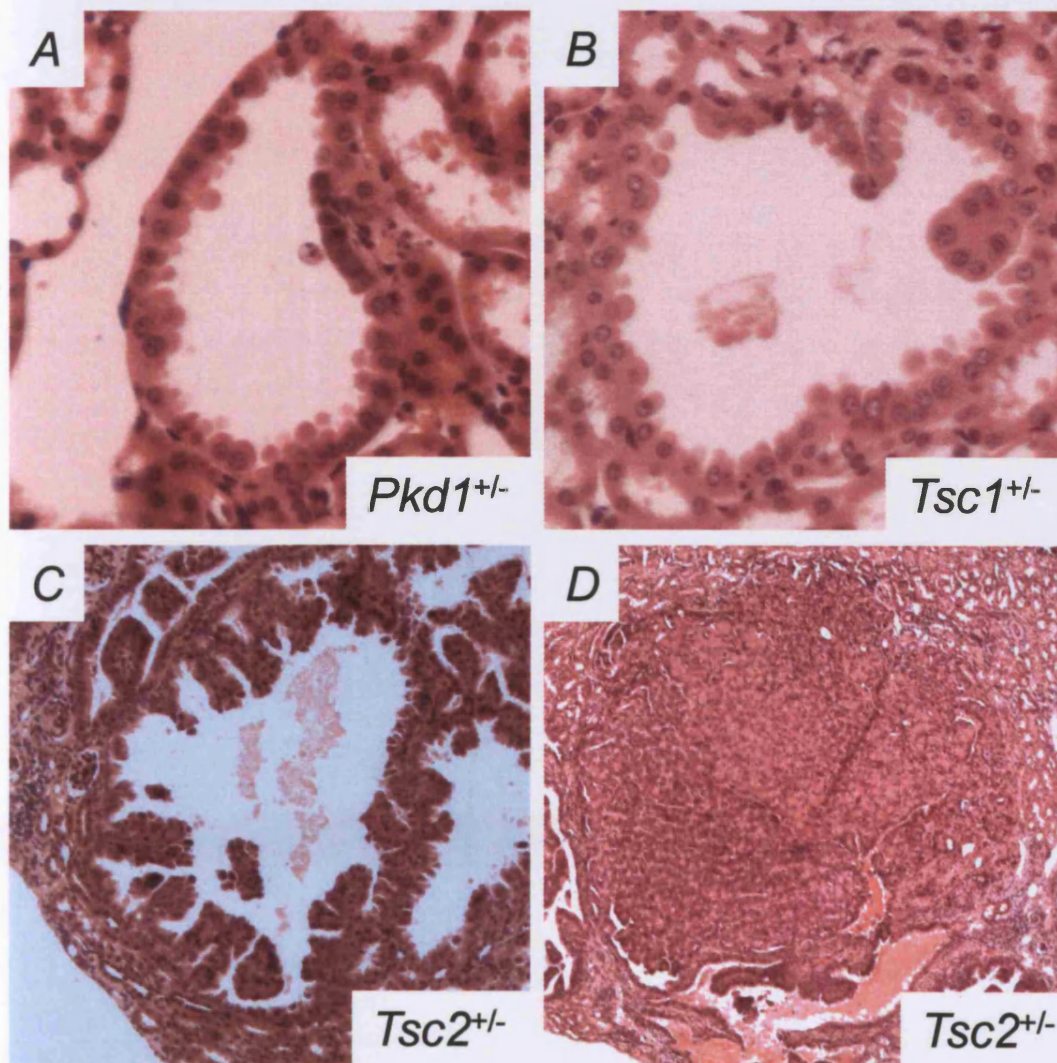


**Figure 3.1** Microscopic analyses of H&E stained renal lesions from 9-12 month old *Pkd1*<sup>+/-</sup>, *Tsc1*<sup>+/-</sup> and *Tsc2*<sup>+/-</sup> mice. Examples are included of a simple cyst (A), a branching lesion (B), a cystadenoma (C) and a renal cell carcinoma (D).



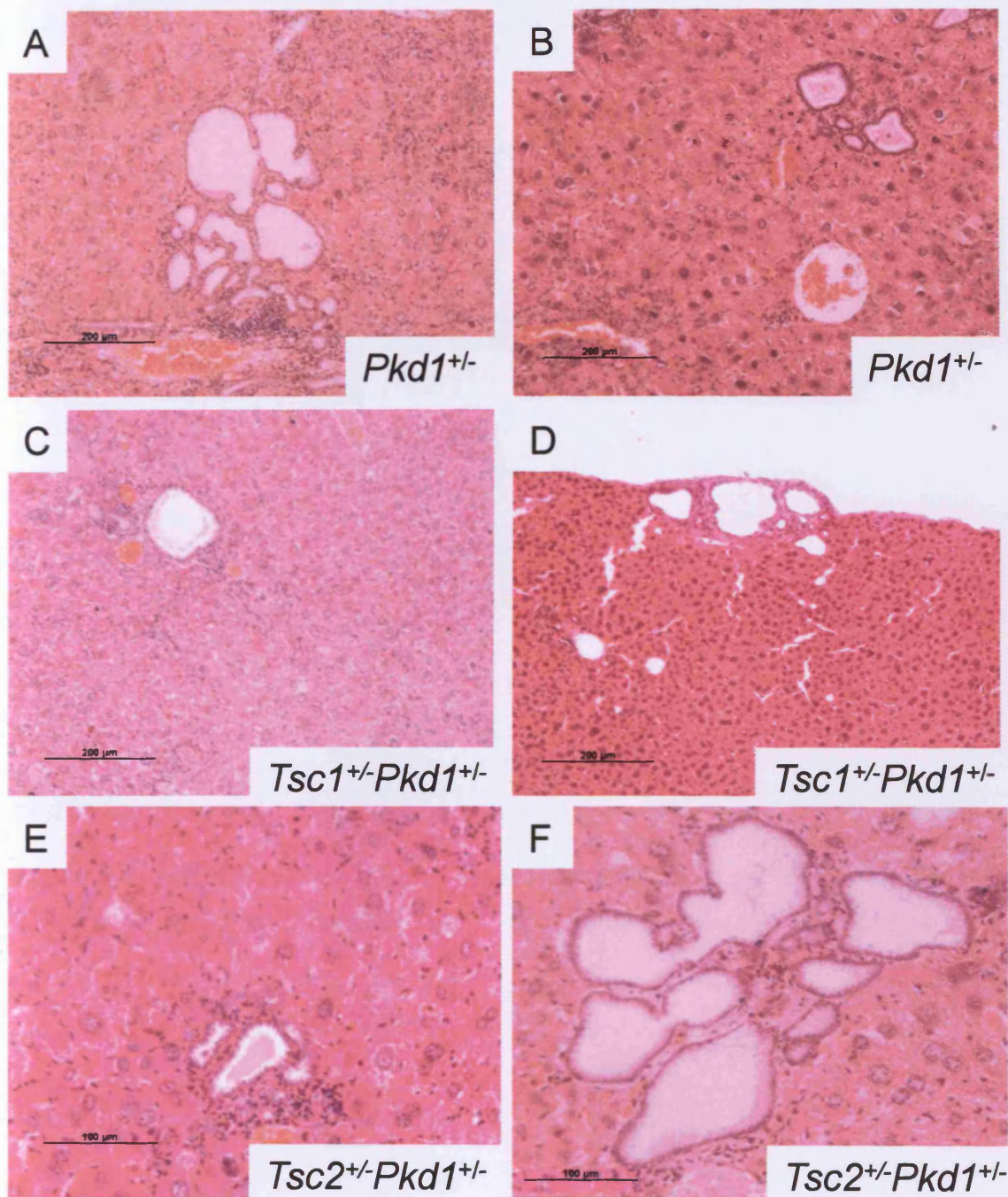


**Figure 3.2** Microscopic analysis of small H&E stained hepatic lesions from (A-B) multi-cystic regions found in the liver of *Pkd1*<sup>+/-</sup> (C-D), *Tsc1*<sup>+/-</sup>*Pkd1*<sup>+/-</sup> and (E-F) *Tsc2*<sup>+/-</sup>*Pkd1*<sup>+/-</sup> mice at 15-18 months of age.

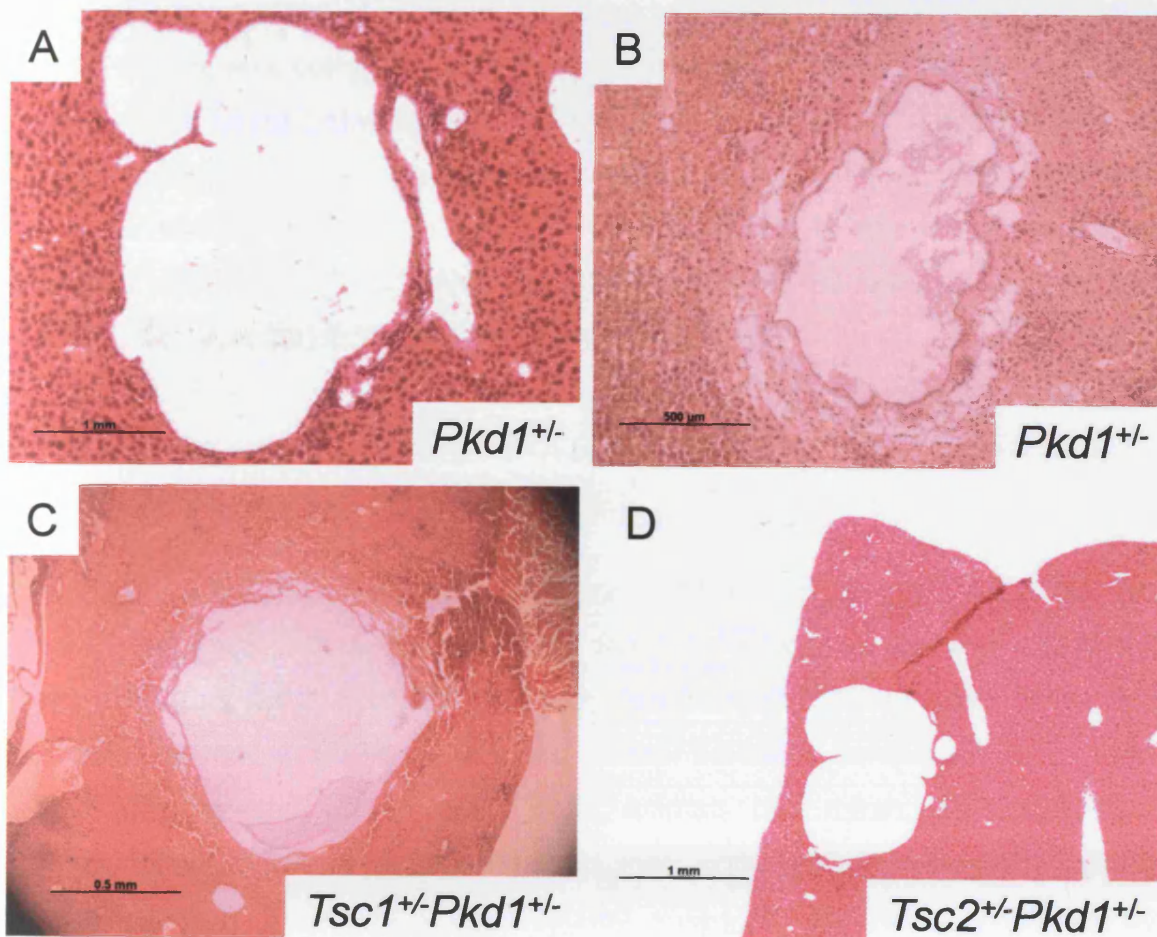


**Figure 3.3** Microscopic analysis of large H&E stained hepatic lesions from (A-B) *Pkd1*<sup>+/-</sup> (C) *Tsc1*<sup>+/-</sup>*Pkd1*<sup>+/-</sup> and (D) *Tsc2*<sup>+/-</sup>*Pkd1*<sup>+/-</sup> mice at 15-18 months of age.

measurements, median = 6.86 $\mu$ m, 3 mice), a difference of 4.77%. The non-parametric data was compared with a two-tailed Mann-Whitney test. No significant difference was found between the medians ( $P=0.242$ ). Care must be taken when interpreting this result, as stronger tests that require normality and equal variance were not available. Statistically, it may not be necessary to age match mice when comparing cilium lengths, but given the difference of 4.77% between the two ages we selected to age match all mice in subsequent studies.

### 3.3.2.3 Primary cilia in pre-cystic renal tubules

We studied the lengths of primary cilia in pre-cystic renal collecting tubule cells from 3 month old  $Tsc1^{+/-}$ ,  $Tsc2^{+/-}$  and  $Pkd1^{+/-}$  mice by scanning electron microscopy (SEM). We found that the lengths of primary cilia from  $Pkd1^{+/-}$  mice were ~5% longer than those found in wild-type animals (mean 2.333 $\mu$ m compared to 2.233 $\mu$ m,  $P=0.02$ ). Interestingly,  $Tsc1^{+/-}$  and  $Tsc2^{+/-}$  animals had mean cilium lengths of 2.122 $\mu$ m and 2.016 $\mu$ m, measurements that were ~5% and ~10% shorter respectively than those from age-matched wild-type littermates ( $P=0.016$  and  $P<0.001$ , respectively) (Table 3.2). The lengths of primary cilia from pre-cystic collecting tubule cells from  $Tsc1^{+/-} Pkd1^{+/-}$  (2.389 $\mu$ m) and  $Tsc2^{+/-} Pkd1^{+/-}$  (2.356 $\mu$ m) mice were significantly longer than found in  $Tsc1^{+/-}$  and  $Tsc2^{+/-}$  mice ( $P<0.001$  for both) and were of a similar length to those found in  $Pkd1^{+/-}$  mice (Table 3.2).

### 3.3.2.4 Primary cilia in pre-cystic liver cholangiocytes

We examined cholangiocyte primary cilia, which project into the lumen of bile ducts throughout the liver. Bile ducts have a distinct morphology and are commonly adjacent to hepatic vasculature. The epithelial cells lining these ducts have defined boundaries and are fairly uniform in size. It has previously been established (Huang *et al.* 2006) that bile duct diameter correlates with cilia length, with large bile ducts having cilia up to two times the size seen in small ones (<15 $\mu$ m). During this study, bile duct diameter was determined before cilium measurements, to ensure only large (diameter between 15 $\mu$ m and 100 $\mu$ m) bile ducts were used.



Genotype	N	Cell size (mean largest diameter) ( $\pm$ SD)	Pearson correlation (r)	Spearman's rank correlation ( $r_s$ )	P value	Critical value	Result
Wild type	86	6.14 $\mu$ m ( $\pm$ 1.6)	0.117		0.282	0.207	No Significant Association
<i>Tsc1</i> <sup>+/-</sup>	91	5.86 $\mu$ m ( $\pm$ 1.1)		0.023		0.207	No Significant Association
<i>Tsc2</i> <sup>+/-</sup>	68	6.38 $\mu$ m ( $\pm$ 1.4)	0.178		0.146	0.235	No Significant Association
<i>Pkd1</i> <sup>+/-</sup>	86	5.76 $\mu$ m ( $\pm$ 1.0)		0.167		0.207	No Significant Association
<i>sc1</i> <sup>+/-</sup> <i>Pkd1</i> <sup>+/-</sup>	97	6.552 $\mu$ m ( $\pm$ 1.4)	0.174		0.089	0.197	No Significant Association
<i>sc2</i> <sup>+/-</sup> <i>Pkd1</i> <sup>+/-</sup>	65	6.61 $\mu$ m ( $\pm$ 1.5)	0.133		0.290	0.235	No Significant Association

**Table 3.1** The relationship between cholangiocyte cell size (measured by taking the maximum cell diameter) and primary cilium length in *Tsc1*<sup>+/-</sup>, *Tsc2*<sup>+/-</sup>, *Pkd1*<sup>+/-</sup>, *Tsc1*<sup>+/-</sup>*Pkd1*<sup>+/-</sup> and *Tsc2*<sup>+/-</sup>*Pkd1*<sup>+/-</sup> mice. Association was tested in normally distributed data (as confirmed by the Anderson-Darling test) with Pearson's correlation coefficient (where no association is indicated when  $P > 0.05$  and when the calculated correlation coefficient is less than the associated critical value at that particular N value). Non-parametric data was ranked and analysed with Spearman's rank correlation coefficient. No significant correlation in this test is indicated by the  $r_s$  value being less than the critical value at  $P = 0.05$ . All critical values taken from Minitab 14.



Genotype	N	Average renal tubule primary cilium length ( $\mu\text{m}$ ) ( $\pm\text{SD}$ )	Percentage change from wild type (%) (P value if significantly different)
Wild type	205	2.233 $\mu\text{m}$ ( $\pm 0.45$ )	n/a
<i>Tsc1</i> <sup>+/-</sup>	126	2.122 $\mu\text{m}$ ( $\pm 0.54$ )	-4.97% (P=0.016)
<i>Tsc2</i> <sup>+/-</sup>	255	2.016 $\mu\text{m}$ ( $\pm 0.41$ )	-9.72% (P<0.001)
<i>Pkd1</i> <sup>+/-</sup>	285	2.333 $\mu\text{m}$ ( $\pm 0.40$ )	+4.48% (P=0.02)
<i>Tsc1</i> <sup>+/-</sup> <i>Pkd1</i> <sup>+/-</sup>	269	2.389 $\mu\text{m}$ ( $\pm 0.46$ )	+6.99% (P<0.001)
<i>Tsc2</i> <sup>+/-</sup> <i>Pkd1</i> <sup>+/-</sup>	261	2.356 $\mu\text{m}$ ( $\pm 0.59$ )	+5.51% (P=0.043)

**Table 3.2** Primary cilium lengths from pre-cystic renal tubule cells. N value denotes the number of primary cilia measured from 5 mice of each genotype. P values refer to associated genotype primary cilium length compared to wild type cilia length.

Primary cilia from pre-cystic 3 month old bile ducts showed no abnormal morphology and were uniformly present as single projections, with no evidence of multiple cilia per cell (Figure 3.4). Cholangiocyte primary cilia from wild-type mice had a mean length of 7.34µm (SD=1.4), and were several times longer than primary cilia found lining kidney tubules in age matched mice from the same strain (mean 2.233µm, SD=0.45). Cholangiocyte primary cilia from *Tsc1*<sup>+/-</sup>, *Tsc2*<sup>+/-</sup> and *Pkd1*<sup>+/-</sup> mice were significantly shorter compared to cilia measurements from wild-type littermates matched for age (-15.8%, -12.8% and -17.6% respectively, *P*<0.001). Double heterozygote mice revealed significant shortening compared to wild-type measurements by comparable amounts (*Tsc1*<sup>+/-</sup>*Pkd1*<sup>+/-</sup> were shorter by -18.1% and *Tsc2*<sup>+/-</sup>*Pkd1*<sup>+/-</sup> by -17.3%, *P*<0.001) (Table 3.3 and Figure 3.5). All measurements were taken from bile ducts of equivalent size.

### 3.3.3 Primary cilia in hepatic cyst epithelia

Hepatic cyst sections were dissected from 20 month old *Pkd1*<sup>+/-</sup>, *Tsc1*<sup>+/-</sup>*Pkd1*<sup>+/-</sup> and *Tsc2*<sup>+/-</sup>*Pkd1*<sup>+/-</sup> mice and analysed via SEM. Many measurements were possible as cilia carpeted the cyst lumen, with clubbed cilia commonly occurring (Figure 3.6). In all three genotypes, cyst primary cilia showed a large amount of variability in length compared to pre-cystic bile duct cilia. Despite containing occasional extremely long primary cilia, the mean lengths of primary cilia from epithelial cells lining cysts in *Pkd1*<sup>+/-</sup> (5.56µm, SD=2.8), *Tsc1*<sup>+/-</sup>*Pkd1*<sup>+/-</sup> (4.29µm, SD=1.6) and *Tsc2*<sup>+/-</sup>*Pkd1*<sup>+/-</sup> (4.05µm, SD=1.9) mice were all significantly shorter than measurements from the bile ducts of 3 month old wild-type mice (*P*<0.001) (Table 3.4). All of these data (Sections 3.3.1.1, 3.3.1.3, 3.3.2.3, 3.3.2.4 and 3.3.3) support a functional relationship between polycystin-1 and hamartin / tuberlin that affects primary cilium length.

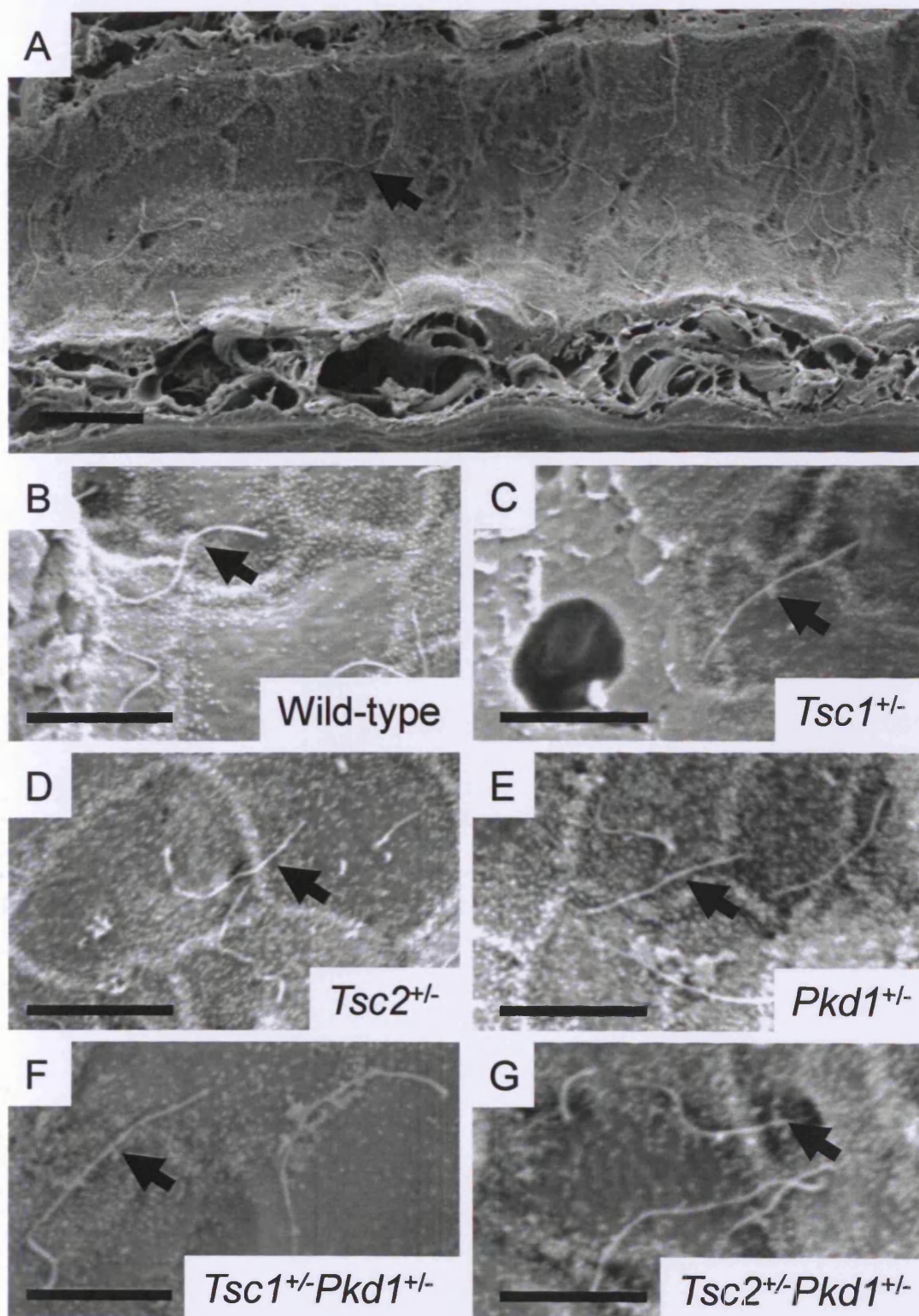


**Figure 3.4** Scanning electron micrographs of cholangiocyte primary cilia in pre-cystic hepatic bile ducts (**A-G**). **Panel A**: overall morphology of a typical mouse bile duct at 3 months of age. **Panels B-G**: Magnified micrographs of cholangiocyte primary cilia. Hepatic primary cilia are indicated with arrow heads. **Scale bars**: 5µm.

Genotype	Sample number	Pre-cystic cholangiocyte primary cilia mean length (μm) (with SD)	Percentage shorter than average wild-type cilium
Wild-type	72	7.34 (1.4)	n/a
<i>Tsc1</i> <sup>+/-</sup>	87	6.18 (1.5)	-15.8% ( <i>P</i> <0.001)
<i>Tsc2</i> <sup>+/-</sup>	94	6.4 (1.4)	-12.8% ( <i>P</i> <0.001)
<i>Pkd1</i> <sup>+/-</sup>	102	6.05 (1.5)	-17.6% ( <i>P</i> <0.001)
<i>Tsc1</i> <sup>+/-</sup> <i>Pkd1</i> <sup>+/-</sup>	134	6.01 (1.2)	-18.1% ( <i>P</i> <0.001)
<i>Tsc2</i> <sup>+/-</sup> <i>Pkd1</i> <sup>+/-</sup>	92	6.07 (1.8)	-17.3% ( <i>P</i> <0.001)

**Table 3.3** Measurements of primary cilia length (μm) from pre-cystic hepatic bile ducts, matched for age and duct diameter.

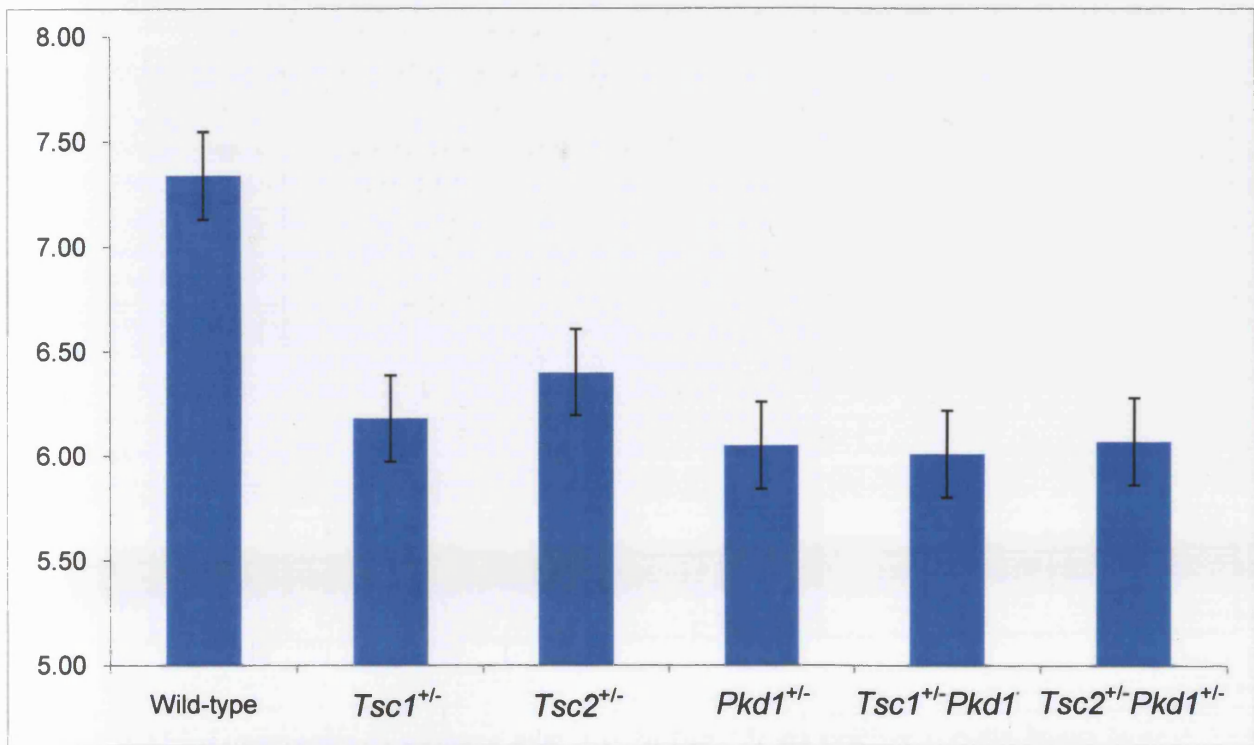


**Figure 3.5** Graph showing distribution of mean primary cilia lengths (μm) from pre-cystic hepatic bile ducts, matched for age and duct diameter. A significant shortening of the primary cilia is seen across pre-cystic haploinsufficient cells ( $P < 0.001$ ) compared to wild-type. Standard error bars are included.

Genotype	Sample number	Epithelial cells lining cysts primary cilia mean length (μm) (with SD)	Percentage shorter than average wild-type cilium
Wild-type	72	7.34 (1.4)	n/a
<i>Tsc1</i> <sup>+/-</sup>	n/a	n/a	n/a
<i>Tsc2</i> <sup>+/-</sup>	n/a	n/a	n/a
<i>Pkd1</i> <sup>+/-</sup>	1932	5.56 (2.8)	-24.3% (P<0.001)
<i>Tsc1</i> <sup>+/-</sup> <i>Pkd1</i> <sup>+/-</sup>	623	4.29 (1.6)	-41.6% (P<0.001)
<i>Tsc2</i> <sup>+/-</sup> <i>Pkd1</i> <sup>+/-</sup>	3818	4.05 (1.9)	-44.8% (P<0.001)

**Table 3.4** Measurements of primary cilia length (μm) from epithelial cells lining liver cysts in 20 month old mice. Sample numbers indicate the total number of primary cilia measured from 3 mice in each genotype. *Tsc1*<sup>+/-</sup> and *Tsc2*<sup>+/-</sup> mice do not experience hepatic cystogenesis.



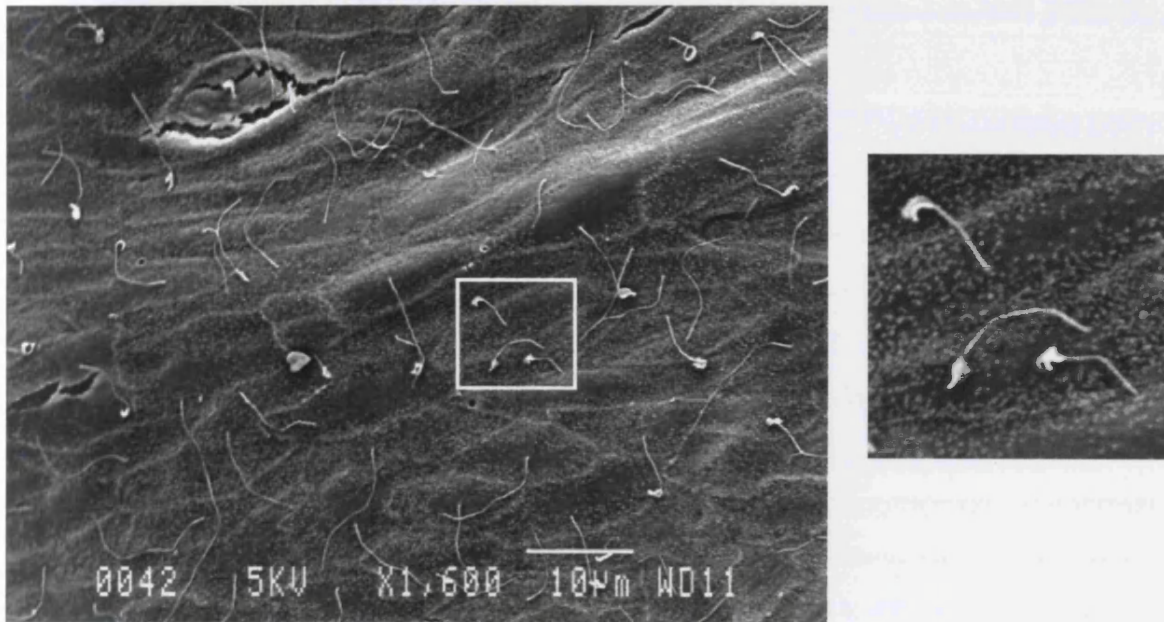


**Figure 3.6 Main Panel:** Scanning electron micrograph of the luminal surface of a liver cyst from a 20 month old *Tsc2*<sup>+/-</sup>*Pkd1*<sup>+/-</sup> mouse. **Inset:** An enlarged area of the micrograph showing the occasional presence of extremely long (>10µm) and abnormally clubbed primary cilia.

### 3.3.4 Investigating the role of hamartin, tuberin and polycystin-1 in cell polarity

#### 3.3.4.1 Pre-cystic renal tubules

We sought defects in cell polarity in our mice by assessing the mitotic orientations of dividing pre-cystic cells from the renal proximal tubule, collecting duct and loop of Henle/distal convoluted tubule from mice at 48 hrs of age. For wild-type mice, we found that 78% of dividing cells from the proximal tubule, 82% from the collecting duct and 78% from the loop of Henle/distal convoluted tubule divided within 10° of the longitudinal axis, demonstrating that, in agreement with others (Fischer *et al.* 2006), oriented cell division is tightly regulated during tubule lengthening. In contrast, we found significant defects in the mitotic orientations of dividing cells from *Tsc1*<sup>+/-</sup>, *Tsc2*<sup>+/-</sup> and *Pkd1*<sup>+/-</sup> mice. For *Tsc1*<sup>+/-</sup> mice, we found that 41% of dividing cells from the proximal tubule, 45% from the collecting duct and 53% from the loop of Henle/distal convoluted tubule divided within 10° of the longitudinal axis ( $P=0.002$ ,  $0.003$  and  $0.039$ , respectively, compared to wild-type), for *Tsc2*<sup>+/-</sup> mice, we found that 46% of dividing cells from the proximal tubule, 27% from the collecting duct and 44% from the loop of Henle/distal convoluted tubule divided within 10° of the longitudinal axis ( $P=0.003$ ,  $<0.001$  and  $0.009$ , respectively, compared to wild-type) and for *Pkd1*<sup>+/-</sup> mice, we found that 61% of dividing cells from the proximal tubule, 47% from the collecting duct and 44% from the loop of Henle/distal convoluted tubule divided within 10° of the longitudinal axis ( $P=0.133$ ,  $0.001$  and  $0.002$ , respectively, compared to wild-type). We also studied dividing cells from mice at 10 days of age and observed identical results to our studies at 48 hrs of age.

#### 3.3.4.2 Pre-cystic hepatic bile ducts

We addressed whether defects in cell polarity were present in hepatic tissues from our mouse models. We assessed the mitotic orientations of dividing pre-cystic cells from the hepatic bile ducts of mice at 10 days of age. For wild-type mice, we found that 94% (16/17) of cells from the bile duct divided within 10° of the longitudinal axis, demonstrating that, similar to the developing renal tubule, orientated cell division is tightly regulated during bile duct lengthening (Figure 3.7). Consistent with the abnormalities that we detected in renal tubules, we found significant defects in the



mitotic orientations of dividing hepatic cells from *Tsc1*<sup>+/-</sup>, *Tsc2*<sup>+/-</sup> and *Pkd1*<sup>+/-</sup> mice. For *Tsc1*<sup>+/-</sup> mice, we found that 33% (7/21) of cells divided within 10° of the longitudinal axis, for *Tsc2*<sup>+/-</sup> mice, we found that 29% (6/21) of cells divided within 10° of the longitudinal axis and for *Pkd1*<sup>+/-</sup> mice, we found that 45% (9/20) of cells divided within 10° of the longitudinal axis ( $P < 0.001$  for all, compared to wild-type).

We also observed that in *Tsc1*<sup>+/-</sup> mice, 28% of dividing cells from hepatic bile ducts showed an 'extreme' dysregulation of mitotic orientation (with divisions between 60° and 90° to the duct axis) and similarly, in *Tsc2*<sup>+/-</sup> mice, 38.1% of dividing cells displayed this severe phenotype. Such dysregulation was observed less frequently in dividing cells from *Pkd1*<sup>+/-</sup> mice (15%) and was not observed in wild-type littermates.

#### 3.3.4.3 Genotype and aberrant polarity

In the kidney, we found no difference between *Tsc1*- and *Tsc2*-associated polarity defects. As expected, we did find significant differences in the orientations of dividing cells from *Tsc1*<sup>+/-</sup> *Pkd1*<sup>+/-</sup> and *Tsc2*<sup>+/-</sup> *Pkd1*<sup>+/-</sup> mice as compared to their wild-type littermates, but did not observe any differences between *Tsc1*<sup>+/-</sup> *Pkd1*<sup>+/-</sup> and *Tsc2*<sup>+/-</sup> *Pkd1*<sup>+/-</sup> mice, or their corresponding single heterozygote littermates (all were similarly misorientated). In the liver, no significant difference was found between the *Tsc1*-, *Tsc2*- and *Pkd1*-associated polarity defects, implying all genotypes had bile duct cells that were similarly misorientated during mitosis.

### 3.4 Discussion

#### 3.4.1 A genetic interaction between *Tsc1*, *Tsc2* and *Pkd1*

A genetic interaction between *TSC2* and *PKD1* is implied by the severe early onset cystic kidney phenotype seen in patients with a contiguous deletion of *TSC2* and the adjacent *PKD1* gene (Brook-Carter *et al.* 1994, Sampson *et al.* 2997). In an attempt to recapitulate this phenotype, we bred *Tsc2*<sup>+/-</sup> mice with *Pkd1*<sup>+/-</sup> mice and analysed renal and hepatic lesions at 9 - 12 months of age. While more renal lesions were

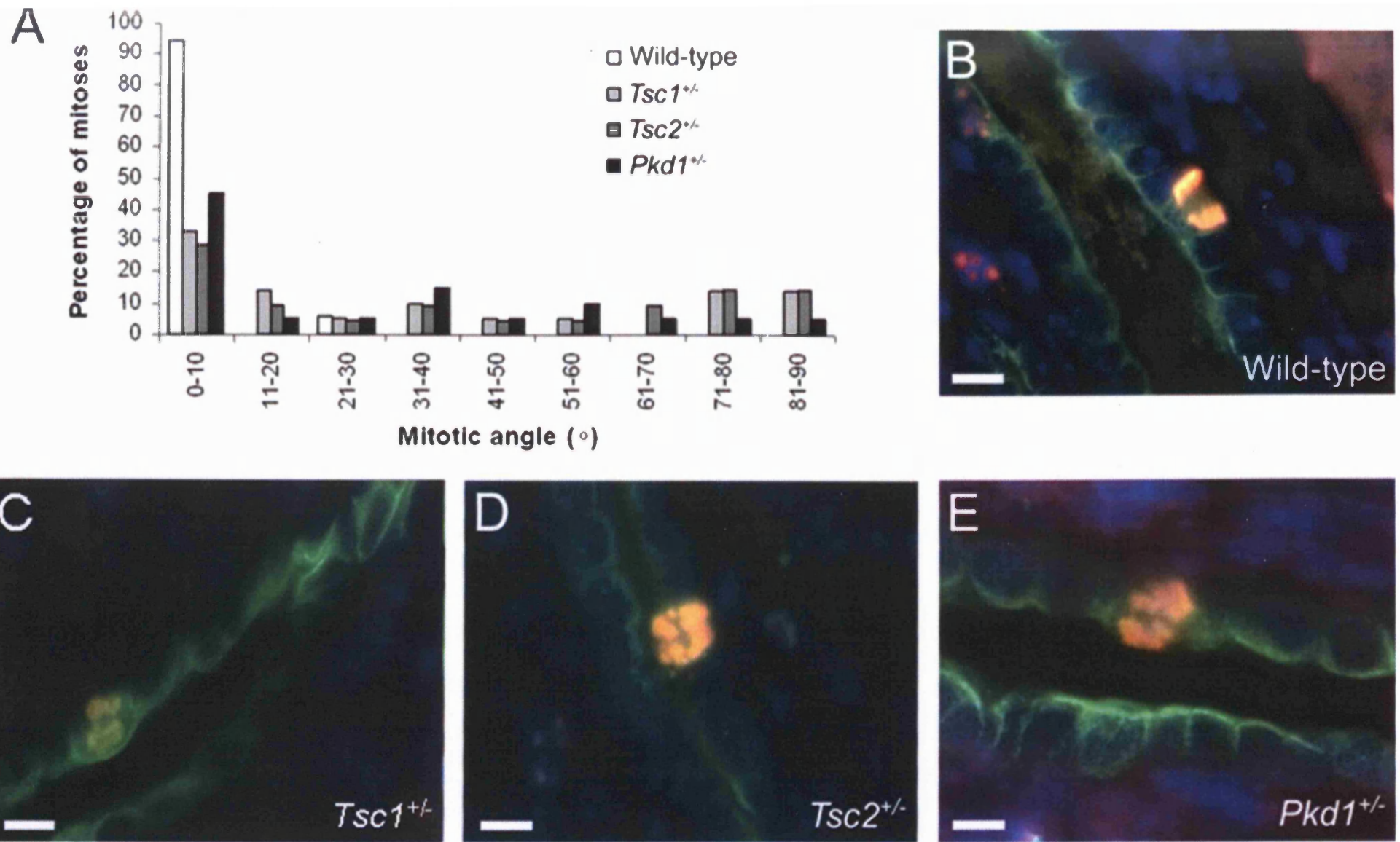


**Figure 3.7** Mitotic orientations of dividing pre-cystic hepatic bile duct cells from 10 day old mice. Graph showing distribution of mitotic angles of division in relation to longitudinal bile duct plane from wild-type, *Tsc1*<sup>+/-</sup>, *Tsc2*<sup>+/-</sup> and *Pkd1*<sup>+/-</sup> mice (A). Fluorescent micrographs showing examples of mitotic orientation in wild-type (B), *Tsc1*<sup>+/-</sup> (C), *Tsc2*<sup>+/-</sup> (D) and *Pkd1*<sup>+/-</sup> (E) mice stained for dividing chromosomes (red) with anti-H3pS10, DAPI for nuclear staining (blue) and cholangiocytes (green) with anti-CK19. Scale bars: 10µm.

found in our *Tsc2<sup>+/-</sup>Pkd1<sup>+/-</sup>* crosses when compared to single heterozygous *Tsc2<sup>+/-</sup>* or *Pkd1<sup>+/-</sup>* animals, the results seen were not on the same scale as the human contiguous deletion syndrome. Rather than massive cystogenesis across newborn kidneys leading to early kidney failure, our compound heterozygote mice presented with moderately increased levels of simple cysts, as well as more advanced lesions, such as cystadenomas and RCCs.

Because tuberin and hamartin have been shown to physically interact and form a tumour suppressor complex (van Slegtenhorst *et al.* 1998, Tee *et al.* 2003), we also investigated the effects of a compound *Tsc1<sup>+/-</sup>Pkd1<sup>+/-</sup>* phenotype in our mice. No severe early onset cystogenesis was seen in our animals, although significantly more renal lesions (cyst, cystadenomas and RCCs) were observed in these mice compared to single heterozygote littermates.

Mice deficient in hamartin or tuberin did not experience any hepatic phenotype at 15-18 months of age. The *Pkd1<sup>+/-</sup>* mice and associated crosses (*Tsc1<sup>+/-</sup>Pkd1<sup>+/-</sup>* and *Tsc2<sup>+/-</sup>Pkd1<sup>+/-</sup>*) developed liver cysts at an incidence of ~30-75%. Renal cysts are known to occur in both the *Pkd1* and the *Tsc* animals. This would suggest a polycystin-1 deficiency is required for the appearance of cysts in the liver. The appearance of a hepatic cystic phenotype in our *Pkd1<sup>+/-</sup>* mice at 15-18 months is a rare event, but is slightly increased in frequency under compound *Tsc1* or *Tsc2* mutation. However, average hepatic lesion number was not significantly different between *Pkd1<sup>+/-</sup>*, *Tsc1<sup>+/-</sup>Pkd1<sup>+/-</sup>* and *Tsc2<sup>+/-</sup>Pkd1<sup>+/-</sup>* mice.

Several reasons may underlie the modulation of the renal phenotype. A compound heterozygote (such as *Tsc1<sup>+/-</sup>Pkd1<sup>+/-</sup>*) has two genes mutated at a germline level, leaving the possibility of a second somatic hit in either gene more likely than in a single heterozygote animal. This second hit to completely remove gene function is likely to exacerbate the cellular phenotype seen with haploinsufficient protein levels and may drive such a cell towards cystogenesis. If such a relationship was a

straightforward link between germline gene mutation and cyst incidence, one would expect an additive increase in lesion number rather than the more complex pattern seen in our animals. Furthermore, several studies (Wilson *et al.* 2006, Onda *et al.* 1999, Koptides *et al.* 2000) have also found that second hits are not always observable in TSC and ADPKD-associated lesions.

Tissue specific factors are relevant in the interpretation of our results, as a compound heterozygous mouse will experience a greatly exaggerated renal phenotype but only a marginally raised incidence of hepatic cysts. A functional interaction between tuberin, hamartin and polycystin-1 has been suggested in the kidney to account for such a large increase in lesion burden, but the data is not so compelling in hepatic samples. Tuberin and polycystin-1 have been shown to functionally and physically interact, with the *TSC2* product trafficking polycystin-1 to the cell membrane from the Golgi (Kleymenova *et al.* 2001). At this point, other groups (Shillingford *et al.* 2006, Mostov *et al.* 2006) have suggested that the cytoplasmic C-terminal tail of polycystin-1 mediates assembly into a complex with tuberin and mTOR. This high level of co-dependency and functional interaction may explain the renal cystic phenotype seen in our compound heterozygous mice but it is likely that additional layers of complexity exist in cholangiocytes, such as alternative signalling pathways, a different cellular signalling environment and a reduction in cellular requirement for hamartin/tuberin/polycystin-1 interaction.

The histological appearance of the liver lesions was similar across all genotypes – focal growths dispersed across the organ, with a single epithelial cell lining and no papillae projections. Size did vary from under a millimetre to several centimetres, with a tendency for larger cysts to be discovered in older animals. This is different to the situation in kidneys, where advanced cysts developed papillae projections and progress towards a cystadenoma. Foci of cystic growth are uncommon in renal samples, while it is a normal finding in the liver. This is likely due to tissue specific differences. For example, under histological examination, hepatic tissue is tightly packed and therefore restrictive to cyst expansion. Cysts in the liver may naturally

expand to fill available space / areas of reduced compaction, in much the same manner as a balloon expanding in a complex 3D shape might. The resultant cyst foci seen in hepatic tissue may be the result of a cross section through this complex shape. Kidney tissue (which certainly appears more spacious under a microscope) may not be so restrictive to cyst expansion, and allow a lesion to expand in a roughly circular shape, compressing the surrounding tissue.

The overall picture appears to suggest that kidneys are much more susceptible to cystic growth and progression compared to livers. An additional *Pkd1*<sup>+/-</sup> mutation is required to drive any sort of hepatic phenotype in our *Tsc* animals. The resulting compound heterozygotes have a slightly raised risk of hepatic cyst incidence but nowhere near the levels seen in kidneys from these same animals. The liver cysts do not progress towards a cancerous phenotype (as seen in kidneys) demonstrating a possible resistance to cyst progression. However, hepatic cysts are much rarer than kidney cysts and may require more time to form in sufficient numbers before advanced lesions may emerge.

### **3.4.2 Differences between the *Pkd1*<sup>+/-</sup> mouse models and humans with ADPKD**

Humans with ADPKD are subject to a progressive formation of bilateral, multiple renal cysts. In around 70% of patients, cysts will also occur in the liver (Yoder *et al.* 2006). In our *Pkd1*<sup>+/-</sup> mouse model, renal cyst incidence has been placed at 50% of 9 month old animals (Boulter *et al.* 2001), with liver cysts occurring in 29% (2/7) of 15-18 month olds. The cystic kidney phenotype seen in *Pkd1*<sup>+/-</sup> animals appears less pronounced than in human counterparts. Additionally, the incidence of hepatic cystogenesis is reduced in the mouse model, although similarities exist in the origins of cyst development – both appear to arise from epithelial cells contained in the biliary tree (Lu *et al.* 1999). Although several groups (Lu *et al.* 1999) have underlined the importance of the *Pkd1*<sup>+/-</sup> mouse model in recapitulating human ADPKD in terms of renal and hepatic cystogenesis, there is a need to appreciate differences exist in cystic kidney disease between humans and mice (specifically with regards to onset and severity).

### **3.4.3 Mice from *Tsc2*<sup>+/-</sup> and *Pkd1*<sup>+/-</sup> crosses occasionally experience a severe early onset kidney disease**

As discussed previously (Chapter 1), humans born with a contiguous deletion of *TSC2* and the adjacent *PKD1* gene experience a severe infantile polycystic kidney syndrome. Interestingly, lesion studies in our *Tsc1*<sup>+/-</sup>*Pkd1*<sup>+/-</sup> and *Tsc2*<sup>+/-</sup>*Pkd1*<sup>+/-</sup> mice failed to find a similar gross cystic phenotype. Mice experiencing severe renal cystic disease may have died before 9-12 months of age, so a breeding programme was set up by our lab as part of a separate study, to examine mice at weaning (3-4 weeks old). Although extremely rare, from over 200 mice born through *Tsc2*<sup>+/-</sup> and *Pkd1*<sup>+/-</sup> crosses, we found three animals with a severe polycystic renal phenotype (no cysts in extra renal tissues were observed). Two of these mice were characterised as *Tsc2*<sup>+/-</sup>*Pkd1*<sup>+/+</sup> and one was a *Tsc2*<sup>+/-</sup>*Pkd1*<sup>+/-</sup>. No mice generated from over 200 crosses of *Tsc1*<sup>+/-</sup> and *Pkd1*<sup>+/-</sup> animals were found to have a severe early onset cystic disease.

In all three mice with early onset polycystic kidney disease, the cystogenesis was unilateral, with one normal kidney and one enlarged cystic kidney. Upon longitudinal bisection, microscopic cysts (ranging in size between 1mm and 5mm) were found to be distributed homogenously across the cortical and medullary regions. Despite the young age of the mice, evidence of lesion progression (in the form of cystadenomas) was found in the *Tsc2*<sup>+/-</sup> mouse kidney. The cysts examined in the kidneys of the *Tsc2*<sup>+/-</sup>*Pkd1*<sup>+/-</sup> mice resembled cysts found in later *Pkd1*<sup>+/-</sup> animals. Similar to our findings, Cai *et al.* (2003) have found three young Eker rats (>3 months of age) with severe polycystic kidney disease. They found cysts, cystadenomas and RCCs in these animals to be present across the cortex and medulla, but the cystogenesis seen was bilateral, not unilateral as in our mice. Cai *et al.* also noted extra-renal lesions in the spleen and uterus, while no evidence of this was found in our early onset animals. Molecular analysis revealed renal cells had lost their functional copy of *Tsc2*, and the authors attributed this to a mutational event during embryogenesis (probably chromosomal nondisjunction). Thus the affected animals were mosaics for loss of *Tsc2* gene function. A similar event may have occurred in our mice, accounting the rarity of this early onset phenotype. The fact that our mice displayed

unilateral cystogenesis while the Eker model produced bilateral cysts implies that loss of the wild-type allele occurred later in embryogenesis. This is supported by the lack of extra-renal lesions in our mice, compared to the wider cystic phenotype seen in the early onset Eker rats.

It is likely that somatic genetic differences account for the discrepancy between contiguous *TSC2/PKD1* syndrome patients and our *Tsc2<sup>+/-</sup>Pkd1<sup>+/-</sup>* mouse lines. In humans, *TSC2* and *PKD1* lie adjacent on chromosome 16. In our mice, *Tsc2* and *Pkd1* are adjacent on chromosome 17, but the gene targeting constructs will lie on different alleles in compound heterozygote animals. The result of this makes biallelic inactivation of the remaining wild-type *TSC2* and *PKD1* genes much more likely in humans (through a single large deletion mutation) than in mice, which would require two further mutational events to completely remove *Tsc2* and *Pkd1* gene function.

#### **3.4.4 Hamartin, tuberin and polycystin-1 play a role in renal and hepatic ciliogenesis**

Following SEM measurement of primary cilia in renal tubules and bile ducts, we found hamartin, tuberin and polycystin-1 play a role in maintaining the length of these organelles in pre-cystic cells. In cholangiocytes, there was a significant decrease in length in all mutant genotypes when compared to wild-type littermates, matched for age and bile duct size. Renal tubule cells experienced disruption in their primary cilia too, with shortening in *Tsc1<sup>+/-</sup>* and *Tsc2<sup>+/-</sup>* animals, and lengthening in *Pkd1<sup>+/-</sup>* mice. These measurements support a role for these proteins in renal and hepatic ciliogenesis, and suggest that a deficiency in hamartin, tuberin or polycystin-1 can lead to haploinsufficient ciliary abnormalities that pre-date cyst development. Clearly ciliogenesis is perturbed in both tissues but the effect of polycystin-1 deficiency appears to vary with tissue type.

Work done by Hartman *et al.* (2009) found that in *Tsc1* and *Tsc2* null mouse embryonic fibroblasts (MEFs) there was a 17-27% increase in primary cilia length when compared to wild-type cells. This would be at odds with our *in vivo* hepatic and renal data but several factors may account for this difference. The MEFs used were



immortalised, through spontaneous means (*Tsc1*<sup>-/-</sup>) or through a targeted p53 knockout (*Tsc2*<sup>-/-</sup>). Either way, there is potential for other pathways to be disrupted, any of which may have a bearing on the ciliary phenotype. The experiments were also conducted under conditions that are removed from liver or kidney physiological conditions and with tubular / ductal flow removed from the ciliated cell environment. While an underlying ciliary disruption may well be present in these cell lines, there is perhaps an issue with recapitulating the physiological setting that a primary cilium would experience in vivo, and so caution must be exercised when drawing comparisons.

Primary cilia lengths from epithelial cells lining hepatic cysts from *Pkd1*<sup>+/-</sup>, *Tsc1*<sup>+/-</sup> *Pkd1*<sup>+/-</sup> and *Tsc2*<sup>+/-</sup> *Pkd1*<sup>+/-</sup> lesions echoed the shortening seen in pre-cystic lesions, although to a greater degree. The primary cilia projecting into the cyst lumen of our 20 month old mice were visibly malformed and significantly shorter than primary cilia in the bile ducts of our 3 month old wild-type mice. One standout feature of the cyst cilia data was the massive range of lengths found. While pre-cystic cilia from across the genotypes occasionally reached 10µm, several *Pkd1*<sup>+/-</sup> and *Tsc2*<sup>+/-</sup> *Pkd1*<sup>+/-</sup> cyst cilia reached sizes exceeding 18µm, with the longest reaching 20µm (almost 3 times the size of a wild-type cilium). This was accompanied by a large number of foreshortened cilia, leading to an overall low average length and large range. Interestingly, this variability was not seen in *Tsc1*<sup>+/-</sup> *Pkd1*<sup>+/-</sup> mice although smaller cysts were used and less measurements taken. The massive variation indicates an extreme loss of control over cilia structure, and additional defects such as clubbing and multi-ciliated cells would support this. Large differences in cilium lengths have previously been observed in renal cysts from these same mice (Bonnet *et al.* 2009). There, a 200% increase in renal cilia length was reported in *Tsc1*<sup>+/-</sup> and *Tsc2*<sup>+/-</sup> mice, changing from a relatively modest 5-10% difference in pre-cystic cells. Taken together with the liver data, we see an extreme loss of length control when moving from a pre-cystic to cystic setting. This may be accounted for by the acquisition of additional mutations during cystogenesis. As these cysts progress, second hits may occur in the remaining *Tsc1*, *Tsc2* or *Pkd1* genes, compounding any effects seen and amplifying the phenotype. Ciliary clubbing seen in the liver was not found in the kidney studies and may well be another tissue specific difference.

Interestingly, *Pkd1*<sup>+/-</sup> in the kidney appears to play a different modifying role, by causing an increase in primary cilium length when compared to the wild-type measurements. This may be another example of tissue specific differences in the roles of primary ciliary proteins and cilium length maintenance, but could also suggest an underlying inconsistency in the ciliogenesis and imply defects seen in this organelle are simply a symptom of disrupted polarity (discussed later).

#### **3.4.5 A physiological consequence to abnormal primary cilia?**

The ciliary membrane is rich in receptors, ion channels and signalling proteins, with the potential for activation by mechanical or chemical means (Rosenbaum *et al.* 2002). Consistent with the loss of such a high concentration of signal transducing proteins, cells lacking primary cilia experience negative cellular effects, such as reduced sensitivity to fluid flow mediated calcium influx (Nauli *et al.* 2003, Praetorius *et al.* 2003, Lin *et al.* 2003). Our mice have disrupted renal tubule and cholangiocyte primary cilia, but it is unclear if a modest reduction in length of ~10-20% can exert similar a pathophysiological effect on pre-cystic cells. Work using the *orpk* mouse model of autosomal recessive polycystic kidney disease looked at a similar situation in renal tubules (Brown *et al.* 2003). It was found that while the observed correlation between reduction in cilia length and formation of renal cysts in *orpk* mutants might indicate a link between reduced ciliogenesis and cystic disease, this hypothesis was not borne out through additional analysis of *orpk* and knockout rescue models. These rescue models revealed discrepancies between levels of ciliogenesis and cystogenesis, implying the two may well be separate processes and not intrinsically linked.

More recent work by Verghese *et al.* (2008) has shown renal cells to alter primary cilia lengths as a cellular response to ischemic renal injury. An initial ciliary shortening was observed following loss of blood flow to the proximal tubule but this was proceeded by lengthening of cilia in several regions of the kidney tubule network. It was suggested that this lengthening was a cellular attempt to increase sensitivity to fluid flow and maintain an epithelial phenotype in the face of hostile factors promoting desensitisation and dedifferentiation. This theory would explain the

accentuated phenotype seen in cystic cell cilium lengths. The cyst has been described as a hostile environment and as such, cellular stresses may be indicated through drastic lengthening and shortening of primary cilia.

Taken together, these observations imply foreshortening of renal and cholangiocyte primary cilia may be a symptom or compounding factor of perturbed cellular signalling and not a direct cause of pathophysiological effects. Uncertainty arises through the reciprocal relationship between primary cilia and cell signalling. For example, defects in primary cilia structure and function have been shown to affect Wnt signalling, but conversely, Wnt pathway proteins are responsible for ciliary formation (Simons *et al.* 2005, Corbit *et al.* 2008).

### **3.4.6 Role of hamartin, tuberin and polycystin-1 in bile duct and renal tubule cell polarity**

In the livers of our mice, wild-type bile duct cholangiocytes behave similarly to renal tubule cells and divide in a tightly controlled manner. Pre-cystic 10 day old mutant mice were then assessed to measure duct polarity during biliary tree development. Significantly less cell divisions in *Tsc1*<sup>+/-</sup>, *Tsc2*<sup>+/-</sup> and *Pkd1*<sup>+/-</sup> mice occurred inside 10° to the axis of the bile duct. Additionally, while no wild-type cell divisions occurred at an extreme angle to the plane, it was found significant levels of *Tsc1*<sup>+/-</sup>, *Tsc2*<sup>+/-</sup> and *Pkd1*<sup>+/-</sup> duct cells divided at an angle greater than 60°.

It is important to note that crucial differences exists between the liver and kidney – a bisected kidney will reveal thousands of tubule cells, many of which are likely to be in the correct plane for measurement if dividing. A dissected liver will unfortunately not. Chance plays a large part in catching a bile duct in the correct orientation with dividing cells, and combined with the small numbers of ducts present on a section, this results in a much smaller number of cells being counted. Every effort was made to obtain sufficient numbers of cell divisions to give an overview of polarity in the liver and the picture that has emerged appears to mirror the situation that occurs in the much more extensively measured kidney.

It has been suggested that it may be appropriate to generate more comprehensive, three dimensional images of aberrant mitotic orientations in renal tubules and bile

ducts to ensure divisions that appear in or outside the tissue plane are not artefactual. Using confocal microscopy, work in the kidney has found similar results using fluorescent staining and 3D techniques, implying the method used here is reliable (Bonnet *et al.* 2009).

On the basis of these results, our data show for the first time that hamartin, tuberin and polycystin-1 have a role to play in bile duct and renal tubule cell polarity. Mice that have reduced levels of these proteins in their cholangiocytes or tubule cells have a deficiency in controlling the orientation of their cell divisions that, alongside the altered lengths of the primary cilia, are abnormal changes that pre-date hepatic and renal cystogenesis.

Potential reasons behind this disruption in polarity are numerous. All three proteins have strong links to the primary cilium, and are known to cause abnormalities in cilia length when levels are diminished through germline mutation (as previously discussed). The primary cilium is thought to modulate planar cell polarity (PCP) (Simons *et al.* 2005) and so a poorly formed organelle may translate to reduced control over mitotic divisions. As an alternative to a cilium-led hypothesis, it is also possible that defective cellular polarity has caused the abnormality in primary cilia lengths (which are polar structures and require functional polarity to form). In this instance, the malformed organelles would be a symptom of an underlying defect (caused directly by a reduction in one of the three proteins) and is therefore a passenger, rather than driver, factor in cystogenesis. To support this hypothesis, several lines of evidence link the ciliary proteins directly to cell polarity signalling. Work by Massey-Harroche *et al.* (2007) using a two-hybrid assay has shown a molecular interaction between the C-terminal domain of tuberin and PDZ 2 and 3 of PATJ. PATJ is a scaffold member of the Crumbs 3 complex in mammalian epithelial cells and is required for normal polarity. Overexpression of the Crumbs 3 complex or knockdown of PATJ (Shin *et al.* 2005) results in polarity defects and a delay in apical morphogenesis in MDCK cells (Roh *et al.* 2003, Lemmers *et al.* 2004). Another group has demonstrated in cell line work that the C-terminal tail of polycystin-1 is able to undergo cleavage, localise and bind to  $\beta$ -catenin in the nucleus. It is thought this binding inhibits  $\beta$ -catenin-dependent Wnt signalling and TCF-dependent gene transcription. Disrupted levels of *Pkd1* expression may therefore activate canonical

Wnt signalling (Lal *et al.* 2008), and dysregulate planar cell polarity (which requires precise switching between canonical and non-canonical Wnt signalling).

These defects in cell polarity are likely to be occurring as a result of haploinsufficiency rather than as a consequence of secondary somatic mutations. The mitotic misorientations took place in very young mice (2 and 10 days old) and at this age it is unlikely that second hits will have occurred in the bile ducts or renal tubules to give rise to such widespread defective polarity. Additional work in the brain provides an interesting parallel, where haploinsufficient levels of hamartin or tuberin appear to dysregulate polarity. Polarisation of neurons is crucial for correct formation of axons and dendrites, and proteins called SAD (synapses of amphids defective)- A and B were found to play a key role in this process in mice (Kishi *et al.* 2005). Inactivation of *Tsc1/2* was shown to promote axonal growth via upregulation of SAD-A, a protein noted to be elevated in the cortical tubers of a TSC patient (Choi *et al.* 2008). LOH of wild-type *TSC1* or *TSC2* in cortical tubers is thought to be a rare event (Henske *et al.* 1996, Niida *et al.* 2001) and so one defective copy may be enough to induce signalling effects (such as upregulation of SAD-A) and promote dysregulation of polarity.

#### **3.4.7 Planar cell polarity or apical/basal polarity?**

To perform many of their functions, epithelial cells (such as renal tubule cells or bile duct cholangiocytes) need to be polarised within the plane of the epithelium, and this is termed PCP (Jenny *et al.* 2006). Apical-basolateral (A/B) polarity is perpendicular to the plane of the epithelial sheet and allows cells to directionally transport molecules across a cell layer and selectively excrete extracellular matrix components to form a basal lamina (Eaton *et al.* 1995). PCP is known to be important in formation of the vertebrate inner ear (specifically the orientation of stereociliary bundles in the organ of Corti) and convergent extension during gastrulation and neurulation (Wallingford *et al.* 2002, Keller *et al.* 2002).

Close examination of misorientated bile duct and renal tubule cells revealed that a significant proportion of these cells were dividing in a plane perpendicular to the epithelial sheet, consistent with defects in PCP (which would be a failure to polarise

cells in the plane of the epithelium). However, further work on our mice examining the organ of Corti failed to find evidence of defective polarity in the stereociliary bundles (Bonnet *et al.* 2009). As previously mentioned, these are orientated through PCP, implying either the PCP defects seen are tissue specific, or it is A/B polarity that has been affected. No defects in gastrulation have been reported either. Finally, primary cilia are the most apical structures in the cholangiocytes and defects seen there could well be accounted for by aberrant A/B polarity. These pieces of data would suggest A/B polarity and not PCP has been affected in our mice. However, evidence for a direct link between A/B polarity and PCP has been shown in recent research. The *drosophila* PATJ equivalent, *dPatj*, is known to play a key role in A/B polarity, and binds to the cytoplasmic tail of Frizzled (Fz1) which recruits aPKC, and in turn phosphorylates and inhibits Fz1-dependant PCP, thereby providing a direct link between A/B polarity and PCP (Djiane *et al.* 2005). Hence, defects in one signalling pathway, such as PCP and misaligned cell division, may spill over and affect A/B polarity in certain tissues, for example by foreshortening primary cilia. The literature on cell signalling would place *Tsc2* at the heart of this switching mechanism and may explain why aspects of both polarity pathways appear to be involved.

#### **3.4.8 Wild-type misorientated cell division**

Data from wild-type renal tubules suggests 78% of dividing cells in the proximal tubule, 82% from the collecting duct and 78% from the Loop of Henle/distal convoluted tubule divided within  $10^\circ$  of the longitudinal axis. While this demonstrates tight orientation of cell division, it is important to note the system is not perfect. Several divisions are occurring outside the tubule plane in non-mutant, wild-type mice. Similarly, in liver bile ducts, an instance of wild-type cell division occurring at an angle outside  $10^\circ$  was found. Taken together, this data implies wild-type cells do occasionally experience misorientated cell divisions, but are found at a much lower level than in our mutant mice. Because tubule and duct architecture is maintained in wild-type animals, this would indicate a mechanism exists to remove the occasional misorientated cell from the liver or kidney.

## **CHAPTER FOUR: Defective apoptosis may promote TSC-associated renal cystogenesis.**

### **4.1 Introduction**

The TSC proteins function as negative regulators in the mTOR signalling pathway. Many lesions from TSC patients and animal models stain positively for activation of mTOR, and clinical trials to treat advanced tumours with mTOR inhibitors such as Rapamycin have been conducted with reasonable success (Bissler *et al.* 2008, Davies *et al.* 2008). A study by Kenerson *et al.* (2005) in the Eker rat model of TSC highlighted a subset of smaller lesions that were unresponsive to Rapamycin treatment and lacked evidence of apoptosis. Additionally, when looking at mTOR inhibition in preventing renal lesion development, it was found that Rapamycin reduced the progression but not incidence of precursor lesions. Further work in a *Tsc2*<sup>+/-</sup> mouse model suggested CCI-779 (a Rapamycin analogue) treatment could cause regression of later lesions but found no effect on the appearance of early kidney lesions (Messina *et al.* 2007). Clearly, mTOR activation is an important part of kidney lesion progression (as illustrated by the effects of mTOR inhibition on tumour volume and advancement), but other factors may influence the formation of a new cyst.

We have demonstrated that primary cilia and cell polarity are perturbed in renal tubule cells from 2- and 10-day old *Tsc1*<sup>+/-</sup> and *Tsc2*<sup>+/-</sup> mice (Chapter 3), but what is unclear is why these early pre-cystic changes do not manifest as widespread tubule dilation and cystogenesis until around 3-6 months of age (Wilson *et al.* 2005). The simple cysts that eventually arise commonly do not stain positive for mTOR activation, implying alternative signalling pathways may contribute to the initiation of TSC-associated cystogenesis in renal tissue.

It has been suggested in other tissues (such as the mammary gland) that apoptosis can act as an important level of control in maintaining epithelial cell structures, in a process suppressed by contact with the extracellular matrix (Frisch *et al.* 1997, Pullan *et al.* 1996). In a similar fashion, a misorientated renal tubule cell division at an extreme angle to the plane of the tubule may result in a daughter cell displaced



from the basement membrane, isolated in terms of cell-cell contact and further removed from pro-survival signals. Apoptosis is known to play an important role in normal tubule development (Igarashi 1994) but we sought to ascertain if the process could be triggered in misorientated renal tubules as a rescue mechanism.

Here, we studied developing renal tubules from *Tsc1*<sup>+/-</sup>, *Tsc2*<sup>+/-</sup> and *Pkd1*<sup>+/-</sup> mice and wild-type littermates, stained for a marker of apoptosis to assess the role this process may play in rescuing a defective polarity phenotype. Furthermore, we studied the nature of TSC-associated mTOR-independent renal cystogenesis through the examination of lesions from *Tsc1*<sup>+/-</sup> (Wilson *et al.* 2005) and *Tsc2*<sup>+/-</sup> (Onda *et al.* 1999) mice. Apoptosis in these lesions was evaluated to test for a correlation between mTOR status and programmed cell death.,

## **4.2 Materials and methods**

### **4.2.1 Animal care, genotyping and tissue preparation**

All matters relating to animal husbandry, care and genotyping were carried out as previously described. *Tsc1*<sup>+/-</sup>, *Tsc2*<sup>+/-</sup> and *Pkd1*<sup>+/-</sup> mice were obtained along with wild-type littermates for control purposes. Four mice from each genotype (*Tsc1*<sup>+/-</sup> and *Tsc2*<sup>+/-</sup>) were sacrificed at 9-12 months and dissected to obtain paraffin-embedded kidneys as previously described. Two day old kidneys, required for tubule apoptosis counts, were removed from *Tsc1*<sup>+/-</sup>, *Tsc2*<sup>+/-</sup> and *Pkd1*<sup>+/-</sup> mice and wild-type littermates. These were embedded in paraffin wax as previously described.

### **4.2.2 Immunohistochemistry**

Paraffin-embedded kidneys from 2 day old wild-type (N=6), *Tsc1*<sup>+/-</sup> (N=6), *Tsc2*<sup>+/-</sup> (N=6) and *Pkd1*<sup>+/-</sup> (N=5) mice were serially sectioned at 5µm and renal tubules were stained for apoptosis (active caspase-3) as previously described. Slides were counterstained with haematoxylin to reveal tubule cell morphology and analysed under an Olympus BX51 light microscope at x100 magnification. Levels of apoptosis taking place in pre-cystic renal tubules from these animals were based on the amount of positively stained tubule cells compared to the number of tubule cells

counted. A counter was used to manually record tubule (collecting duct, proximal tubule and Loop of Henle/ distal convoluted tubule) cell numbers from representative sections of the young kidneys. Stain grading was performed by an observer blinded to genotype.

Whole kidneys from 9-12 month *Tsc1*<sup>+/-</sup> (N=4) and *Tsc2*<sup>+/-</sup> (N=4) mice were serially sectioned at 5µm onto clear Superfrost Plus slides. The resulting bank of kidney tissue was then assessed for Tsc-associated lesions through staining every 6<sup>th</sup> slide with H&E (to reveal abnormal tissue architecture). Following identification of a lesion, further IHC stains were carried out on adjacent slides known to contain the same cyst. A marker of mTOR activation, anti-phospho-S6 ribosomal protein (Ser<sup>240-244</sup>), and a marker of active apoptosis, anti-cleaved caspase-3 (Asp<sup>175</sup>) were used to categorise the cysts. Simple cysts were defined as cysts having a single epithelial cell boundary, with no evidence of multicellular projections (Wilson *et al.* 2006). Cysts with multicellular projections, branching lesions, cyst adenomas and renal cell carcinomas were classified as advanced lesions. Following ABC peroxidase treatment as previously described, slides were graded on stain intensity to assess the mTOR and apoptotic status of the cyst. Lesion analysis was performed by an observer blinded to genotype.

#### **4.2.3 Cell size measurement**

As previously discussed, serial sections of kidneys were obtained from *Tsc1*<sup>+/-</sup> and *Tsc2*<sup>+/-</sup> mice, stained for pS6 and caspase-3, and categorised into simple cysts (96 cysts) and advanced lesions (111 lesions). These were analysed under a light microscope, photographed and measured with AxioVision software. Cross sectional area (in µm<sup>2</sup>) was assessed by measuring all available sections containing a cyst, and taking the largest single area (rather than an average) to represent that lesion. Data was then tested for normality with an Anderson-Darling test and compared using the Mann-Whitney test for non-parametric data.

#### 4.2.4 Statistics

Cyst staining data was compared using Fisher's exact test with contingency tables. Larger samples ( $N > 6$  in all categories) were analysed with a Chi-squared test. To analyse the levels of apoptosis in 2 day old renal tubules, Chi-squared contingency tables were used, as the data was categorical and non-parametric. Cell sizes were compared with Mann-Whitney test.

#### 4.3 Results

##### 4.3.1 Apoptosis in developing mouse renal tubules

To test the hypothesis that apoptosis could be triggered to destroy misaligned tubule cells in *Tsc1*<sup>+/-</sup>, *Tsc2*<sup>+/-</sup> and *Pkd1*<sup>+/-</sup> mice, we stained developing renal tubules from 2 day old mice for cleaved Caspase-3 (a marker of apoptosis). Tubule polarity defects have previously been established in these mice (see Chapter 3). We found that  $11.6 \times 10^{-4}$  (76/65337) and  $11.8 \times 10^{-4}$  (53/44963) tubule cells from *Tsc1* and *Tsc2* mice, respectively, were undergoing apoptosis which was ~1.5 fold higher than found in wild type littermates ( $7.8 \times 10^{-4}$  [50/64246] tubule cells;  $P=0.026$  and  $P=0.034$ , respectively). *Pkd1*<sup>+/-</sup> mice demonstrated similar levels of elevated renal tubule apoptosis when compared to wild-type littermates ( $14.9 \times 10^{-4}$  [69/46322] tubule cells,  $P < 0.001$ ) (Figure 4.1, Table 4.1).

##### 4.3.2 mTOR activation in TSC-associated renal lesions

We stained 41 simple cysts, defined as having no multicellular projections or branches into the lumen and 40 advanced lesions (branching cysts, cystadenomas and RCCs) from *Tsc1*<sup>+/-</sup> mice ( $N=4$ ) and 55 simple cysts and 71 advanced lesions from *Tsc2*<sup>+/-</sup> mice ( $N=4$ ) for phospho-S6, a marker of mTOR activation. In agreement with our previous studies (Wilson *et al.* 2006), we found that mTOR was not active in 39% (16/41) and 40% (22/55) of simple cysts from *Tsc1* and *Tsc2* mice, respectively, whereas almost all advanced lesions from these mice were mTOR-active (40/40, 100% for *Tsc1* and 70/71, 98.6% for *Tsc2*,  $P < 0.005$  for both as compared to cysts) (Figure 4.2). No significant difference was found between *Tsc1* and *Tsc2* simple cysts in terms of mTOR activation.

### 4.3.3 Caspase-3 and mTOR activation in TSC lesions

We stained simple kidney cysts from 9-12 month-old *Tsc1*<sup>+/-</sup> (N=4) and *Tsc2*<sup>+/-</sup> mice (N=4) with caspase-3 and, on adjacent serial sections, pS6. We found that 17/41 (41.5%) and 18/55 (32.7%) of cysts from *Tsc1*<sup>+/-</sup> and *Tsc2*<sup>+/-</sup> mice, respectively, stained for caspase-3. In the context of mTOR activity, almost all cysts without mTOR activation did not have caspase-3 activation (36/38, 94.7%), whereas many cysts with mTOR activation also had caspase-3 activation (25/58, 43%;  $P < 0.001$  as compared to mTOR-inactive cysts) (Figure 4.3, Table 4.2 and 4.3).

### 4.3.4 Cyst size investigation

As previously discussed, simple and advanced lesions from 9-12 month-old *Tsc1*<sup>+/-</sup> (N=4) and *Tsc2*<sup>+/-</sup> mice (N=4) were defined on the basis of H&E stained sections and categorised on levels of phospho-S6 and cleaved caspase-3 staining. To further characterise the cystogenesis seen in our Tsc mouse models, these lesions were measured under an Olympus BX51 light microscope with AxioVision software. In the 207 lesions found in our 8 mice (111 advanced lesions, 96 simple cysts), the variability in size was considerable, with the smallest cyst measuring 362 $\mu\text{m}^2$  and the largest being 1,688,362 $\mu\text{m}^2$ . No significant difference was found between the sizes of our mTOR positive and negative simple cysts ( $P = 0.7502$ ), although both mTOR positive and negative simple cysts were significantly smaller than mTOR active advanced lesions ( $P < 0.0001$  and  $P = 0.0002$  respectively). No significant difference was detected between the sizes of *Tsc1*<sup>+/-</sup> and *Tsc2*<sup>+/-</sup> simple cysts ( $P > 0.05$ ). No significant difference was detected between the sizes of *Tsc1*<sup>+/-</sup> and *Tsc2*<sup>+/-</sup> advanced lesions ( $P > 0.05$ ). In simple cysts, mTOR activation (pS6+/C3- compared to pS6-/C3-) does not significantly alter cyst size ( $P = 0.1894$ ). However, active apoptosis (pS6+/C3+ compared to pS6+/C3-) correlated with a significantly larger average cyst size ( $P = 0.0247$ ). Simple cysts with no mTOR activation and no apoptosis were found to contain both the smallest and the largest recorded cyst sizes in all 96 simple cysts (362 $\mu\text{m}^2$  and 400,000 $\mu\text{m}^2$ , respectively). Advanced lesions were nearly all mTOR active, but when compared for size in the context of caspase-3 staining (pS6+/C3+ compared to pS6+/C3-), it was found cysts with inactive apoptosis were significantly smaller (Figure 4.4, Table 4.4).

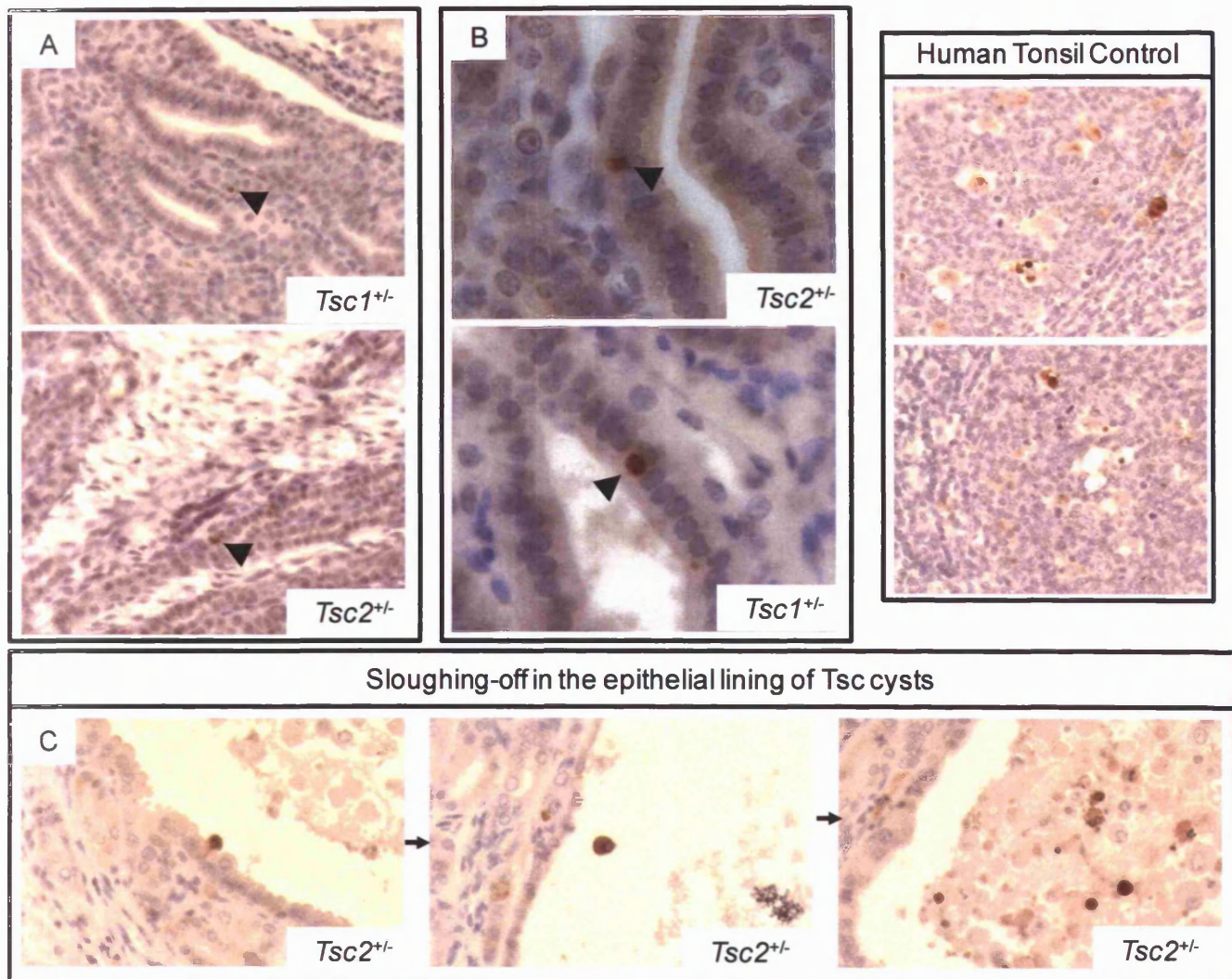


**Figure 4.1** Apoptosis in 2-day old mouse renal tubules. **Panel A:** Haematoxylin and cleaved-caspase 3 stained mouse renal tubules. Cell counts were made from all sections of the kidney (collecting duct, proximal tubule and Loop of Henle/ distal convoluted tubule). **Panel B:** 100x magnification images of apoptotic events taking place in *Tsc1*<sup>+/-</sup> and *Tsc2*<sup>+/-</sup> mouse renal tubules. **Panel C:** Apoptosis taking place in the lining of cyst epithelium (from 9-12 month old mice). Occasionally, sloughing-off may be seen, when a recently deceased cyst cell is forced into the cyst lumen, leading to the collection of apoptotic bodies in the central vacuation.



Genotype	Number of slides used	Number of apoptotic events	Apoptotic events per slide	Projected number of tubule cells	Percentage of tubule cells undergoing apoptosis	Percentage increase compared to wild-type
Wild-type	34	50	1.47	64246	0.078	n/a
<i>Tsc1</i> <sup>+/-</sup>	25	76	3.04	65337	0.117 ( <i>P</i> =0.026)	+33%
<i>Tsc2</i> <sup>+/-</sup>	28	53	1.89	44963	0.118 ( <i>P</i> =0.034)	+34%
<i>Pkd1</i> <sup>+/-</sup>	25	69	2.76	46322	0.149 ( <i>P</i> <0.001)	+48%

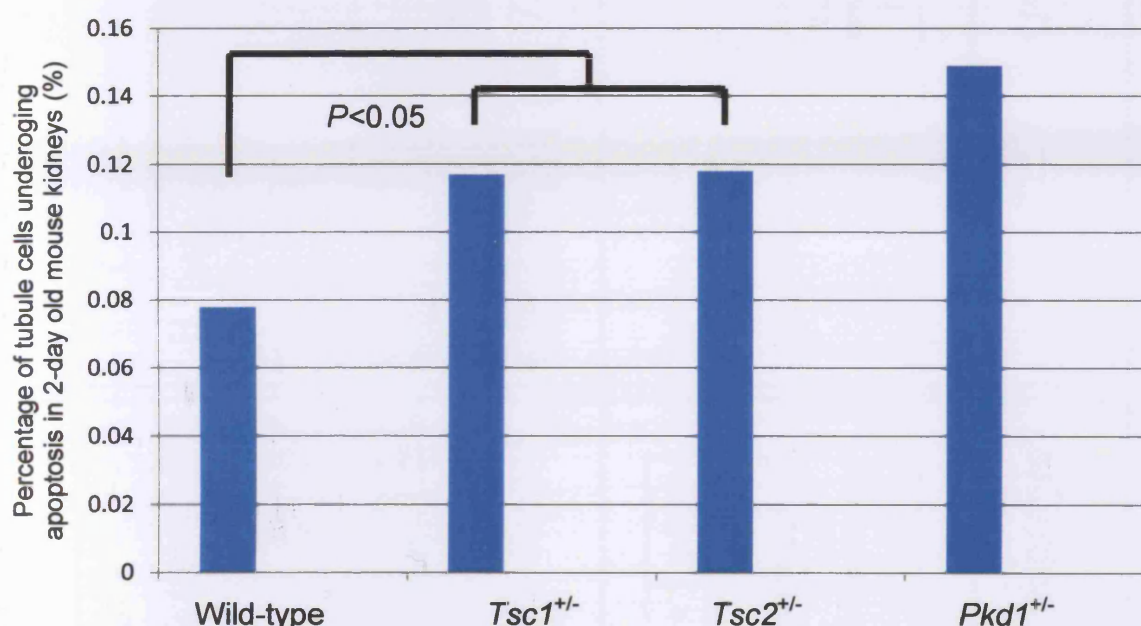


**Table 4.1** Levels of apoptosis in the developing renal tubules of *Tsc1*<sup>+/-</sup>, *Tsc2*<sup>+/-</sup>, *Pkd1*<sup>+/-</sup> and wild-type mice at 2 days of age. An average of 6 mice was used in each genotype, with tubule counts performed on representative kidney sections. Apoptotic lesions found across these slides were expressed as a percentage of total tubule cells, calculated from the representative sections. No significant difference was found in the levels of apoptosis between *Tsc1* or *Tsc2* mice and *Pkd1* mice. All three mutant mouse lines had significantly more renal tubule apoptosis compared to wild-type littermates (*P*=0.026 *Tsc1*<sup>+/-</sup>, *P*=0.034 *Tsc2*<sup>+/-</sup> and *P*<0.001 *Pkd1*<sup>+/-</sup>).

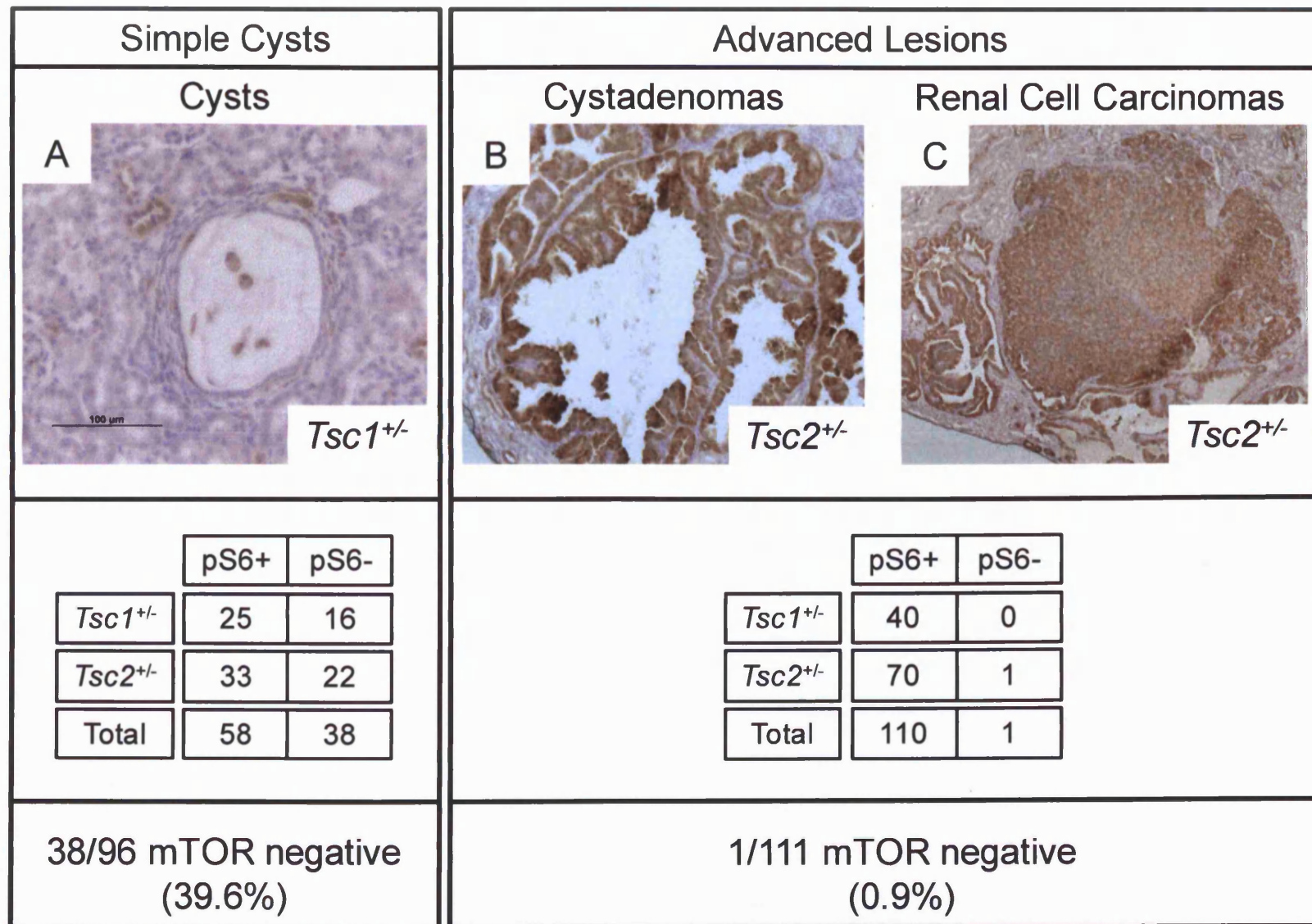


**Figure 4.2** Many simple cysts (A) do not stain positive for mTOR activity (indicated by the absence of a strong brown stain), while later and more advanced lesions (B and C) commonly do ( $P < 0.005$ ). Simple cysts are defined as having a single epithelial cell boundary, with no evidence of multicellular projections. Photos were taken from the serial sectioned kidneys of 9-12 month old *Tsc1*<sup>+/-</sup> and *Tsc2*<sup>+/-</sup> mice.



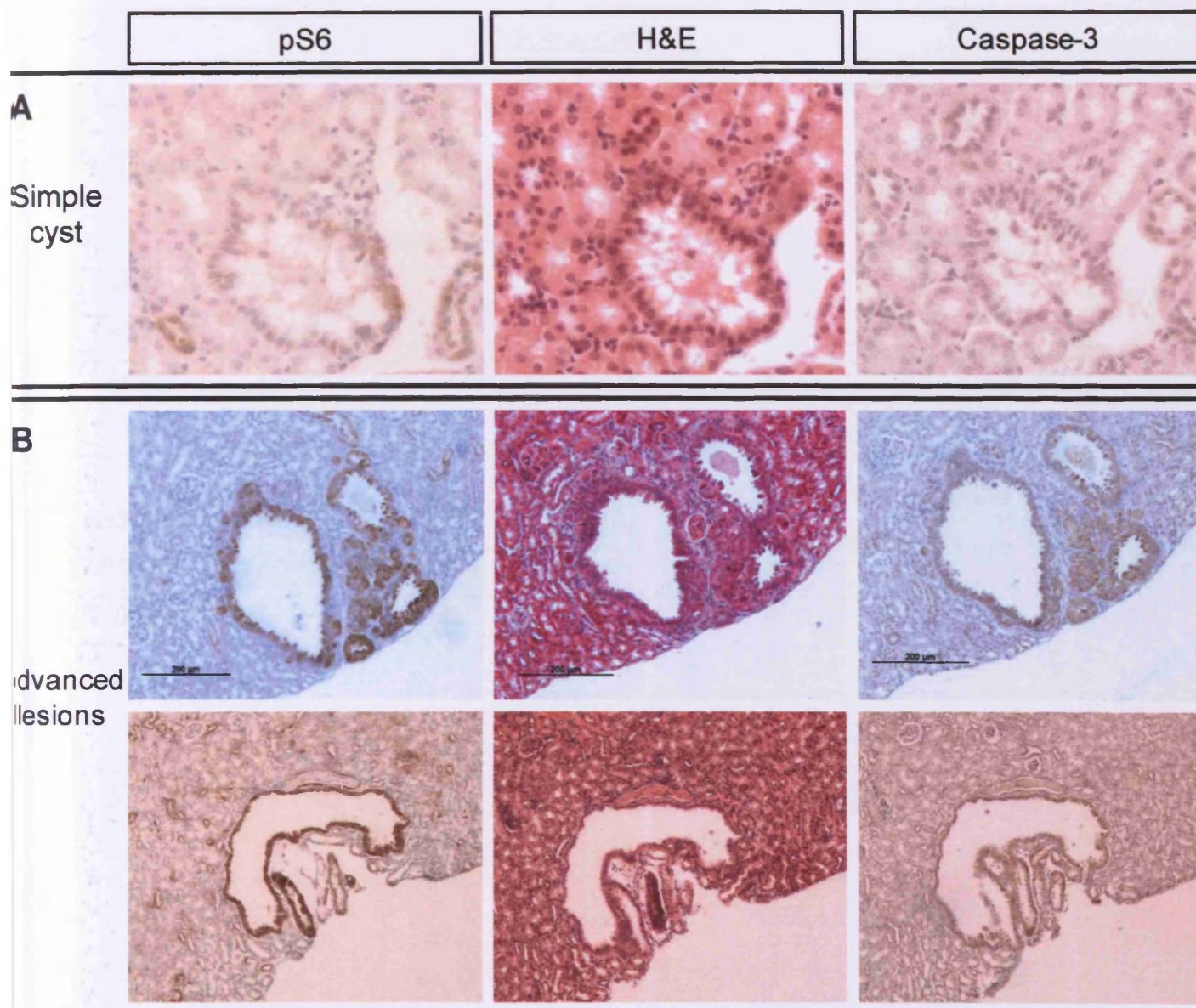


**Figure 4.3** Apoptotic and mTOR status of early and late lesions in Tsc cystogenesis. Serially sectioned kidneys from *Tsc1*<sup>+/-</sup> and *Tsc2*<sup>+/-</sup> were stained for mTOR and apoptosis. **Panel A:** Many simple cysts do not demonstrate mTOR activation, and these particular lesions are also negative for apoptosis. **Panel B:** Advanced lesions commonly stain strongly for both markers.

### Simple cysts

Mouse ID	Genotype	Negative pS6 / Negative caspase-3	Negative pS6 / Positive caspase-3	Positive pS6 / Negative caspase-3	Positive pS6 / Positive caspase-3	Total
6448A12	<i>Tsc1</i> <sup>+/-</sup>	6	0	4	1	41
6439624	<i>Tsc1</i> <sup>+/-</sup>	3	0	0	3	
64493AB	<i>Tsc1</i> <sup>+/-</sup>	6	0	2	7	
64387E7	<i>Tsc1</i> <sup>+/-</sup>	0	1	3	5	
B659B634	<i>Tsc2</i> <sup>+/-</sup>	3	0	3	3	55
B6596E10	<i>Tsc2</i> <sup>+/-</sup>	7	0	6	9	
B659B336	<i>Tsc2</i> <sup>+/-</sup>	2	1	3	3	
B659F8FA	<i>Tsc2</i> <sup>+/-</sup>	9	0	4	2	
		36	2	25	33	96

		Apoptotic Status	
		caspase-3 positive	caspase-3 negative
mTOR status	pS6 positive	33/58 (56.9%)	25/58 (43.1%)
	pS6 negative	2/38 (5.3%)	36/38 (94.7%)

**Table 4.2** Apoptotic and mTOR status of simple cysts in Tsc-associated renal cystogenesis. Eight mouse kidneys, four from each genotype, were serially sectioned and stained for mTOR and apoptotic status. Cysts were split into four subgroups, where it was found the mTOR negative subgroup were highly likely to contain cysts that did not stain for active apoptosis ( $P<0.001$ ).



### Advanced lesions

Mouse ID	Genotype	Negative pS6 / Negative caspase-3	Negative pS6 / Positive caspase-3	Positive pS6 / Negative caspase-3	Positive pS6 / Positive caspase-3	Total
6448A12	<i>Tsc1</i> <sup>+/-</sup>	0	0	7	10	40
6439624	<i>Tsc1</i> <sup>+/-</sup>	0	0	7	3	
64493AB	<i>Tsc1</i> <sup>+/-</sup>	0	0	6	3	
64387E7	<i>Tsc1</i> <sup>+/-</sup>	0	0	3	1	
B659B634	<i>Tsc2</i> <sup>+/-</sup>	0	0	5	10	71
B6596E10	<i>Tsc2</i> <sup>+/-</sup>	0	0	3	20	
B659B336	<i>Tsc2</i> <sup>+/-</sup>	0	0	8	12	
B659F8FA	<i>Tsc2</i> <sup>+/-</sup>	0	1	5	7	
		0	1	44	66	111

		Apoptotic Status	
		caspase-3 positive	caspase-3 negative
mTOR status	pS6 positive	66/110 (60%)	44/110 (40%)
	pS6 negative	1/1	0/1

**Table 4.3** Apoptotic and mTOR status of advanced lesions in Tsc-associated renal cystogenesis. Eight mouse kidneys, four from each genotype, were serially sectioned and stained for mTOR and apoptosis. Cysts were split into four subgroups, where it was found the vast majority of advanced lesions were positive for mTOR signalling but were equally likely to be positive or negative for apoptosis.

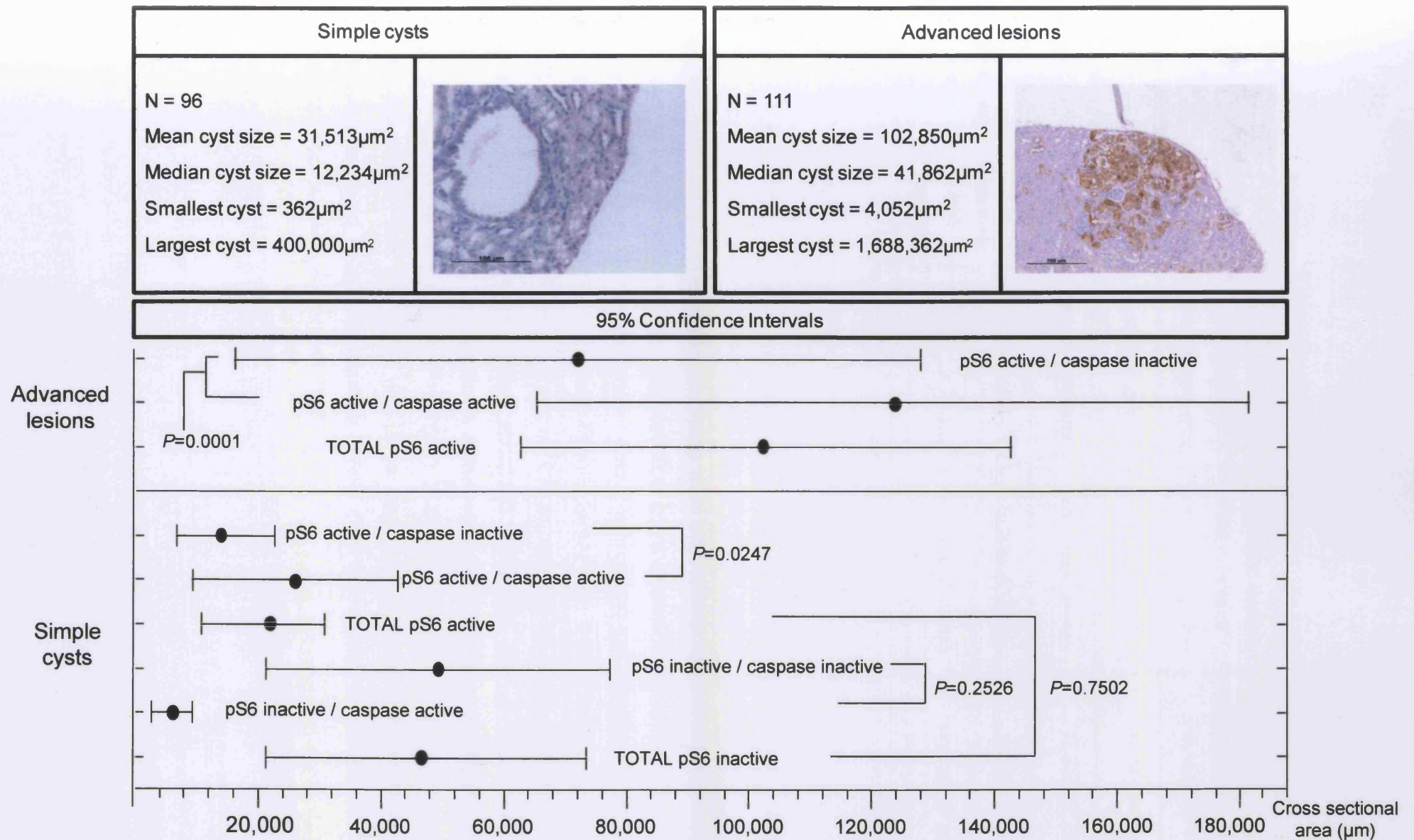


**Figure 4.4** The effect of mTOR activation and apoptosis on lesion size. Lesions from *Tsc1*<sup>+/-</sup> and *Tsc2*<sup>+/-</sup> mice at 9-12 months were categorised as simple or advanced, measured (cross sectional area, μm<sup>2</sup>) and compared. Simple cysts with mTOR activation were significantly larger with active apoptosis than those without ( $P=0.0247$ ). No significant difference was found between sizes of simple cysts from *Tsc1*<sup>+/-</sup> and *Tsc2*<sup>+/-</sup> mice.

Lesion classification	mTOR status	caspase-3 negative (N= number of individual cysts used)	caspase-3 positive (N= number of individual cysts used)	Mean lesion size based on pS6 status (N= number of individual cysts used)
Simple cysts	pS6 negative	49,682 $\mu\text{m}^2$ (N=36)	7,130 $\mu\text{m}^2$ (N=2)	47,443 $\mu\text{m}^2$ (N=38)
	pS6 positive	14,692 $\mu\text{m}^2$ (N=25)	25,913 $\mu\text{m}^2$ (N=33)	21,976 $\mu\text{m}^2$ (N=58)
Advanced lesions	pS6 negative	n/a (N=0)	70,208 $\mu\text{m}^2$ (N=1)	70,208 $\mu\text{m}^2$ (N=1)
	pS6 positive	72,015 $\mu\text{m}^2$ (N=44)	123,900 $\mu\text{m}^2$ (N=66)	103,146 $\mu\text{m}^2$ (N=110)

**Table 4.4** The effect of mTOR and apoptotic status on lesion size in *Tsc1<sup>+/-</sup>* and *Tsc2<sup>+/-</sup>* mice. Lesion size was categorised into advanced lesions and simple cysts. The sizes were then broken down according to mTOR status. Finally, lesions were assessed on their apoptotic status. All statistical comparisons were carried out with the Mann-Whitney test for non-parametric data. Perhaps not surprisingly, advanced lesions with mTOR activation were significantly larger than both simple cysts with mTOR activation ( $P<0.0001$ ) and without mTOR activation ( $P=0.0002$ ). In advanced lesions with mTOR activation, active apoptosis correlated with a larger cross sectional area ( $P=0.0001$ ). No significant difference was found between the mTOR positive and negative simple cysts ( $P=0.7502$ ). In simple cysts with mTOR activation, apoptosis activation was associated with larger cyst sizes ( $P=0.0247$ ). No significant difference was found in mTOR negative simple cyst sizes when compared in the context of apoptosis activation ( $P=0.2526$ ),

## **4.4 Discussion**

### **4.4.1 Latency in TSC-associated cystogenesis**

The *Tsc1*<sup>+/-</sup> and *Tsc2*<sup>+/-</sup> mice used in our study develop renal lesions in an age-dependent manner. New born mice will have no lesions, 3-6 month old mice may have a low number of simple cysts, 9-12 month old mice commonly have a range of cysts and cystadenomas, while older mice (18 months up) start to develop a significant amount of renal cell carcinomas (Wilson *et al.* 2005, Onda *et al.* 1999). A clear latency period exists where renal tissue from mice heterozygous for hamartin or tuberin is indistinguishable to wild-type littermates. This latency period has previously been cited as the time needed to provide a somatic mutation in the remaining *Tsc1* or *Tsc2* allele and induce cyst formation through loss of control over the mTOR pathway. This would follow the classic progression of TSG loss of function outlined by Knudson, but data from Wilson *et al.* (2006) in our *Tsc1*<sup>+/-</sup> mice suggests many of the earliest lesions do not stain for mTOR activation. Furthermore, we have discovered subtle but significant changes in the renal tubules and hepatic bile ducts of 2- and 10-day old *Tsc1*<sup>+/-</sup> and *Tsc2*<sup>+/-</sup> mice that predate cystogenesis (Chapter 3). These changes in primary cilium lengths and cell polarity are likely to occur in the absence of secondary hits in the TSC genes, given the early time scales involved and lack of cyst formation apparent at this age. Therefore, what we are seeing in our mice may not be a simple waiting period for a second hit in the mTOR pathway.

### **4.4.2 A significant proportion of Tsc-associated simple cysts do not stain for mTOR activation**

Since the discovery that the *TSC1* and *TSC2* gene products inhibit mTOR activity through modulation of Rheb GTP levels (Inoki *et al.* 2002, Tee *et al.* 2002), the majority of TSC research has centred on the mTOR pathway. Interestingly, in kidneys from our 9-12 month old *Tsc1*<sup>+/-</sup> and *Tsc2*<sup>+/-</sup> mice, we have found many simple cysts do not stain for pS6 (a marker of mTOR activity), while many later lesions do. This supports and builds upon previous work from our group that analysed *Tsc1*<sup>+/-</sup> mice to show 37% (20/54) of cysts showed little or no mTOR

activity, compared with 7% (7/98) of advanced lesions ( $P<0.001$ ) (Wilson *et al.* 2006). Cysts were stained across several sections where possible, and in all cases, pS6 staining was consistent across all lesions.

Data present here, along with similar studies by Kenerson *et al.* (2005) and Messina *et al.* (2007), suggest cysts associated with TSC can develop without activation of the mTOR pathway.

#### **4.4.3 Advanced lesions are highly likely to be positive for mTOR activation**

Nearly all later lesions (cystadenomas and RCCs) were found to be positive for mTOR signalling, which suggests that dysregulation of this pathway is something acquired as cysts progress and become more advanced. Downstream targets of active mTOR signalling involve stimulation of transcription, translation, cell growth and proliferation. These are all outcomes that may promote cystogenesis and lesion progression, perhaps explaining why mTOR activation is so commonly seen in advanced lesions.

#### **4.4.4 Apoptosis is elevated in developing renal tubules with defective polarity**

It was found that apoptosis was elevated in the renal tubules of our 2-day old *Tsc1*<sup>+/-</sup>, *Tsc2*<sup>+/-</sup> and *Pkd1*<sup>+/-</sup> mice when compared to wild-type littermates. This is another subtle, pre-cystic change that occurs alongside primary cilia defects and aberrant polarity. Since epithelial cells displaced from the extracellular matrix are subject to apoptotic cell death (Frisch *et al.* 1997), we suggest that apoptosis is acting as a rescue mechanism in renal tubules to prevent aberrant cell divisions from surviving. Under this hypothesis, the elevated levels of apoptosis seen in our mutant kidneys is an outward sign of the mechanism clearing misaligned cells from the developing renal tubules. Tubules with evidence of misorientated cell divisions (previously demonstrated in *Tsc1*<sup>+/-</sup>, *Tsc2*<sup>+/-</sup> and *Pkd1*<sup>+/-</sup> mice) are therefore likely to have raised levels of apoptosis to cope with this challenge to tubule architecture. In addition to elevated cell death in the lining of the 2-day old tubules, apoptotic bodies were also found in the tubule lumen, suggesting recently killed cells are sloughed off from the



tubule lining and enter the adjacent fluid to be cleared from the tissue. Because apoptotic cell death is a quick process (Green 2005), and the products of this process seem to be removed with efficient sloughing-off, IHC analysis of a kidney will detect a reduced portion of the total apoptotic events taking place. This highly efficient induction and clearance may explain why under widespread defective polarity conditions, levels of tubule apoptosis appear elevated only ~1.5 times in our *Tsc1*<sup>+/-</sup>, *Tsc2*<sup>+/-</sup> and *Pkd1*<sup>+/-</sup> mice compared to wild-types.

#### **4.4.5 Apoptosis is important in wild-type kidney development**

While apoptosis may be acting as a rescue mechanism in the renal tubules of mice with defective polarity (*Tsc1*<sup>+/-</sup>, *Tsc2*<sup>+/-</sup> and *Pkd1*<sup>+/-</sup>), the process is clearly important in normal tissue development too. This is illustrated by the presence of apoptotic cells in the lining of wild-type renal tubules. Our lab has shown cell orientation in wild-type mice to be a tightly controlled process, but the occasional division does take place outside the plane of the renal tubule. Some of the apoptosis seen in renal tubules from wild-type mice may be accounted for by the occasional cell that has mis-divided and become removed from cell-cell contacts and the basement membrane. Aside from this, wild-type tubule cells could be stimulated to die for a range of physiological reasons, such as occurrence of spontaneous mutations, DNA damage, the need to control cell numbers or simply in the process of sculpting the renal architecture (Brill *et al.* 1999).

#### **4.4.6 Simple cysts that are negative for activation of the mTOR pathway are not likely to display apoptosis**

Following the identification of apoptosis as a potential rescue mechanism in kidneys with defective polarity, we then analysed simple cysts for signs of apoptosis. Simple cysts which did not demonstrate mTOR activity were highly likely to be negative for caspase-3 activity. This result implies a strong correlation between cyst development, lack of mTOR activation and lack of apoptosis. It may be defects in misaligned cell removal, such as through inappropriate survival may eventually

produce a cyst through mTOR-independent means. Mutations that render a progenitor cyst cell to be unresponsive to death cues following an aberrant division are likely to persist through to the eventual cyst as our Tsc lesions are clonal. The higher levels of apoptosis seen in advanced lesions may be explained by the cyst environment itself, which has previously been noted to be hostile, hypoxic and nutrient deprived. mTOR activation is present in the majority of these advanced lesions, and the elevated apoptosis rates could also be due to consequences of dysregulated mTOR signalling.

#### **4.4.7 Caspase and mTOR activation modulate cyst size**

Renal lesions were assessed for cell size in the context of mTOR activation and apoptotic status. The subset of simple cysts that were negative for mTOR and apoptosis contained the largest and smallest of all simple cysts measured. Between these two extremes, huge variability was seen in cyst size in mice from the same age group. Without loss of mTOR control to drive cyst size, an observer may expect mTOR negative cysts to remain relatively small, but this evidently not always the case. Cyst size is therefore influenced by more factors than mTOR status alone, although this is clearly important given mTOR's cellular functions and the role of hamartin and tuberlin in its repression. Cysts that are developing without functional apoptotic machinery (contained within the caspase-3 inactive subset) may not be subject to the growth restriction experienced by other caspase-3 active cysts. Factors such as contact-inhibition of growth and self-limiting cell proliferation may restrict the expansion of other cysts (even though they may have more cellular stimuli driving their enlargement).

In the mTOR active simple and advanced lesions, we found that absence of caspase staining correlated strongly with a smaller average lesion size. This may seem counter-intuitive, because a lack of apoptosis should lead to more cells being present in the lesion, and therefore a larger lesion size. However, mTOR active lesions are likely to be highly proliferative (for reasons outlined above, and in Chapter 1, Section 1.3.6) and may be able to offset the cells lost through apoptosis to an overall net gain in lesion size. Similarly, mTOR active lesions without caspase staining may be weakly proliferative, so as to not trigger cell cycle-induced

apoptosis. It may be possible that apoptosis is a marker for cysts and lesions with the capacity to become large and progressive. This is because apoptosis is so closely linked to cell proliferation, a key determinant of overall lesion size.

Perhaps not surprisingly, it was found mTOR active advanced lesions had a significantly larger cross sectional area compared to mTOR active, and mTOR inactive simple cysts in the same *Tsc1*<sup>+/-</sup> and *Tsc2*<sup>+/-</sup> mice. Between the simple cysts, mTOR activation was not found to modify lesion size. The mTOR pathway has well characterised roles in cell growth and proliferation, explaining why mTOR positive advanced lesions tend to be larger than mTOR negative simple cysts. The cells that compose the lesion will be more proliferative and larger than cyst cells that can control mTOR signalling. Because these advanced lesions are also larger than mTOR positive simple cysts, it may be reasonable to assume a certain level of progression is required for lesion size to increase under dysregulated mTOR signalling. All these lesions have come from the same group of 9-12 month old mice, but lesions may develop at different rates and at different starting points. For a cyst to become advanced and far removed from normal renal tissue, various mutations are likely to be collected on the way towards a lesion with multiple papillae projections or a solid carcinoma centre. Therefore, by selecting for a comparison between advanced lesions and simple cysts, we are comparing the relative purity of a fresh lesion to the genetic chaos present in a progressive renal tumour. The advanced lesion may have acquired numerous mutations outside the mTOR pathway, some of which could pertain to overall lesion size (through changes to genes that alter the cellular response to growth factors, vascularisation factors or nutrient uptake, for example).

Finally, it is important to note that the absence of a caspase stain in a cyst does not necessarily mean that the lesion does not contain functional apoptotic machinery. It simply means that when the IHC stain was performed, no apoptosis was taking place. This could be due to a defect, lack of pro-death stimulation or strong pro-survival signalling.

## **CHAPTER FIVE: Activation of the Jak/Stat signalling pathway in Tsc-associated cystogenesis**

### **5.1 Introduction**

Previous work has revealed widespread polarity defects in both renal and hepatic tissue from Tsc mice (see Chapter 3). While polarity has been strongly linked to cystogenesis (Bissler *et al.* 2005), there is a significant delay between widespread misaligned cell divisions taking place (2 and 10-day old mice) and disruption of renal architecture with tubule dilation and cystogenesis (around 6 months). Work in developing renal tubules suggest that apoptosis may be acting as a rescue mechanism to clear aberrant cell divisions from the organ, as cleaved caspase-3 levels are elevated in mice with defective polarity compared to wild-type littermates (see Chapter 4). Further data in simple cysts has highlighted a subset of lesions that have developed without mTOR activation and are also negative for a marker of active apoptosis (see Chapter 4). A failure to initiate apoptosis in response to a misaligned cell division may be the first step towards the formation of some TSC-associated cysts.

How could a misguided cell division be selected for apoptotic cell death in a renal tubule or hepatic bile duct? The working hypothesis put forward by our lab is that a misorientated cell division at an extreme angle to the plane of the tubule or duct will result in a daughter cell a) more distant from the tubule basement membrane b) more isolated in terms of cell / cell contact and c) further removed from pro-survival signals. Indeed, it has been shown in mammary glands (Pullen *et al.* 1996) that cells require survival signals from the basement membrane to prevent the engagement of apoptosis, and that this survival is enhanced by cell-cell contact.

Aberrantly divided cells may well lack tight junctions with adjacent tubule cells, leading to isolation and loss of cellular communication (both associated with apoptosis). Cells in these tubules that are dividing incorrectly may be subject to this level of intrinsic control and will undergo apoptotic death and slough-off into the flow of the adjacent lumen. It may be through this control that aberrantly divided cells are prevented from dilating the tubule and leading the organ towards cyst formation.

As reviewed in Chapter 1 (Section 1.3.6), apoptosis is controlled cell death through two general routes. Internal apoptosis involves a signalling phase (such as a toxic insult, cell injury, DNA damage or removal of survival signals) to stimulate a shift in the internal balance of Bcl2 family members towards mitochondrial membrane permeabilisation and cytochrome c release. External apoptosis is characterised by a different signalling phase, and involves the stimulation of specific cell surface receptors by cell death associated ligands. Both forms of apoptosis proceed to an execution phase that involves the activation of caspases, which mediate the cleavage of key structures and bring about characteristic morphological changes. This includes chromatin fragmentation, membrane blebbing (surface changes) and the eventual formation of apoptotic bodies. These are commonly sloughed-off from surrounding, healthy cells and subjected to phagocytosis. Apoptosis is thought to be the consequence of an intricate balancing act by the cell, with factors supporting and inhibiting the process. It is crucial for maintaining appropriate cell numbers and tissue organisation, and is also implicated in many pathogenic conditions. In cyst formation specifically, several animal models with aberrant apoptosis experience a renal cystic phenotype (reviewed in Chapter 1, Section 1.3.6.2). Gene mutation involved in removal of this apoptotic control is more likely to be a single gain-of-function mutation (the activation of a proto-oncogene) rather than two separate hits to remove a tumour suppressor gene function.

Anoikis (reviewed in Gilmore 2005 and Zhan *et al.* 2004) is defined as a subset of apoptotic cell death arising through inadequate or inappropriate cell-matrix interactions. It is commonly called anchorage-related apoptosis. Examples of anoikis include the apoptosis after detachment and shedding of terminally differentiated colon epithelial cells into the lumen (Strater *et al.* 1996), and the apoptosis of mammary epithelial cells upon regression of the mammary gland (Lund *et al.* 1996). It has also been observed in kidney epithelial cells (Frisch *et al.* 1994) where the term anoikis was first coined. Communication exists between cells and their surroundings, such as specific interactions with the extracellular matrix (ECM) and also neighbouring cells. A removal or disruption of either of these interactions can be sufficient to induce anoikis in a cell. Several groups have published data showing how cells deprived of ECM contact undergo classical apoptosis (Frisch *et al.* 1994, Meredith *et al.* 1993). A crucial finding in these papers was that anoikis was inhibited

by overexpression of *Bcl2* indicating apoptosis was taking place through the intrinsic, mitochondrial route. They also noted that not all cell types are equally sensitive to anoikis, with epithelial cells (such as the ones lining kidney tubules) being more sensitive than fibroblasts. Oncogenic transformation (conferred by mutations in cell-cell adhesion molecules, integrins, integrin-associated signalling molecules or apoptotic regulators) can cause these epithelial cells to become anoikis insensitive. Many of these cellular interactions are mediated by adhesion receptors, which function in an analogous way to growth factor receptors (GFRs) and activate many of the same downstream pathways (Gilmore 2005). Indeed, GFRs themselves can relay important spatial information to a newly divided cell, as distance to the basement membrane (and pro-survival GFs) is a function of the cell's position. Incorrect attachment by the cell to the immediate environment is conveyed by integrins and growth factors to result in suppression of pro-survival signalling (such as through PI3K and ERK pathways) and activation of pro-apoptotic signalling (for example through p53 induction and modulation of the *Bcl2* family of genes).

It is important to note that correct attachment to the environment is not sufficient on its own to provide a survival signal. Cell spreading and shape can profoundly influence phenotype, with the role played by the cytoskeleton in these aspects of adhesion signalling being critical. Additionally, integrins crosstalk directly with GFRs to permit cells to fully respond to growth factor signalling when correctly orientated in their surroundings (Gilmore 2005).

While strong evidence exists to support this form of cell death occurring through the intrinsic route (Frisch *et al.* 1996, Ilic *et al.* 1998), some studies suggest the external route of apoptosis can be involved too. Epithelial cells overexpressing a dominant-negative form of FADD (which blocks caspase-8 recruitment to the DISC) inhibits anoikis (Frisch *et al.* 1999, Rytomaa *et al.* 1999). This implicates both types of apoptosis in controlling the correct position of cells within tissues.

We hypothesised that our cysts that have arisen without mTOR activation may have done so through gain-of-function mutations in pro-survival signalling pathways. We therefore stained our cysts for a variety of markers to provide information on the pathways activated and repressed. Because the library of cysts constructed in Chapter 4 was a scarce resource, it was important to identify the key regulatory

proteins in cell survival signalling that could lead to defective apoptosis in renal tubules. Figure 5.1 reviews the apoptotic and anoikis signalling network and highlights important proteins in the pathways.

Bcl2 is an integral outer mitochondrial membrane protein which regulates cell death by controlling permeability of this membrane to cytochrome c. It is a member of a large family of both pro- (Bid, Bak, Bax, Puma and Noxa) and anti- (Bcl2 and BclxL) apoptotic factors. While many of these family members differ in specific protein domains, most will contain a C-terminal transmembrane domain that targets these proteins to the outer mitochondrial membrane. Once released through the action of pro-apoptotic factors, cytochrome c will induce apoptosis by activating caspase-9 and subsequently, caspase-3. Bcl2 exerts its anti-apoptotic function in two ways, firstly by preventing the activation of caspases by inhibiting the release of cytochrome c from mitochondria, and secondly by binding to the apoptosis activating factor (APAF1). Previous work has suggested that expression levels of Bcl2 family members may determine the sensitivity of a cell to anoikis (Strasser *et al.* 2000), and overexpression of this protein may protect cells from anchorage-mediated death (Frisch *et al.* 1996). We therefore selected to stain for elevated Bcl2 in our cohort of cysts.

Stat3, also called Acute Phase Response Factor (APRF), is a member of the STAT (signal transducers and activators of transcription) family. It is activated as a result of signalling by a variety of cytokines, growth factors and other stimuli. It has been suggested to play both a pro-apoptotic role (for example, during mammary gland involution) and a pro-survival role (in numerous human and mouse malignancies) (Yu *et al.* 2009). Tyrosine phosphorylation at a single site near the carboxyl-terminus of Stat3 (Tyr<sup>705</sup>) is required for dimerisation, nuclear translocation and DNA binding (Lo *et al.* 2003). However, full transcriptional activity of the Tyr<sup>705</sup> homodimer is only achieved through further phosphorylation at a site within the transactivation domain (Ser<sup>727</sup>). JAKs phosphorylate Stat3 at Tyr<sup>705</sup>, while Ser<sup>727</sup> can be phosphorylated by several means, discussed later. We opted to stain for the Tyr<sup>705</sup> form of the protein.

JAK2 is widely expressed member of the Janus family of tyrosine kinases and its importance is highlighted by its susceptibility to mutational activation which leads to cell transformation (Kurzer *et al.* 2006). Commonly, JAK signalling is induced by



interaction of an internal FERM domain with activated cytokine receptors. While these receptors have no intrinsic catalytic ability, binding of cytokines (such as erythropoietin, interleukins and interferons) to the receptor leads to recruitment and activation of JAK tyrosine kinases. The JAK/STAT axis is of interest to our studies because it is a key mediator of cell survival. Furthermore, it is constitutively activated in a number of human diseases, such as RCCs (Wu *et al.* 2007) and various other inflammatory diseases and cancers (Yu *et al.* 2009). Activation of JAK2 has been strongly correlated with elevated STAT3 signalling in human diseases such as polycythemia vera and essential thrombocythemia (Constantinescu *et al.* 2007). It has two sites that are associated with kinase activity, Tyr<sup>1007</sup> and Tyr<sup>1008</sup> (with Tyr<sup>1007</sup> likely to be more important) and we opted to use an antibody that recognised this double phosphorylated, active form of Jak2 (Feng *et al.* 1997).

NF-κB is a protein complex that controls transcription of DNA. It is found in most cells and is activated in response to cell stress, cytokine signalling and bacterial / viral antigens (providing a link to the immune system). NF-κB is a heterodimer of subunits that translocate to the nucleus upon activation to modulate a wide variety of genes (Baldwin 1996, May *et al.* 1997). These subunits have two general classes; Class I, which includes p100 and p105 (these are large precursors and are processed to p52 and p50 respectively) and Class II, which includes p65 (also called RelA). NF-κB is not considered a strong activator of transcription unless the signalling complex includes p65. This subunit is phosphorylated by protein kinase A (PKA) on serine 726 to activate signalling (Zhong *et al.* 1998), and it is this form of p65 that we opted to stain for in our simple cysts. Because NF-κB does not require new protein synthesis to be activated it is an extremely fast acting transcription factor signalling pathway and a first responder to harmful cellular stimuli. It is a widely expressed regulator of genes that control cell proliferation and survival, and as such, is frequently constitutively activated in disease (Karin 2006). Cancers such as pancreatic and breast have been found to have upregulated NF-κB signalling (reviewed in Rayet *et al.* 1999, Cascinu *et al.* 2007). Chronic inflammation has been linked to cystogenesis in renal tissue in conditions such as ADPKD, and NF-κB signalling is known to be activated by pro-inflammatory cytokines such as IFNα. Because of these numerous links to proliferation, survival and responses to

cytokines and inflammatory signalling molecules, we opted to stain for transcriptionally active NF- $\kappa$ B in our cysts.

HGF is known to be mitogenic and anti-apoptotic in renal tubule cells (Horie *et al.* 1994) and a mouse model that overexpresses HGF experiences a renal cystic disease similar to our Tsc mice, with tubular cystic dilation (Takayama *et al.* 1997). It is known HGF signalling leads to inhibition of Anoikis in cancerous cell lines, via PI3K/Akt activation and MAPK pathways (Xiao *et al.* 2001). This has obvious interesting implications for our mice as it may well be that disruption of cell-cell interactions / removal of ECM survival signals is pushing a misdivided cell to undergo apoptosis. We opted to stain for the activated form of the high affinity HGF receptor, c-Met, to ensure stains were tightly localised to the cystic epithelia, rather than diffuse across the tissue section (as may be the case with a soluble GF).

Akt, also called Protein Kinase B (PKB), is Serine/Threonine kinase. Its principle role in the cell is to promote growth factor mediated cell survival and to block apoptotic cell death. To be fully activated, it requires phosphorylation at two regulatory residues, Threonine 308 (by PDK1) (Alessi *et al.* 1996) and Serine 473 (by mTORC2) (Sarbasov *et al.* 2005). The initial phosphorylation event (Thr<sup>308</sup>) appears to 'prime' the kinase, while the additional phosphorylation (Ser<sup>473</sup>) enhances activity (Pommier *et al.* 2004). We used an antibody that recognises the Ser<sup>473</sup> form of Akt, the enhanced form of the activated kinase, used in many publications for a similar purpose (Engelman *et al.* 2008, Allard *et al.* 2008, Segrelles *et al.* 2008). The kinase has many links to inappropriate cell survival in human and mouse cancers, with interestingly links to the mTOR axis. Although we are primarily looking for activation of pathways outside the mTOR axis, Akt is an important staining target because it has been shown to be activated in other TSC lesions (Han *et al.* 2004).

Finally, p53 is the most commonly mutated gene in human cancers (Cheah *et al.* 2001), and this reflects its role as a cell cycle regulator and mediator of apoptosis. It is normally kept at low levels through continuous degradation, but is increased and activated under periods of cell stress. In contrast to most other proteins, it is regulated through protein modification rather than transcriptional or translational upregulation. It is primarily through interaction with its regulatory binding partner, Mdm2 that mediates this control through targeting the heterodimer for ubiquitination

and proteasome degradation. Phosphorylation of p53 at the N-terminus interrupts this interaction and leads to elevated p53 in the cytosol and the nucleus (due to a nuclear localisation domain). Further modification of p53 can then enhance specificity for binding elements of downstream genes that control cycle progression and cell survival. Mutations in p53 that arise in cancer commonly occur in the DNA binding domain of the protein, rendering it unable to modulate gene function in the face of cellular stress. Because cysts are known to be highly hostile environments and may display dysregulated cell proliferation and apoptosis, we therefore opted to stain for elevated p53 in our cohort of cysts.

Here, we investigate if pathways that are generally outside the mTOR/TSC axis are dysregulated and contributing to inappropriate cell survival in early cystogenesis. To do this, the panel of 96 simple cysts previously assessed for mTOR activity (positive or negative for pS6) and apoptotic activity (positive or negative for cleaved caspase-3) (see Chapter 4) were screened for a variety of markers of cell survival. The selection of staining targets for this investigation was the result of careful analysis of current literature, pathways and animal models. These proteins were finalised as the following: Bcl2, Stat3, p65, c-Met, Akt, p53 and Jak2.

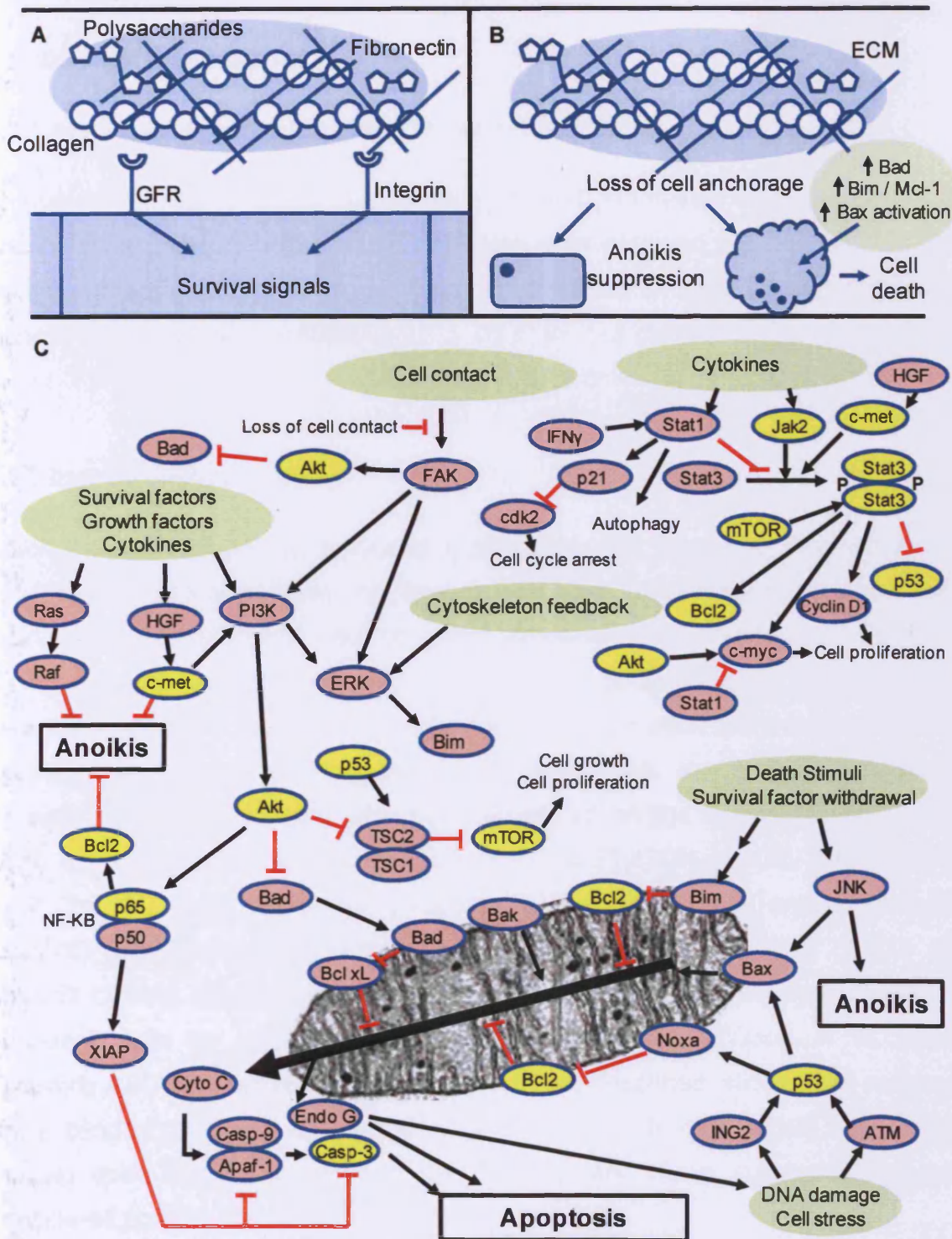


**Figure 5.1** Identification of key proteins within anoikis and apoptosis signalling. **Panel A:** Cell contact with the ECM or other cells promotes cell survival. It does this through many of the same pathways as GFR signalling. The ECM is also a source of survival signals that stimulate GFRs. **Panel B:** Loss of cell anchorage leads to upregulation of pro-apoptotic Bcl2 family members and cell death. **Panel C:** The Bcl2 family of proteins regulate apoptosis by controlling mitochondrial permeability. Anti-apoptotic Bcl2 and BclxL are located on the outer mitochondrial membrane, where they inhibit cytochrome c release. Pro-apoptotic family members such as Bad, Bak, Bax and Bim are cytosolic until activated by death signalling. The ultimate release of cytochrome c and resultant apoptosis is the result of a precise interplay between many cellular proteins (which centre on activation / repression of the Bcl2 family). Yellow colour indicates a protein analysed in our study.

## **5.2 Materials and methods**

### **5.2.1 Animal care, genotyping and tissue preparation**

All matters relating to animal husbandry, care and genotyping were carried out as previously described. *Tsc1*<sup>+/-</sup> and *Tsc2*<sup>+/-</sup> mice were obtained at 9-12 months. Four mice from each genotype were sacrificed and dissected to obtain paraffin-embedded kidneys as previously described.

### **5.2.2 Immunohistochemistry**

Whole kidneys were serially sectioned at 5µm onto clear Superfrost Plus slides. The resulting bank of kidney tissue was then assessed for Tsc-associated lesions through staining every 6<sup>th</sup> slide with H&E (to reveal abnormal tissue architecture). Following identification of a lesion, further IHC stains were carried out on adjacent slides known to contain the same cyst. A marker of mTOR activation and a marker of active apoptosis were used to categorise the bank of cysts as previously discussed (Chapter 4). Further staining was then carried out on the remaining serial slides using the following antibodies: anti-phospho-Stat3 (Tyr705) (1:100), anti-phospho-Jak2 (Tyr1007/1008) (1:50), anti-phospho-Akt (Ser473) (1:100), anti-phospho-p65 (Ser276) (1:50), anti-phospho-Met (Tyr1234/1235) (1:150), anti-Bcl2 (1:100) and anti-p53 (1:100). Simple cysts were defined as cysts having a single epithelial cell boundary, with no evidence of multicellular projections (Wilson *et al.* 2006). Following ABC peroxidase treatment as previously described, slides were assessed under blinded conditions. A grading system was used to differentiate the staining, ranging from G0 (no staining) to G4 (heavy, dark brown staining); G3/4 was considered positive and compared to G0-2.

### **5.2.3 Statistical analysis**

Cyst staining data was compared using Fisher's exact test with contingency tables. Larger samples (N>6 in all categories) were analysed with a Chi-squared test.

## 5.3 Results

### 5.3.1 Delineating the pro-survival mechanism in mTOR-inactive simple cysts from *Tsc1*<sup>+/-</sup> and *Tsc2*<sup>+/-</sup> mice

In cysts without mTOR activation and that were not undergoing apoptosis, we did not find activation of c-Met (Y1234/Y1235) (0/12 cysts stained strongly), Akt (S473) (0/14 cysts stained strongly) or p65 (NF-κB) (S726) (0/11 cysts stained strongly) (Table 5.1) (Figure 5.2). In contrast, we did observe activation of Jak2 (Y1007/Y1008) (10/12 cysts stained strongly) and its downstream targets Stat3 (Y705) (9/10 cysts stained strongly) and Bcl2 (7/13 cysts stained strongly) (Figures 5.3, 5.4 and 5.5 respectively). As expected, activation of the Jak2-Stat3-Bcl2 pathway was significantly less frequent in cysts with mTOR activation and that were undergoing apoptosis (phospho-Jak2 4/14 cysts stained,  $P=0.008$ ; phospho-Stat3 3/12 cysts,  $P=0.004$ ; Bcl2 1/12 cysts,  $P=0.030$ ) (Table 5.1 and 5.2). No mice had germline variants in the regulatory region of the *Jak2* gene (discussed in full in Chapter 6).

To determine whether activation of the Jak2/Stat3 pathway was occurring in an mTOR-independent manner, we analysed cysts that showed activation of mTOR but that were not undergoing apoptosis. We found significantly less of these cysts stained for activated Jak2 (Y1007/Y1008) (5/15 cysts,  $P=0.019$ ) and Stat3 (Y705) (4/14 cysts,  $P=0.005$ ) as compared to the mTOR-inactive, caspase-3 negative, cysts. Interestingly, Bcl2 was elevated in similar proportions of mTOR-active (6/13 cysts stained) and mTOR-inactive (7/13 cysts) cysts that were not undergoing apoptosis.

We also stained for levels of p53 to determine if this pro-apoptotic protein was elevated in our simple cysts (Table 5.1, 5.2 and Figure 5.6). We found 4/15 cysts that were mTOR inactive and caspase-3 inactive stained strongly for p53. However, no significant difference was found between the levels of strong p53 staining when this was compared to mTOR active / caspase-3 inactive cysts (1/9 cysts,  $P=0.615$ ) or mTOR active / caspase-3 active cysts (1/10 cysts,  $P=0.615$ ).

	mTOR inactive / caspase-3 inactive	mTOR active / caspase-3 inactive	mTOR active / caspase-3 active
phospho-Met (Y1234/Y1235)	0/12	0/9 ( $P=1.000$ )	0/9 ( $P=1.000$ )
phospho-Jak2 (Y1007/Y1008)	10/12	5/15 ( $P=0.019$ )	4/14 ( $P=0.008$ )
phospho-Akt (S473)	0/14	0/12 ( $P=1.000$ )	0/12 ( $P=1.000$ )
phospho-Stat3 (Y705)	9/10	4/14 ( $P=0.005$ )	3/12 ( $P=0.004$ )
phospho-p65 (S276)	0/11	2/11 ( $P=0.476$ )	1/10 ( $P=0.476$ )
Bcl2	7/13	6/13 ( $P=0.695$ )	1/12 ( $P=0.030$ )
p53	4/15	1/9 ( $P=0.615$ )	1/10 ( $P=0.615$ )

**Table 5.1** Simple cysts staining strongly (G3/4) for phospho-Met, phospho-Jak2, phospho-Akt, phospho-Stat3, phospho-p65, Bcl2 and p53. Results are categorised by their mTOR and caspase-3 activity. All  $P$  values are in comparison to strong staining events in mTOR inactive / caspase-3 inactive simple cysts.



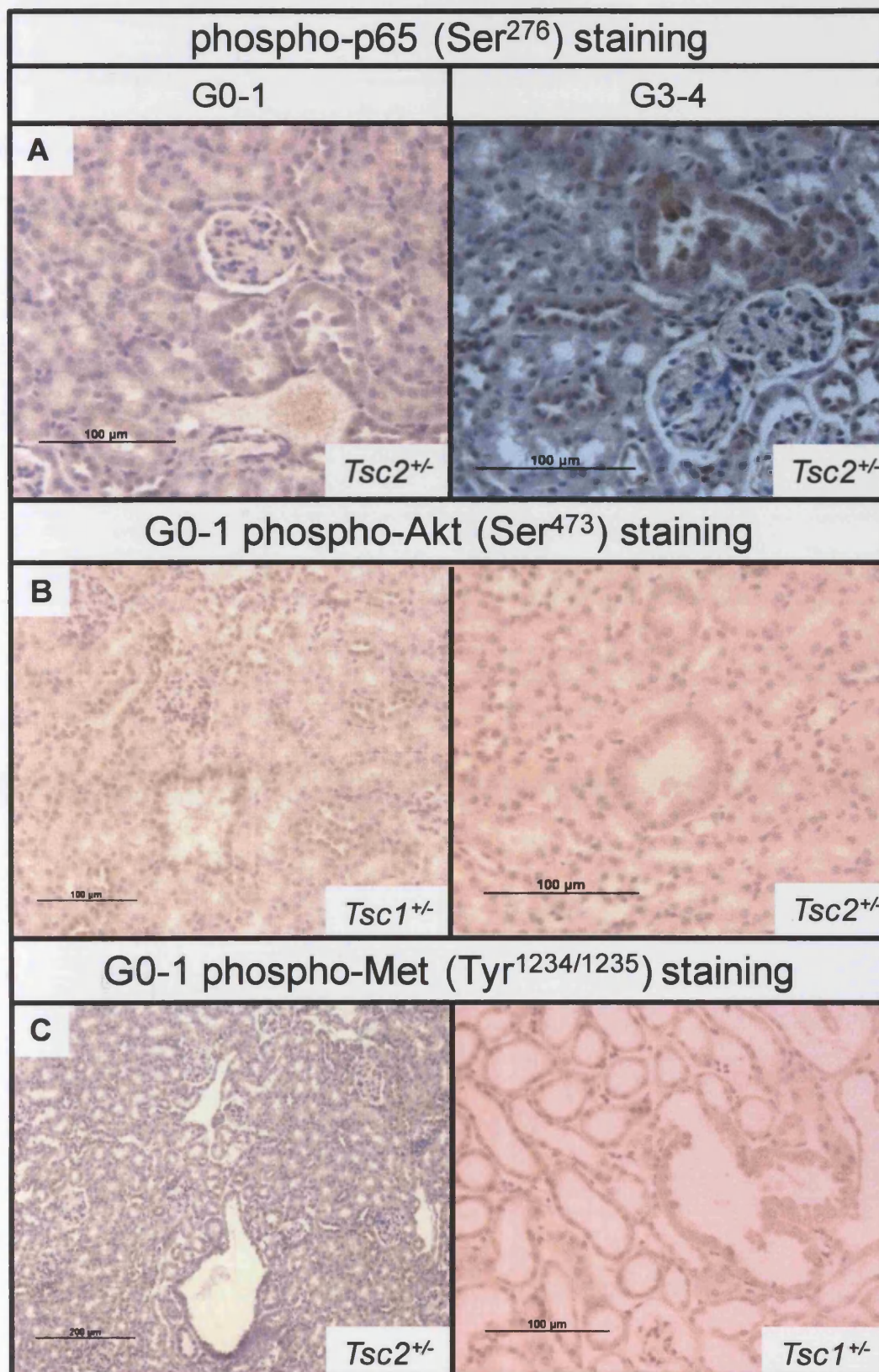


**Figure 5.2** mTOR inactive / caspase-3 inactive simple cysts do not show activation of Akt, c-Met or p65. **Panel A:** phospho-p65 weak and strong staining in mTOR inactive (left) and active (right) cysts. **Panel B:** no simple cysts stained strongly for phospho-Akt, regardless of mTOR / apoptotic status. **Panel C:** no simple cysts stained strongly for phospho-Met, regardless of mTOR / apoptotic status



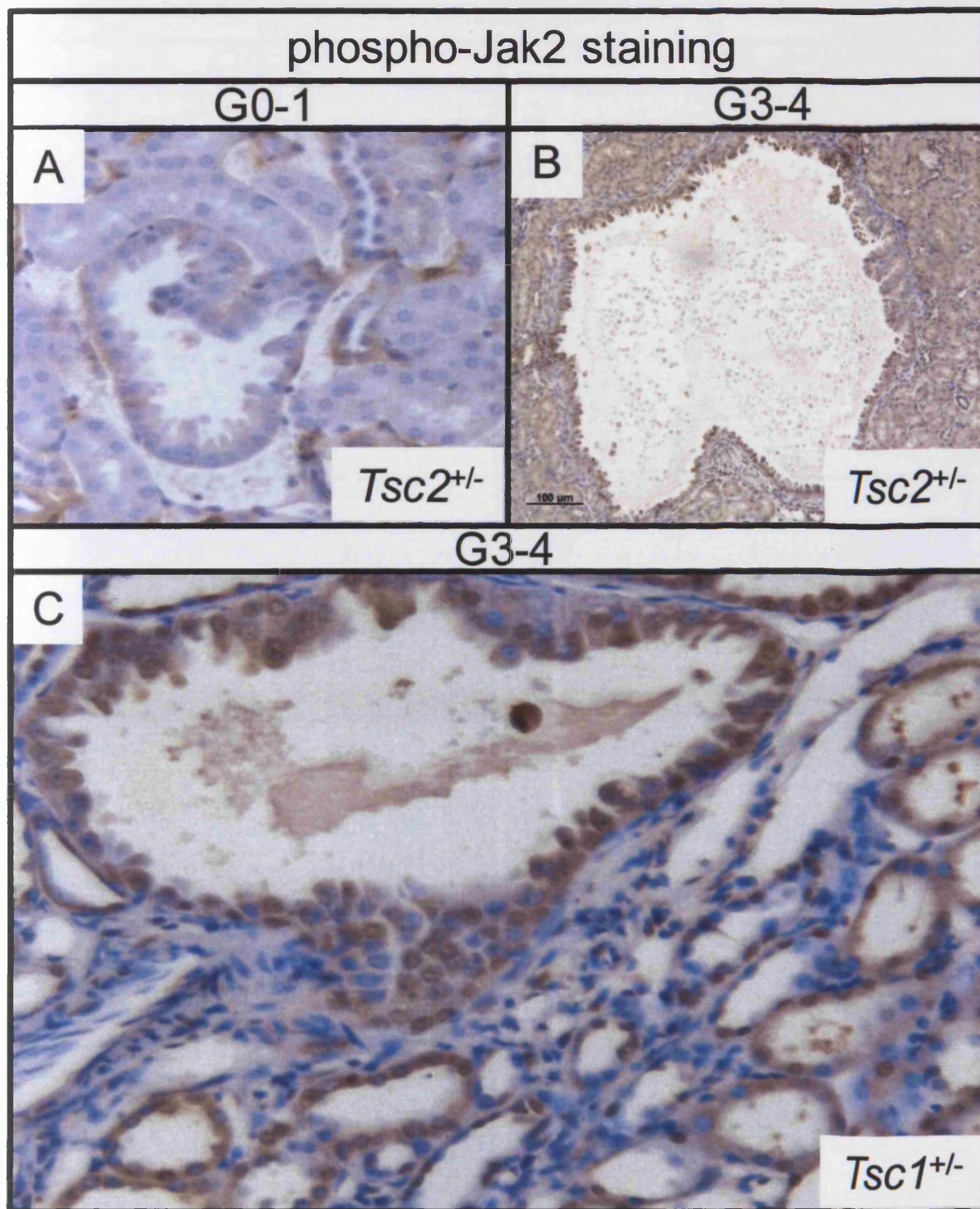


**Figure 5.3** Activation of Jak2 in simple cysts from *Tsc1<sup>+/-</sup>* and *Tsc2<sup>+/-</sup>* mice, with examples of weak (**Panel A**) and strong (**Panels B and C**) staining. Jak2 was found activated in significantly more mTOR inactive / caspase-3 inactive lesions compared to mTOR active / caspase-3 inactive and mTOR active / caspase-3 active cysts.



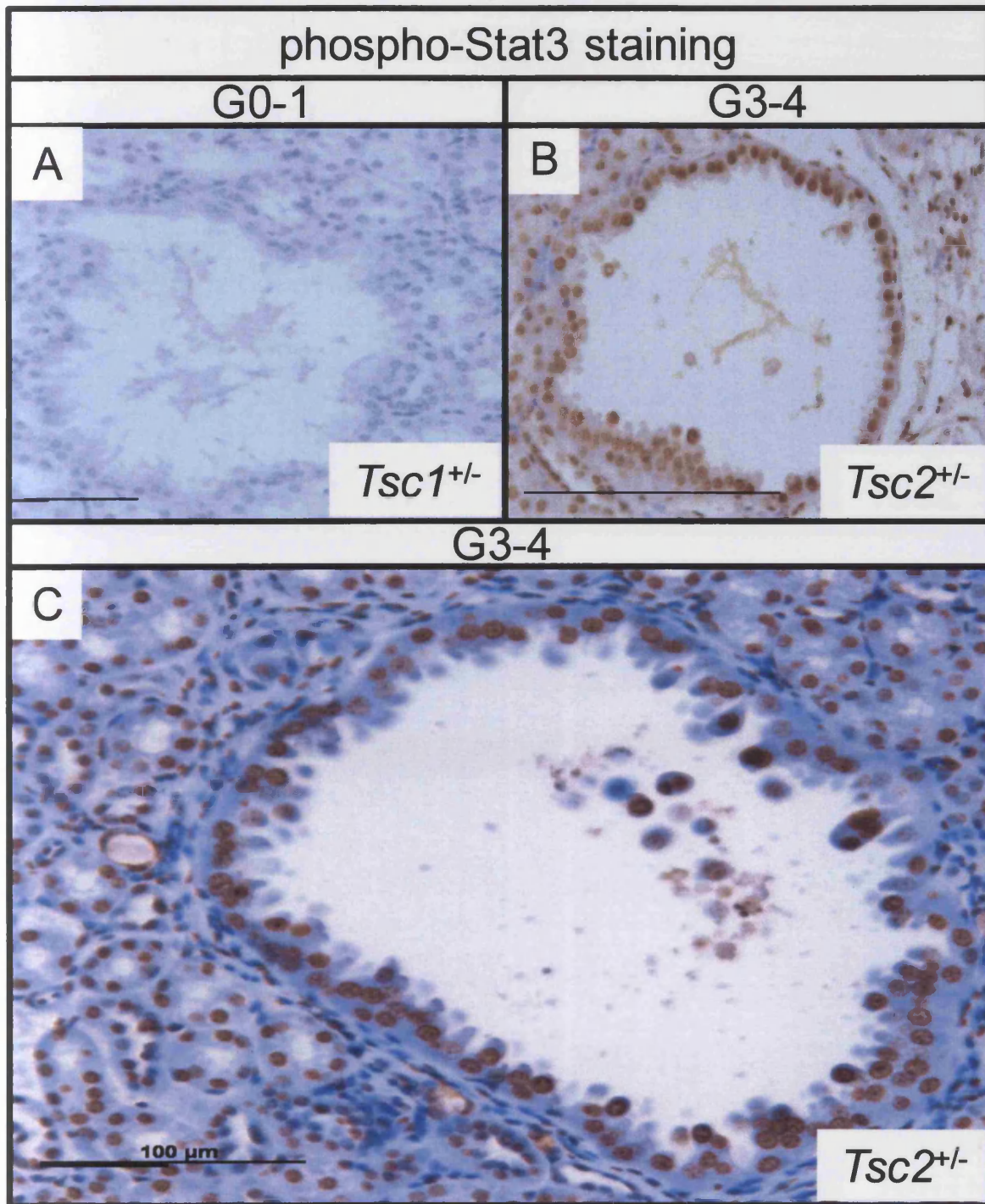


**Figure 5.4** Activation of Stat3 in simple cysts from *Tsc1<sup>+/-</sup>* and *Tsc2<sup>+/-</sup>* mice, with examples of weak (**Panel A**) and strong (**Panels B and C**) staining. Stat3 was found activated in significantly more mTOR inactive / caspase-3 inactive lesions compared to mTOR active / caspase-3 inactive and mTOR active / caspase-3 active cysts.



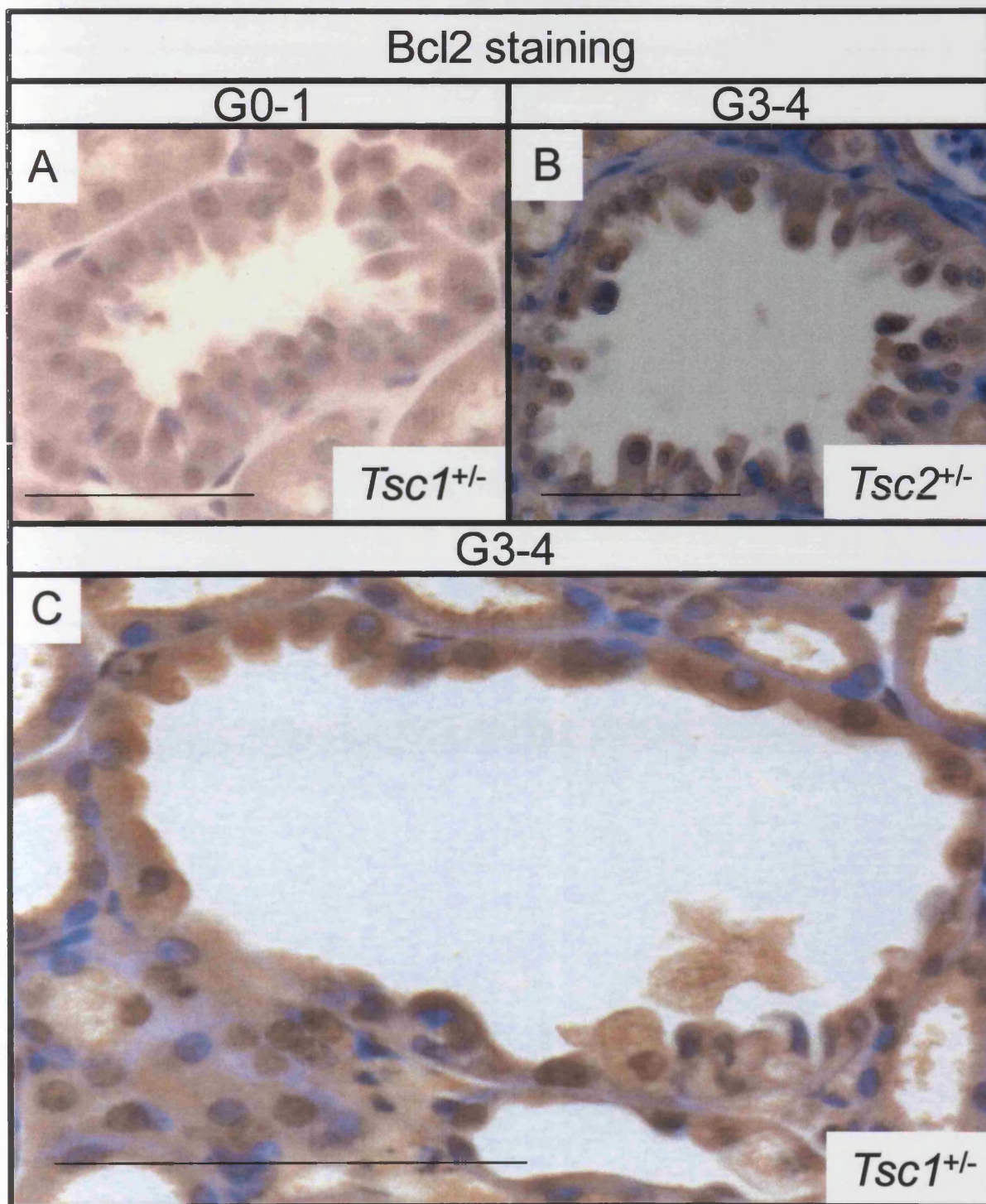


**Figure 5.5** Upregulation of Bcl2 in caspase-3 inactive simple cysts from *Tsc1<sup>+/-</sup>* and *Tsc2<sup>+/-</sup>* mice, with examples of weak (**Panel A**) and strong (**Panels B and C**) staining. Bcl2 was found upregulated in significantly more caspase-3 inactive lesions compared to cysts undergoing apoptosis. No significant difference was found between the frequency of strong staining events in mTOR active / caspase-3 inactive and mTOR inactive / caspase-3 inactive cysts.



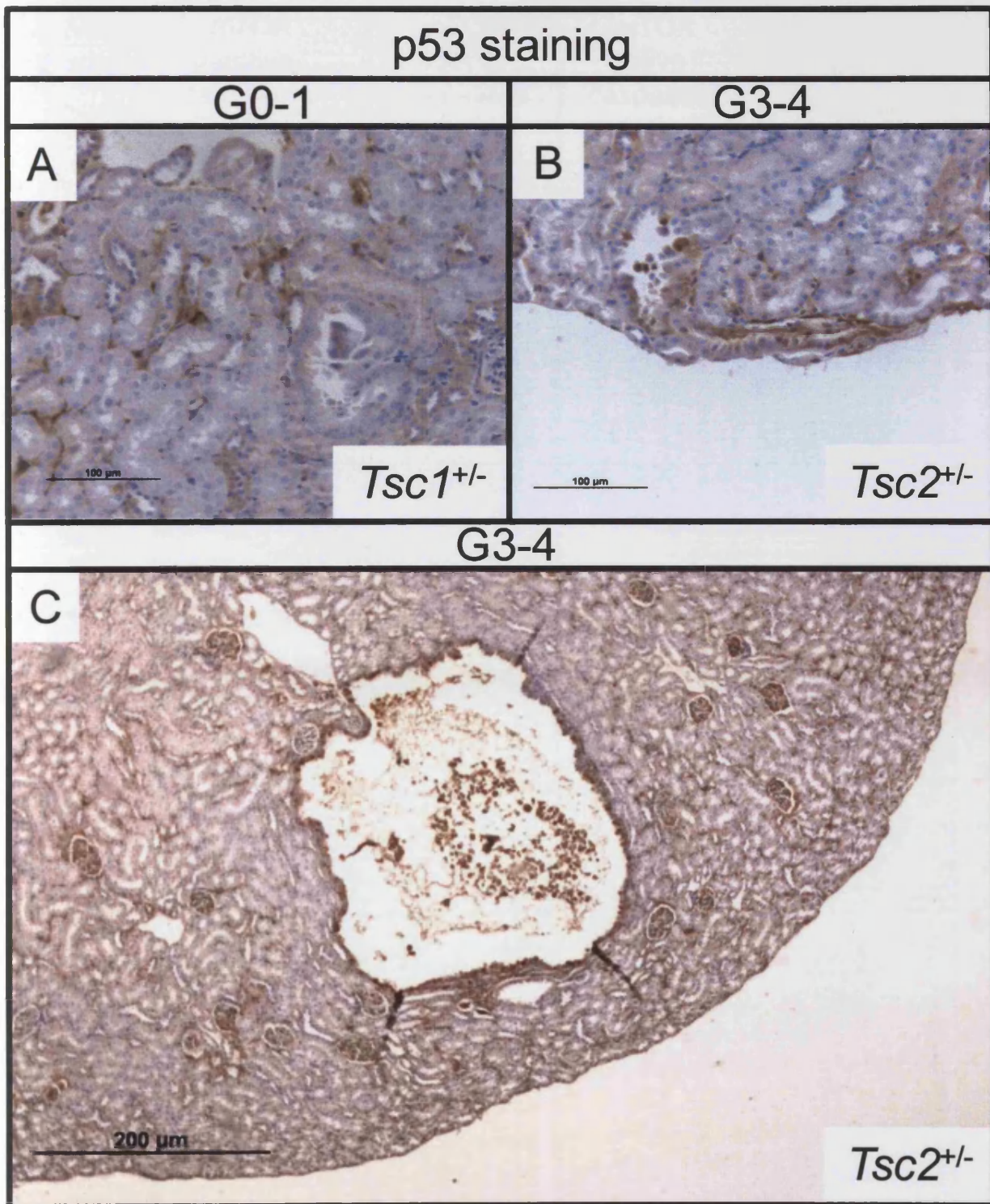


**Figure 5.6** Upregulation of p53 is seen in a selection of lesions from *Tsc1<sup>+/-</sup>* and *Tsc2<sup>+/-</sup>* mice. **Panel A and B:** Weak and strong staining (respectively) for p53 in simple cysts with inactive mTOR and inactive caspase-3 from *Tsc1<sup>+/-</sup>* and *Tsc2<sup>+/-</sup>* mice. **Panel C:** A cyst from a *Tsc2<sup>+/-</sup>* mouse with active mTOR and caspase-3 signalling, displaying strong p53 staining.



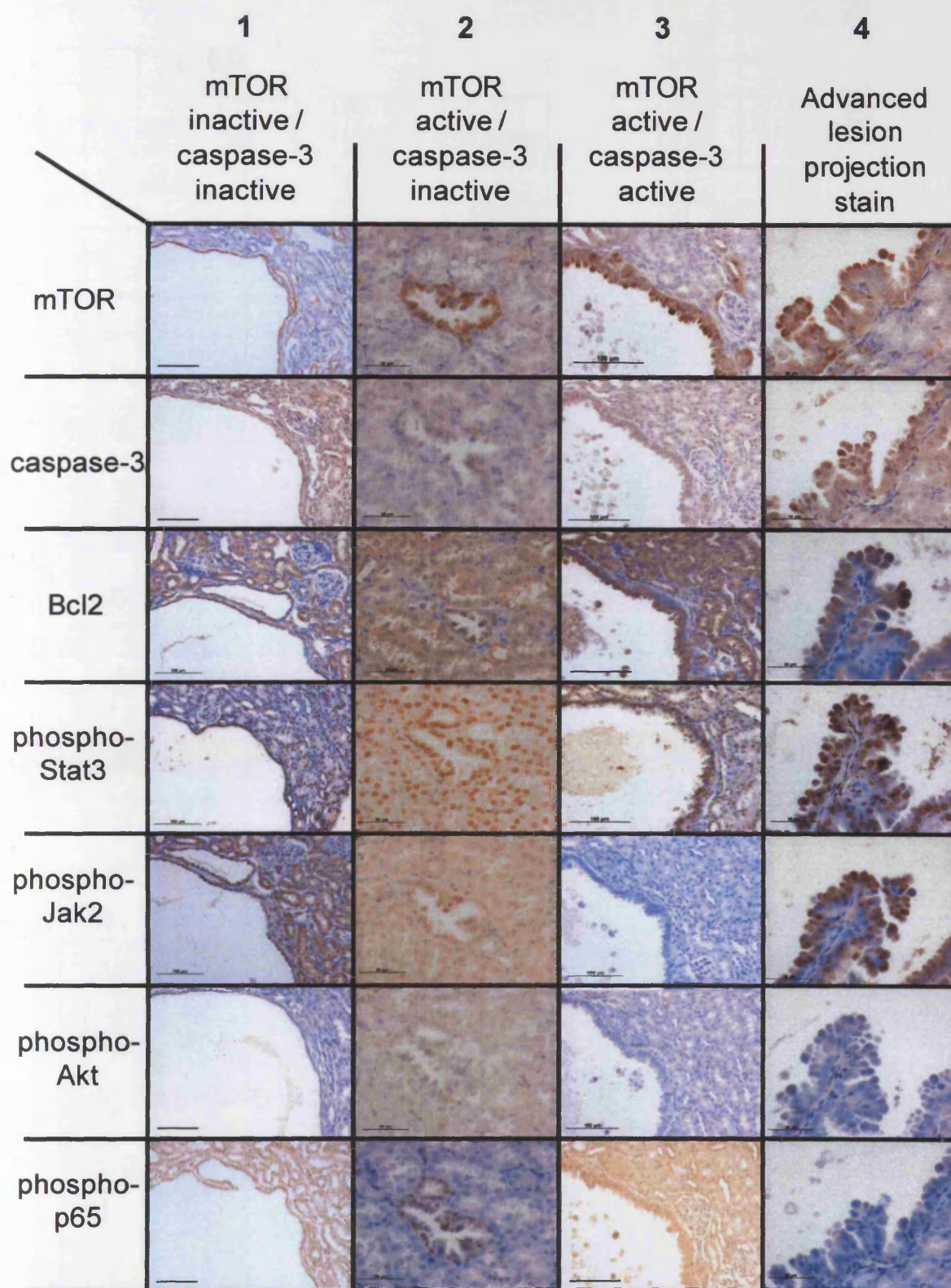


**Figure 5.7 Columns 1-3:** Serial mTOR inactive / caspase-3 inactive (1), mTOR active / caspase-3 inactive (2), mTOR active / caspase-3 active (3) simple cyst sections stained for mTOR, caspase-3, Bcl2, phospho-Stat3, phospho-Jak2, phospho-Akt and phospho-p65. **Column 4:** Serial sections of a multicellular projection from an advanced lesion stained for the same markers.



### mTOR inactive / caspase-3 inactive cysts

Pro-survival  
signalling

	3	7	31	36	49	50	51	55	64	85	103	105	108	110	112	115	117	121	123	126	145	152	164	170	177	180	183	196
phospho-Akt (S473)	Red				Red			Red		Red		Red		Red		Red		Red		Red		Red						
phospho-p65 (S276)	Red		Red	Red				Red		Red		Red		Red		Red		Red		Red							Red	Red
p53	Red	Red				Green	Green			Red		Red		Red		Red		Red				Red						
phospho-Met (Y1234/Y1235)			Red	Red						Red		Red		Red		Red		Red							Red	Red		
phospho-Stat3 (Y705)	Green		Green				Green			Green		Red		Green	Green		Green		Green									Green
phospho-Jak2 (Y1007/Y1008)	Green		Red			Green		Green		Green		Green	Green		Green	Green			Green					Green				Red
Bcl2	Green		Red			Red		Red		Green		Green	Green		Green	Red		Green	Red							Red		Green

### mTOR active / caspase-3 inactive cysts

Pro-survival  
signalling

	6	12	14	34	35	44	47	58	60	62	69	77	84	94	107	128	129	136	142	182	191	211	216	222	226
phospho-Akt (S473)	Red						Red				Red	Red				Red	Red	Red	Red	Red		Red	Red	Red	
phospho-p65 (S276)				Red	Red			Red			Red								Red		Red	Green	Green		Red
p53	Red	Red	Red			Red	Green					Red			Red									Red	
phospho-Met (Y1234/Y1235)				Red	Red				Red	Red	Red		Red					Red						Red	
phospho-Stat3 (Y705)	Red	Red	Green		Red		Green					Red	Red	Red					Green	Red	Green	Red	Red	Red	
phospho-Jak2 (Y1007/Y1008)			Red		Red	Green	Green				Red	Red	Green	Red	Red				Green	Red	Green	Red	Red	Red	
Bcl2			Green			Green	Red	Green			Red	Red					Red	Red		Green	Green	Green	Red	Red	

### mTOR active / caspase-3 active cysts

No activation  
of pro-survival  
signalling

	2	11	20	33	38	43	46	52	59	65	66	67	73	86	96	98	114	122	137	163	175	176	187	198	199	200	204	205	206	209	210	214	220	
phospho-Akt (S473)																																		
phospho-p65 (S276)																																		
p53																																		
phospho-Met (Y1234/Y1235)																																		
phospho-Stat3 (Y705)																																		
phospho-Jak2 (Y1007/Y1008)																																		
Bcl2																																		

**Table 5.2** Patterns of activation in simple cysts stained for activation of Akt, p65, p53, c-Met, Stat3, Jak2 and Bcl2, assessed with regards to mTOR and caspase-3 activation status. **Green:** strong staining (G3/4) **Red:** weak staining (G0-2). Numbers across the table refer to individual cysts, followed across serial sections and stained for activation of specific pathways.



## **5.4 Discussion**

### **5.4.1 The pro-survival signalling in our simple cysts deficient in apoptosis appears to be Bcl2 mediated**

We sought to determine the basis of cell survival in our cysts and analysed levels of Bcl2, a common mediator of inappropriate cell survival. We found expression levels of Bcl2 to be significantly elevated in the caspase-3 negative subsets of our simple cysts when compared to the cysts actively undergoing apoptosis, implying that this was mediating the cell survival. Because no difference was found between mTOR active / caspase-3 inactive and mTOR inactive / caspase-3 inactive cysts, we suggest that Bcl2 induction may be a general mediator of cell survival in cysts and not specific to mTOR positive or negative pathways. In this way, Bcl2 induction represents a point for signalling pathways to converge on, and this is in agreement with current literature (Tsujimoto 2001).

Previous work in *Tsc2<sup>+/-</sup>* mice has shown these animals develop tumours and cysts that express gelsolin (Onda *et al.* 1999). Interestingly, gelsolin is a known repressor of apoptosis (Ohtsu *et al.* 1997), a function it mediates through its ability to prevent apoptotic changes of mitochondria (Koya *et al.* 2000). Taken with the Bcl2 data, we suggest that the mitochondrial cell death pathway is exploited during cystogenesis.

### **5.4.2 Simple cysts that do not display apoptosis or mTOR activation are likely to have increased levels of activated Stat3 and Jak2**

Following confirmation of elevated Bcl2 in our simple cysts with no apoptosis, we then sought to ascertain the cause of the pro-survival signalling. We stained our panel of early cysts for activated Stat3 (a known regulatory of the Bcl2 family) and activated Jak2 (a pro-survival signalling molecule and activator of the STAT pathway).

Stat3 has previously been shown to mediate cell survival by inducing anti-apoptotic genes like *Bcl2* (Bhattacharya *et al.* 2005) and *BclxL* (Lu *et al.* 2006). In our simple cysts, we found activated Stat3 (indicated by strong staining [G3-4]) in significantly

more mTOR inactive cysts than equivalent mTOR active lesions, in an expression pattern that correlated with Bcl2 elevation. This implies phospho-Stat3 signalling may mediate the high levels of Bcl2 seen in our mTOR inactive category of cysts. Activated phospho-Stat3 was seen in both mTOR active / caspase-3 inactive and mTOR inactive / caspase-3 inactive cysts. This suggests a correlation with repression of apoptosis, but the association was only significant in the mTOR inactive category (implying this effect is mTOR independent). Our observations of Stat3 activation in *Tsc1*<sup>+/-</sup> and *Tsc2*<sup>+/-</sup> cysts is in agreement with current literature, where elevated pSTAT3 Tyr705 levels have been reported in *Tsc2* null neuroepithelial progenitor cells (Onda *et al.* 2002), *Tsc1* and *Tsc2* null MEFs (El-Hashemite *et al.* 2004), TSC-associated LAM (El-Hashemite *et al.* 2005) and renal AMLs (El-Hashemite *et al.* 2005). This elevated Stat3 signalling has previously been linked to Bcl2 mediated resistance to apoptosis (El-Hashemite *et al.* 2004). What may be contentious however, is whether Stat3 can be activated in the absence of mTOR signalling (as observed in our simple cysts). This is discussed later on.

In human cancers, no STAT3 gain-of-function mutations have been reported (Constantinescu *et al.* 2007). However, STAT3 is frequently activated in a variety of cancers (Calo *et al.* 2003), so commonly a cell will have dysregulation of upstream STAT activators. We sought these mTOR-independent defects by examining several Stat3 activators, including Jak2.

We found phospho-Jak2 to be activated in significantly more mTOR inactive / caspase-3 inactive simple cysts than mTOR active / caspase-3 inactive and mTOR active / caspase-3 active cysts. When plotted for activation of Jak2, along with the other staining targets in the context of mTOR and caspase-3 status, we saw a strong correlation with the expression profiles of Jak2, Bcl2 and phospho-Stat3 in these mTOR inactive / caspase-3 inactive cysts. While the Bcl2 elevation appears to be independent of mTOR status (suggesting a convergence point), phospho-Stat3 and phospho-Jak2 are activated in cysts without mTOR signalling, providing an alternative means of cyst initiation.

Interestingly, a steady flow over endothelial cells in culture has been found by Ni *et al.* (2004) to suppress Jak2/Stat3 signalling induced by IL-6 signalling. This may have implications in our Tsc mice because the renal cysts they experience will likely

repress fluid flow in two ways – firstly through expansion and occlusion of nearby tubules, and secondly through blockage and distortion of cystic tubules. Furthermore, haploinsufficiency in the Tsc proteins has previously been shown to produce structural abnormalities in primary cilia (see Chapter 3) and these are key mechanosensors of fluid flow in the kidney. The defects produced by a *Tsc1*<sup>+/-</sup> or *Tsc2*<sup>+/-</sup> genotype may be sufficient to reduce responsiveness to fluid flow in renal tubules and activate the Jak2/Stat3 signalling pathway in an mTOR-independent manner. Similarly, Gatsios *et al.* (1998) published that renal cell injury through hyperosmolarity resulted in Jak2 phosphorylation and induction of Stat3 following cell shrinkage. Whether the cyst cells we see in Tsc are osmotically abnormal remains to be discovered. Renal injury, which has been proposed as a mechanism for precipitating cystogenesis in TSC kidneys, was shown by Kuratsune *et al.* (2007) to lead to six times the endogenous level of phospho-Stat3 in rat renal tubules.

The SOCS proteins play an inhibitory role in JAK/STAT signalling (Constantinescu *et al.* 2007) and inactivating mutations in the SOCS genes are known to cause dysregulation of STAT signalling in human cancers such as B cell lymphomas (Melzner *et al.* 2005), hepatocellular carcinoma (Ogata *et al.* 2006) and Hodgkin's lymphoma (Weniger *et al.* 2006). Mutations in these SOCS proteins would be another mTOR-independent route of Stat3 / Bcl2 activation, although the high levels of phospho-Jak2 staining in our cysts would suggest this is not the main route for Stat3 activation.

#### **5.4.3 Activation of Stat3 can be mTOR-dependent or independent**

Stat3 is a member of the STAT family and contains multiple phosphorylation sites that are crucial for its activation and signalling function. As previously discussed, phosphorylation at Tyr<sup>705</sup> leads to monomer dimerisation, nuclear localisation and DNA binding. Further phosphorylation at Tyr<sup>727</sup> is required for maximal transcriptional activity. Separate kinases are thought to be responsible for these phosphorylation events, with Jak1 / 2 acting at Tyr<sup>705</sup> and a variety of kinases acting Tyr<sup>727</sup>. Kinases linked to this site include JNK-1 (Lim *et al.* 1999), MEKK1 (Lim *et al.* 2001), ERK (Kuroki *et al.* 1999), Protein Kinase C (Gartsbein *et al.* 2006, Jain *et al.* 1999) and mTOR (Kim *et al.* 2008, Yokogami *et al.* 2000). While the Y727 site is important, as illustrated by the defective embryonic development and elevated apoptosis seen in

mouse lines lacking a 727 tyrosine residue (Shen *et al.* 2004), we have opted to look at the Tyr<sup>705</sup> form of phospho-Stat3. This is because we are interested in mTOR independent signalling pathways that may lead to cystogenesis. Although our results refer to the mTOR-independent form of activated Stat3, it is important to remember that further activation events will come in downstream to maximise the transcriptional response of this transcription factor. Hence, while levels of active phospho-Stat3 (Tyr<sup>705</sup>) may be mTOR-independent, ultimate Stat3-lead transcription may not be. However, other kinases apart from mTOR have been shown to carry out this secondary phosphorylation event, and so the whole pro-survival pathway could be outside the mTOR axis. Cell line work done by Chung *et al.* (1997) suggests activation at Tyr<sup>727</sup> may negatively feedback to repress Tyr<sup>705</sup> phosphorylation, providing another point that mTOR could impact upon activation of Stat3. Our phospho-Stat3 data in simple cysts suggests mTOR activity is not required for phosphorylation of Stat3 at Tyr<sup>705</sup>, in agreement with current literature. mTOR positive cysts had markedly reduced levels of phospho-Tyr<sup>705</sup>, which may be explained by the feedback mechanism proposed by Chung *et al.* (1997).

#### **5.4.4 ADPKD and JAK2 / STAT3**

Work by Talbot *et al.* (2011) has found membrane-bound polycystin-1 is able to activate STAT3 in a JAK2-dependent manner, leading to tyrosine phosphorylation and transcriptional activity. Furthermore, it is thought polycystin-1 can also activate STAT1, -3 and -6 following cleavage and nuclear translocation of its cytosolic tail. In ADPKD kidneys, polycystin-1 tail fragments are overexpressed. Interestingly, STAT3 was found to be activated in human ADPKD renal cysts by the same group, suggesting this cellular interaction carries over to the cystic phenotype. HGF, an activator of JAK2, has been found in cystic fluids in ADPKD (Horie *et al.* 1994), while transgenic mice overexpressing HGF develop renal cysts (Takayama *et al.* 1997). The previous work in ADPKD goes some way to validate the observations we have made in our Tsc-kidneys. Activation of the JAK2/STAT3 signalling pathway is associated with cystogenesis in humans and mice with dysregulated polycystin-1 tail signalling, and we have now shown similar Jak2-mediated activation of Stat3 is associated with a cystic phenotype in our *Tsc1*<sup>+/-</sup> and *Tsc2*<sup>+/-</sup> mice.

#### **5.4.5 NF- $\kappa$ B is not activated in simple cysts from our *Tsc1*<sup>+/-</sup> and *Tsc2*<sup>+/-</sup> mice**

We found that phospho-p65 was rarely activated (IHC stain of G3-4) in our simple cysts. The only cysts found to contain active NF- $\kappa$ B signalling were also positive for mTOR activation, although some had evidence of apoptosis and some did not. This implies NF- $\kappa$ B signalling is not significantly involved in early cystogenesis, either in concert with mTOR signalling or as an alternative route of cell proliferation and survival. The lack of correlation between strong NF- $\kappa$ B staining and apoptotic status indicates that this pathway is probably not involved in mediating any effects on cyst apoptosis. Active NF- $\kappa$ B signalling is able to induce the release of cytokines which can then activate the JAK/STAT signalling pathway (Ward 2002), but this is unlikely to be the means of Jak2/Stat3 activation in our cohort of cysts because of the low levels of NF- $\kappa$ B activation.

The lack of NF- $\kappa$ B activation in our cysts is an interesting result because this pathway is known to be upregulated in other cystic disorders. It is widely used by eukaryotic cells as a regulator of genes that control survival and proliferation. Following stimulation of NF- $\kappa$ B signalling by cytokines, cell stress and growth factors (Baldwin 2001), the pathway can be active within minutes. A study by Konda *et al.* (2008) found weak phospho-p65 in normal tissue and upregulation of NF- $\kappa$ B signalling in the tubules and cysts of renal samples from patients with acquired cystic disease of the kidney. These cysts develop papillae projections and progress to RCC (as in TSC), and active NF- $\kappa$ B was found elevated in these tumours too. The researchers concluded that activated NF- $\kappa$ B signalling may drive the progression of a simple cyst towards epithelial hyperplasia and eventually to RCC. NF- $\kappa$ B is also known to be induced by hypoxic renal injury (Melvin *et al.* 2011), a factor that has been implicated in early cystogenesis (Pollard *et al.* 2007, Konda *et al.* 2008, Belebi *et al.* 2011). Because NF- $\kappa$ B is such a quickly induced signalling pathway, it may be that this pathway is activated in our young mice following renal injury, stimulates cystogenesis through tubule hyperproliferation and inappropriate survival, and then quickly returns to normal levels as other pathways like mTOR or Jak/Stat signalling take over. The simple cysts we are looking at may miss this narrow window. Finally, the strong links between NF- $\kappa$ B and cytokine / growth factor signalling and the lack

of activation seen in this pathway imply that our cysts may not be initiated by external signalling events and could be arising through internal malfunctions.

#### **5.4.6 HGF signalling is not activated in simple cysts from our *Tsc1*<sup>+/-</sup> and *Tsc2*<sup>+/-</sup> mice**

Hepatocyte growth factor (HGF) is a secreted GF that acts on responsive cells via a high affinity cell surface c-Met receptor. We decided to stain our cysts for the activated form of the HGF receptor, phospho-c-Met, to ensure positive stains would be localised to the cyst lumen and not dispersed across the kidney (as HGF is a soluble GF). The antibody we used stains c-Met when phosphorylated at Tyr1234 and Tyr1235 - this selects for the receptor activated by HGF signalling. HGF induces STAT3 during tubule development, and both the GF and its receptor have been shown to be overexpressed in many human cancers, including RCC (Zhang *et al.* 2004). In humans with ADPKD and simple renal cysts, studies have found elevated HGF in the cell walls of many lesions studied (Horie *et al.* 1994). Furthermore, cyst fluid from another disease, acquired renal cystic disease (a disorder that progresses to RCC in a similar manner to TSC) has been found to contain high levels of the soluble GF, suggesting it may play a role in promoting cyst progression (Konda *et al.* 2004).

Despite an animal model that experiences renal cysts with HGF overexpression, links to cystic progression and a clear anti-apoptotic role, we failed to find HGF / c-Met signalling elevated in any of our simple cysts. It may be that HGF signalling becomes an important factor later on in cyst progression but does not have a bearing on the early events in cystogenesis. However, the dilated tubules and cysts experienced by HGF overexpression suggest it can be activated to initiate cyst formation. In these mice with aberrant HGF signalling, it is possible that they have defective apoptosis, and therefore, a misdivided cell in these tubules (which we have suggested can happen in wild-type mice, see Chapter 3), would persist and constitute the first step towards tubule dilation and cyst formation. The fact that we did not observe any abnormal HGF activation perhaps suggests this is a rare occurrence in a mouse kidney, and something that only takes place as a lesion progresses and becomes more genetically unstable.



#### **5.4.7 Akt signalling is not activated in simple cysts from our *Tsc1*<sup>+/-</sup> and *Tsc2*<sup>+/-</sup> mice**

Activation of PI3K stimulates cell growth, proliferation and survival primarily through Akt-directed phosphorylation (Manning *et al.* 2005). It is this PI3K-Akt axis that stimulates mTOR under growth factor signalling, whereby the main mechanism of activation appears to be phosphorylation and inhibition of TSC2 (Inoki *et al.* 2002, Manning *et al.* 2002). Interestingly, it has been noted that homozygous loss of *Tsc1* or *Tsc2* in MEFs and *Drosophila* results in strong inhibition of PI3K signalling (Radimerski *et al.* 2002, Zhang *et al.* 2003, Harrington *et al.* 2004). Manning *et al.* (2005) carried out further work in *Tsc2*<sup>+/-</sup> and *Pten*<sup>+/-</sup> mice and suggested that loss of *Tsc2* expression in developing tumours triggers an upregulation of mTOR activation and a subsequent feedback inhibition of Akt signalling. It is this feedback inhibition that may limit the growth of TSC-related tumours and account for the benign nature of many of the tumours that arise in the disease. The same feedback inhibition could cause the absence of strong active Akt staining in our mTOR active cysts. We also saw no strong staining in our mTOR inactive / caspase-3 inactive cysts, implying Akt has not become activated in these lesions either. This would suggest these early cysts are developing without strong GF stimulation (which can be important in other renal cystic diseases), because this would be likely to feed in through the PI3K-Akt pathway. It may be possible that crosstalk from other mTORC1-independent signalling pathways is acting to repress activation of Akt, such as via ER stress (Chen *et al.* 2011), or PTEN signalling. PTEN is a major negative regulator of the PI3K/Akt pathway (Cantley *et al.* 1999) and is controlled by phosphorylation and cellular localisation (Meili *et al.* 2005). The small G protein Rho has been implicated in this activation (Meili *et al.* 2005) and both TSC1 (Lamb *et al.* 2000) and TSC2 (Goncharova *et al.* 2004) have been shown to activate Rho. Hence, in a cyst with functional TSC proteins (in which mTOR is inactive) there could be activated Rho, and consequently PTEN signalling may be elevated and repressing activation of Akt. While good antibodies exist for the detection of activated Rho and PTEN, constraints on the amount of cysts available for our IHC studies has lead this particular line of research to be left for future work. Furthermore, while activated Akt signalling is associated with resistance to apoptosis and inappropriate cell survival in other conditions, such as breast cancer (Bose *et al.* 2006), we can confirm it does not

appear activated in our simple cysts, irrespective of whether the cyst is displaying apoptosis or not.

#### **5.4.8 p53 in cystogenesis**

Our IHC analysis showed p53 was strongly activated in several cysts, both positive and negative for mTOR activation. The p53 transcription factor is known to sense a variety of cell stress signals which may reduce the fidelity of cell growth and division. It also can prevent misdirected growth in endothelial cell culture assays. Its role is therefore to initiate cell cycle arrest, senescence or apoptosis. While strong activation of p53 is perhaps not surprising considering the high rates of cell stress and proliferation in a developing cyst, it appears mTOR activation status does not definitively correlate with p53 levels in a Tsc lesion. Several groups have previously examined the links between mTOR and p53. *TSC2* has been shown to be a p53-regulated target gene, with levels of tuberin rising following p53 induction in cell line work and p53 binding elements found in the *TSC2* gene (Feng *et al.* 2005, Feng *et al.* 2007). This suggests that p53 signalling may downregulate the mTOR pathway as tuberin is a negative regulator of mTOR signalling. Furthermore, p53 is also known to upregulate *PTEN* (Stambolic *et al.* 2001), a phosphatase upstream from the mTOR complex and generally associated with mTOR repression. Although high levels of p53 should correlate with low levels of mTOR signalling, this is not the case in our cysts, where both mTOR active and inactive simple cysts stained strongly for p53. It is important to note that this strong staining was a rare event when compared to the total number of cysts stained. This implies many levels of complexity exist between p53 induction, target gene modulation and overall effects on mTOR signalling. Similarly, although p53 is linked to apoptosis induction, strong staining was witnessed in caspase 3 active and inactive cysts. It is likely that many factors play a modulating role in the final outcome of cell death, and upregulated p53 is clearly not a precise marker for apoptosis. Indeed, p53 activation alone may not be sufficient for induction of apoptosis, and Weber *et al.* (2003) have shown it may take a coordination of several factors to illicit a death response. A marker such as cleaved caspase-3 is much better for finding cells undergoing apoptosis because it is directly involved in the cell death pathway as one of the terminal effectors of this process. It is one of the last caspases to become activated, by which point, cells are wholly committed to fulfilment apoptosis.

#### **5.4.9 Activation of pro-survival signalling in simple cysts without mTOR dysregulation**

In conclusion, we have found simple cysts that did not stain for caspase-3, were significantly more likely to stain strongly for Bcl2 when compared to cysts that were undergoing apoptosis. This induction of Bcl2 was seen in both mTOR active and inactive lesions, implying the pro-survival protein is a general mediator of anti-apoptotic signalling in our Tsc cysts and may represent a convergence point for mTOR-mediated and mTOR –independent cell survival. Furthermore, we have shown that active phospho-Jak2 and phospho-Stat3 correlate strongly with this induction of Bcl2 in our mTOR inactive cysts that are not undergoing apoptosis. This pathway does not appear to be activated in mTOR active cysts that are non-apoptotic. We therefore suggest that inappropriate cell survival (mediated by Jak2-Stat3-Bcl2 signalling) can lead to the development of dilated tubules and simple cysts in *Tsc1*<sup>+/-</sup> and *Tsc2*<sup>+/-</sup> mice, when placed in the context of widespread defective renal tubule polarity (previously discussed in Chapter 3). This mechanism of cyst formation appears to be mTOR-independent and represents an important step towards fully understanding the processes behind the formation of a Tsc renal lesion. To confirm our IHC findings, evidence of gain-of-function mutations in *Jak2* were sought from a panel of *Tsc1*<sup>+/-</sup> and *Tsc2*<sup>+/-</sup> simple cysts (discussed in Chapter 6).

## **CHAPTER SIX: Oncogenic somatic *Jak2* mutations may promote TSC-associated renal cystogenesis**

### **6.1 Introduction**

We have shown for the first time that the majority of mTOR-inactive simple cysts from Tsc murine models do not show signs of apoptosis, suggesting that they have somatically activated a pro-survival pathway. In support of this, we found strong activation of Jak2 and its downstream target, Stat3, in the majority of these cysts (Chapter 5).

JAK2 is a member of the Janus family of non-receptor protein tyrosine kinases, which also includes JAK1, JAK3 and TYK2 (Zou *et al.* 2011). The kinase is widely expressed and found in virtually all cell types (Sayyah *et al.* 2009). The JAK-STAT pathway mediates signalling by cytokines, which control cell survival, proliferation and differentiation of many cell types. Based on their primary structure, members of the JAK family are characterised by the presence of seven regions of conserved homology, denoted JAK homology (JH) domains 1–7 (Harpur *et al.* 1992). A somatic JAK2 mutation, V617F, in the JH2 domain is present in the majority of patients with myeloproliferative neoplasms (MPNs) including polycythemia vera (PV). The mutation leads to constitutive kinase activity (Zhao *et al.* 2005), which activates the JAK2 signalling pathway in a cytokine-independent manner and is believed to be a critical driver of excess proliferation. Other neoplastic conditions that display constitutive JAK2 or its downstream target, STAT3 activation include RCCs (Horiguchi *et al.* 2010), melanomas (Kong *et al.* 2008), and other cancers of the breast, neck, ovaries, lung and prostate (Yu *et al.* 2004). Many of the gain-of-function JAK2 mutations are contained within the same region of the protein, a section called the pseudokinase domain (JH2), which has basic structural features of a kinase domain but no catalytic activity. It is involved in the autoregulation of the adjacent kinase domain, and amino acid substitutions have been shown to produce conformational changes that disrupt the inhibitory function of this region (Zhao *et al.* 2005). While the *JAK2* gene in humans and mice spans 24 exons, many gain-of-function mutations occur within the JH2 domain (exons 11-17), providing a suitable target for molecular analysis in our simple cysts.

We have previously shown that the Jak2-Stat3-Bcl2 signalling pathway is upregulated in our mTOR inactive cysts, and that growth factor / cytokine signalling is unlikely to drive initiation of these lesions (as indicated by weak staining for active c-Met, Akt or NF-κB) (Chapter 5). We therefore sought evidence of activating mutations in *Jak2* in Tsc-associated cysts to support our IHC findings.

## **6.2 Materials and methods**

### **6.2.1 Animal care, genotyping and tissue preparation**

All matters relating to animal husbandry, care and genotyping were carried out as previously described. *Tsc1*<sup>+/-</sup> (N=10) and *Tsc2*<sup>+/-</sup> (N=11) mice were obtained at 11-12 months along with wild-type littermates. Following cervical dislocation and dissection, kidneys were bisected longitudinally and snap frozen in OCT as previously described. Kidneys for lesion progression analysis were taken from *Tsc2*<sup>+/-</sup> mice, while wild-type mice were used for a separate cyst incidence study. Kidneys from both studies were matched for age and formalin fixed / paraffin embedded as previously described.

### **6.2.2 DNA isolation from simple cysts**

Snap frozen kidneys were serial sectioned at 10µm onto 1.0 PEN membrane PALM slides using a freezing-stage microtome, and stained with toluidine blue dye. This stain was used to reveal lesions for microdissection. Samples were viewed and cysts dissected on a PALM Microlaser system. Great care was taken not to include any surrounding tissue in the areas selected for dissection, and cysts were dissected over several sequential slides where possible to maximise the amount of DNA captured. DNA was extracted from cysts using QIAamp DNA mini-kits, re-suspended in distilled water, and stored at -20°C. A total of 71 simple cysts were identified and DNA extracted.

### 6.2.3 *Jak2* sequencing

Primers were designed using Primer3 (Rozen *et al.* 2000) to amplify exons 11-17 of the murine *Jak2* gene (Gene ID: 16452): 11F 5'-AGTTTTGCTGTGCTTTGCTT-3', 11R 5'-GACACTGCTTTAAAGGGACAAA-3'; 12F 5'-CATTTCCTGTCATTGAATATGTTTCC-3', 12R 5'-TCTCACATGCATCTAATGTGC-3'; 13F 5'-CAGGGGTATCTTTCTGAGTTCTG-3', 13R 5'-TCCAAGGTTTTGCTGACACC-3'; 14F 5'-TTGCCTGTTGTATCCACAAGT-3', 14R 5'-TCCTTCTGGTTGCCAGGTTA-3'; 15F 5'-ATCTGTACTGTAGTTTTGGGCATA-3', 15R 5'-CAGCAATAAACTAGAATGAAAGGAA-3'; 16F 5'-CAAGTAAGTTTGGAAGCTCTTCACA-3', 16R 5'-TAGAAGGGCCAGGAACACAC-3'; 17F 5'-CCTGGCCCTTCTAATTGTGA-3', 17R 5'-GACTGTCTCAGATGGAGCTAAAAA-3'. PCR products were purified with Exonuclease I and Shrimp Alkaline Phosphatase and Sanger sequenced using the BigDye Terminator Cycle Sequencing kit (Version 1.1 and 3.1) on an ABI 3100 Genetic Analyser.

### 6.2.4 Cyst progression in *Tsc2*<sup>+/-</sup> mice with and without germline *Jak2* changes

To study the effects that germline *Jak2* changes at K575E and G614G have on lesion progression, we sequenced exons 12 and 13 of *Jak2* using tail DNA from a cohort of *Tsc2*<sup>+/-</sup> mice. We assembled the mice into groups matched for age and background (at 7-12 months [N=22] and 17-23 months [N=8]) and cut 5 representative slides at 5µm (taken at 200µm intervals) from across the kidney. Slides were stained with H&E to reveal the lesions, and counted by an observer blinded to the *Jak2* status of the mice. Renal abnormalities were mapped throughout the kidney to ensure the same lesion was not counted multiple times.

### 6.2.5 Cyst analysis in wild-type mice with and without germline *Jak2* changes

To study the effects that germline *Jak2* changes at K575E and G614G had on cyst initiation in mice, we sequenced exons 12 and 13 of *Jak2* using tail DNA from a cohort of wild-type mice. We assembled the mice into groups matched for age and background (10-16 months [N=11]). The first 150µm of each kidney was serial sectioned at 5µm and stained with H&E. Slides were analysed under a Motic B3 professional series light microscope and assessed for the presence of lesions by an



observer blinded to the germline *Jak2* status of the mice. Lesions were mapped throughout the kidney to ensure the same cyst was not counted multiple times.

### 6.2.6 SNP severity prediction

We used a web-based algorithm to anticipate how amino acid substitutions would affect *Jak2* protein function. AlignGVGD, ([http://agvgd.iarc.fr/agvgd\\_input.php](http://agvgd.iarc.fr/agvgd_input.php)) makes predictions based on sequence homology and the biophysical properties of an amino acid. Sequence homology between species was ascertained using ClustalW2 (<http://www.ebi.ac.uk/Tools/msa/clustalw2>), which is a general purpose multi-sequence alignment program for DNA. Accession numbers for the protein sequence of *Jak2* in humans (*Homo Sapiens*) (NP\_004963.1), orang-utan (*Pongo Albeii*) (NP\_001125600.1), mouse (*Mus Muscularis*) (NP\_001041642.1), rat (*Rattus Novegicus*) (NP\_113702.1), chicken (*Gallus Gallus*) (NP\_001025709.1) and zebrafish (*Danio Rerio*) (NP\_571168.1) were taken from NCBI.

### 6.2.7 Statistical analysis

Frequencies of renal cyst formation in wild-type mice (with and without germline changes in *Jak2*) were compared using Fisher's exact test. Comparisons between frequencies of renal cystogenesis in *Tsc2*<sup>+/-</sup> mice with and without germline *Jak2* mutations were compared using the Mann-Whitney test for non-parametric data.

## 6.3 Results

### 6.3.1 Germline *Jak2* variations are present in our *Tsc1*<sup>+/-</sup> and *Tsc2*<sup>+/-</sup> mice

Here, we analysed DNA from 71 simple cysts from 11-12 month old *Tsc1*<sup>+/-</sup> (N=10) and *Tsc2*<sup>+/-</sup> (N=11) mice to test for activating mutations in the regulatory domain (exons 11-17) of *Jak2*. We identified six single base changes in this pseudokinase domain, four of which were somatically acquired (discussed in Section 6.3.2) and two which were present in all 9 cysts removed from the same *Tsc2*<sup>+/-</sup> mouse. Upon

testing the tail DNA from this same animal, we confirmed that the two variants were germline changes. These were K575E (exon 12) and G614G (exon13), and both have been previously characterised (rs37008700 and rs13483586, respectively) (Figure 6.1).

### **6.3.2 Somatic *Jak2* mutations are present in the cysts of our *Tsc1*<sup>+/-</sup> and *Tsc2*<sup>+/-</sup> mice**

Four variants were detected during our sequencing of the regulatory region of *Jak2* in the cyst DNA of our *Tsc1*<sup>+/-</sup> and *Tsc2*<sup>+/-</sup> mice (Figure 6.2). These were all somatic mutations, confirmed by sequencing of tail DNA to prove the absence of the mutation. Each somatic mutation was identified just once. In DNA extracted from a *Tsc2*<sup>+/-</sup> simple cyst, we found an I522T mutation in exon 11 of *Jak2*, which is a non-conservative change from Isoleucine (hydrophobic) to Threonine (hydrophilic). The intronic region downstream of *Jak2* exon 11 was found to contain a base substitution in DNA from a *Tsc2*<sup>+/-</sup> simple cyst, 12 bases away from codon 547 (termed c547+12T>C). In DNA extracted from a *Tsc2*<sup>+/-</sup> simple cyst, we found a single incidence of a V617A change in exon 13 of *Jak2*, a conservative substitution but at a key position. Finally, DNA from a *Tsc1*<sup>+/-</sup> simple cyst was found to contain a single base mutation in exon 16 of *Jak2*, N726N, which did not lead to a change in the amino acid encoded (Asparagine).

### **6.3.3 *Jak2* mutation analysis**

#### **6.3.3.1 Evolutionary conservation**

We sought to determine the fidelity of this regulatory region and the mutations contained within it by aligning the murine *Jak2* sequence with that of *JAK2* in humans, orang-utan, rat, chicken and zebrafish (Figure 6.3). The alignment revealed a high level of conservation at V617, implying this is an important residue in the function of *Jak2*. Across the species, the I522 and K575 residues are not found to be conserved, indicating these amino acids may not be so crucial to the properties of the kinase.

### 6.3.3.2 Severity of residue change

Finally, an *in silico* analysis was performed to test the consequences of our non-synonymous SNPs on the function of *Jak2*. AlignGVGD revealed I522T and V617A were 'very likely' to interfere with *Jak2* function (C65), while K575E was predicted to be 'likely' to interfere (C55).

### 6.3.4 Germline variants in *Jak2* at K575E and G614G may modulate cyst burden in *Tsc2*<sup>+/-</sup> animals

We observed that the 12 month old *Tsc2*<sup>+/-</sup> mouse with germline K575E and G614G variants in *Jak2* experienced an unusually large number of cysts across its kidneys. By looking at the number of cysts removed for LCM in this mouse and the other 20 animals without *Jak2* germline variants, we found it had approximately 3x as many lesions (22 cysts compared to an average of 8.14). We therefore sought to address whether the presence of these germline *Jak2* variants can influence levels of cystogenesis in *Tsc*. We set up a study looking at *Tsc2*<sup>+/-</sup> mice at 7-12 months and at 17-23 months of age. These were tested for the presence of the two *Jak2* germline changes in exon 12 and 13 (hereafter termed *Tsc2*<sup>+/-</sup> *Jak2*<sup>K575E/+</sup>). Mice that tested positive (*Tsc2*<sup>+/-</sup> *Jak2*<sup>K575E/+</sup>) were matched for age and generation with *Tsc2*<sup>+/-</sup> *Jak2*<sup>+/+</sup> mice, and assessed for cyst incidence. Kidneys were embedded and sectioned as previously described, with one 5µm section being cut every 200µm, to obtain 5 representative sections (H&E stained) throughout the organ.

As expected, we found an increase in all types of lesion with age. The younger age group, 7-12 months, contained 10 *Tsc2*<sup>+/-</sup> *Jak2*<sup>K575E/+</sup> mice and 12 *Tsc2*<sup>+/-</sup> *Jak2*<sup>+/+</sup> mice. No significant difference was found between the number of simple cysts (2.9 per animal compared to 2.5, respectively [*P*=0.59]), the number of branching cysts (1.3 per animal compared to 0.7, respectively [*P*=0.24]), the number of cystadenomas (0.5 per animal compared to 1.2, respectively [*P*=0.30]) or the number of RCCs (0.4 compared to 0.2 per animal, respectively [*P*=0.78]). Total lesion incidence was 5.1 lesions per *Tsc2*<sup>+/-</sup> *Jak2*<sup>K575E/+</sup> animal compared to 4.5 lesions per *Tsc2*<sup>+/-</sup> *Jak2*<sup>+/+</sup> animal (*P*=0.59), an increase of 1.13 fold.

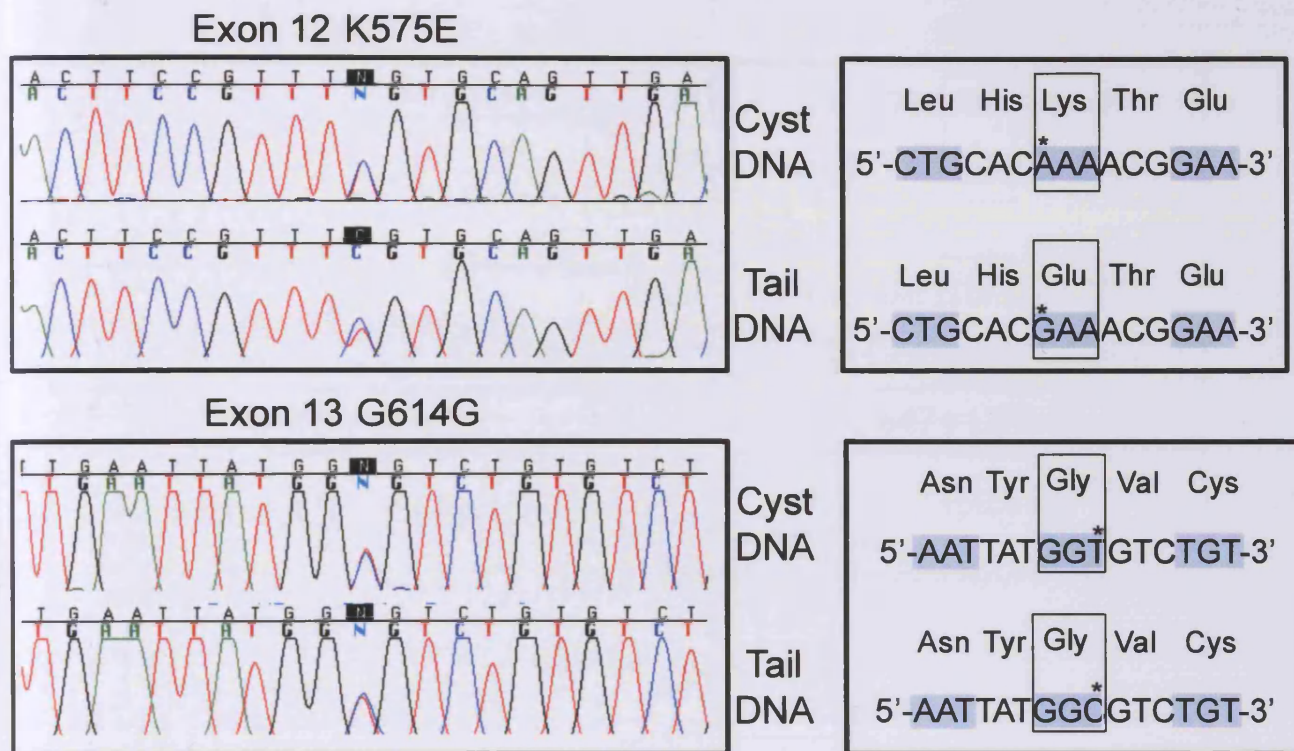


**Figure 6.1** Germline changes in *Jak2* were found in all 9 simple cysts taken from one of our *Tsc2*<sup>+/-</sup> mice. Sequencing of tail DNA confirmed the changes were present in the germline. The mutation at K575E is a non-conservative change from a positively charge amino acid to a negatively charged residue. The change at G614G does not alter the amino acid encoded.

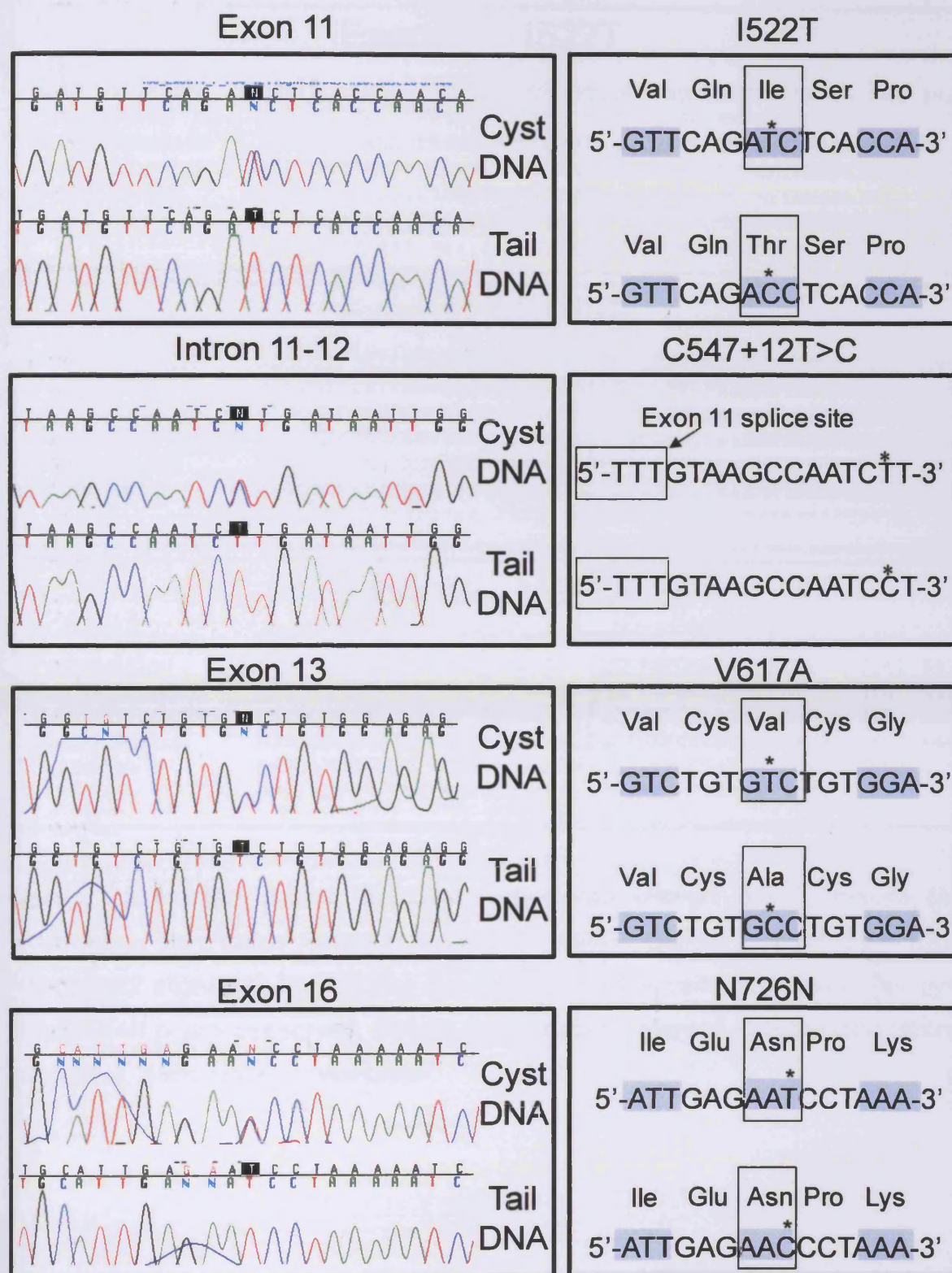


**Figure 6.2** Somatic changes in *Jak2* were found in four separate cysts from *Tsc1*<sup>+/-</sup> and *Tsc2*<sup>+/-</sup> mice. The somatic status of these mutations was confirmed through sequencing of tail DNA from the same animal.



### Exon 11 – I522T

<i>Homo Sapiens</i>	PPKPKDKSNLLVFRITNGVSDVPTSPTLQRP THMNQMV FHKIRNEDLIFNE	549
<i>Pongo Albeii</i>	PPKPKDKSNLLVFRITNGVSDVPTSPTLQRP THMNQMV FHKIRNEDLIFNE	549
<i>Mus Muscularis</i>	PPKPKDKSNLLVFRITNGISDVQISPTLQRHNNVNQMV FHKIRNEDLIFNE	549
<i>Rattus Norvegicus</i>	PPKPKDKSNLLVFRITNGVSDVQLSPTLQRHNNVNQMV FHKIRNEDLIFNE	549
<i>Gallus Gallus</i>	PPKPKDKSNLLVFRSNSVSDVPSSPTLQRHN-VSQMV FHKIRNEDLIFEE	546
<i>Danio Rerio</i>	SPRPKEKSSLLVCRSHRGLEVP LSSSLQRHN-ISQMV FHKIKKEDLELGE	532
	.*:***:***.*** *: : * *:*** . :.*****:*** : *	

### Exon 12 - K575E

<i>Homo Sapiens</i>	SLGQGTFTKIFKGVRRREVGDYQQLHETEVL LKVL DKAHRNYESSFFEAAS	599
<i>Pongo Albeii</i>	SLGQGTFTKIFKGVRRREVGDYQQLHETEVL LKVL DKAHRNYESSFFEAAS	599
<i>Mus Muscularis</i>	SLGQGTFTKIFKGVRRREVGDYQQLHKTEVL LKVL DKAHRNYESSFFEAAS	599
<i>Rattus Norvegicus</i>	SLGQGTFTKIFKGVRRREVGDYQQLHETEVL LKVL DKAHRNYESSFFEAAS	599
<i>Gallus Gallus</i>	SLGQGTFTKIFKGI RKEVGDYQQLHQTEVL LKVL DKVHRNYESSFFEAAS	596
<i>Danio Rerio</i>	SQGQGTFTKIFKGI RKEQGDYGETHKTEVIVKVL DKAHRNYESSFFEAAS	582
	* *****:*: * *****: *:***: *****.*****	

### Exon 13 – V617A

<i>Homo Sapiens</i>	MMSKLSHKHLVLN YGV CVC G DENILVQEFVKFGSLDTYLKKNKN--CINI	647
<i>Pongo Albeii</i>	MMSKLSHKHLVLN YGV CVC G DENILVQEFVKFGSLDTYLKKNKN--CINI	647
<i>Mus Muscularis</i>	MMSQLSHKHLVLN YGV CVC G EENILVQEFVKFGSLDTYLKKNKN--SINI	647
<i>Rattus Norvegicus</i>	MMSQLSHKHLVLN YGV CVC G EENILVQEFVKFGSLDTYLKKNKN--SINI	647
<i>Gallus Gallus</i>	MMSQLSYKHLVLN YGV CVC G EENILVQEYVKFGSLDTYLKKNKN--VINI	644
<i>Danio Rerio</i>	MMSQLTHKHLVLTYGICVC G DENIMVQEYVKFGSLDTYLKKNKSSVSVNI	632
	***:*. : *****. **: *****: ***: ***: *****.*****. : **	

**Figure 6.3** Human (*Homo Sapiens*), orang-utan (*Pongo Albeii*), mouse (*Mus Muscularis*), rat (*Rattus Novegicus*), chicken (*Gallus Gallus*) and zebrafish (*Danio Rerio*) *Jak2* alignment, highlighting the positions of the variants found in our cysts. **No symbol:** poorly conserved, **Single dot:** weakly conserved, **Double dot:** Strongly conserved, **Star:** 100% conservation.



The older age group, 17-23 months, included 4 *Tsc2*<sup>+/-</sup>*Jak2*<sup>K575E/+</sup> mice and 4 *Tsc2*<sup>+/-</sup>*Jak2*<sup>+/+</sup> mice. No significant difference was found between the number of simple cysts (6.0 per animal compared to 4.75, respectively [*P*=0.37]), the number of branching cysts (5.0 per animal compared to 4.75, respectively [*P*=0.89]), the number of cystadenomas (4.5 per animal compared to 1.75, respectively [*P*=0.24]) or the number of RCCs (3.0 compared to 0.75 per animal, respectively [*P*=0.23]). Total lesion incidence was 18.5 lesions per *Tsc2*<sup>+/-</sup>*Jak2*<sup>K575E/+</sup> animal compared to 12.0 lesions per *Tsc2*<sup>+/-</sup>*Jak2*<sup>+/+</sup> animal (*P*=0.25), which is a modest increase of approximate 1.5 fold (Table 6.1, Figure 6.4).

### **6.3.5 Wild-type mice with germline variants in *Jak2* at K575E and G614G experience a low level of renal cystogenesis**

We then investigated the effect of the *Jak2* germline variants on cystogenesis in wild-type mice. We selected animals previously genotyped as wild-type for *Tsc1*, *Tsc2* and *Pkd1* and tested for the presence of the K575E and G614G germline *Jak2* variants. We found 8 wild-type mice with the *Jak2* variants between the ages of 10-11 months of age where tissue was available for sectioning. These kidneys were serial sectioned for 150µm and assessed for the presence of cysts. We found a low level of cystogenesis occurring in these animals, with the maximum number of cysts found in one mouse being 6. However, several had no lesions, and the overall average was 2.38 cysts per mouse (Figure 6.5). All lesions found were small simple cysts, with evidence of dilated renal tubules in many of the kidneys. Two 13 month old wild-type mice with no *Jak2* germline variants were used as controls, and no evidence of dilated tubules or cysts were found in their kidneys. In addition, previous studies have reproduced the finding that no wild-type mice at 15 months get renal cysts on a range of genetic backgrounds (Wilson *et al.* 2006, Bonnet *et al.* 2009), All mice used in this study were genotyped multiple times to ensure they carried no germline mutations in *Tsc1*, *Tsc2* or *Pkd1*.

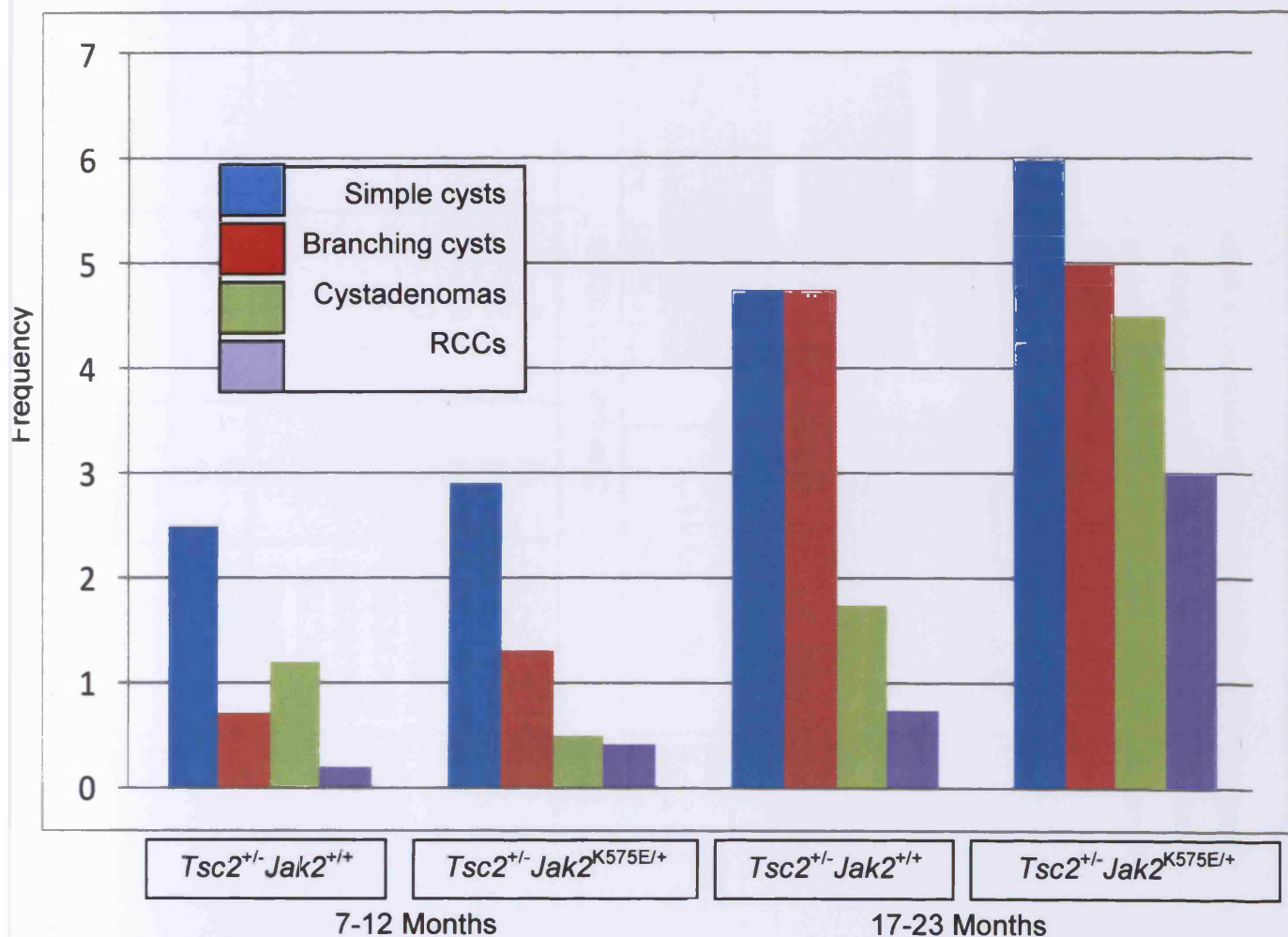


**Figure 6.4** Germline changes in *Jak2* at K575E and G614G may modestly affect lesion incidence in *Tsc2*<sup>+/-</sup> mice. A 1.13 fold increase in total lesions per mouse was observed at 7-12 months in the kidneys of our *Tsc2*<sup>+/-</sup>*Jak2*<sup>K575E/+</sup> mice compared to *Tsc2*<sup>+/-</sup>*Jak2*<sup>+/+</sup> animals (5.1 average lesions per mouse compared to 4.5, respectively). When examined at 17-23 months of age, this difference between *Tsc2*<sup>+/-</sup>*Jak2*<sup>K575E/+</sup> and *Tsc2*<sup>+/-</sup>*Jak2*<sup>+/+</sup> animals had increased to 1.54 fold (18.5 average lesions per mouse compared to 12, respectively). Neither increase was statistically significant.

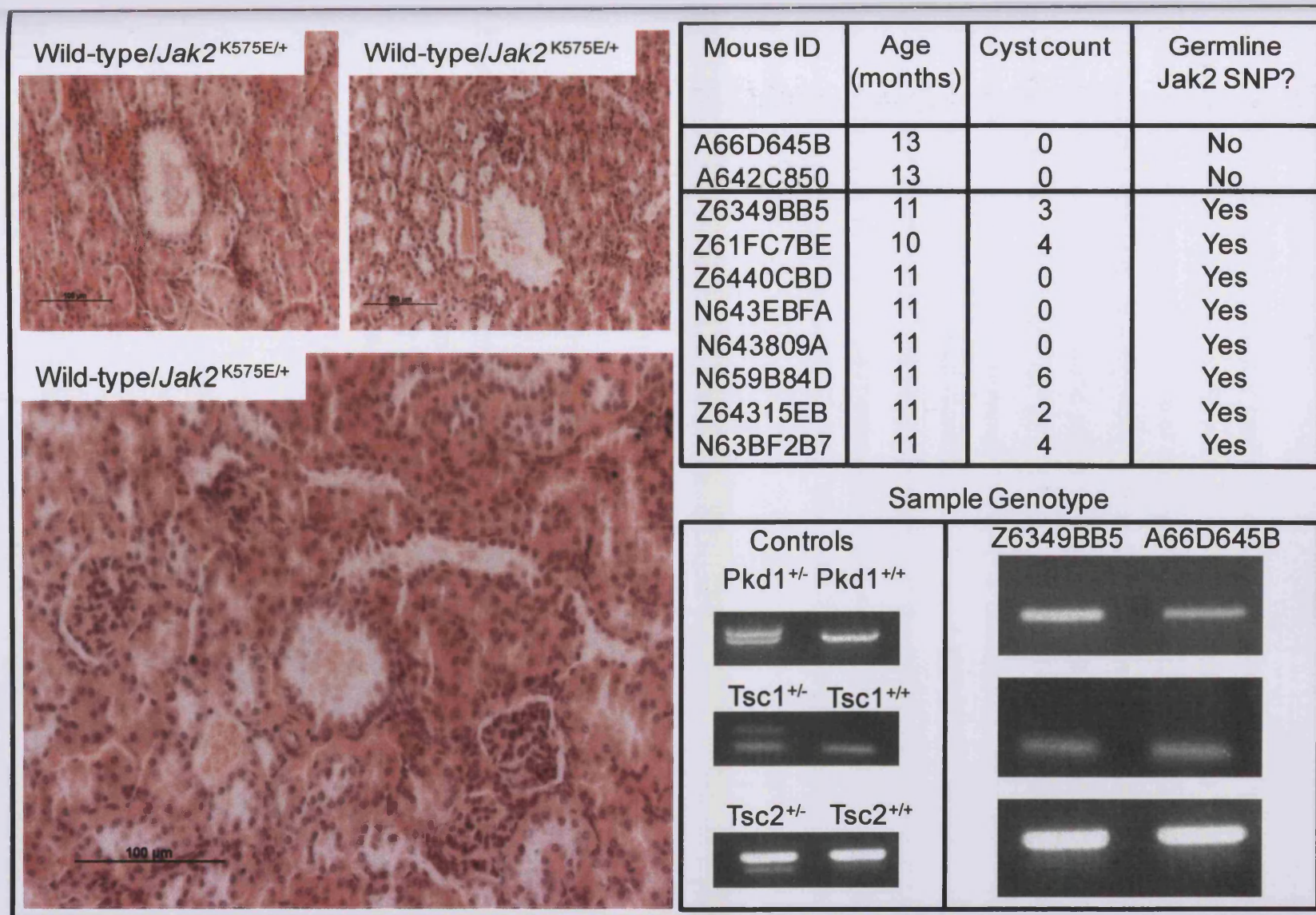


**Figure 6.5** Germline changes in *Jak2* at K575E and G614G may cause wild-type (*Tsc1*<sup>+/-</sup> and *Tsc2*<sup>+/-</sup>) mice to develop renal cysts. Several examples of renal cystogenesis were observed in mice that were confirmed as definitely negative for mutations in *Tsc1*, *Tsc2* and *Pkd1*. The presence of a *Jak2* germline change was confirmed by sequencing tail DNA from the animal. No cysts were seen in our wild-type controls, nor have any been reported by other groups using the same mouse lines.

## **6.4 Discussion**

### **6.4.1 *Jak2* mutations in *Tsc1*<sup>+/-</sup> and *Tsc2*<sup>+/-</sup> simple cysts**

The *JAK2* locus has previously been reported to be susceptible to point mutations, rearrangements or deletions (Sayyah *et al.* 2009), and we have found a range of *Jak2* mutations in the renal cysts of our *Tsc1*<sup>+/-</sup> and *Tsc2*<sup>+/-</sup> mice. Despite being a mix of exonic / intronic, synonymous / non-synonymous and conservative / non-conservative changes, we found all four somatic mutations were T to C transitions. It is perhaps not surprising that all the changes found were base substitutions, as these are among the most common mutations observed in mice and humans. In finding evidence of *Jak2* mutations in the DNA extracted from simple cysts in our *Tsc1*<sup>+/-</sup> and *Tsc2*<sup>+/-</sup> mice, we have strengthened the IHC observations in Chapter 5 and demonstrated a possible mechanism of pro-survival signalling taking place. This is the first time that mutations outside the mTOR pathway have been identified in simple Tsc cysts.

### **6.4.2 Somatic *Jak2* mutations in Tsc-associated renal cysts**

In total, we found three exonic somatic mutations in our cysts, I522T, V617A and N726N. We found a further intronic somatic mutation 12 base pairs downstream from the 3' end of exon 11 (termed c547+12T>C). These were all separately confirmed to be true somatic events through sequencing matched tail DNA.

The I522T variant is a non-conservative substitution from a hydrophobic amino acid (Isoleucine) to a hydrophilic residue (Threonine). Sequence alignments revealed the I522 position to be poorly conserved, indicating a substitution here may not lead to drastic effects on protein function. The human and orang-utan forms of *Jak2* actually have a Threonine at this position in place of Isoleucine. However, *in silico* analysis with GVG D software suggests an I522T mutation was very likely to alter protein function.

The c547+12T>C variant was detected between exon 11 and exon 12 of *Jak2*. Although it does not lead to a coding change, the variant may still be of interest



because of its proximity to the end of exon 11. The area adjacent to the end of an exon is often conserved to facilitate complex gene splicing, and non-coding mutations such as c547+12T>C may disrupt this and lead to protein abnormalities. Disruption in a 5' donor splice site can lead to exclusion of exonic coding sequence in the mature mRNA (Bateman *et al.* 1994) and work by Saharinen *et al.* (2000) has shown deletions within the pseudokinase domain of *Jak2* to lead to constitutive activation of the tyrosine kinase and induction of Stat transcription factors. However, the base pair involved is just outside the region covered by the characterised consensus sequence (which normally extends ~6 bases into the intron from the 5' splice site) and therefore may not affect the splicing of *Jak2*. Outside of this 5' donor site sequence, other consensus sequences are required for correct formation of the 'lariat' intermediate (the 'branch point') and the final correctly assembled *Jak2* mRNA (the 3' acceptor splice site). These are unlikely to be disrupted by the c547+12T>C change because they lie much further downstream (the intron between exon 11 and 12 of *Jak2* is 2,365bp long, with the 3' acceptor splice site lying adjacent to the start of exon 12, and the branch point commonly occurs ~25bp upstream from there). One more factor to be considered by intronic mutations is the possibility of disrupting an intronic splicing enhancer (ISE) or intronic splicing silencer (ISS). These short sequences can modulate splice site selection and alter the coding sequence included in the final mRNA transcript. Splicing defects in the regulatory domain of *JAK2* have previously been linked to pathological conditions such as chronic myeloproliferative neoplasms (Ma *et al.* 2010).

The V617A mutation, found in exon 13 of *Jak2*, is the most likely to have pathological consequences to the regulation of *Jak2* kinase function. Indeed, several other mutations at residue 617 (V617I, V617L, V617M, and V617W) have also been shown to be able to induce constitutive signalling *in vitro* (Dusa *et al.* 2008). The *in silico* analysis supports these claims, as the V617 residue is highly conserved from humans to zebrafish, indicating that changes here are poorly tolerated. This V617 residue is commonly mutated in polycythemia vera (PV) as V617F (Zhao *et al.* 2005), where it has been shown to be present in the blood of 20 out of 24 PV patients. In these samples, the substitution to a phenylalanine constitutes a gain-of-function mutation in *JAK2* and leads to unrestrained STAT3 activation. Although the change we have discovered in our cystic DNA is more conservative (a Valine to an

Alanine), the position is clearly vital to the inhibitory properties of the pseudokinase domain. We therefore suggest that the cyst cells expressing the V617A *Jak2* mutant are likely to have enhanced kinase activity and constitutive Stat3 activity.

Finally, the N726N variant did not lead to a change in the amino acid encoded (Asparagine). However, work done by Juboa *et al.* (2003) and Capon *et al.* (2004) suggests 'silent' synonymous mutations can actually impact on protein function through altering mRNA folding, and lead to changes in stability and levels of translation. In this context, the silent AAT→AAC change may still alter the levels of *Jak2* available for activation and Stat signalling.

#### **6.4.3 Low levels of *Jak2* mutation detection**

In total, four somatic *Jak2* mutations were found across exons 11-17 in cysts from our *Tsc1*<sup>+/-</sup> and *Tsc2*<sup>+/-</sup> mice. Of the total 65 cysts sequenced for each exon, 37.5% (36/96, see Chapter 4) of these would be expected to be mTOR and caspase inactive. From this subset, previous work in Chapter 5 has shown ~80% (10/12, see Chapter 5) will show *Jak2* activation. We therefore expected to find 19.5 variants in our cohort of mice (65 cysts x 0.375 x 0.8). This means that we are seeing fairly low levels of mutation in the *Jak2* gene, which can be accounted for in several ways. Due to restrictions on cyst DNA levels, only a small portion of the total *Jak2* gene was sequenced. When isolating advanced tumour DNA via LCM, large quantities of genetic material can be collected due to the solid and densely packed nature of most tumours. Unfortunately, cysts have a central vacuation, leaving a single cell lining to collect DNA from. The sequencing approach was specifically designed to make the most of our small amounts of DNA, and cover the areas of *Jak2* most likely to contain gain-of-function mutations, but clearly many exons have been left out of our molecular analysis. This means mutations in exons 1-10 and exons 18-24 could be present but were not searched for in our samples. Another weakness of LCM tissue collection from cysts is the possibility of wild-type cells contaminating the sample and reducing the mutant allele frequency to a level that may not be detectable by standard sequencing techniques. It is also possible that some cysts that stained positive for phospho-*Jak2* in Chapter 5 did so through normal activation or renal injury, not through mutation driven gain-of-function signalling. This would therefore reduce the expected level of *Jak2* mutations. Finally, the Stat3 and Bcl2 activation



seen in our cysts could be brought about through *Jak2*-independent means (such as dysregulated polycystin-1 tail signalling) further reducing the expected levels of *Jak2* mutations.

Repressors of this signalling pathway are another important consideration when interpreting these findings. The SOCS proteins act to negatively regulate JAK-STAT signalling through three distinct means – by direct inhibition of JAKs by binding to the kinase activation loop (Endo *et al.* 1997), by competing for binding sites on the receptor with other molecules containing the SH2 domain (STATs) (Matsumoto *et al.* 1997) and by targeting the receptor complex and associated proteins for proteasome-mediated degradation (Hilton *et al.* 1998, Zhang *et al.* 1999). Constitutive activation of the JAK-STAT pathway can be induced by mutations in the SOCS genes and are associated with human disease; for example, mutations in *SOCS1* are associated with primary mediastinal B cell lymphoma (Melzner *et al.* 2005), hepatocellular carcinoma (HCC) (Yoshikawa *et al.* 2001) and Hodgkin's lymphoma (Weniger *et al.* 2006). Other studies have suggested promoter methylation may lead to silencing of the *SOCS3* gene and cause persistent anti-apoptotic signalling under weak JAK-STAT activation (Constantinescu *et al.* 2007). This has been linked to HCC, as Ogata *et al.* (2006) have shown *SOCS3* expression to be reduced in HCC areas compared to non-HCC tissue in the same patients. Liver specific deletion of *SOCS3* enhances carcinogen-stimulated hepatic tumour development in mice, and correlated with increased expression of several anti-apoptotic genes (Ogata *et al.* 2006). Therefore, mutations in SOCS genes in our mice that reduce repression on the JAK-STAT axis may contribute to pro-survival signalling. However, because these proteins are acting as tumour suppressor genes, it is probable that two separate hits are required to remove their regulatory function. This is less likely than a single gain-of-function mutation occurring higher up the pathway in a proto-oncogene.

#### **6.4.4 Germline *Jak2* mutations**

We observed two *Jak2* variants (K575E and G614G) that were present in both cyst DNA and tail DNA of a *Tsc2*<sup>+/-</sup> mouse. These were found together in exons 12 and 13 (respectively) in all samples analysed from that mouse. Through lineage analysis, we traced the mutation back to a cd1/129 founder mouse, which had a homozygous

change for GAA (and not AAA) at 575 (encoding Glutamic acid rather than Lysine), and GGC (and not GGT) at 614 (still encoding Glycine). Because this mouse was a progenitor *Pkd1*<sup>+/-</sup> mouse in our colony, we then tested the germline status of *Jak2* in all the mice used in our studies. None of the mice used in Chapters 3, 4 or 5 were found to contain the *Jak2* K575E / G614G changes.

The K575E change occurs at a residue which is relatively strongly conserved, indicating its alteration may have consequences for *Jak2* regulation. *In silico* analysis through GVGD software supports this suggestion by grading the change as C55 (likely to interfere with function). Humans, Orang-utans and rats all encode a Glutamic acid at position 575, implying this change can be tolerated in these animals. However, it was noted that the *Tsc2*<sup>+/-</sup> mouse containing these two mutations was heavily burdened with cysts compared to age matched *Tsc1*<sup>+/-</sup> and *Tsc2*<sup>+/-</sup> littermates used in the same study. This was the impetus for a further study into the effects of these germline *Jak2* mutations on cystic load (see Section 6.4.5 and 6.4.6).

#### **6.4.5 The effects of germline changes in *Jak2* on Tsc-associated renal cystogenesis**

Due to the high number of renal cysts experienced by the *Tsc2*<sup>+/-</sup> mouse with germline changes in *Jak2* at K575E and G614G, we sought to address whether these variants could modulate cystic load. Following careful age and strain matching, we collected data at two different ages to provide a complete picture of lesion development in *Tsc2*<sup>+/-</sup> *Jak2*<sup>K575E/+</sup> and *Tsc2*<sup>+/-</sup> *Jak2*<sup>+/+</sup> animals. We found no significant difference between simple cysts or more advanced lesions in 7-12 month old or 17-23 month old mice. However, the presence of a germline change in *Jak2* did increase the incidence of most types of lesions in both age groups. In terms of fold difference, the average number of simple cysts forming in 7-12 month old mice increased by x1.2 in the context of a *Tsc2*<sup>+/-</sup> *Jak2*<sup>K575E/+</sup> genotype compared to a *Tsc2*<sup>+/-</sup> *Jak2*<sup>+/+</sup> animals. This difference increases to x1.3 in the older age category. The number of advanced lesions (branching cysts, cystadenomas and RCCs) also appears to be modulated with the germline change, with the incidence of RCCs in 17-23 month old animals

being increased x4 under a *Tsc2*<sup>+/-</sup>*Jak2*<sup>K575E/+</sup> genotype compared to *Tsc2*<sup>+/-</sup>*Jak2*<sup>+/+</sup> animals. Perhaps the most encompassing way to compare the effects of germline *Jak2* changes on cystogenesis is to compare total lesion counts, because advanced lesions have developed directly from cysts and the frequencies of both will be closely related. We saw a modest x1.1 fold increase in total lesions per mouse at 7-12 months when comparing *Tsc2*<sup>+/-</sup>*Jak2*<sup>K575E/+</sup> mice to *Tsc2*<sup>+/-</sup>*Jak2*<sup>+/+</sup> animals. As before, age appears to amplify this difference, with the difference between total lesions per mouse increasing to x1.5 fold (comparing *Tsc2*<sup>+/-</sup>*Jak2*<sup>K575E/+</sup> mice to *Tsc2*<sup>+/-</sup>*Jak2*<sup>+/+</sup> animals) at 17-23 months of age.

These data suggest a germline *Jak2* mutation may be having a subtle effect on cyst formation and progression. However, caution should be taken when interpreting the results because these changes were not statistically significant. The fact that wider differences are not seen may reflect the subtle nature of genetic changes to *Jak2* – with K575E taking place at a relatively well tolerated position and G614G being a synonymous mutation. Any difference in cyst data being observed under these relatively mild *Jak2* changes underlines a strong role for the Jak2/Stat3 signalling axis in cystogenesis.

#### **6.4.6 Wild-type mice with germline changes in Jak2 experience a low level of renal cysts**

To conclude our study on the effects of germline changes in *Jak2* at K575E and G614G, we analysed kidneys from wild-type mice both with and without these variants. Interestingly, although previous studies have noted that our mice do not experience renal cysts when wild-type for *Tsc1*, *Tsc2* or *Pkd1*, we discovered clear cut examples of cystogenesis in a selection of wild-type mice. All these mice were confirmed to have the germline changes in *Jak2* at K575E and G614G, while control animals with no changes in *Jak2* did not show signs of any renal cysts. Great care was taken with the genotyping of these animals, and it is highly unlikely that mutant *Tsc* or *Pkd* mice were included in our counts. Furthermore, the levels of cystogenesis were well below that expected in animals of the same age with *Tsc1*,

*Tsc2* or *Pkd1* mutations, implying that what we are seeing here is independent of classic Tsc / Pkd cystogenesis.

Wild-type mice may experience a very mild cystic phenotype due to inappropriate cell survival following misorientation of a renal tubule cell division. Although cell polarity is not massively disrupted in these wild-type animals (Chapter 3), a proportion of cell divisions were found to occur outside the plane of the renal tubule in wild-type animals. We hypothesize that these misdivisions are normally killed off through activation of apoptosis, possibly via anchorage dependent cell death. Under inappropriate survival signalling, which may be upregulated in the renal tubules of our germline *Jak2* mutants, some of these cells may persist, cause tubule dilation / pinching and constitute the first steps towards cyst formation. The dispersed and focal nature of the cysts suggests other factors may be required before a cyst can form, possibly as a result of localised renal injury or a somatic mutation in an unknown pathway. The germline changes found in *Jak2* may be just one characterised example of a wide range of variants in pro-survival genes that cumulatively contribute towards a cystic phenotype.

## CHAPTER SEVEN: General discussion

### 7.1 Haploinsufficiency in TSC and ADPKD

We have observed abnormalities in renal and hepatic tissue from mice heterozygote for *Tsc1*, *Tsc2* and *Pkd1*. Due to the young age of these animals (2 days old), it is unlikely that these events are mediated by a somatic removal of functional hamartin, tuberlin or polycystin-1. The suggestion that deficiency in *Tsc1*, *Tsc2* or *Pkd1* may induce haploinsufficient pathological effects is supported by wide ranging studies from other groups.

#### 7.1.1 Haploinsufficiency in TSC and other hamartoma syndromes

Stoyanova *et al.* (2004) have previously shown aberrant gene expression profiles in renal epithelial cells cultured from patients with a germline TSC mutation when compared to control cells under microarray analysis. These epithelial cells were reported to be microscopically normal but demonstrated upregulation of factors involved in protein synthesis, such as eukaryotic translation initiation factor 3 and several ribosomal proteins (L6, L21, S6, S25). Furthermore, TSC haploinsufficiency was able to increase levels of HIF1 $\alpha$  subunit mRNA, hypoxia-inducible protein 2 and hypoxia-induced gene 1, all involved in cellular oxygen sensing and HIF signalling.

Uhlmann *et al.* (2002) found *Tsc2*<sup>+/-</sup> astrocytes to have reduced levels of the cell cycle control protein, p27-Kip1 compared to wild-type cells. This decrease was suggested to mediate the 1.5 fold increase in *Tsc2*<sup>+/-</sup> astrocyte number (uniformly distributed throughout the brain) *in vivo*, by providing a growth advantage in heterozygous cells. *Tsc2* heterozygosity was then coupled with mutations in other genes (*Tsc1* and *p53*) to test for an additional growth advantage. *Tsc1*<sup>+/-</sup>*Tsc2*<sup>+/-</sup> mice displayed a cooperative astrocyte growth advantage which underlines the much studied functional interaction between tuberlin and hamartin (van Slegtenhorst *et al.* 1998, Plank *et al.* 1998, Nellist *et al.* 1999). Unlike *Nf1*<sup>+/-</sup>*p53*<sup>+/-</sup> mouse crosses (which do demonstrate significant genetic cooperation) (Bajenaru *et al.* 2001), the *Tsc2*<sup>+/-</sup>*p53*<sup>+/-</sup> mice showed no such effect.

Further evidence that heterozygosity for *TSC1* or *TSC2* may be sufficient to trigger cell abnormalities has come from mutational analysis studies of brain lesions in TSC (Henske *et al.* 1996, Parry *et al.* 2000), where lesions do not (or rarely) demonstrate bi-allelic inactivation of *TSC1* or *TSC2*. Goorden *et al.* (2007) reported that *Tsc1*<sup>+/-</sup> mice with no apparent cerebral pathology showed impaired learning in hippocampus-orientated tasks (Morris water maze trials) and abnormal social behaviour (reduced nest building).

A link between tuberin and DNA repair has been proposed by Habib *et al.* (2008), through using Eker rats (*Tsc2*<sup>+/-</sup>). Under heterozygous levels of tuberin, a decrease in the levels of expressed 8-oxoguanine DNA glycosylase (OGG1) was noted in the renal tissue of the Eker rats when compared to controls. OGG1 initiates base excision repair in mammalian cells and is the main defence against the mutagenic effects of the oxidised DNA product, 8-oxo-2'deoxyguanosine (8-oxo-dG). The researchers suggest that this haploinsufficiency for *Tsc2* makes the Eker rats more susceptible to oxidative DNA damage. The kidney is known to have unusually high levels of oxygen metabolism and furthermore, high concentrations of urea are able to trigger oxidative stress in kidney cells (Audebert *et al.* 2000). Haploinsufficient defects in this pathway may have severe repercussions for the genetic integrity of the kidney and lead to the acquisition of further mutations.

Our laboratory has contributed to this area of TSC research by finding a lack of *Tsc1* second hits in 68.4% of renal cysts compared to ~20% of advanced lesions (cystadenomas and RCCs) from *Tsc1*<sup>+/-</sup> mice. Second hits were tested for by LOH analyses and direct sequencing of the entire *Tsc1* ORF, and the absence of these events in many early lesions suggests haploinsufficiency for *Tsc1* may be sufficient to initiate renal cystogenesis (Wilson *et al.* 2006). The work in this thesis adds to these renal findings by providing further evidence for haploinsufficient *Tsc1* and *Tsc2* cystogenesis, as indicated by the finding that a significant proportion of simple cysts are mTOR inactive (Chapter 4). In addition, we report other subtle, pre-cystic changes in renal tubule cell primary cilium lengths, hepatic cholangiocyte primary cilium lengths and defects in mitotic orientation of tubule / duct cells in both organs (Chapter 3). Furthermore, apoptosis rates in developing renal tubules in our heterozygote mice (*Tsc1*<sup>+/-</sup> and *Tsc2*<sup>+/-</sup>) were found to be elevated when compared to



wild-type littermates. Our findings are likely to be the earliest events in cystogenesis and support the theory that haploinsufficiency of *Tsc1* or *Tsc2* is able to instigate cyst formation (Figure 7.1).

Aside from TSC, there is evidence for haploinsufficient tumour initiation in several related hamartoma (hyperplastic disorganised growth) syndromes (such as Peutz-Jeghers syndrome [PJS], PTEN hamartoma syndromes and juvenile polyposis syndrome [JPS]) (reviewed in Santarosa *et al.* 2004). Data from these syndromes support the Tsc renal findings, where many advanced lesions will display second hits in their corresponding wild-type gene while earlier lesions will demonstrate haploinsufficiency. For example, LOH of the wild-type *LKB1* gene is almost always found in carcinomas from PJS patients, but is only seen in 38% of benign hamartomatous polyps (Entius *et al.* 2001). Furthermore, heterozygosity for *Lkb1* is sufficient to induce gastrointestinal polyps in *Lkb1*<sup>+/-</sup> mice (Miyoshi *et al.* 2002, Rossi *et al.* 2002, Jishage *et al.* 2002). Loss of wild-type *Pten* does not occur in the hyperplastic / dysplastic changes of the colon mucosa and polyps in the lower gastrointestinal tract in *Pten*<sup>+/-</sup> mice (Di Cristofano *et al.* 1998), and PTEN haploinsufficiency can induce gene expression changes in subventricular zone precursor cells (Li *et al.* 2003). Finally, LOH of the *Smad4* allele (associated with JPS) is rare in early gastrointestinal lesions from *Smad4*<sup>+/-</sup> mice (Xu *et al.* 2000, Alberici *et al.* 2006), and data from humans with JPS suggests a similar low level (9%) of *SMAD4* LOH in gastrointestinal polyps (Howe *et al.* 1998).

Due to the higher frequency of biallelic inactivation in advanced lesions when compared to early lesions, it is likely that one hit in *Tsc1* or *Tsc2* will prime cells for tumourigenesis and a second hit will promote tumour progression. As a lesion develops and becomes increasingly genetically unstable, further mutations are acquired and the initiating factors in tumourigenesis become masked. A cyst that has arisen though reductions in the cellular levels of tuberin or hamartin (but not complete removal, as indicated by control over the mTOR pathway) will have strong selection pressures for a second mutational event at the wild-type *Tsc1* or *Tsc2* loci to remove mTOR control and increase cell proliferation and translation. We suggest that by looking in pre-cystic cells from Tsc heterozygous mice we are observing effects of hamartin and tuberin haploinsufficiency (alterations of primary cilium

lengths, aberrant cell polarity and elevated apoptosis) before confounding factors can obscure what is critical to lesion formation.

### 7.1.2 Haploinsufficiency in ADPKD

Second hits in *PKD1* or *PKD2* are unable to be found in a significant proportion of cysts from ADPKD patients (see Chapter 1, Section 1.2.8) (Jiang *et al.* 2006). Furthermore, many ADPKD cyst epithelia stain strongly for polycystin-1 and -2 (Ong *et al.* 1999a, Ong *et al.* 1999b), implying that complete loss of these proteins is not strictly required for cystogenesis in this condition. A reduced dosage of wild-type *Pkd1* was sufficient for cyst formation in a mouse model with 15-20% normally spliced polycystin-1 (Lantinga-van Leeuwen *et al.* 2004). Jiang *et al.* (2006) found similar results in a conditional *Pkd1* knockout mouse model. Ahrabi *et al.* (2007) studied a non-cystic *Pkd1*<sup>+/-</sup> mouse model and found a reduction in polycystin-1 to be associated with a phenotype of inappropriate antidiuresis (reduction of urinary volume) reflecting decreased intracellular Ca<sup>2+</sup> concentration, decreased activity of RhoA and abnormal expression of Arginine vasopressin in the brain. Haploinsufficiency has also been demonstrated in *Pkd2* mice, where Chang *et al.* (2006) found *Pkd2* heterozygous mice to have an elevated proliferative index in non-cystic renal tubules, when compared to wild-type littermates. When non-cystic tubules of ADPKD patients were analysed by the same group, a similar increase in the proliferative index was seen, implying this increase in cell proliferation is an event that pre-dates cystogenesis and can result from haploinsufficiency at *PKD2*.

In our *Pkd1*<sup>+/-</sup> mice, we found pre-cystic defects in the lengths of primary cilia projecting from renal tubule cells and cholangiocytes lining the hepatic bile ducts. We also observed a disruption in pre-cystic renal tubule and bile duct cell polarity, reflected in high levels of misaligned mitoses. Developing renal tubules in our *Pkd1*<sup>+/-</sup> mice exhibited elevated apoptosis when compared to wild-type littermates, and these changes, together with the above studies, make a clear case for haploinsufficiency at *Pkd1* causing pre-cystic abnormalities.

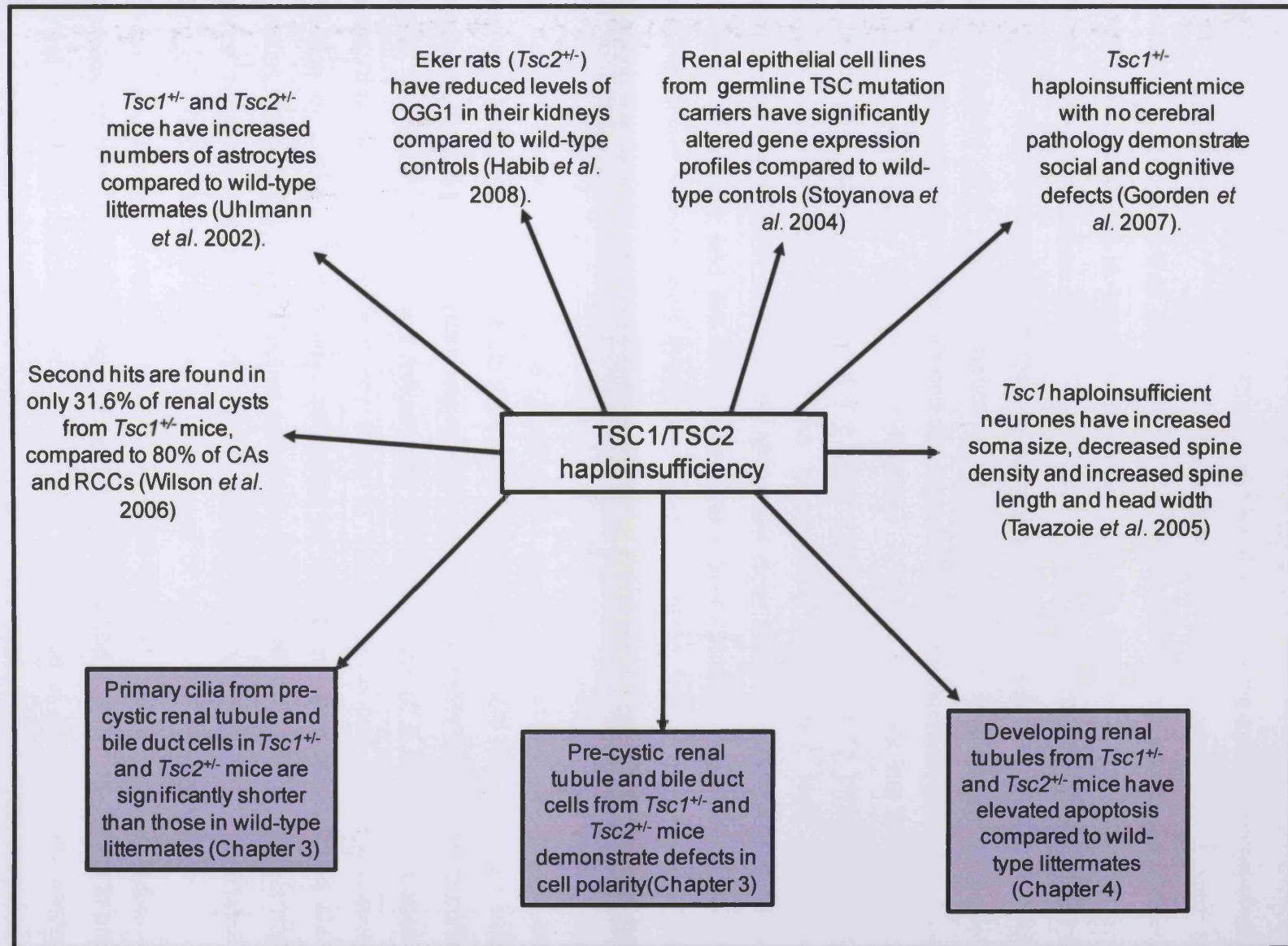


**Figure 7.1** Consequences of haploinsufficiency in *Tsc1* and *Tsc2*. **Purple boxes:** contributions to the field contained within this thesis.

## 7.2 Mechanisms of cystogenesis

We have shown that PCP or A/B polarity is disrupted in the pre-cystic kidneys of our *Tsc1*<sup>+/-</sup>, *Tsc2*<sup>+/-</sup> and *Pkd1*<sup>+/-</sup> mice. This dysregulation of mitotic orientation is likely to underlie cystic changes that occur later in the kidneys of these mice. Similar polarity defects were observed in hepatic bile ducts from the same animals, although the lack of a cystic phenotype in *Tsc1*<sup>+/-</sup> and *Tsc2*<sup>+/-</sup> mice suggests polycystin-1 plays a particularly important role in hepatic cystogenesis. Our data from wild-type mice suggest tubule and duct elongation during development is a tightly controlled process, with carefully orientated cell divisions ensuring an increase in tubule / duct length but maintenance of a constant diameter. Aberrant divisions into the lumen of the developing tubule will restrict the passageway and lead to pinching / fluid retention. Aberrant divisions into the surrounding tissue will lead to tubule enlargement and dilation. Both eventualities are clear steps towards an abnormally dilated tubule / duct and are likely to create highly cystogenic conditions in our haploinsufficient kidneys and livers. However, a striking feature first noted when observing the tubules / ducts of 2-3 month old *Tsc1*<sup>+/-</sup>, *Tsc2*<sup>+/-</sup> or *Pkd1*<sup>+/-</sup> mice is the lack of evidence for these misdivisions. No dilated renal tubules are seen, no dilated bile ducts are seen and no cells growing into or out of tubule / duct lumen are observed. Indeed, mutant animals ultimately form tubules / ducts that are structurally indistinguishable from wild-type mice, and do not develop cysts for several months. Clearly, secondary factors are influencing the expression of a cystic phenotype. These may be numerous, but are likely to include enhanced cell proliferation, induction of the mTOR pathway, cessation of fluid flow, aberrant GF and Ca<sup>2+</sup> signalling, renal injury and defective apoptosis. We hypothesise that apoptosis may 'rescue' renal tubules and hepatic bile ducts from aberrant divisions by selectively killing off cells that have misdivided. This level of selection is suggested to occur through lack of cell-cell contact, removal of ECM survival signals and the triggering of anoikis. Defects in this process, through gain-of-function somatic mutations in pro-survival signalling, could therefore lead to the persistence of an aberrantly divided cell and the subsequent clonal expansion of a new cyst. These cysts may have sufficient heterozygous levels of tuberin / hamartin to retain mTOR control, but secondary mutations in pro-survival pathways. We have now identified Bcl2 as the mediator of this survival, and put forward Stat3 and Jak2 as likely inducers of this

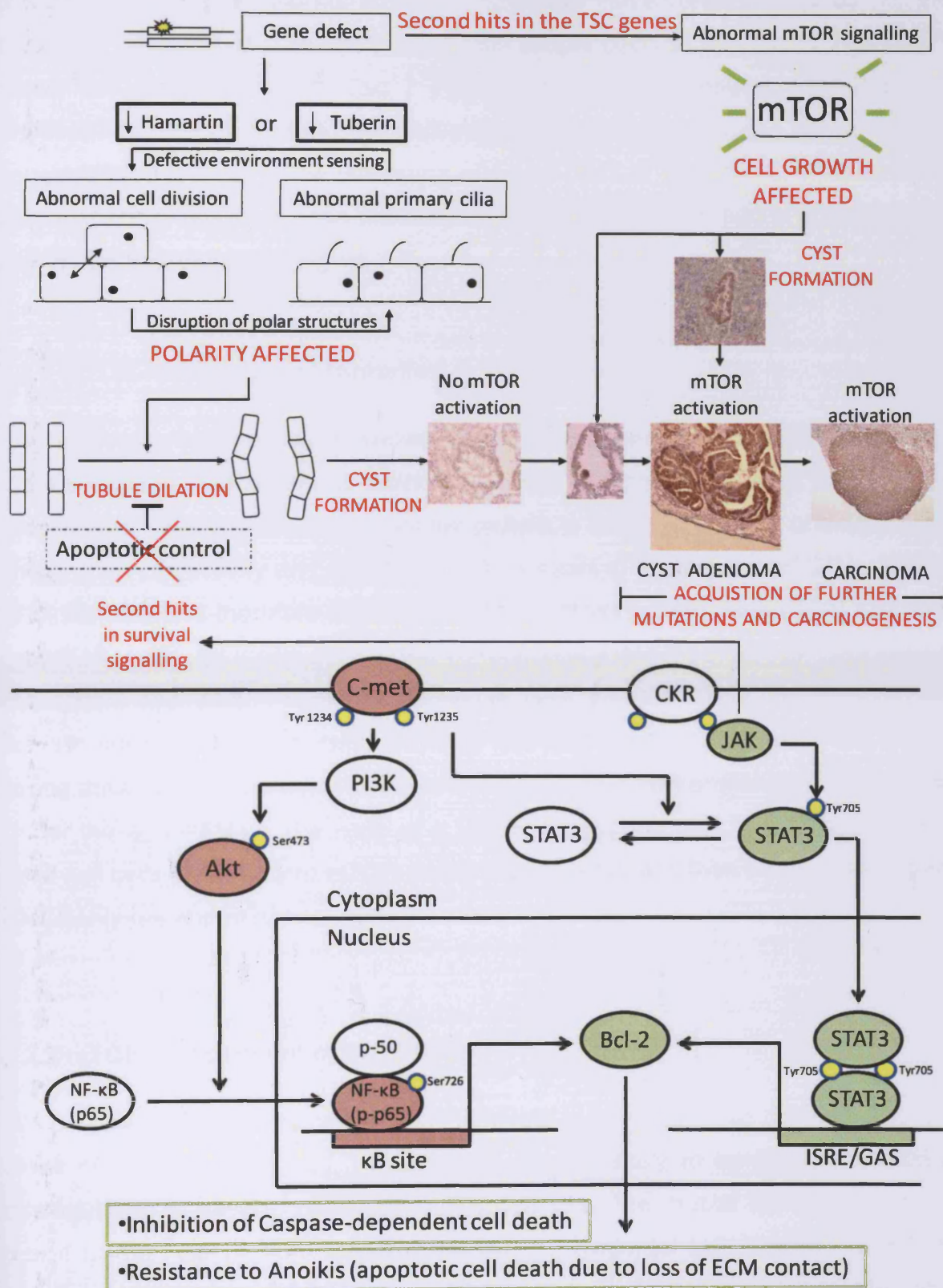


**Figure 7.2** mTOR-dependent and independent cystogenesis in TSC. All lesions pictured have been stained for active pS6. Green / red colouring in the pro-survival signalling diagram indicates activation / inactivation, respectively.



protein. Furthermore, gain-of-function mutations have been observed in the regulatory region of *Jak2* in DNA taken from simple cysts in our *Tsc1*<sup>+/-</sup> and *Tsc2*<sup>+/-</sup> mice. The delay period in Tsc / Pkd-associated cystogenesis may therefore represent the time needed for activating secondary mutations, which do not necessarily have to be in the remaining wild-type *Tsc1* or *Tsc2* locus. We propose a model where cystogenesis can occur by two distinct routes (termed mTOR-mediated and mTOR-independent) (Figure 7.2).

### 7.2.1 mTOR-mediated cyst formation

Our laboratory has previously shown somatic mutations in *Tsc1* are infrequent in cysts but common in advanced lesions from *Tsc1*<sup>+/-</sup> mice (Wilson *et al.* 2006). When assessed for mTOR activation, a similar pattern is seen, with ~60% of simple cysts showing mTOR activity and advanced lesions staining positive for mTOR activation all of the time. We therefore suggest, but have not yet proven, that mTOR activation occurs after somatic inactivation of the corresponding wild-type *Tsc1* or *Tsc2* allele in our *Tsc1*<sup>+/-</sup> and *Tsc2*<sup>+/-</sup> mice. Renal tubule cells in *Tsc1*<sup>+/-</sup> and *Tsc2*<sup>+/-</sup> mice with somatic inactivation of the corresponding wild-type *Tsc1* or *Tsc2* allele will have a strong drive towards cystogenesis due to mTOR-dependent proliferation and growth. Under these conditions, the walls of a tubule will expand with hyperplastic *Tsc1* or *Tsc2* null cells, develop into mTOR-active simple cysts, and then advance through to cystadenomas and RCCs.

### 7.2.2 mTOR-independent cyst formation

We propose that TSC-associated cystogenesis is a multifaceted process. The end result of a cyst in our *Tsc1*<sup>+/-</sup> and *Tsc2*<sup>+/-</sup> mice is likely to be the culmination of dysregulation in several pathways and processes. The crucial contribution of this thesis to the field of TSC research will be the evidence collected for an mTOR-independent route of TSC-associated cystogenesis. The heart of this alternative theory of cyst formation is that haploinsufficiency for *Tsc1* or *Tsc2* will lead to widespread polarity defects across the kidney and liver. This provides the context for all other cystic changes to take place in. How this defective polarity is brought about



is a perhaps less clear (Figure 7.3), with evidence for both abnormal primary cilia-mediated polarity defects and a reduction in hamartin-tuberin leading to direct disruption of polarity signalling through PatJ. We suggest that abnormal primary cilia are a symptom of these polarity defects, due to their highly polar nature. The role hamartin, tuberin and polycystin-1 play in ciliogenesis cannot be ignored either (Chapter 1, Sections 1.1.10 and 1.3.2). Against the background of defective polarity, additional factors, such as renal injury or defective apoptosis can then drive cystogenesis in the absence of mTOR dysregulation. Ischemic renal injury (IRI) has been shown to promote cell proliferation in surviving tubular epithelial cells. Patel *et al.* (2008) and Takakura *et al.* (2009) found that following unilateral IRI, *Kif3a* mutant mice and *Pkd1* mutant mice developed renal cysts, whilst no cyst formation was observed in the uninjured corresponding kidney. In this case, it appears the sudden stimulation of cell proliferation was enough to tip the balance towards cystogenesis, in much the same way as induction of the mTOR pathway. Alternatively, or perhaps concurrently, defects in apoptosis are likely to promote polarity-driven cystogenesis through unopposed misorientated divisions. The somatic mutations we have found (Figure 7.4) in the regulatory region of *Jak2* in DNA from cysts in *Tsc1*<sup>+/-</sup> and *Tsc2*<sup>+/-</sup> animals suggest this is a valid and physiologically relevant mechanism of cyst formation. The random occurrence of these second hits may explain both the focal nature, and delayed appearance of TSC-associated cystogenesis. The model of apoptosis as a rescue mechanism for defective polarity in renal tubules is supported by our findings of elevated cell death in the developing tubules of *Tsc1*<sup>+/-</sup>, *Tsc2*<sup>+/-</sup> and *Pkd1*<sup>+/-</sup> mice, compared to wild-type littermates. This elevation is the third pre-cystic haploinsufficient change we detected in our mutant mice (Figure 7.1), and is likely to not represent a disease-causing process, but rather the attempt by the kidney to resist pathogenesis.

### 7.2.3 mTOR-dependent cyst progression

We occasionally found cysts that were clearly negative for mTOR activation but displayed a positive pS6 papillae projection (Figure 7.2). We suggest that these cysts may have arisen through defective polarity but eventually acquired a second hit in *Tsc1* or *Tsc2* in a single cell of the cyst epithelium. The subsequent mTOR

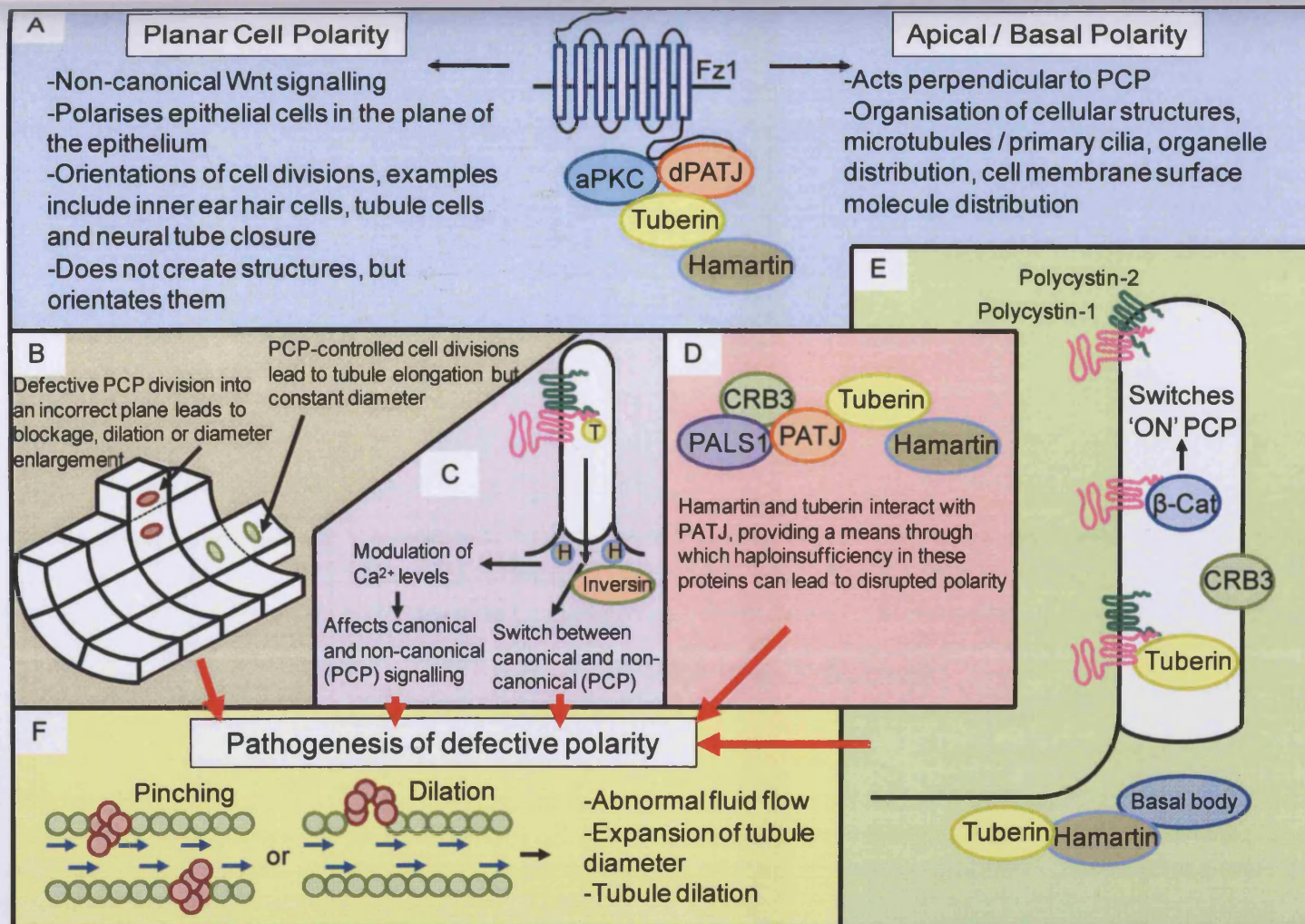


**Figure 7.3** Hamartin, tuberin and polycystin-1 have links to A/B and planar cell polarity. **Panel A:** PCP and A/B polarity are able to organise tissue sheets into functional systems. Through its interaction with dPatJ (PatJ in mice, PATJ in humans), tuberin is suggested to inhibit the canonical Wnt receptor, Fz1, and in doing so, it acts as a switch between A/B and PCP. **Panel B:** Aberrant PCP leads to misaligned cell divisions in renal tubules / hepatic bile ducts, and causes morphogenic defects. **Panel C:** Primary cilia are mediators of PCP, with key polarity proteins such as Inversin localised to the ciliary body. They are also likely to provide an sensory input as the tissue is shaped (for example, through  $Ca^{2+}$ ). **Panel D:** Tuberin and hamartin directly interact with PATJ. **Panel E:** Polycystin-1 is able to interact with  $\beta$ -Catenin and switch on PCP signalling by inhibiting the canonical Wnt pathway. Tuberin, hamartin and CRB3 have all been localised to the primary cilium, making it a likely mediator of cell polarity. **Panel F:** Defects in A/B and/or PCP signalling cause cystic changes in renal tubules.

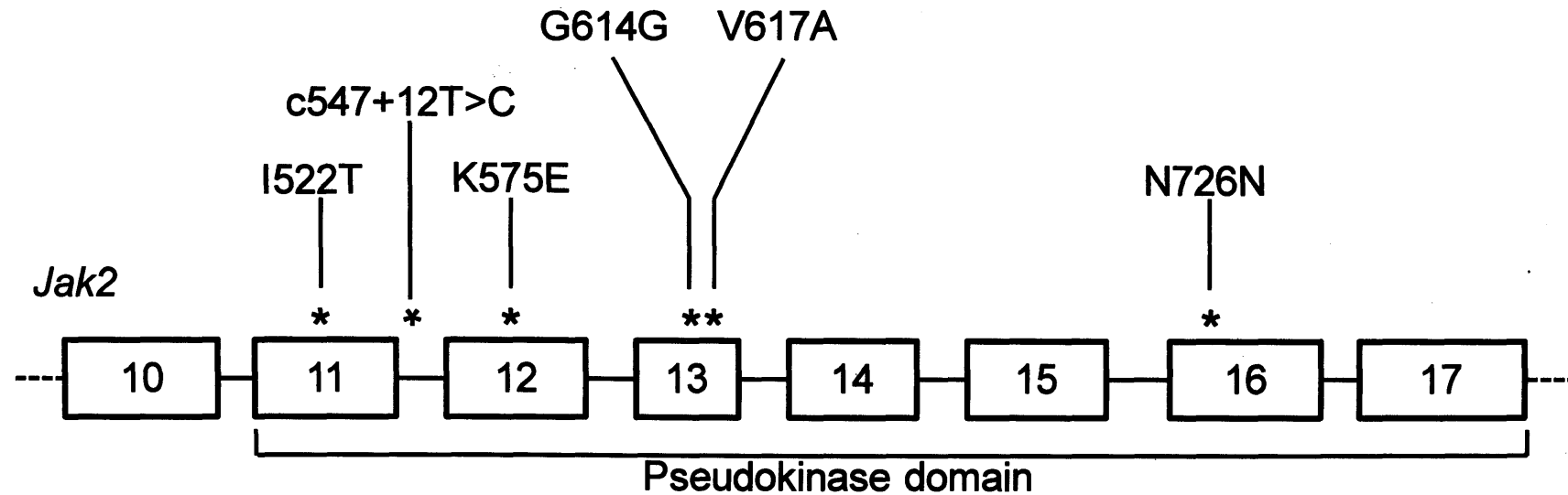


**Figure 7.4** Distribution of variants identified across the pseudokinase domain of *Jak2*. A total of 6 changes were found, two of which were concurrent germline mutations and present in all cysts analysed from a single *Tsc2*<sup>+/-</sup> mouse. Somatic changes, which were a mixture of synonymous and non-synonymous mutations, were confirmed by sequencing tail DNA to prove the absence of the variant. No mutations were detected in exons 14, 15 or 17 of *Jak2* in our cysts.



activation and clonal expansion could then promote formation of a papillae projection, which given enough time, would progress through to a cystadenoma and eventually, a RCC. These cysts are rare events to capture under the microscope, as not only would the cyst need to be negative for mTOR activation, but must also be in the early stages of acquiring localised mTOR activation. The massive growth and proliferation advantages offered by dysregulation of the mTOR pathway will probably mean these early hits are quickly hidden by rapid clonal expansion of the activated cell. However, examples of such a cyst go some way to explain why mTOR activation appears so strongly correlated with lesion progression. It also demonstrates that multiple routes of cystogenesis are viable in TSC.

### **7.3 Implications for clinical trials**

Due to the role hamartin and tuberlin play in the regulation of mTORC1 signalling, a large portion of TSC treatment has focussed on restoring repression to the TSC1/2-mTOR axis, primarily through specific inhibitors such as Rapamycin. Similarly, mTOR has been shown to be aberrantly activated in ADPKD (Shillingford *et al.* 2010), leading to trials of Rapamycin to treat the renal and hepatic phenotype associated with this disease. We have used animal models to recapitulate these diseases and we now discuss the clinical implications of our findings.

#### **7.3.1 Inhibition of the mTOR pathway in TSC**

As reviewed in Chapter 1 (Section 1.1.10.5), Rapamycin is a naturally occurring inhibitor of the mTORC1 complex. Through repression of this signalling axis, control can theoretically be restored to TSC1/2 mutant cells with dysregulated mTOR activation. Human trials have returned mixed results, with reports of lesion regression following cessation of treatment and poor effects on lesion initiation. The data collected in this thesis may go some way to explain the unfortunate inefficacy of this drug. A key problem with targeting the mTOR pathway in the treatment of a TSC kidney phenotype is that while the majority of later lesions in our Tsc mice have mTOR activation, many of the earliest cysts do not. By exclusively targeting mTOR, many lesions may still develop through pathways outside the mTOR axis. Indeed,

Kenerson *et al.* (2005) treated Eker rats with Rapamycin and found no effect on the numbers of microscopic precursor lesions. Interestingly, inhibition of this pathway may be beneficial in the advanced stages of a TSC-associated renal phenotype because volume reductions in later kidney lesions have been reported by two separate studies (Bissler *et al.* 2008, Davies *et al.* 2008). While Rapamycin can help control tumour progression, it cannot completely prevent lesion initiation because our work shows these early cysts may have arisen through an mTOR-independent mechanism. We suggest that mTOR inhibition should remain in treating the renal phenotype associated with TSC, but by targeting this one axis alone, opportunities are missed to effectively block renal cyst initiation. The ultimate answer may therefore lie in combination therapy to target multiple routes of cyst formation (discussed in Section 7.3.2). Additionally, the TSC patient's stage of renal disease could be taken into account, with early preventative therapy targeting multiple routes of cyst initiation, and later stage Rapamycin-heavy treatment to induce regression of strongly mTOR-active lesions.

### **7.3.2 JAK2 or STAT3 inhibitors in TSC?**

We have shown a route of cyst initiation that is mTOR-independent and instead relies on defective polarity (through haploinsufficiency of tuberin / hamartin) and inappropriate cell survival. Jak2-Stat3-Bcl2 signalling pathway appears to be mediating this survival in our mTOR inactive cysts, and so novel therapeutic options may now be available in treating the renal cystic manifestations of TSC. JAK2 has a role in signalling through cytokine receptors, such as those that bind erythropoietin and thrombopoietin, and activation of this molecule is linked to haematologic malignancies (Yu *et al.* 2004), and much work has already been done on developing inhibitors to suppress aberrant JAK2 signalling. Currently no JAK2 inhibitors are approved for human use, although clinical trials are underway (Sayyah *et al.* 2009).

The first JAK2 inhibitor identified was AG490 (Meydan *et al.* 1996), which is able to block constitutive Jak2 signalling and trigger caspase-dependent apoptosis in leukemic cells derived from human patients. Although potent, this inhibitor lacks specificity for Jak2 (Gu *et al.* 2001), which is actually a widespread problem across

this class of drugs. For example, Atilimod has been shown to reduce levels of phosphorylated STAT3, STAT5 and Akt, coupled with an induction of apoptosis and caspase-3 activity (Faderl *et al.* 2007) in constitutively active JAK2 cells, but targets both JAK2 and JAK3 molecules (Quintas-Cardama *et al.* 2010). Non-specific pathway disruption may have unforeseen consequences in the human body and possible deleterious effects. Chemicals that target STATs directly appear to have higher specificity (Yu *et al.* 2004).

Numerous groups have reported on the induction of apoptosis that follows blocking constitutively activated STAT3 in tumour cells (Bowman *et al.* 2000, Buettner *et al.* 2002, Battle *et al.* 2002). Promisingly, blocking STAT3 in normal cells does not generally lead to apoptosis (Bowman *et al.* 2001, Turkson *et al.* 2001), suggesting an exploitable difference between STAT3 activated and normal cells. This selective inhibition of growth may reflect an irreversible dependence of STAT3-activated cells on the stimulatory outcomes of STAT3 signalling, with normal cells being able to withstand lower levels of STAT3 activity or use alternative pathways (Yu *et al.* 2004).

Small molecule inhibitors of STAT3 would have increased specificity, although direct inhibition of specific transcription factors is notoriously challenging. However, progress has been made towards this goal, with STAT3 peptide inhibitors (based on rational design) showing specific blocking of STAT3 dimerisation / activity and induction of tumour cell death, with little effect on normal cells (Turkson *et al.* 2001).

During development, STAT3 is activated by HGF and mediates epithelial tubulogenesis (regulating genes responsible for forming branched tubule structures) (Boccaccio *et al.* 1998), along with roles in cell differentiation (Bonni *et al.* 1998) and suppression of apoptosis (Akira 1999). The need for this protein is highlighted by Stat3 null mice that die early embryogenesis, prior to gastrulation (Takeda *et al.* 1997).

Several groups have investigated using IFN $\gamma$  as a treatment for TSC, as it has been previously shown that elevated IFN $\gamma$  expression is associated with decreased severity of kidney tumours in TSC patients and mouse models (Dabora *et al.* 2002, Hino *et al.* 2002b). IFN $\gamma$  is an activator of the JAK/STAT signalling pathway, specifically inducing STAT1 phosphorylation at Tyr701 through JAK1 and JAK2



(Ramana *et al.* 2002). Treatment of *Tsc1* or *Tsc2* null cell lines with IFN $\gamma$  caused elevation of phospho-Stat1 (Y701), a reduction in both phospho-Stat3 (Y705) and *bcl2*, with a subsequent induction of apoptosis (El-Hashemite *et al.* 2004). Clearly IFN $\gamma$  is an exciting prospect in TSC treatment and appears to be able to abolish aberrant Stat3 and Bcl2-mediated cell survival in cell lines and mouse models. While IFN $\gamma$  could block aberrant pro-survival signalling in cysts that develop outside the mTOR pathway, it may be wise to treat the renal phenotype of TSC with a combination of IFN $\gamma$  and Rapamycin to block multiple cyst initiation routes. Reports of synergism between the action of these drugs in *Tsc1* / *Tsc2* null cell lines in raising phospho-Stat1 (Y701) levels and reducing the *bcl2* expression provides early support for this line of treatment (El-Hashemite *et al.* 2004). Furthermore, Rapamycin has been shown to stimulate IFN $\gamma$  secretion *in vitro* in a dose dependent manner, in a signalling pathway likely to involve repression of mTOR (El-Hashemite *et al.* 2004).

In conclusion, our results highlight a role for hamartin, tuberlin and polycystin-1 in the polarity of renal tubule epithelial cells and hepatic bile duct cholangiocytes. The precise mechanism of this role remains undefined, but multiple links have emerged between these proteins and polarity signalling. The interaction between A/B, PCP and the primary cilium also remains unclear, but our data suggest defects in these processes are the earliest pathogenic mechanisms in disease progression. We have suggested a rescue mechanism may prevent early cystogenesis, and have subsequently found evidence for its dysregulation in a proportion of our simple cysts. The identification of the Bcl2-Stat3-Jak2 axis as a route to cystogenesis outside the mTOR pathway is an important finding and one which may lead to new and exciting therapeutic options for TSC patients.

## References

- Abbott, K. C., Agodoa, L. Y. (2002) Polycystic kidney disease in patients on the renal transplant waiting list: trends in haematocrit and survival. *BMC Nephrol.*, 3: 7.
- Abraham, R. T., Wiederrecht, G. J. (1996) Immunopharmacology of rapamycin. *Annu Rev Immunol.*, 14: 483-510.
- Adhvaryu, K., Shanbag, P., Vaidya, M. (2004) Tuberous sclerosis with hypothyroidism and precocious puberty. *Indian J Pediatr.*, 71: 273-275.
- Akira, S., (1999) Functions and roles of STAT family proteins: lessons from knockout mice. *Stem Cells*, 17: 138-146.
- Alberici, P., Jagmohan-Changur, S., De Pater, E., Van Der Valk, M., Smits, R., Hohenstein, P., Fodde, R. (2006) *Smad4* haploinsufficiency in mouse models for intestinal cancer. *Oncogene*, 25: 1841-1851.
- Alessi, D. R., Andjelkovic, M., Caudwell, B., Cron, P., Morrice, N., Cohen, P., Hemmings, B. A. (1996) Mechanism of activation of PKB by Insulin and IGF-1. *EMBO J.*, 15: 6541-6551.
- Ali, S. M., Wong, V. Y., Kikly, K., Fredrickson, T. A., Keller, P. M., DeWolf, W. E., Lee, D., Brooks, D. P. (2000) Apoptosis in polycystic kidney disease: involvement of caspases. *Am J Physiol Regulatory Integrative Comp Physiol.*, 278: 763-769.
- Allard, D., Figg, N., Bennett, M. R., Littlewood, T. D. (2008) Akt regulates the survival of vascular smooth muscle cells inhibition of FOXO3a and GSK3. *J Bio Chem.*, 283: 19739-19747.
- Alper, J. C., Holmes, L. B. (1983) The incidence and significance of birthmarks in a cohort of 4,641 newborns. *Ped Dermatol.*, 1: 58-68.

Alpini, G., Glaser, S., Robertson, W., Rodgers, R. E. D., Phinizy, J. L., Lasater, J., Lesage, G. D. (1997) Large but not small intrahepatic bile ducts are involved in secretin-regulated ductal bile secretion. *Am Phys Soc.*, 272: 1064-1074.

Al-Saleem, T., Wessner, L. L., Scheithauer, B. W., Patterson, K., Roach, E. S., Dreyer, S. J., Fujikawa, K., Bjornsson, J., Bernstein, J., Henske, E. P. (1998) Malignant tumours of the kidney, brain and soft tissues in children and young adults with the tuberous sclerosis complex. *Cancer*, 83: 2208-2216.

Alvaro, D., Mancino, M. G., Onori, P. (2006) Estrogens and the pathophysiology of the biliary tree. *World J Gastroenterol.*, 12: 3537-3545.

Ariza, M., Alvarez, V., Marin, R., Aguado, S., Lopez-Larrea, C., Alvarez, J., Menendez, M. J., Coto, E. (1997) A family with a milder form of adult polycystic kidney disease not linked to the *PKD1* (16p) or *PKD2* (4q) genes. *J Med Genet.*, 34: 587-589.

Astrinidis, A., Cash, T. P., Hunter, D. S., Walker, C. L., Chernoff, J., Henske, E. P. (2002) Tuberin, the tuberous sclerosis complex 2 tumour suppressor gene product regulates Rho activation, cell adhesion and migration. *Oncogene*, 21: 8470-8476.

Astrinidis, A., Senapedis, W., Coleman, T. R., Henske, E. P. (2003) Cell cycle-regulated of phosphorylation of hamartin, the product of the tuberous sclerosis complex-1 gene, by cyclin-dependent kinase 1/cyclin B. *J Biol Chem.*, 278: 51372-51379.

Astrinidis, A., Henske, E. P. (2005) Regulation of cell growth and differentiation by the TSC gene. *Oncogene*, 24: 7475-7481.

Astrinidis, A., Senapedis, W., Henske, E. P. (2006) Hamartin, the tuberous sclerosis complex 1 gene product, interacts with polo-like kinase-1 in a phosphorylation-dependent manner. *Hum Mol Genet.*, 15: 287- 297.

Bateman, A., Sandford, R. (1999) The PLAT domain: a new piece in the *PKD1* puzzle. *Curr Biol.*, 9: 588-590.

Bateman, J. F., Chan, D., Moeller, I., Hannagan, M., Cole, W. G. (1994) A 5' splice site mutation affecting the pre-mRNA splicing of two upstream exons in the collagen COL1A1 gene: Exon 8 skipping and altered definition of exon 7 generates truncated procollagen chains with a non-collagenous insertion destabilizing the triple helix. *Biochem J.*, 302: 729-735.

Battle, T. E., Frank, D. A. (2002) The role of STATs in apoptosis. *Curr Mol Med.*, 2: 381-392.

Battini, L., Fedorova, E., Macip, S., Li, X., Wilson, P. D., Gusella, G. L. (2006) Stable knockdown of polycystin 1 confers integrin- $\alpha 2\beta 1$ -mediated anoikis resistance. *Am J Soc Nephrol.*, 17: 3049-3058.

Beall, S., Delaney, P. (1983) Tuberous sclerosis with intracranial aneurysm. *Arch Neurol.*, 40: 826-827.

Belibi, F., Zafar, I., Ravichandran, K., Bauer Segvic, A., Jani, A., Ljubanovic, D. G., Edelstein, C. L. (2011) Hypoxia-inducible factor 1a (HIF1a) and autophagy in polycystic kidney disease (PKD). *Am J Physiol Renal Physiol.*, 300: 235-243.

Bender, B. L. and Yunis, E. J. (1981) Splenic involvement in tuberous sclerosis. *Pathol Anat.*, 391: 363-369.

Bénit, P., Bonnefont, J. P., Kara Mostefa, A., Francannet, C., Munnich, A., Ray, P. F. (2001) Denaturing high-performance liquid chromatography (DHPLC)-based prenatal diagnosis for tuberous sclerosis. *Prenat Diagn.*, 21: 279-283.

Benvenuto, G., Li, S., Brown, S. J., Braverman, R., Vass, W. C., Cheadle, J. P., Halley, D. J., Sampson, J. R., Wienecke, R., DeClue, J. E. (2000) The tuberous sclerosis-1 (TSC1) gene product hamartin suppresses cell growth and augments the

expression of the TSC2 product tuberlin by inhibiting its ubiquination. *Oncogene*, 19: 6306-6316.

Berg, H. (1913) Vererbung der tuberosen sklerose durch zwei bzw. Drei generationen. *Z Ges Neurol Psychiatri.*, 19: 528-539.

Bernstein, J. and Robbins, T. O. (1991) Renal involvement in tuberous sclerosis. *Ann New York Acad Sci.*, 615: 36-49.

Bhattacharya, S., Ray, R. M., Johnson, L. R. (2005) STAT3-mediated transcription of Bcl-2, Mcl-1 and c-IAP2 prevents apoptosis in polyamine-depleted cells. *Biochem J.*, 392: 335-344.

Bhunja, A. K., Piontek, K., Boletta, A., Liu, L., Qian, F., Xu, P. N., Germino, F. J., Germino, G. G. (2002) *PKD1* induces p21<sup>waf1</sup> and regulation of the cell cycle via direct activation of the JAK-STAT signalling pathway in a process requiring *PKD2*. *Cell*, 109: 157-168.

Bisgrove, B. W., Yost, H. J. (2006) The roles of cilia in developmental disorders and disease. *Development*, 133: 4131-4143.

Bissler, J. J. and Kingswood, J. C. (2004) Renal angiomyolipomata. *Kidney Int.*, 66: 924-934.

Bissler, J. J., McCormack, F. X., Young, L. R., Elwing, J. M., Chuck, G., Leonard, J. M., Schmithorst, V. J., Laor, T., Brody, A. S., Bean, J., *et al.* (2008) Sirolimus for angiomyolipoma in tuberous sclerosis complex or lymphangioleiomyomatosis. *N Eng J Med.*, 358:140-151.

Bjornsson, J., Short, M., Kwiatkowski, D. J., Henske, E. P. (1996) Tuberous sclerosis-associated renal cell carcinoma. *Am J Pathol.*, 149: 1201-1208.

Blancquaert, S., Wang, L., Paternot, S., Coulonval, K., Dumont, J. E., Harris, T. E., Roger, P. P. (2010) cAMP dependent activation of mammalian target of rapamycin in thyroid cells. Implications in mitogenesis and activation of CDK4. *Mol Endocrine*, 24: 1453-1468.

Boccaccio, C., Ando, M., Tamagnone, L. (1998) Induction of epithelial tubules by growth factor HGF depends on the STAT pathway. *Nature*, 391: 285-288.

Boletta, A., Germino, G. G. (2003) Role of polycystins in renal tubulogenesis. *Trends Cell Biol.*, 13: 484-492.

Boletta, A. (2009) Emerging evidence of a link between the polycystins and the mTOR pathways. *Pathogenet.*, 2: 1-16.

Bonnet, C. S., Aldred, M., von Ruhland, C., Harris, R., Sandford, R., Cheadle, J. P. (2009) Defects in cell polarity underlie TSC and ADPKD associated cystogenesis. *Hum Mol Genet.*, 18: 2166-2176.

Bonni, A., Sun, Y., Nadal-Vicens, M. (1998) Regulation of gliogenesis in the central nervous system by the JAK-STAT signalling pathway. *Science*, 276: 477-483.

Bose, S., Chandran, S., Mirocha, J. M., Bose, N. (2006) The Akt pathway in human breast cancer: A tissue array based analysis. *Mod Pathol.*, 19: 238-245.

Boulter, C., Mulroy, S., Webb, S., Fleming, S., Brindle, K., Sandford, R. (2001) Cardiovascular, skeletal and renal defects in mice with a targeted disruption of the *Pkd1* gene. *Proc Nat Acad Sci USA*, 98: 12174-12179.

Bourneville, D. M. (1880) Sclérose tubéreuse des circonvolutions cérébrales: idiotie et épilepsie hémiplégique. *Arch Neurol.* (Paris), 1: 81-91.

Bowman, T., Garcia, R., Turkson, J., Jove, R. (2000) STATs in oncogenesis. *Oncogene*, 19: 2472-2488.



Bowman, T., Broome, M. A., Sinibaldi, D., Wharton, W., Pledger, W. J., Sedivy, J. M., Irby, R., Yeatman, T., Courtneidge, S. A., Jove, R. (2001) Stat3-mediated Myc expression is required for Src transformation and PDGF-induced mitogenesis. *Proc Nat Acad Sci USA.*, 98: 7319-7324.

Brasier, J. L., Henske, E. P. (1997) Loss of the polycystic kidney disease (*PKD1*) region of chromosome 16p13 in renal cyst cells supports a loss of functional model for cyst pathogenesis. *J Clin Invest.*, 99: 194-199.

Braun, W. E. (2009) Autosomal dominant polycystin kidney disease: emerging concepts of pathogenesis and new treatments. *Clev Clin J Med.*, 76:97-104.

Brill, A., Torchinsky, A., Carp, H., Toder, V. (1999) *J Ass Reprod Genet.*, 16: 512-519.

Brook-Carter, P. T., Peral, B., Ward, C. J., Thompson, P., Hughes, J., Maheshwar, M. M., Nellist, M., Gamble, V., Harris, P. C., Sampson, J. R. (1994) Deletion of the *TSC2* and *PKD1* genes associated with severe infantile polycystic kidney disease – a contiguous gene syndrome. *Nat Genet.*, 8: 328-332.

Brown, N. E., Murcia, N. S. (2003) Delayed cystogenesis and increased ciliogenesis associated with the re-expression of polaris in *Tg737* mutant mice. *Kid Int.*, 63: 1220-1229.

Buckle, V. J., Higgs, D. R., Wilkie, A. O., Super, M., Weatherall, D. J. (1988) Localisation of human alpha globin to 16p13.3-pter. *J Med Genet.*, 25: 847-849.

Buettner, R., Mora, L. B., Jove, R. (2002) Activated STAT signalling in human tumours provides novel molecular targets for therapeutic intervention. *Clin Cancer Res.*, 8: 945-954.

Cai, S., Everitt, J. I., Kugo, H., Cook, J., Kleymenova, E., Walker, C. L. (2003) Polycystic kidney disease as a result of loss of the tuberous sclerosis 2 tumour suppressor gene during development. *Am J Pathol.*, 162: 457-468.

Cai, Y., Maeda, Y., Cedzich, A., Torres, V. E., Wu, G., Hayashi, T., Mochizuki, T., Park, J. H., Witzgall, R., Somlo, S. (1999) Identification and characterisation of polycystin-2, the *PKD2* gene product. *J Biol Chem.*, 274: 28557-28565.

Caló, V., Migliavacca, M., Bazan, V., Macaluso, M., Buscemi, M., Gebbia, N., Russo, A. (2003) STAT proteins: from normal control of cellular events to tumourigenesis. *J Cell Physiol.*, 197: 157-168.

Cantley, L. C., Neel, B. G. (1999) New insights into tumour suppression: PTEN suppresses tumour formation by restraining the phosphoinositide 3-kinase/ Akt pathway. *Proc Nat Acad Sci USA.*, 8: 4240-4245.

Carbonara, C., Longa, L., Grosso, E., Borrone, C., Garre, M., Brisigotti, M., Migone, N. (1994) 9q34 loss of heterozygosity in a tuberous sclerosis astrocytoma suggests a growth suppressor-like activity also for the *TSC1* gene. *Hum Mol Genet.*, 3: 1829-1832.

Carmody, E., Yeung, E., McLoughlin, M. (1994) Angiomyolipomas of the liver in tuberous sclerosis. *Abdo Imag.*, 19: 537-539.

Casper, K. A., Donnelly, L. F., Chen, B., Bissler, J. J. (2002) Tuberous sclerosis complex: renal imaging findings. *Radiology*, 225: 451-456.

Casteels, I. (2010) Retinal findings in Tuberous sclerosis syndrome. *Bull Soc Belge Ophthalmol.*, 314: 55-56.

Chang, M. Y., Parker, E., Ibrahim, S., Sandford, J. R., Nahas, M. E., Haylor, J. L., Ong, A. C. M. (2006) Haploinsufficiency of *Pkd2* is associated with increased tubular cell proliferation and interstitial fibrosis in two murine *Pkd2* models. *Nephrol Dial Transplant*, 21: 2078-2084.

Chapman, A. B., Johnson, A., Gabow, P. A., Schrier, R. W. (1990) The rennin-angiotensin-aldosterone system and autosomal dominant polycystic kidney disease. *N Engl J Med.*, 323: 1091-1096.

Chauvet, V., Tian, X., Husson, H., Grimm, D. H., Wang, T., Hiesberger, T., Igarashi, P., Bennett, A. M., Ibraghimov-Beskrovnaya, O., Somlo, S. (2004) Mechanical stimuli induce cleavage and nuclear translocation of the polycystin-1 C terminus. *J Clin Invest.*, 114: 1433-1443.

Cheadle, J. R., Reeve, M. P., Sampson, J. R., Kwiatkowski, D. J. (2000) Molecular genetic advances in tuberous sclerosis. *Hum Genet.*, 107: 97-114.

Cheah, P. L., Looi, L. M. (2001) p53: an overview of over two decades of study. *Malays J Pathol.*, 23: 9-16.

Chen, C-H., Shaikenov, T., Peterson, T. R., Aimbetov, R., Bissenbaev, A. K., Lee, S-W., Wu, J., Lin, H-K., Sarbassov, D. D. (2011) ER stress inhibits mTORC2 and Akt signalling through GSK-3 $\beta$  mediated phosphorylation of Rictor. *Sci Signal.*, 4: ra10.

Choi, Y. J., Di Nardo, A., Kramvis, I., Meikle, L., Kwiatkowski, D. J., Sahin, M., He, X. (2008) Tuberous sclerosis complex proteins control axon formation. *Genes Dev.*, 22: 2485-2495.

Chung, J., Uchida, E., Grammer, T. C., Blenis, J. (1997) STAT3 serine phosphorylation by ERK-dependent and -independent pathways negatively modulates its tyrosine phosphorylation. *Mol Cell Biol.*, 17: 6508-16.

Ciruna, B., Jenny, A., Lee, D. (2006) Planar cell polarity signalling couples cell division and morphogenesis during neurulation. *Nature*, 439: 220-224.

Cohen, H. T. and McGovern, F. J. (2005) Renal-cell carcinoma. *New Eng J Med.*, 353: 2477-2490.

Constantinescu, S. N., Girardot, M., Pecquet, C. (2007) Mining for JAK-STAT mutations in cancer. *TIBS.*, 33: 122-131.

Cook, J. A., Oliver, K., Mueller, R. F., Sampson, J. R. (1996) A cross sectional study of renal involvement in tuberous sclerosis. *J Med Genet.*, 33: 480-484.

Capon, F., Allen, M. H., Ameen, M., Burden, A. D., Tillman, D., Barker, J. N., Trembath, R. C. (2004) A synonymous SNP of the corneodesmosin gene leads to increased mRNA stability and demonstrates association with psoriasis across diverse ethnic groups.

Corbit, K. C., Shyer, A. E., Dowdle, W. E., Gaulden, J., Singla, V., Chen, M., Chaung, P. T., Reiter, J. F. (2008) Kif3a constrains beta-catenin-dependent Wnt signalling through dual ciliary and non-ciliary mechanisms. *Nat Cell Biol.*, 10: 70-76.

Creagh, E. M., Conroy, H., Martin, S. J. (2003) Caspase activation pathways in apoptosis and immunity. *Immuno Rev.*, 193: 10-21.

Dabora, S. L., Jowiak, S., Franz, D. N., Roberts, P. S., Nieto, A., Chung, J., Choy, Y., Reeve, M. P., Thiele, E., Egelhoff, J. C., *et al.* (2001) Mutational analysis in a cohort of 224 tuberous sclerosis patients indicates increased severity of *TSC2*, compared with *TSC1*, disease in multiple organs. *Am J Hum Genet.*, 68: 64-80.

Dabora, S. L., Roberts, P., Nieto, A., (2002) Association between a high-expressing interferon- $\gamma$  allele and a lower frequency of kidney angiomyolipomas in *TSC2* patients. *Am J Hum Genet.*, 71: 750-758.

D'Agata, I. D., Jonas, M. M., Perez-Atayde, A. R., Guay-Woodford, L. M. (1994) Combined cystic disease of the liver and kidney. *Semin Liver Dis.*, 14: 215-228.

Dalgaard, O. Z. (1957) Bilateral polycystic disease of the kidneys; a follow up of two hundred and eighty four patients and their families. *Acta Med Scand Suppl.*, 328: 1-255.

Daoust, M. C., Reynolds, D. M., Bichet, D. G., Somlo, S. (1995) Evidence for a third genetic locus for autosomal dominant polycystic kidney disease. *Genomics*, 25: 733-736.

Davies, M. D., Johnson, S. R., Tattersfield, A. E., Kingswood, J. C., Cox, J. A., McCartney, D. L., Doyle, T., Elmslie, F., Saggar, A., de Vries, P. J., Sampson, J. R. (2008) Sirolimus therapy in tuberous sclerosis or sporadic lymphangioleiomyomatosis. *N Eng J Med.*, 358: 200-203.

Davies, M. D., Sampson, J. R. (2010) Small-molecule signal transduction inhibitors: targeted therapeutic agents for single-gene disorders. *J Med Genet.*, 47: 145-149.

De Almeida, S., de Almedia, E., Peters, D., Pinto, J. R., Tavora, I., Lavinha, J., Breuning, M., Prata, M. M. (1995) Autosomal dominant polycystic kidney disease: evidence for the existence of a third locus in a Portuguese family. *Hum Genet.*, 96: 83-88.

Deane, J. A., Ricardo, S. D. (2007) Polycystic kidney disease and the renal cilium. *Nephrol.*, 12: 559-564.

Delmas, P., Normura, H., Li, X., Lakkis, M., Luo, Y., Segal, Y., Fernandez-Fernandez, J. M., Harris, P., Frischauf, A. M., Brown, D. A., Zhou, J. (2002) Constitutive activation of G-proteins by polycystin-1 is antagonized by polycystin-2. *J Biol Chem.*, 277: 11276-11283.

Delmas, P., Padilla, F., Osorio, N., Coste, B., Raoux, M., Crest, M. (2004) Polycystins, calcium signalling and human diseases. *Biochem Biophys Res Commun.*, 322: 1374-1383.

Deisseroth, A., Hendrick, D. (1977) Human alpha-globin gene expression following chromosomal dependant gene transfer into mouse erythroleukemia cells. *Cell*, 15: 55-63.

Dickerson, W. W. (1951) Familial occurrence of tuberous sclerosis. *Arch Neurol Psychiatr.*, 65: 683-702.

Di Cristofano, A., Pesce, B., Cordon-Cardo, C., Pandolfi, P., P. (1998) *Pten* is essential for embryonic development and tumour suppression. *Nat Genet.*, 19: 348-355.

Dijane, A., Yogev, S., Mlodzik, M. (2005) The apical determinants aPKC and dPatj regulate Frizzled-dependant planar cell polarity in the drosophila eye. *Cell*, 121: 621-631.

Distefano, G., Boca, M., Rowe, I., Wodarczyk, C., Ma, L., Piontek, K. B., Germino, G. G., Pandolfi, P. P., Boletta, A. (2009) Polycystin-1 regulates extracellular signal-regulated kinase-dependent phosphorylation of tuberin to control cell size through mTOR and its downstream effectors, S6K and 4EBP1. *Mol Cell Biol.*, 29: 2359-2371.

Dobin, A., Kimberling, W. J., Pettinger, W., Bailey-Wilson, J. E., Shugart, Y. Y., Gabow, P. A. (1993) Segregation analysis of autosomal dominant polycystic kidney disease. *Genet Epidemiol.*, 10: 189-200.

Dusa, A., Staerk, J., Elliott, J., Pecquet, C., Poirel, H. A., Johnston, J. A., Constantinescu, S. N. (2008) Substitution of pseudokinase domain residue Val-617 by large non-polar amino acids causes activation of JAK2. *J Biol Chem.* 283:12941-12948.

Eaton, S., Simons, K. (1995) Apical, basal and lateral cues for epithelial polarisation. *Cell*, 82: 5-8.

Eisenmann, D. M. (2005) Wnt signalling. *Wormbook*. Jun 25: 1-17.

Eker, R. (1954) Familial renal adenomas in Wistar rats. *Acta Pathol Microbiol Scand.*, 34: 554-562.



Eker, R. and Mossige, J. (1961) A dominant gene for renal adenomas in the rat. *Nature*, 189: 858-859.

Eker, R., Mossige, J., Johannessen, J. V., Aars, H. (1981) Hereditary renal adenomas and adenocarcinomas in rats. *Diagn. Histopathol.*, 4: 99-110.

Eley, L., Yates, L. M., Goodship, J. A. (2005) Cilia and disease. *Curr Opin Genet Dev.*, 15: 308-314.

El-Hashemite, N., Zhang, H., Walker, V., Hoffmeister, K. M., Kwiatkowski, D. J. (2004) Perturbed IFN-gamma-Jak-Signal transducers and activators of transcription signalling in tuberous sclerosis mouse models: synergistic effects of rapamycin-IFN-gamma treatment. *Cancer Res.*, 64: 3436-3443.

El-Hashemite, N., Kwiatkowski, D. J. (2005) Interferon- $\gamma$ -Jak-Stat Signaling in Pulmonary Lymphangiomyomatosis and Renal Angiomyolipoma: A Potential Therapeutic Target. *Am J Respir Cell Mol Biol.*, 33: 227-230.

Elzinga, L. W., Barry, J. M., Torres, V. E. (1992) Cyst decompression surgery for autosomal dominant polycystic kidney disease. *J Am Soc Nephrol.*, 2: 1219-1226.

Elzinga, L. W., Bennett, W. M. (1996) Miscellaneous renal and systemic complications of autosomal dominant polycystic kidney disease including infection. In: Watson, M. L., Torres, V. E. (eds.) Polycystic kidney disease. Oxford: Oxford Medical Publications, pp483-499.

Endo, T. A., Masuhara, M., Yokouchi, M., Suzuki, R., Sakamoto, H., Mitsui, K., Matsumoto, A., Tanimura, S., Ohtsubo, M., Misawa, H., Miyazaki, T., Leonor, N., Taniguchi, T., Fujita, T., Kanakura, Y., Komiyama, S., Yoshimura, A. (1997) A new protein containing an SH2 domain that inhibits JAK kinases, *Nature* 387: 921-924.

Engelman, J. A., Chen, L., Tan, X., Crosby, K., Guimaraes, A. R., Upadhyay, R., Maira, M., McNamara, K., Perera, S. A., Song, Y., Chirieac, L. R., Kaur, R., Lightbown, A., Simendinger, J., Li, T., Padera, R. F., García-Echeverría, C.,

Weissleder, R., Mahmood, U., Cantley, L. C., Wong, K. K. (2008) Effective use of PI3K and MEK inhibitors to treat mutant Kras G12D and PIK3CA H1047R murine lung cancers. *Nat Med.*, 14: 1351-1356.

Entius, M. M., Keller, J. J., Westerman, A. M., van Rees, B. P., van Velthuysen, M. L., de Goeij, A. F., Wilson, J. H., Giardiello, F. M., Offerhaus, G. J. (2001) Molecular genetic alterations in hamartomatous polyps and carcinomas of patients with Peutz-Jeghers syndrome. *J Clin Pathol.*, 54: 126-131.

European Chromosome 16 Tuberous Sclerosis Consortium (1993) Identification and characterisation of the tuberous sclerosis gene on chromosome 16. *Cell*, 75: 1305-1315.

European Chromosome 16 Tuberous Sclerosis Consortium (1994) The polycystic kidney disease 1 gene encodes a 14kb transcript and lies within a duplicated region on chromosome 16. *Cell*, 77: 881-894.

European Polycystic Kidney Disease Consortium (1994) The polycystic kidney disease 1 gene encodes a 14kb transcript and lies within a duplicated region on chromosome 16. *Cell*, 77: 881-894.

Everitt, J. I., Goldsworthy, T. L., Wolf, D. C., Walker, C. L. (1992) Hereditary renal cell carcinoma in the Eker rat: a rodent familial cancer syndrome. *J Urol.*, 148: 1932-1936.

Everitt, J. I., Goldsworthy, T. L., Wolf, D. C., Walker, C. L. (1995) Hereditary renal cell carcinoma in the Eker rat: a unique model for the study of cancer susceptibility. *Toxicol Let.*, 82: 621-625.

Everson, G. T. (1990) Hepatic cysts in ADPKD. *Mayo Clin Proc.*, 65: 1020-1025.

Everson, G. T. (1990) Functional similarities of hepatic and biliary epithelium: studies of fluid constituents and *in vivo* secretion in response to secretin. *Hepatology*, 11: 557-565.

Everson, G. T. (1993) Hepatic cysts in autosomal dominant polycystic kidney disease. *Am J Kidney Dis.*, 22: 520-525.

Everson, G. T., Taylor, M. R. G., Doctor, B. R. (2004) Polycystic disease of the liver. *Hepatology*, 40: 774-782.

Ewalt, D. H., Sheffield, E., Sparagana, S. P., Delgado, M. R., Roach, E. S. (1998) Renal lesion growth in children with tuberous sclerosis complex. *J Urol.*, 160: 141-145.

Faderl, S., Ferrajoli, A., Harris, D., Van, Q., Kantarjian, H. M., Estrov, Z. (2007) Atiprimod blocks phosphorylation of JAK-STAT and inhibits proliferation of acute myeloid leukemia (AML) cells. *Leuk Res.*, 31: 91-95.

Feng, J., Witthuhn, B. A., Matsuda, T., Kohlhuber, F., Kerr, I. M., Ihle, J. (1997) Activation of JAK2 catalytic activity requires phosphorylation of Y1007 in the kinase activation loop. *Mol Cell Biol.*, 17: 2497-2501.

Feng, Z., Zhang, H., Levine, A. J., Jin, S. (2005) The coordinate regulation of the p53 and mTOR pathways in cells. *Proc Nat Acad Sci USA.*, 102: 8204-8209.

Feng, Z., Hu, W., Stanchina, E., Teresky, A. K., Jin, S., Lowe, S., Levine, A. J. (2007) The regulation of AMPK  $\beta$ 1, TSC2 and PTEN expression by p53: Stress, Cell and Tissue specificity and the role of these gene products in modulating the IGF-1-AKT-mTOR pathways. *Cancer Res.*, 67: 3043-3053.

Fischer, E., Legue, E., Doyen, A., Nato, F., Nicolas, J. F., Torres, V., Yaniv, M., Pontoglio, M. (2006) Defective planar cell polarity in polycystic kidney disease. *Nat Genet.*, 38: 21-23.

Fliegauf, M., Benzing, T., Omran, T. (2007) When cilia go bad: cilia defects and ciliopathies. *Nat Rev Mol Cell Biol.*, 8: 880-893.

Foggensteiner, L., Bevan, A. P., Thomas, R., Coleman, N., Boulter, C., Bradley, J., Ibraghimov-Beskrovnaya, O., Klinger, K., Sandford, R. (2000) Cellular and subcellular distribution of polycystin-2, the protein product of the *PKD2* gene. *J Am Soc Nephrol.*, 11: 814-827.

Franz, D. N., Leonard, J., Tudor, C., Chuck, G., Care, M., Sethuraman, G., Dinopoulos, A., Thomas, G., Crone, K. R. (2006) Rapamycin causes regression of astrocytomas in tuberous sclerosis complex. *Ann Neurol.*, 59: 490-498.

Fricke, B. L., Donnelly, L. F., Casper, K. A., Bissler, J. J. (2004) Frequency and imaging appearance of hepatic angiomyolipomas in paediatric and adult patients with tuberous sclerosis. *Am J Roent.*, 182: 1027-1030.

Frisch, S. M., Francis, H., (1994) Disruption of epithelial cell matrix interactions induces apoptosis. *J Cell Biol.*, 124: 619-626

Frisch, S. M., Vuori, K., Kelaita, D., Sicks, S. (1996) A role for Jun-N-terminal kinase in anoikis; suppression by bcl-2 and crmA. *J Cell Biol.*, 135: 1377-1382.

Frisch, S. M., Ruoslahti, E. (1997) Integrins and anoikis. *Curr Opin Cell Biol.*, 9: 701-706.

Frisch, S. M. (1999) Evidence for a function of death receptor related, death domain containing proteins in anoikis. *Curr Biol.*, 9: 1047-1049.

Fryer, A. E., Chalmers, A. H., Connor, J. M., Fraser, I., Povey, S., Yates, A. D., Yates, J. R., Osborne, J. P. (1987) Evidence that the gene for tuberous sclerosis is on chromosome 9. *Lancet*, 1: 659-661.

Fujiwara, S., Takaki, T., Hikita, T., Nishio, S. (1989) Sub-ependymal giant cell astrocytoma associated with tuberous sclerosis: do sub-ependymal nodules grow? *Childs Nerv Syst.*, 5: 43-44.

- Fukuda, T., Kobayashi, T., Momose, S., Yasui, H., Hino, O. (2000) Distribution of Tsc1 protein detected by immunohistochemistry in various normal rat tissues and the renal carcinomas of Eker rat: detection of limited colocalisation with Tsc1 and Tsc2 gene products in vivo. *Lab Invest.*, 80: 1347-1357.
- Fulda, S., Debatin, K-M. (2006) Intrinsic versus extrinsic apoptosis pathways in anticancer chemotherapy. *Oncogene*, 25: 4798-4811.
- Gabow, P. A., Johnson, A. M., Kaehny, W. D., Manco-Johnson, M. L., Duley, I. T., Everson, G. T. (1990) Risk factors for the development of hepatic cysts in autosomal dominant polycystic kidney disease. *Hepatology*, 11: 1033-1037.
- Gabow, P. A., Chapman, A. B., Johnson, A. M. (1990) Renal structure and hypertension in autosomal dominant polycystic kidney disease. *Kidney Int.*, 38: 117-1180.
- Gabow, P. A. (1991) Polycystic kidney disease: clues to pathogenesis. *Kidney Int.*, 40: 989-996.
- Gabow, P. A., Johnson, A. M., Kaehny, W. D., Kimberling, W. J., Lezotte, D. C., Duley, I. T., Jones, R. H. (1992) Factors affecting the progression of renal cystic disease in autosomal dominant polycystic kidney disease. *Kidney Int.*, 41: 1311-1319.
- Gabow, P. A. (1993) Autosomal dominant polycystic kidney disease. *N Engl J Med.*, 329: 332-342.
- Galant, J., Marti-Bonmati, L., Ripollés, T., Martinez-Rodrigo, J., Ferrer, M. D. (1995) Hepatic manifestations of tuberous sclerosis studied by US and CT. *Eur Radiol.*, 5: 486-491.
- Gallagher, A. R., Germino, G. G., Somlo, S. (2010) Molecular advances in autosomal dominant polycystic kidney disease. *Adv Chronic Kidney Dis.*, 17: 118-130.

Gao, X. and Pan, D. (2001) *TSC1* and *TSC2* tumour suppressors antagonise insulin signalling in cell growth. *Genes Dev.*, 15: 1383-1392.

Gao, X., Zhang, Y., Arrazola, P., Hino, O., Kobayashi, T., Yeung, R. S., Ru, B., Pan, D. (2002) Tsc tumour suppressor proteins antagonise amino acid TOR signalling. *Nat Cell Biol.*, 9: 699-704.

Garcia-Gonzalez, M. A., Jones, J. G., Allen, S. K. (2007) Evaluating the clinical utility of a molecular genetic test for polycystic kidney disease. *Mol Genet Metab.*, 92: 160-167.

Gartsbein, M., Alt, A., Hashimoto, K., Nakajima, K., Kuroki, T., Tennebaum, T. (2006) The role of protein kinase C; activation and STAT3 Ser727 phosphorylation in insulin-induced keratinocyte proliferation. *J Cell Sci.*, 119: 470-481.

Gatsios, P., Terstegen, L., Schliess, F., Haussinger, D., Kerr, I. M. Heinrich, P. C., Graeve, L. (1998) Activation of the Janus Kinase / Signal Transducer and activator of transcription pathway by osmotic shock. *J Biol Chem.*, 273: 33962-22968.

Geist, R. T., Gutmann, D. H. (1995) The tuberous sclerosis 2 gene is expressed at high levels in the cerebellum and developing spinal cord. *Cell Growth Differ.*, 6: 1477-1483.

Geng, L., Segal, Y., Pavolva, A., Barros, E. J., Lohning, C., Lu, W., Nigam, S. K., Frischauf, A. M., Reeders, S. T., Zhou, J. (1997) Distribution and developmentally regulated expression of murine polycystin. *Am J Physiol.*, 272: 451-459.

Geng, L., Okuhara, D., Yu, Z., Tian, X., Cai, Y., Shibasaki, S., Somlo, S. (2006) Polycystin-2 trafficks to cilia independently of polycystin-1 by using an N-terminal RVxP motif. *J Cell Sci.*, 119: 1383-1395.

Gerard, G. and Weisberg, L. (1987) Tuberous sclerosis: CT findings and differential diagnosis. *Comp Radiol.*, 11: 189-192.



Germino, G. G. (2005) Linking cilia to Wnts. *Nat Genet.*, 37: 455-457.

Gilmore, A. P. (2005) Anoikis. *Cell Death Diff.*, 12: 1473-1477.

Gingras, A. C., Raught, B., Gygi, S. P., Niedzwiecka, A., Miron, M., Burley, S. K., Polakiewicz, R. D., Wyslouch-Cieszyńska, A., Aebersold, R., Sonenberg, N. (2001) Hierarchical phosphorylation of the translation inhibitor 4E-BP1. *Genes Dev.*, 15: 2852-2864.

Gomez, M. R. (1979) *Tuberous sclerosis, First Edition*. Raven Press, Ltd., New York.

Gomez, M. R. (1988) *Tuberous sclerosis, Second Edition*. Raven Press, Ltd., New York.

Gomez, M. R., Sampson, J. R., Whittemore, V. H. (1999) *The tuberous sclerosis complex*. Oxford University Press, Oxford, UK.

Goncharova, E., Goncharov, D., Noonan, D., Krymskaya, V. P. (2004) TSC2 modulates actin cytoskeleton and focal adhesion through TSC1-binding domain and the Rac1 GTPase. *J Cell Biol.*, 167: 1171-1182.

Goorden, S. M., van Woerden, G. M., van der Weerd, L., Cheadle, J. P., Elgersma, Y. (2007) Cognitive defects in Tsc1<sup>+/-</sup> mice in the absence of cerebral lesions and seizures. *Ann Neurol.*, 62: 648-655.

Gould, S. R. (1991) Hamartomatous rectal polyps are common in tuberous sclerosis. *Ann N Y Acad Sci.*, 615: 71-80.

Grantham, J. J. (2003) Polycystic kidney disease. *Sci Med.*, 9: 128-139.

Grantham, J. J., Torres, V. E., Chapman, A. B. (2006) Volume progression in polycystic kidney disease. *N Engl J Med.*, 354: 2122-2130.

Green, A. J., Smith, M., Yates, J. (1994) Loss of heterozygosity on chromosome 16p13.3 in hamartomas from tuberous sclerosis patients. *Nature Genet.*, 6: 193-196.

Green, D. R. (2005) Apoptotic pathways: Ten minutes to dead. *Cell*, 121: 671-674.

Gu, Y., Zuo, Y., Aikawa, R. (2001) Growth hormone signalling and apoptosis in neonatal rat cardiomyocytes. *Mol Cell Biochem.*, 223: 35-46.

Guay-Woodford, L. M. (2003) Murine models of polycystic kidney disease: molecular and therapeutic insights. *Am J Physiol Renal Physiol.*, 285: 1034-1049.

Gunther, M., Penrose, L. S. (1935) The genetics of epiloia. *J Genet.*, 31: 413-430.

Habib, S. L., Simone, S., Barnes, J. J., Abboud, H. E. (2008) Tuberin haploinsufficiency is associated with the loss of OGG1 in rat kidney tumors. *Mol Cancer*, 7: 10.

Haddad, L. A., Smith, N., Bowser, M., Niida, Y., Murthy, V., Gonzalez-Agosti, C., Ramesh, V. (2002) The *TSC1* tumour suppressor hamartin interacts with neurofilament-L and possibly functions as a novel integrator of the neuronal cytoskeleton. *J Biol Chem.*, 277: 44180-44186.

Haines, J. L., Short, M. P., Kwiatkowski, D. J., Jewell, A., Andermann, E., Bejjani, B., Yang, C., Guselle, J. F., Amos, J. A. (1991) Localisation of one gene for tuberous sclerosis within 9q32-9q34, and further evidence for heterogeneity. *Am J Hum Genet.*, 49: 764-772.

Han, S., Santos, T. M., Puga, A., Roy, J., Thiele, E. A., MacCollin, M., Stemmer-Rachamimov, A., Ramesh, V. (2004) Phosphorylation of tuberin as a novel mechanism for somatic inactivation of the tuberous sclerosis complex proteins in brain lesions. *Cancer Res.*, 64: 812-816.

Han, S., Polizzano, C., Nielsen, G. P., Hornicek, F. J., Rosenberg, A. E., Ramesh, V. (2009) Aberrant hyperactivation of Akt and Mammalian target of rapamycin complex 1 in sporadic chordomas. *Clin Cancer Res.*, 15: 1940-1946.

Hanaoka, K., Qian, F., Boletta, A., Bhunia, A. K., Piontek, K., Tsiokas, L., Sukhatme, V. P., Guggino, W. B., Germino, G. G. (2000) Co-assembly of polycystin-1 and polycystin-2 produces unique cation-permeable currents. *Nature*, 408: 990-994.

Harpur AG, Andres AC, Ziemiecki A, Aston RR, Wilks AF. JAK2, a third member of the JAK family of protein tyrosine kinases. *Oncogene*. 1992 Jul;7(7):1347-53.

Harrington, L. S., Findlay, G. M., Gray, A., Tolkacheva, T., Wigfield, S., Rebholz, H., Barnet, J., Leslie, N. R., Cheng, S., Shepherd, P. R. (2004) The TSC1-2 tumour suppressor controls insulin-PI3K signalling via regulation of IRS proteins. *J Cell Biol.*, 166: 213-223.

Harris, P. C., Bae, K., Rossetti, S., Torres, V. E., Grantham, J. J., Chapman, A., Guay-Woodford, L., King, B. F., Wetzel, L. H., Baumgarten, D., Kenney, P. J., Consugar, M., Klahr, S., Bennett, W. M., Meyers, C. M., Zhang, Q., Thompson, P. A., Zhu, F., Miller, J. P. (2006) Cyst number but not the rate of cyst growth is associated with the mutated gene in ADPKD. *J Am Soc Nephrol.*, 17: 3013-3019.

Harris, P. C., Kyongtae, T., Bae, K. T., Rossetti, S. (2007) Cyst number but not the rate of cystic growth is associated with the mutated gene in autosomal dominant polycystic kidney disease. *J Am Soc Nephrol.*, 17: 3013-2019.

Hartman, T. R., Nicolas, E., Klein-Szanto, A., Al-Saleem, T., Cash, T. P., Simon, M. C., Henske, E. P. (2009) The role of the Birt-Hogg-Dubé protein in mTOR activation and renal tumourigenesis. *Oncogene*, 28: 1594-1604.

Hartman, T. R., Liu, D., Zilfou, J. T., Robb, V., Morrison, T., Watnick, T., Henske, E. P. (2009) The tuberous sclerosis proteins regulate formation of the primary cilium via a rapamycin-insensitive and polycystin-1 independent pathway. *Hum Mol Genet.*, 18: 151-163.

Hateboer, N., van Dijk, M. A., Bogdanova, N., Coto, E., Saggar-Malik, A. K., San Millan, J. T., Torra, R., Breuning, M., Ravine, D. (1999) Comparison of phenotypes of polycystic kidney disease types 1 and 2. *Lancet*, 353: 103-107.

Heitman, J., Movva, N. R., Hall, M. N. (1991) Targets for cell cycle arrest by the immunosuppressive drug rapamycin in yeast. *Science*, 253: 905-909.

Henske, E. P., Scheithauer, B. W., Short, W. P., Wollman, R., Nahmias, J., Hornigold, N., van Slegtenhorst, M., Welsh, C. T., Kwiatkowski, D. J. (1996) Allelic loss is frequent in tuberous sclerosis kidney lesions but rare in brain lesions. *Am J Hum Genet.*, 59: 400-406.

Henske, E. P. (2005) Tuberous Sclerosis and the kidney: from mesenchyme to epithelium, and beyond. *Pediatr Nephrol.*, 20: 854-857.

Hernandez, O., Way, S., McKenna, J., Gambello, M. J. (2007) Generation of a conditional disruption of the *Tsc2* gene. *Genesis*, 45: 101-106.

Hildebrandt, F., Otto, E. (2005) Cilia and centrosomes: a unifying pathogenic concept for cystic kidney disease? *Nat Genet.*, 6: 928-940.

Hilton, D. J., Richardson, R. T., Alexander, W. S., Viney, E. M., Willson, T. A., Sprigg, N. S., Starr, R., Nicholson, S. E., Metcalf D., Nicola, N. A. (1998) Twenty proteins containing a C-terminal SOCS box form five structural classes, *Proc Nat Acad Sci USA.*, 95: 114–119.

Hino, O., Mitani, H., Sakaurai, J. (2002) "Second hit" of *Tsc2* gene in radiation induced renal tumours of Eker rat model. *Int Cong Series*, 1236: 163-174.

Hino, O., Hino O, Kobayashi T, Mitani H. (2002b) Prevention of hereditary carcinogenesis. *Proc Japan Acad.*, 78: 30–32.

Hite, S. H., Kuo, J. S., Cheng, E. Y. (1998) Axillary aneurysm in tuberous sclerosis: cross-sectional imaging findings. *Pediatr Radiol.*, 28: 554-556.

Hockenberry, D. M. (2003) Nailing down a link between tuberin and renal cysts. *Am J Pathol.*, 162: 369-371.

Hodges, A. K., Li, S., Maynard, J., Parry, L., Braverman, R., Cheadle, J. P., DeClue, J. E., Sampson, J. R. (2001) Pathological mutations in *TSC1* and *TSC2* disrupt the interaction between hamartin and tuberin. *Hum Mol Genet.*, 10: 2899-2905.

Horie, S., Higashihara, E., Nutahara, K., Mikami, Y., Okubo, A., Kano, M., Kawabe, K. (1994) Mediation of renal cyst formation by hepatocyte growth factor. *Lancet*, 344: 789-791.

Horiguchi, A., Asano, T., Kuroda, K., Sato, A., Asakuma, J., Ito, K., Hayakawa, M., Sumitomo, M., Asano, T. (2010) STAT3 inhibitor WP1066 as a novel therapeutic agent for renal cell carcinoma. *B J Cancer*, 102: 1592-1599.

Horvath, C. M. (2000) STAT proteins and transcriptional responses to extracellular events. *TIBS.*, 25: 496-502.

Howe, J. R., Roth, S., Ringold, J. C., Summers, R. W., Jarvinen, H. J., Sistonen, P., Tomlinson, I. P., Houlston, R. S., Bevan, S., Mitros, F. A., Stone, E. M., Aaltonen, L. A. (1998) Mutations in the *SMAD4/DPC4* gene in juvenile polyposis. *Science*, 280: 1086-1088.

Huang, B. Q., Masyuk, T. V., Muff, M. A., Tietz, P. S., Masyuk, A. I., LaRusso, N. F. (2006) Isolation and characterisation of cholangiocyte primary cilia. *Am J Physiol.*, 291: 500-509.

Huang, J., Manning, B. D. (2008) The *TSC1-TSC2* complex: a molecular switchboard controlling cell growth. *Biochem J.*, 412: 179-190.

Hughes, E. and Hodder, R. (1987) Pulmonary lymphangioliomyomatosis complicating pregnancy. A case report. *J Reprod Med.*, 32: 553-557.

Hughes, J., Ward, C. J., Peral, B., Aspinwall, R., Clark, K., San Millan, J. L., Gamble, V., Harris, P. C. (1995) The polycystic kidney disease 1 (*PKD1*) gene encodes a novel protein with multiple cell recognition domains. *Nat Genet.*, 10: 151-160.

Ibraghimov-Beskrovnaya, O., Bukanov, N. O., Donohue, L. C., Dackowski, W., Klinger, K. W., Landes, G. M. (2000) Strong homophilic interactions of the Ig-like domains of polycystin-1, the protein product of an autosomal dominant polycystic kidney disease gene, *PKD1*. *Hum Mol Genet.*, 9: 1641-1649.

Ibrahim, R. E., Weinberg, D. S., Weidner, N. (1989) Atypical cysts and carcinomas of the kidneys in the phacomatoses: a quantitative DNA study using static and flow cytometry. *Cancer*, 63: 148-157.

Igarashi, P. (1994) Transcription factors and apoptosis in kidney development. *Curr Opin Nephrol Hypertens.*, 3: 308-317.

Iglesias, C. G., Torres, V. E., Offord, K. P., Holley, K. E., Beard, C. M., Kurland, L. T. (1983) Epidemiology of adult polycystic kidney disease, Olmsted County, Minnesota. *Am J Kidney Dis.*, 2: 630-639.

Ikeda, M., Guggino, W. B. (2002) Do polycystins function as cation channels? *Curr Opin Nephrol Hypertens.*, 11: 539-545.

Ilgren, E. B. and Westmoreland, D. (1984) Tuberous sclerosis: unusual associations in four cases. *J Clin Pathol.*, 37: 272-278.

Ilic, D., Almedia, E. A. C., Schlaepfer, D. D., Dazin, P., Aizawa, S., Damsky, C. H. (1998) Extracellular matrix survival signals transduced by focal adhesion kinase suppress p53 mediated apoptosis. *J Cell Biol.*, 143: 547-560.

Inoki, K., Li, Y., Zhu, T., Wu, J., Guan, K. L. (2002) TSC2 is phosphorylated and inhibited by Akt and suppresses mTOR signalling. *Nat Cell Biol.*, 4: 648-657.

Inoki, K., Li, Y., Xu, T., Guan, K. L. (2003) Rheb GTPase is a direct target of TSC2 GAP activity and regulates mTOR signalling. *Genes Dev.*, 17: 1829-1834.

Inoki, K., Corradetti, M. N., Guan, K. (2005) Dysregulation of the TSC-mTOR pathway in human disease. *Nature Genet.*, 37: 19-24.

Inoue, H., Uyama, T., Suzuki, T., Kazami, M., Hino, O., Kobayashi, T., Kobayashi, K-I., Tadokoro, T., Yamamoto, Y. (2009) Phosphorylated hamartin-Hsp70 complex regulates apoptosis via mitochondrial localisation. *Biochem biophys Res Comm.*, 391: 1148-1153.

Ito, N. and Rubin, G. M. (1999) *Gigas*, a Drosophila homolog of tuberous sclerosis gene product-2, regulates the cell cycle. *Cell*, 96: 529-539.

Jacinto, E., Loewith, R., Schmidt, A., Lin, S., Ruegg, M. A., Hall, A., Hall, M. N. (2004) Mammalian TOR complex 2 controls the actin cytoskeleton and is rapamycin insensitive. *Nat Cell Biol.*, 6: 1122-1128.

Jain, N., Zhang, T., Kee, W. H., Li, W., Cao, X. (1999) Protein Kinase C  $\delta$  Associates with and Phosphorylates Stat3 in an Interleukin-6-dependent Manner. *J Biol Chem.*, 274: 24392-24400.

Jenny, A., Mlodzik, M. (2006) Planar Cell Polarity Signalling: A common mechanism for cellular polarisation. *M Sinai J Med.*, 73: 738-750.

Jiang, S. T., Chiou, Y. Y., Wang, E., Lin, H. K., Lin, Y. T., Chi, Y. C., Wang, C. K., Tang, M. J., Li, H. (2006) Defining a link with autosomal dominant polycystic kidney disease in mice with congenitally low expression of *Pkd1*. *Am J Pathol.*, 168: 205-220.



Jimenez, R. E., Eble, J. N., Reuter, V. E., Epstein, J. I., Folpe, A. L., Peralta-Venturina, M., Tamboli, P., Ansell, D., Grignon, D. J., Young, R. H., Amin, M. B. (2001) Concurrent angiomyolipoma and renal cell neoplasia: a study of 36 cases. *Mod Pathol.*, 14: 157-163.

Jishage, K., Nezu, J., Kawase, Y., Iwata, T., Watanabe, M., Miyoshi, A., Ose, A., Habu, K., Kake, T., Kamada, N., *et al.* (2002) Role of *Lkb1*, the causative gene of Peutz-Jeghers syndrome, in embryogenesis and polyposis. *Proc Nat Acad Sci USA.*, 99: 8903-8908.

Johnson, M. W., Kerfoot, C., Bushnell, T., Li, M., Vinters, H. V. (2001) Hamartin and tuberin expression in human tissues. *Mod Pathol.*, 14: 202-210.

Jones, A. C., Daniells, C. E., Snell, R. G., Tachataki, M., Idziaszczyk, S. A., Krawczak, M., Sampson, J. R., Cheadle, J. P. (1997) Molecular genetic and phenotypic analysis reveals differences between *TSC1* and *TSC2* associated familial and sporadic tuberous sclerosis. *Hum Mol Genet.*, 6: 2155-2161.

Jones, A. C., Shyamsundar, M. M., Thomas, M. W., Maynard, J., Idziaszczyk, S. A., Tomkins, S., Sampson, J. R., Cheadle, J. P. (1999) Comprehensive mutation analysis of *TSC1* and *TSC2* and phenotypic correlations in 150 families with tuberous sclerosis. *Am J Hum Genet.*, 64: 1305-1315.

Jones, A. C., Sampson, J. R., Cheadle, J. P. (2001) Low level mosaicism detected by DHPLC but not by direct sequencing. *Hum Mutation*, 17: 233-234.

Jonsson, E., Sueoka, B., Spielgel, P. K., Richardson, J. R., Heaney, J. A. (1991) Angiographic management of retroperitoneal haemorrhage from renal angiomyolipoma in polycystic kidney disease. *J Urol.*, 145; 1248-1250.

Jóźwiak, S., Pedich, M., Rajszyk, P., Michalowicz, R. (1992) Incidence of hepatic hamartomas in tuberous sclerosis. *Arch Dis Child.*, 67: 1363-1365.

Józwiak, J., Józwiak, S., Włodarski, P. (2008) Possible mechanisms for disease development in tuberous sclerosis. *Lancet Oncol.*, 9: 73-79.

Juboa, D., Wainwright, M. S., Comeron, J. M., Saitou, N., Sanders, A. R., Gelernter, J., Gejman, P. V. (2003) Synonymous mutations in the human dopamine receptor D2 (DRD2) may affect mRNA stability and synthesis of the receptor. *Hum Mol Genet.*, 12: 205-216.

Kamada, S., Shimono, A., Shinto, Y., Tsujimura, T., Takahashi, T., Noda, T., Kitamura, Y., Kondoh, H., Tsujimoto, Y. (1995) bcl2 deficiency in mice leads to pleiotropic abnormalities: accelerated lymphoid cell death in thymus and spleen, polycystic kidney, hair hypopigmentation, and distorted small intestines. *Cancer Res.*, 55: 354-359.

Kandt, R. S., Haines, J. L., Smith, M., Northrup, H., Gardner, R. J., Short, M. P., Dumars, K., Roach, E. S., Steingold, S., Wall, S., *et al.* (1992) Linkage of an important gene locus for tuberous sclerosis to a chromosome 16 marker for polycystic kidney disease. *Nature Genet.*, 2: 37-41.

Karner, C. M., Chirumamilla, R., Aoki, S., Igarashi, P., Wallingford, J. B., Carroll, T. J. (2009) Wnt9b signalling regulates planar cell polarity and kidney tubule morphogenesis. *Nat Genet.*, 41: 793-799.

Kelleher, C. L., McFann, K. K., Johnson, A. M., Schrier, R. W. (2004) Characteristics of hypertension in young adults with autosomal dominant polycystic kidney disease compared with the general US population. *Am J Hypertens.*, 17: 1029-1034.

Keller, R. (2002) Shaping the vertebrate body plan by polarised embryonic cell movements. *Science*, 298: 1950-1954.

Kenerson, H., Dundon, T. A., Yeung, R. S. (2005) Effects of rapamycin in the Eker rat model of tuberous sclerosis complex. *Pediatr Res.*, 57: 67-75.

Khan, A., Pepio, A. M., Sossin, W. S. (2001) Serotonin activates S6 kinase in a rapamycin-sensitive manner in *Aplysia* synaptosomes. *J Neurosci.*, 21: 382-391.

Kim, E., Arnould, T., Sellin, L. K., Benzing, T., Fan, M. J., Gruning, W., Sokol, S. Y., Drummond, I., Walz, G. (1999) The polycystic kidney disease 1 gene product modulates Wnt signalling. *J Biol Chem.*, 274: 4947-4953.

Kim, H., Kerr, A., Morehouse, H. (1995) The association between tuberous sclerosis and insulinoma. *Am J Neuroradiol.*, 16:1543-1544.

Kim, J.-H., Kim, J. E., Liu, H. Y., Cao, W., Chen, J. (2008) Regulation of Interleukin-6-induced Hepatic Insulin Resistance by Mammalian Target of Rapamycin through the STAT3-SOCS3 Pathway. *J Biol Chem.*, 283: 708-715.

Kimberling, W. J., Fain, P. R., Kenyon, J. B., Goldgar, D., Sujansky, E., Gabow, P. A. (1988) Linkage heterogeneity of autosomal dominant polycystic kidney disease. *N Engl J Med.*, 319: 913-918.

Kimberling, W. J., Kumar, S., Gabow, P. A., Kenyon, J. B., Connolly, C. J., Somlo, S. (1993) Autosomal dominant polycystic kidney disease: localisation of the second gene to chromosome 4q13-q23. *Genomics*, 18: 467-472.

Kirpicznik, J. (1910) Ein fall von tuberöser sklerose und gleichzeitigen multiplen nierengeschwulsten. *Virchows Arch F Path Anat.*, 202: 358.

Kishi, M., Pan, Y. A., Crump, J. G., Sanes, J. R. (2005) Mammalian SAD kinases are required for neuronal polarisation. *Science*, 307: 929-932.

Kleymenova, E., Ibraghimov-Beskrovnaya, O., Kugoh, H., Everitt, J., Xu, H., Kiguchi, K., Landes, G., Harris, P., Walker, C. (2001) Tuberin-dependent membrane localisation of polycystin-1: a functional link between polycystic kidney disease and the *TSC2* tumour suppressor gene. *Mol Cell.*, 7: 823-832.

Knudson, A. G. J. (1971) Mutation and cancer: statistical study of retinoblastoma. *Proc Natl Acad Sci USA.*, 68: 820-823.

Kobayashi, T., Hirayama, Y., Kobayashi, E., Kubo, Y., Hino, O. (1995) A germline insertion in the tuberous sclerosis (Tsc2) gene gives rise to the Eker rat model of dominantly inherited cancer. *Nature*, 9: 70-74.

Kobayashi, T., Urakami, S., Hirayama, Y., Yamamoto, T., Nishizawa, M., Takahara, T., Kubo, Y., Hino, O. (1997) Intragenic Tsc2 somatic mutations as Knudson's second hit in spontaneous and chemically induced renal carcinomas in the Eker rat model. *Jpn J Cancer Res.*, 88: 254-261.

Kobayashi, T., Minowa, O., Kuno, J., Mitani, H., Hino, O., Noda, T. (1999) Renal carcinogenesis, hepatic hemangiomatosis and embryonic lethality caused by a germline *Tsc2* mutation in mice. *Cancer Res.*, 59: 1206-1211.

Kobayashi, T., Minowa, O., Sugitani, Y., Takai, S., Mitani, H., Kobayashi, E., Noda, T., Hino, O. (2001) A germ-line *Tsc1* mutation causes tumour development and embryonic lethality that are similar but not identical to those caused by *Tsc2* mutation in mice. *Proc Nat Acad Sci USA.*, 98: 8762-8767.

Kobe, B., Deisenhofer, J. (1994) The Leucine-rich repeat: a versatile binding motif. *Trends Biochem Sci.*, 19: 415-421.

Kobe, B., Kajava, A. V. (2001) The leucine rich repeat as a protein recognition motif. *Curr Opin Struct Biol.*, 11: 725-732.

Konda, R., Sato, H., Hatafuku, F., Nozawa, T., Ioritani, N., Fujioka, T. (2004) Expression of hepatocyte growth factor and its receptor, c-met, in acquired renal cystic disease associated with renal cell carcinoma. *J Urol.*, 171: 2166-2170.

Konda, R., Sugimura, J., Sohma, F., Katagiri, T., Nakamura, Y., Fujioka, T. (2008) Over expression of Hypoxia-inducible protein 2, hypoxia-inducible factor-1a and nuclear factor  $\kappa$ B is putatively involved in acquired renal cyst formation and

subsequent tumour transformation in patients with end stage renal failure. *J Urol.*, 180: 481-485.

Kong, L-Y., Abou-Ghazal, M. K., Wei, J., Chakraborty, A., Sun, W., Qiao, W., Fuller, G. N., Fokt, I., Grimm, E. A., Schmittling, R. J., Archer, G. E., Sampson, J. H., Priebe, W., Heimberger, A. B. (2008) A novel inhibitor of signal transducers and activators of transcription 3 activation is efficacious against established central nervous system melanoma and inhibits regulatory T cells. *Clin Cancer Res.*, 14: 5759-5768.

Koptides, M., Hadjimichael, C., Koupepidou, P., Pierides, A., Constantinou Deltas, C. (1999) Germinal and somatic mutations in the *PKD2* gene of renal cysts in autosomal dominant polycystic kidney disease. *Hum Mol Genet.*, 8: 509-513.

Koptides, M., Mean, R., Demetriou, K., Pierides, A., Deltas, C. C. (2000) Genetic evidence for a trans-heterozygous mouse model for cystogenesis in autosomal dominant polycystic kidney disease. *Hum Mol Genet.*, 9: 447-452.

Koulen, P., Cai, Y., Geng, L., Maeda, Y., Nishimura, S., Witzgall, R., Ehrlich, B. E., Somlo, S. (2002) Polycystin-2 is an intracellular calcium release channel. *Nat Cell Biol.*, 4: 191-197.

Koya, R. C., Fujita, H., Shimizu, S., Ohtsu, M., Takimoto, M., Tsujimoto, Y., Kuzumaki, N. (2000) Gelsolin inhibits apoptosis by blocking mitochondrial membrane potential loss and cytochrome c release. *J Biol Chem.*, 275:15343–15349.

Krymskaya, V. P. (2003) Tumour suppressors hamartin and tuberlin: intracellular signalling. *Cell Signal.*, 15: 729-739.

Kubo, Y., Mitani, H., Hino, O. (1994) Allelic loss at the predisposing gene locus in spontaneous and chemically induced renal cell carcinomas in the eker rat. *Cancer Res.*, 54: 2633-2635.

Kuratsune, M., Masaki, T., Hirai, T., Kiribayashi, K., Yokoyama, Y., Arakawa, T., Yorioka, N., Kohno, N. (2007) Signal transducer and activator of transcription 3 involvement in the development of renal interstitial fibrosis after unilateral ureteral obstruction. *Nephrol.*, 12: 565-571.

Kuroki, M., O'Flaherty, J.T. (1999) Extracellular signal-regulated protein kinase (ERK)-dependent and ERK-independent pathways target STAT3 on serine-727 in human neutrophils stimulated by chemotactic factors and cytokines. *J Biochem.*, 341: 691-696.

Kurzer, J. H., Saharinen, P., Silvennoinen, O., Carter-Su, C. (2006) Binding of SH2-B family members within a potential negative regulatory region maintains JAK2 in an active state. *Mol Cell Biol.*, 26: 6381-6394.

Kwiatkowska, J., Jozwiak, S., Hall, F., Henske, E., Haines, J., McNamara, P., Braiser, J., Wigowska-Sowinska, J., Kasprzyk-Obara, J., Short, M. P., Kwiatkowski, D. J. (1998) Comprehensive analysis of the *TSC1* gene: observations on frequency of mutation, associated features and nonpenetrance. *Ann Hum Genet.*, 62: 277-285.

Kwiatkowski, D. J. and Short, M. P. (1994) Tuberous sclerosis. *Arch Dermatol.*, 130: 348-354.

Kwiatkowski, D. J., Humprey, D., van Slechtenhorst, M. (1996) A dense str map of 1.5Mb region of 9q34: small reduction in the *TSC1* critical region. In: Abstracts of the 5<sup>th</sup> international chromosome 9 workshop; Oxford, UK. 17.

Kwiatkowski, D. J., Zhang, H., Bandura, J. L., Heiberger, K. M., Glogauer, M., el-Hashemite, H., Onda, H. (2002) A mouse model of *TSC1* reveals sex-dependent lethality from liver haemangioma and up-regulation of p70S6 kinase activity in *Tsc1* null cells. *Hum Mol Genet.*, 64: 93-121.

Kwiatkowski, D. J. (2003) Rhebbling up mTOR: new insights on *TSC1* and *TSC2*, and the pathogenesis of tuberous sclerosis. *Cancer Biol Ther.*, 2: 471-476.

Kwiatkowski, D. J. (2005) *TSC1, TSC2, TSC3? Or mosaicism? Eur J Hum Genet.*, 13: 695-696.

Kwiatkowski, D. J. (2010) Animal models of Lymphangioleiomyomatosis and tuberous sclerosis complex. *Lymph Res and Biol.*, 8: 51- 57.

Kwiatkowski, D. J., Whittemore, V. H., Thiele, E. (2010) Tuberous Sclerosis Complex. Genes, Clinical features and therapeutics. , First edition, Wiley-Blackwell, Germany.

Laas, M. W., Spiegel, M., Jauch, A., Hahn, G., Rupprecht, E., Vogelberg, C., Bartsch, O., Huebner, A. (2004) Tuberous sclerosis and polycystic kidney disease in a 3 month old infant. *Pediatr Nephrol.*, 19: 602-608.

Lagos, J. C. and Gomez, M. R. (1967) Tuberous sclerosis: reappraisal of a clinical entity. *Mayo Clin Proc.*, 42: 26-49.

Lal, M., Song, X., Pluznick, J. L., Di Giovanni, V., Merrick, D. M., Rosenbaum, N. D., Chauvet, V., Gottardi, C. J., Pei, Y., Caplan, M. J. (2008) Polycystin-1 C-terminal tail associates with  $\beta$ -catenin and inhibits canonical Wnt signalling. *Hum Mol Genet.*, 17: 3105-3117.

Lamb, R. F., Roy, C., Diefenbach, T. J., Vinters, H. V., Johnson, M. W., Jay, D. G., Hall, A. (2000) The *TSC1* tumour suppressor hamartin regulates cell adhesion through ERM proteins and the GTPase Rho. *Nat Cell Biol.*, 2: 281-287.

Lanoix, J., D'Agati, V., Szabolcs, M., Trudel, M., Dysregulation of cellular proliferation and apoptosis mediates human autosomal dominant polycystic kidney disease (ADPKD). *Oncogene*, 13: 1153-1160.

Lantinga-van Leeuwen, I. S., Dauwerse, J. G., Baelde, H. J., Leonhard, W. N., van de Wal, A., Ward, C. J., Verbeek, S., Deruiter, M. C., Breuning, M. H., de Heer, E., Peters, D. J. (2004) Lowering of *Pkd1* expression is sufficient to cause polycystic kidney disease. *Hum Mol Genet.*, 13: 3069-3077.



Le, N. H., van der Bent, P., Huls, G., van de Wetering, M., Loghman-Adham, M., Ong, A. C., Calvet, J. P., Clevers, H., Breuning, M. H., van Dam, H., Peters, D. J. (2004) Aberrant polycystin-1 expression results in modification of activator protein-1 activity, whereas Wnt signalling remains unaffected. *J Biol Chem.*, 279: 27472-27481.

Lemmers, C., Michel, D., Lane-Guermonprez, L., Delgrossi, M. H., Medina, E., Arsanto, J. P., Le Bivic, A. (2004) CRB3 binds directly to Par6 and regulates the morphogenesis of the tight junctions in mammalian epithelial cells. *Mol Cell Biol.*, 15: 1324-1333.

Lendvay, T. S., Broecker, B., Smith, E. A. (2002) Renal cell carcinoma in a 2-year old with tuberous sclerosis. *J Urol.*, 168: 1131-1132.

Lendvay, T. S. and Marshall, F. F. (2003) The tuberous sclerosis complex and it's highly variable manifestations. *J Urol.*, 169: 1635-1642.

Li, H. P., Geng, L., Burrow, C. R., Wilson, P. D. (1999) Identification of phosphorylation sites in the PKD1-encoded protein C-terminal domain. *Biochem Biophys Res Commun.*, 259: 356-363.

Li, L., He, F., Litofsky, N. S., Recht, L. D., Ross, A. H. (2003) Profiling of genes expressed by *PTEN* haploinsufficient neural precursor cells. *Mol Cell Neurosci.*, 24: 1051-1061.

Li, X., Luo, Y., Starremans, P. G., McNamara, C. A., Pei, Y., Zhou, J. (2005) Polycystin-1 and polycystin-2 regulate the cell cycle through the helix-loop-helix inhibitor Id2. *Nat Cell Biol.*, 7: 1202-1212.

Lim, C.P., Cao, X. (1999) Serine Phosphorylation and Negative Regulation of Stat3 by JNK. *J Biol Chem.*, 274: 31055-31061.

Lim, C.P., Cao, X. (2001) Regulation of Stat3 Activation by MEK Kinase 1. *J Biol Chem.*, 276: 21004-21011.

Lin, F., Hiesberger, T., Cordes, K., Sinclair, A. M., Goldstein, L. S., Somlo, S., Igarashi, P. (2003) Kidney specific inactivation of the KIF3A subunit of kinesin-II inhibits renal ciliogenesis and produces polycystic kidney disease. *Proc Nat Acad Sci U S A*, 100: 5286-5291.

Lin, H-H., Yang, T-P., Jiang, S-T., Yang, H-Y., Tang, M-J. (1999) Bcl2 overexpression prevents apoptosis induced Madin Darby canine kidney simple epithelial cyst formation. *Kidney Int.*, 55: 168-178.

Linehan, W. H., Srinivasan, R., Schmidt, L. S. (2010) The genetic basis of kidney cancer: a metabolic disease. *Nature Rev Urology*, 7: 277-285.

Lo, R. K. H., Cheung, H., Wong, Y. H. (2003) Constitutively active Gα16 stimulates STAT3 via a c-Src/JAK-and ERK dependent mechanism. *J Biol Chem.*, 278: 52154-52165.

Lou, D., Griffith, N., Noonan, D. J. (2001) The tuberous sclerosis 2 gene product can localise to nuclei in a phosphorylation-dependent manner. *Mol Cell Biol Res Commun.*, 4: 374-380.

Low, S. H., Vasanth, S., Larson, C. H., Mukherjee, S., Sharma, N., Kinter, M. T., Kane, M. E., Obara, T., Weimbs, T. (2006) Polycystin-1, STAT6 and P100 function in a pathway that transduces ciliary mechanosensation and is active in polycystic kidney disease. *Dev Cell*, 10: 57-69.

Lu, W., Fan, X., Basora, N., Babakhanlou, H., Law, T., Rifai, N., Harris, P. C., Perez-Atayde, A. R., Rennke, H. G., Zhou, J. (1999) Late onset of renal and hepatic cysts in Pkd1-targeted heterozygotes. *Nat Genet.*, 21: 160-161.

Lu, Y., Fukuyama, S., Yoshida, R., Kobayashi, T., Saeki, K., Shiraishi, H., Yoshimura, A., Takaesu, G. (2006) Loss of SOCS3 gene expression converts

STAT3 function to from anti-apoptotic to pro-apoptotic. *J Biol Chem.*, 281: 36683-36690.

Lund, L. R., Romer, J., Thomasset, N., Solberg, H., Pyke, C., Bissell, M. J., Dano, K., Werb, Z. (1996) Two distinct phases of apoptosis in mammary gland involution: proteinase-independent and dependent pathways. *Devel.*, 122: 181-193.

Luo, Y., Vassilev, P. M., Li, X., Kawanabe, Y., Zhou, J. (2003) Native polycystin-2 functions as a plasma membrane  $\text{Ca}^{2+}$  permeable cation channel in renal epithelia. *Mol Cell Biol.*, 23: 2600-2607.

Ma, W., Kantarjian, H., Zhang, X., Wang, X., Zhang, Z., Yeh, C-H., O'Brien, S., Giles, F., Bruey, J. M., Albitar, M. (2010) JAK2 Exon 14 Deletion in Patients with Chronic Myeloproliferative Neoplasms. *PLoS ONE.*, 5: e12165.

Magistroni, R., He, N., Wang, K., Andrew, R., Johnson, A., Gabow, P., Dicks, E., Parfrey, P., Torra, R., San-Millan, J. L. (2003) Genotype-renal function correlation in type 2 autosomal dominant polycystic kidney disease. *J Am Soc Nephrol.*, 14: 1164-1174.

Maheshwar, M. M., Cheadle, J. P., Jones, A. C., Myring, J., Fryer, A. E., Harris, P. C., Sampson, J. R. (1997) The GAP-related domain of tuberlin, the product of the *TSC2* gene, is a target for missense mutations in tuberous sclerosis. *Hum Mol Genet.*, 5: 1991-1996.

Majno, G., Joris, I. (1995) Apoptosis, oncosis and necrosis: an overview of cell death. *Am J Pathol.*, 146: 3-15.

Mak, B. C., Takemaru, K., Kenerson, H. L., Moon, R. T., Yeung, R. S. (2003) The tuberlin-hamartin complex negatively regulates beta-catenin signalling activity. *J Biol Chem.*, 278: 5947-5951.

Mak, B. C., Kenerson, H. L., Aicher, L. D., Barnes, E. A., Yeung, R. S. (2005) Aberrant beta-catenin signalling in tuberous sclerosis. *Am J Pathol.*, 167: 107-116.

Mamane, Y., Petroulakis, E., Rong, L., Yoshida, K., Ler, L. W., Sonenberg, N. (2004) eIF4E-from translation to transformation. *Oncogene*, 23: 3172-3179.

Manning, B. D., Tee, A. R., Logsdon, M. N., Blenis, J., Cantley, L. C. (2002) Identification of the tuberous sclerosis complex 2 tumour suppressor gene product tuberlin as a target of the phosphoinositide 3-kinase / Akt pathway. *Mol Cell*, 10: 151-162.

Manning, B. D. (2004) Balancing Akt with S6K: implications for both metabolic diseases and tumourigenesis. *J Cell Biol.*, 167: 399-403.

Manning, B. D., Logsdon, M. N., Lipovsky, A. I., Abbott, D., Kwiatkowski, D. J., Cantley, L. C. (2005) Feedback inhibition of Akt signalling limits the growth of tumours lacking *Tsc2*. *Gen Dev.*, 19: 1773-1778.

Mao, Z., Streets, A. J., Ong, A. C. M. (2011) Thiazolidinediones inhibit MDCK cyst growth through disrupting orientate d cell division and apicobasal polarity. *Am J Physiol Renal Physiol.*, E-published ahead of print.

Massey-Harroche, D., Delgrossi, M-H., Lane-Guermonprez, L., Arsanto, J-P., Borg, J-P., Billaud, M., Le Bivic, A. (2007) Evidence for a molecular link between the tuberous sclerosi complex and the Crumbs complex. *Hum Mol Genet.*, 16: 529-536.

Masyuk, T., Huang, B. Q., Ward, C. J., Masyuk, A. I., Yuan, D., Splinter, P. L., Punyashthiti, R., Ritman, E. L., Torres, V. E., Harris, P. C. (2003) Defects in cholangiocyte fibrocystin expression and ciliary structure in the PCK rat. *Gastroenterology*, 125: 1303-1310.

Masyuk, T., LaRusso, N. (2006) Polycystic liver disease: new insights into disease pathogenesis. *Hepatology*, 43: 906-908.

Matsumoto, A., Masuhara, M., Mitsui, K., Yokouchi, M., Ohtsubo, M., Misawa, H., Miyajima, A., Yoshimura, A. (1997) CIS, a cytokine inducible SH2 protein, is a target of the JAK-STAT5 pathway and modulates STAT5 activation, *Blood* 89: 3148–3154.

Matsumoto, S., Bandyopadhyay, A., Kwiatkowski, D. J., Maitra, U., Matsumoto, T. (2002) Role of the Tsc1-Tsc2 complex in signalling and transport across the cell membrane in the fission yeast *Schizosaccharomyces Pombe*. *Nature Genet.*, 161: 1053-1063.

Matsuyama, M., Yoshimura, R., Hase, T., Kawahito, Y., Sano, H., Nakatani, T. (2004) Study of cyclooxygenase-2 in renal ischemia-reperfusion injury. *Transp Proc.*, 37: 370-372.

May, M. J., Ghosh, S. (1996) Rel/ NF- $\kappa$ B and I $\kappa$ B: an overview. *Semin Cancer Biol.*, 8: 63-73.

Meile, R., Sasaki, A. T., Firtel, R. A. (2004) Rho rocks PTEN. *Nat Cell Biol.*, 7: 334-335.

Melvin, A., Mudie, S., Rocha, S. (2011) Mechanism of hypoxia-induced NF- $\kappa$ B. *Cell Cycle*, 10: 879-882.

Melzner, I., Bucur, A. J., Brüderlein, S., Dorsch, K., Hasel, C., Barth, T. F., Leithäuser, F., Möller, P. (2005) Biallelic mutation of SOCS-1 impairs JAK2 degradation and sustains phospho-JAK2 action in the MedB1 mediastinal lymphoma line. *Blood*, 105: 2535-2542.

Meredith, J. E., Fazeli, B., Schwartz, M. A. (1993) The extracellular matrix as a cell survival factor. *Mol Cell Biol.*, 4: 953-961.

Messina, M. P., Rauktys, A., Lee, L., Dabora, S. L. (2007) Tuberous sclerosis preclinical study: timing of treatment, combination of a rapamycin-analogue (CCI-779) and interferon-gamma, and comparison of rapamycin to CCI-779. *BMC Pharmacol.*, 7: 14.

Meydan, N., Grunberger, T., Dadi, H. (1996) Inhibition of acute lymphoblastic leukaemia by a Jak-2 inhibitor. *Nature*, 379: 645-648.

Miyoshi, H., Nakau, M., Ishikawa, T. O., Seldin, M. F., Oshima, M., Taketo, M. M. (2002) Gastrointestinal hamartomatous polyposis in *Lkb1* heterozygous knockout mice. *Cancer Res.*, 62: 2261-2266.

Mizuguchi, M., Takashima, S., Yamanouchi, H., Nakazato, Y., Mitani, H., Hino, O. (2000) Novel cerebral lesions in the Eker rat model of tuberous sclerosis: cortical tuber and anaplastic ganglioglioma. *J Neuropathol Exp Neurol.*, 59: 188-196.

Mochizuki, T., Wu, G., Hayashi, T., Xenophontos, S. L., Veldhuisen, B., Saris, J. J., Reynolds, D. M., Cai, Y., Gabow, P. A., Pierides, A. (1996) *PKD2* a gene for polycystic kidney disease that encodes an integral membrane protein. *Science*, 272: 1339-1342.

Moon, R. T. (2005) Wnt/beta-catenin pathway. *Sci STKE.*, 271: cm1.

Moser, M., Pscherer, A., Roth, C., Becker, J., Mucher, G., Zerrers, K., Dixkens, C., Weis, J., Guay-woodford, L., Buettner, R., Fassler, R. (1997) Enhanced apoptotic cell death of renal epithelial cells in mice lacking transcription factor AP-2 $\beta$ . *Gen Dev.*, 11: 1938-1948.

Mostov, K. E. (2006) mTOR is out of control in polycystic kidney disease. *Proc Natl Acad Sci U S A*, 103: 5247-5248.

Moy, G. W., Mendoza, L. M., Schulz, J. R., Swanson, W. J., Glabe, G. G., Vacquier, V. D. (1996) The sea urchin sperm receptor for egg jelly is a modular protein with extensive homology to the human polycystic kidney disease protein, PKD1. *J Cell Biol.*, 133: 809-817.

Munemura, C., Uemasu, J., Kawasaki, H. (1994) Epidermal growth factor and endothelin in cyst fluid from autosomal dominant polycystic kidney disease cases: possible evidence of heterogeneity in cystogenesis. *Am J Kidney Dis.*, 24: 561-568.

Murgia, M. G., Jordan, S., Kahan, B. D. (1996) The side effect profile of sirolimus: a phase I study in quiescent cyclosporine-prednisone-treated renal transplant patients. *Kid Int.*, 49: 209-216.

Nadasdy, T., Laszik, Z., Lajoie, G., Blick, K. E., Wheeler, D. E., Silva, F. G. (1995) Proliferative activity of cyst epithelium in human renal cystic diseases. *J Am Soc Nephrol.*, 5: 1462-1468.

Nakase, Y., Fukuda, K., Chikashige, Y., Tsutsumi, C., Morita, D., Kawamoto, S., Ohnuki, M., Hiraoka, Y., Matsumoto, T. (2006) A defect in protein Farnesylation suppresses a loss of *Schizosaccharomyces Pombe tsc2<sup>+</sup>*, a homolog of the human gene predisposing to tuberous sclerosis complex. *Nature Genet.*, 173: 569-578.

Nation, J. L. (1983) A new method using hexamethyldisilazane for preparation of soft insect tissues for scanning electron microscopy. *Stain Technol.*, 58: 347-351.

Nauli, S. M., Alenghat, F. J., Luo, Y., Williams, E., Vassilev, P., Li, X., Elia, A. E., Lu, W., Brown, E. M., Quinn, S. J., Ingber, D. E., Zhou, J. (2003) Polycystins 1 and 2 mediate mechanosensation in the primary cilium of kidney cells. *Nat Genet.*, 33: 129-137.

Nellist, M., van Slegtenhorst, M. A., Goedbloed, M., van den Ouweland, A. M., Halley, D. J., van der Sluijs, P. (1999) Characterisation of the cytosolic tuberin-hamartin complex. Tuberin is a cytosolic chaperone for hamartin. *J Biol Chem.*, 274: 35647-35652.

Nellist, M., Sancak, O., Goedbloed, M. A., Rohe, C., van Netten, D., Mayer, K., Tucker-Williams, A., van den Ouweland, A., Halley, D. J. J. (2005) Distinct effects of the single amino-acid changes to tuberin on the function of the tuberin –hamartin complex. *Eur J Hum Genet.*, 13: 59-68.



Nevin, N. C., and Pearce, W. G. (1968) Diagnostic and genetical aspects of tuberous sclerosis. *J Med Genet.*, 5: 273-280.

Ni, C-W., Hsieh, H-J., Chao, Y-J., Wang, D. L. (2004) Interleukin-6 induced JAK2/STAT3 signalling pathway in endothelial cells is suppressed by hemodynamic flow. *Am J Physiol Cell Physiol.*, 287: 771-780.

Nichols, M. T., Gidey, E., Matzakos, T., Dahl, R., Stiegmann, G., Shah, R. J. (2004) Secretion of cytokines and growth factors into autosomal dominant polycystic kidney liver cyst fluid. *Hepatology*, 40: 836-846.

Niida, Y., Lawrence-Smith, N., Banwell, A., Hammer, E., Lewis, J., Beauchamp, R., Sims, K., Ramesh, V., Ozelius, L. (1999) Analysis of both *TSC1* and *TSC2* for germline mutations in 126 unrelated patients with tuberous sclerosis. *Hum Mutat.*, 14: 412-422.

Niida, Y., Stemmer-Rachamimov, A. O., Logrip, M., Tapon, D., Perez, R., Kwiatkowski, D. J., Sims, K., MacCollin, M., Louis, D. N., Ramesh, V. (2001) Survey of somatic mutations in tuberous sclerosis complex (TSC) hamartomas suggests difference genetic mechanisms for pathogenesis of TSC lesions. *Am J Hum Genet.*, 69: 493-503.

Nims, N., Vassmer, D., Maser, R. L. (2003) Transmembrane domain analysis of polycystin-1 the product of the polycystic kidney disease 1 gene: evidence for 11 membrane spanning domains. *Biochemistry*, 42: 13035-13048.

Nir, A., Tajik, A. J., Freeman, W. K., Seward, J. B., Offord, K. P., Edwards, W. D., Mair, D. D., Gomez, M. R. (1995) Tuberous sclerosis and cardiac rhabdomyoma. *Am J Cardiol.*, 76: 419-421.

Nishio, S., Hatano, M., Nagata, M., Horie, S., Koike, T., Tokuhisa, T., Mochizuki, T. (2005) *Pkd1* regulates immortalised proliferation of renal tubular epithelial cells through p53 induction and JNK activation. *J Clin Invest.*, 115: 910-918.

Noonan, D. J., Lou, D., Griffith, N., Vanaman, T. C. (2002) A calmodulin binding site in the tuberous sclerosis 2 gene product is essential for regulation of transcriptional events and is altered by mutations linked to tuberous sclerosis and lymphangiomyomatosis. *Arch Biochem Biophys.*, 398: 132-140.

Northrup, H., Kwiatkowski, D. J., Roach, E. S., Dobyns, W. B., Lewis, R. A., Herman, G. E., Rodriguez, E., Daiger, S. P., Blanton, S. H. (1992) Evidence for genetic heterogeneity in tuberous sclerosis: one locus on chromosome 9 and at least one locus elsewhere. *Am J Hum Genet.*, 51: 709-720.

Nur, S., Chuang, L., Ramaswamy, G. (2006) Immunohistochemical characterisation of cancer antigen in uterine cancers. *Int J Gynecol Cancer*, 16: 1903-1910.

Nyboer, J. H., Robertson, D. M., Gomez, M. R. (1976) Retinal lesions in tuberous sclerosis. *Arch Ophthalmol.*, 94: 1277-1280.

O'Callaghan, F. J., Noakes, M. J., Martyns, C. N., Osborne, J. P. (2004) An epidemiological study of renal pathology in tuberous sclerosis. *BJU Int.*, 94: 853-857.

Oesterling, J. E., Fishman, E. K., Goldman, S. M., Marshall, F. F. (1986) The management of renal angiomyolipoma. *J Urol.*, 135: 1121-1124.

Ogata, H., Kobayashi, T., Chinen, T., Takaki, H., Sanada, T., Minoda, Y., Koga, K., Takaesu, G., Maehara, Y., Lida, M., Yoshimura, A. (2006) Deletion of the SOCS3 gene in liver parenchymal cell promotes hepatitis induced hepatocarcinogenesis. *Gastroent.*, 131: 179-193.

Ohtsu, M., Sakai, N., Fujita, H., Kashiwagi, M., Gasa, S., Shimizu, S., Eguchi, Y., Tsujimoto, Y., Sakiyama, Y., Kobayashi, K., Kuzumaki, N. (1997) Inhibition of apoptosis by the actin-regulatory protein gelsolin. *EMBO J.*, 16: 4650–4656.

Onda, H., Lueck, A., Marks, P. W., Warren, H. B., Kwiatkowski, D. J. (1999) *Tsc2*<sup>+/-</sup> mice develop tumours in multiple sites that express gelsolin and are influenced by genetic background. *J Clin Invest.*, 104: 687-695.

Onda, H., Crino, P. B., Zhang, H., Murphey, R. D., Rastelli, L., Rothberg, B. E. G., Kwiatkowski, D. J. (2002) *Tsc2* null murine neuroepithelial cells are a model for human tuber giant cells, and show activation of an mTOR pathway. *Mol Cell Neurosci.*, 21: 561-574.

Ong, A. C., Ward, C. J., Butler, R. J., Biddolph, S., Bowker, C., Torra, R., Pei, Y., Harris, P. C. (1999a) Coordinate expression of the autosomal dominant polycystic kidney disease proteins, polycystin-2 and polycystin-1, in normal and cystic tissue. *Am J Pathol.*, 154: 1721-1729.

Ong, A. C., Harris, P. C., Davies, D. R., Pritchard, L., Rossetti, S., Biddolph, S., Vaux, D. J., Migone, N., Ward, C. J. (1999b) Polycystin-1 expression in PKD1, early onset PKD1 and TSC2/PKD1 cystic tissue. *Kidney Int.*, 56: 1324-1333.

Orlova, K. A., Crino, P. B. (2010) The tuberous sclerosis complex. *Ann N Y Acad Sci.*, 1184: 87-105.

Osborne, J. P. (1988) Diagnosis of tuberous sclerosis. *Arch Dis Child.*, 63: 1423-1425.

Osborne, J. P., Fryer, A., Webb, D. (1991) Epidemiology of tuberous sclerosis. *Ann NY Acad Sci.*, 615: 125-127.

Ostrom, L., Tang, M. J., Gruss, P., Dressler, G. R. (2000) Reduced *Pax2* gene dosage increases apoptosis and slows the progression of renal cystic disease. *Dev Biol.*, 219: 250-258.

Pagliuca, A., Gallo, P., De Luca, P., Lania, L. (2000) Class A helix-loop-helix proteins are positive regulators of several cyclin-dependent kinase inhibitors' promoter activity and negatively affect cell growth. *Cancer Res.*, 60: 1376-1382.

Pan, D., Dong, J., Zhang, Y., Gao, X. (2004) Tuberous sclerosis complex: from *Drosophila* to human disease. *Trends Cell Biol.*, 14: 78-85.

Pan, J., Snell, W. (2007) The primary cilium: keeper of the key to cell division. *Cell*, 129: 1255-1257.

Park, T. J., Gray, R. S., Sato, A., Habas, R., Wallingford, J. B. (2005) Subcellular localisation and signalling properties of dishevelled in developing vertebrate embryos. *Curr Biol.*, 15: 1039-1044.

Park, T. J., Haigo, S. L., Wallingford, J. B. (2006) Ciliogenesis defects in embryos lacking inturned or fuzzy function are associated with failure of planar cell polarity and Hedgehog signalling. *Nat Genet.*, 38: 303-311.

Parnell, S. C., Magenheimer, B. S., Maser, R. L., Rankin, C. A., Smine, A., Okamoto, T., Calvet, J. P. (1998) The polycystic disease-1 protein, polycystin-1, binds and activates heterotrimeric G proteins in vitro. *Biochem Biophys Res Commun.*, 251: 625-631.

Parnell, S. C., Magenheimer, B. S., Maser, R. L., Calvet, J. P. (1999) Identification of the major site of in vitro PKA phosphorylation in the polycystin-1 C-terminal cytosolic domain. *Biochem Biophys Res Commun.*, 259: 539-543.

Parry, L., Maynard, J. H., Patel, A., Hodges, A. K., von Deimling, A., Sampson, J. R., Cheadle, J. P. (2000) Molecular analysis of the *TSC1* and *TSC2* tumour suppressor genes in sporadic glial and glioneuronal tumours. *Hum Genet.*, 107: 350-356.

Parry, L., Maynard, J. H., Patel, A., Clifford, S. C., Morrissey, C., Maher, E. R., Cheadle, J. P., Sampson, J. R. (2001) Analysis of the *TSC1* and *TSC2* genes in sporadic renal cell carcinoma. *Br J Cancer*, 85: 1226-1230.

Patel, V., Li, L., Cobo-Stark, P., Shao, X., Somlo, S., Lin, F., Igarashi, P. (2008) Acute kidney injury and aberrant planar cell polarity induce cyst formation in mice lacking renal cilia. *Hum Mol Genet.*, 17: 1578-1590.

Paterson, A. D., Pei, Y. (1998) Is there a third gene for autosomal dominant polycystic kidney disease? *Kidney Int.*, 54: 1759-1761.

Paterson, A. D., Pei, Y. (1999) PKD3-to be or not to be? *Nephrol Dial Transplant*, 14: 2965-2966.

Pazour, G. J., Dickert, B. L., Vucica, Y., Seeley, E. S., Rosenbaum, J. L., Witman, G. B., Cole, D. G. (2000) Chlamydomonas IFT88 and its mouse homologue, polycystic kidney disease gene *tg737*, are required for assembly of cilia and flagella. *J Cell Biol.*, 151: 709-718.

Pazour, G. J., San Agustin, J. T., Follit, J. A., Rosenbaum, J. L., Witman, G. B. (2002) Polycystin-2 localises to kidney cilia and the ciliary level is elevated in *orpk* mice with polycystic kidney disease. *Curr Biol.*, 12: R378-380.

Pei, Y., Watnick, T., He, N., Wang, K., Liang, Y., Parfrey, P., Germino, G. G., St George-Hyslop, P. (1999) Somatic *PKD2* mutations in individual kidney and liver cysts support a two hit model of cystogenesis in type 2 autosomal dominant polycystic kidney disease. *J Am Soc Nephrol.*, 10: 1524-1529.

Pei, Y. (2001) A two hit model of cystogenesis in autosomal dominant polycystic kidney disease? *Trends Mol Med.*, 7: 151-156.

Pei, Y., Watnick, T. (2010) Diagnosis and screening of autosomal dominant polycystic kidney disease. *Adv Chronic Kid Dis.*, 17: 140-152.

Perantoni, A. O. (2003) Renal development: perspectives on a Wnt-dependent process. *Semin Cell Dev Biol.*, 14: 201-208.

Peters, B., San Millan, J. L., Hernandez, C., Valero, A., Lathrop, G. M., Beckmann, J. S., Moreno, F. (1993) Estimating locus heterogeneity in autosomal dominant polycystic kidney disease (ADPKD) in the Spanish population. *J Med Genet.*, 30: 910-913.

Petri, E. T., Celic, A., Kennedy, S. D., Ehrlich, B. E., Boggon, T. J., Hodsdon, M. E. (2010) Structure of the EF hand domain in polycystin 2 suggests a mechanism for  $\text{Ca}^{2+}$  dependent regulation of polycystin 2 channel activity. *Proc Nat Acad Sci USA.*, 107: 9176-9181.

Perusini, G. (1905) Über einen Fall von Sclerosis tuberosa hypertrophica. *Monatsschr Psychiatr Neurol.*, 17: 69-255.

Plank, T. L., Yeung, R. S., Henske, E. P. (1998) Hamartin, the product of the tuberous sclerosis 1 (*TSC1*) gene, interacts with tuberin and appears to be localised to cytoplasmic vesicles. *Cancer Res.*, 58: 4766-4770.

Pollard, P., Spencer-Dene, B., Shukla, D., Howarth, K., Nye, E., El-Bahrawy, M., Deheragoda, M., Joannou, M., McDonald, S., Martin, A, Igarashi, P., Varsani-Brown, S., Rosewell, I., Poulsom, R., Maxwell, P., Stamp, G. W., Tomlinson, I. P. M. (2007) Targeted inactivation of Fh1 causes proliferative renal cyst development and activation of the hypoxia pathway. *Cancer Cell*, 11: 311-319.

Pommier, Y., Sordet, O., Antony, S., Hayward, R. L., Kohn, K. W. (2004) Apoptosis defects and chemotherapy resistance: molecular interaction maps and networks. *Oncogene*, 23: 2934-2949.

Ponting, C. P., Hofmann, K., Bork, P. A. (1999) A latrophilin/CL-1 like GPS domain in polycystin-1. *Curr Biol.*, 9: 585-588.

Potter, C. J., Huang, H., Xu, T. (2001) *Drosophila Tsc1* functions with *Tsc2* to antagonise insulin signalling in regulating cell growth, cell proliferation and organ size. *Cell*, 105: 357-368.

Praetorius, H. A., Spring, K. R. (2001) Bending the MDCK cell primary cilium increases intracellular calcium. *J Membr Biol.*, 191: 69-76.

Praetorius, H. A., Spring, K. R. (2003) Removal of the MDCK cell primary cilium increases intracellular calcium. *J Membr Biol.*, 191: 69-76.

Preminger, G. M., Koch, W. E., Fried, F. A., McFarland, E., Murphy, E. D., Mandell, J. (1982) Murine congenital polycystic kidney disease: a model for studying development of cystic disease. *J Urol.*, 127: 556-560.

Pringle, J. J. (1890) A case of congenital adenoma sebaceum. *Br J Dermatol.*, 2: 1-14.

Pullan, S., Wilson, J., Metcalfe, A., Edwards, G. M., Goberdhan, N., Tilly, J., Hickman, J. A., Dive, C., Streuli, C. H. (1996) Requirement of basement membrane for suppression of programmed cell death in mammary epithelium. *J Cell Sci.*, 109: 631-642.

Qian, C. N., Knol, J., Igarashi, P., Lin, F., Zylstra, U., Teh, B. T., Williams, B. O. (2005) Cystic renal neoplasia following conditional inactivation of *apc* in mouse renal tubule epithelium. *J Biol Chem.*, 280: 3938-3945.

Qian, F., Germino, F. J., Cai, Y., Zhang, X., Somlo, S., Germino, G. G. (1997) *PKD1* interacts with *PKD2* through a probable coiled-coil domain. *Nat Genet.*, 16:179-183.

Qian, F., Watnick, T. J., Onuchic, L. F., Germino, G. G. (1996) The molecular basis of focal cyst formation in human autosomal dominant polycystic kidney disease type-1. *Cell*, 87: 979-987.

Qian, F., Boletta, A., Bhunia, A. K., Xu, H., Liu, L., Ahrabi, A. K., Watnick, T. J., Zhou, F., Germino, G. G. (2002) Cleavage of polycystin-1 requires the receptor for egg jelly domain and is disrupted by human autosomal dominant polycystic kidney disease-1 associated mutations. *Proc Nat Acad Sci USA.*, 99: 16981-16986.



Qian, Q., Li, A., King, B. F., Kamath, P. S., Lager, D. J., Huston, J. I. (2003) Clinical profile of autosomal dominant polycystic liver disease. *Hepatology*, 37: 164-171.

Qian, Q., Du, H., King, B. F., Kumar, S., Dean, P. G., Cosio, F. G., Torres, V. E. (2008) Sirolimus reduces polycystic liver volume in ADPKD patients. *J Am Soc Nephrol.*, 19: 631-638.

Qin, W., Kozlowski, P., Taillon, B. E., Bouffard, P., Holmes, A. J., Janne, P., Camposano, S., Thiele, E., Franz, D., Kwiatkowski, D. J. (2010) Ultra deep sequencing detects a low rate of mosaic mutations in tuberous sclerosis complex. *Hum Genet.*, 127: 573-582.

Quintas-Cardama, A., Manshour, T., Estrov, Z., Harris, D., Zhang, Y., Gaikwad, A., Kantarjian, H. M., Verstovsek, S. (2010) Preclinical characterisation of atiprimod, a novel JAK2 and JAK3 inhibitor. *Invest New Drugs*, e-publication ahead of print.

Radimerski, T., Montagne, J., Hemmings-Mieszczak, M., Thomas, G. (2002) Lethality of *Drosophila* lacking TSC tumour suppressor function rescued by reducing dS6K signalling. *Gen Dev.*, 16: 2627-2632.

Rajagopalan, S., Rodrigues, M., Polk, T., Wilson, D., Chader, G. J., Hayden, B. J. (1993) Modulation of retinoblastoma cell characteristics by hexamethylene bis-acetamide and other differentiating agents in culture. *J Histo Chem.*, 41: 1331-1337.

Rakowski, S. K., Winterkorn, E. B., Paul, E., Steele, D. J. R., Halpern, E. F., Thiele, E. A. (2006) Renal manifestations of tuberous sclerosis complex: incidence, prognosis and predictive factors. *Kid Int.*, 70: 1777-1782.

Ramana, C. V., Gil, M. P., Schreiber, R. D., Stark, G. R. (2002) Stat1-dependent and independent pathways in IFN $\gamma$  dependent signalling. *Trends Immunol.*, 23: 96-101.

Raukty, A., Lee, N., Lee, L., Dabora, S. L. (2008) Topical rapamycin inhibits tuberous sclerosis tumour growth in a nude mouse model. *BMC Dermatol.*, 8:1.

Ravine, D., Gibson, R. N., Walker, R. G., Sheffield, L. J., Kincaid-Smith, P., Danks, D. M. (1994) Evaluation of ultrasonographic diagnostic criteria for autosomal dominant polycystic kidney disease. *Lancet*, 343: 824-827.

Reeders, S. T., Breuning, M. H., Davies, K. E., Nicholls, R. D., Jarman, A. P., Higgs, D. R., Pearson, P. L., Weatherall, D. J. (1985) A highly polymorphic DNA marker linked to adult polycystic kidney disease on chromosome 16. *Nature*, 317: 542-544.

Reeders, S. T. (1992) Multilocus polycystic disease. *Nat Genet.*, 1: 235-237.

Resta, N., Simone, C., Mareni, C., Montera, M., Gentile, M., Susca, F., Gristina, R., Pozzi, S., Bertario, L., Bufo, P., et al. (1998) *STK11* mutations in Peutz-Jeghers syndrome and sporadic colon cancer. *Cancer Res.*, 58: 4799-4801.

Roach, E. S., Gomez, M. R., Northrup, H. (1998) Tuberous sclerosis complex consensus conference: Revised clinical diagnostic criteria. *J Child Neurol.*, 13: 624-624.

Roach, E. S. and Sparagana, S. P. (2004) Diagnosis of tuberous sclerosis complex. *J Child Neurol.*, 19: 643-649.

Roberts, P. S., Dabora, S., Thiele, E. A., Franz, D. N., Jozwiak, S., Kwiatkowski, D. J. (2004) Somatic mosaicism is rare in unaffected parents of patients with sporadic tuberous sclerosis. *J Med Genet.*, 41: 69.

Robertson, D. M. (1988) Ophthalmic findings. In *Tuberous sclerosis, Second Edition*. Raven Press, Ltd., New York.

Robertson, D. M. (1991) Ophthalmic manifestations of tuberous sclerosis. *Ann N Y Acad Sci.*, 615: 17-25.

Robertson, F. M., Cendron, M., Klauber, G. T., Harris, B. H. (1996) Renal cell carcinoma in association with tuberous sclerosis in children. *J Pediatr Surg.*, 31: 729-730.

Roh, M. H., Fan, S., Liu, C. J., Margolis, B. (2003) The Crumbs3 – Pals1 complex participates in the establishment of polarity in mammalian epithelial cells. *J Cell Sci.*, 116: 2895-2906.

Romeo, G., Devoto, M., Costa, G., Roncuzzi, L., Catizone, L., Zucchelli, P., Germino, G. G., Keith, T., Weatherall, D. J., Reeders, S. T. (1988) A second genetic locus for autosomal dominant polycystic kidney disease. *Lancet*, 2: 8-11.

Rosenbaum, J. L., Witman, G. B. (2002) Intraflagellar transport. *Nat Rev Mol Cell Biol.*, 3:813-825.

Rosner, M., Hanneder, M., Siegel, N., Valli, A., Hengstschlager, M. (2008) The tuberous sclerosis gene products hamartin and tuberin are multifunctional proteins with a wide spectrum of interacting partners. *Mutation Res.*, 658: 234-246.

Ross, A. J., May-Simera, H., Eichers, E. R. (2005) Disruption of Bardet-Biedl syndrome ciliary proteins perturbs planar cell polarity in vertebrates. *Nat Genet.*, 37: 1135-1140.

Rosser, T., Panigrahy, A., McClintock, W. (2006) The diverse clinical manifestations of tuberous sclerosis complex: a review. *Semin Pediatr Neurol.*, 13: 27-36.

Rossetti, S., Strmecki, L., Gamble, V., (2001) Mutation analysis of the entire *PKD1* gene: genetic and diagnostic implications. *Am J Hum Genet.*, 68: 46-63.

Rossetti, S., Chauveau D., Walker, D. (2002) A complete mutation screen of the ADPKD genes by DHPLC. *Kidney Int.*, 61: 1588-1599.

Rossetti, S., Burton, S., Strmecki, L., Pond, G. R., San Millan, J. L., Zerres, K., Barratt, T. M., Ozen, S., Torres, V. E., Bergstralh, E. J. (2002) The position of the

polycystic kidney disease 1 (*PKD1*) gene mutation correlates with the severity of renal disease. *J Am Soc Nephrol.*, 13: 1230-1237.

Rossetti, S., Consugar, M. B., Chapman, A. B. (2007) Comprehensive molecular diagnostics in autosomal dominant polycystic kidney disease. *J Am Soc Nephrol.*, 18: 2143-2160.

Rossetti, S., Harris, P. C. (2007) Genotype-Phenotype correlations in autosomal dominant and autosomal recessive polycystic kidney disease. *J Am Soc Nephrol.* 18: 1374-1380.

Rossi, D. J., Ylikorkala, A., Korsisaari, N., Salovaara, R., Luukko, K., Launonen, V., Henkemeyer, M., Ristimäki, A., Aaltonen, L. A., Makela, T. P. (2002) Induction of cyclooxygenase-2 in a mouse model of Peutz-Jeghers polyposis. *Proc Nat Acad Sci USA.*, 99: 12327-12332.

Rowley, S. A., O'Callaghan, J. P., Osborne, J. P. (2001) Ophthalmic manifestations of tuberous sclerosis: a population based study. *Br J Ophthalmol.*, 85: 420-423.

Rozen, S., Skaletsky, H. (2000) Primer3 on the WWW for general users and for biologist programmers. *Methods Mol Biol.*, 132: 365-386.

Rytomaa, M., Martins, L. M., Downward, J. (1999) Involvement of FADD and caspase 8 signalling in detachment induced apoptosis. *Curr Biol.*, 9: 1043-1046.

Saadi-Kheddouci, S., Berrebi, D., Romagnolo, B., Cluzeaud, F., Peuchmaur, M., Kahn, A., Vandewalle, A., Perret, C. (2001) Early development of polycystic kidney disease in transgenic mice expressing an activated mutant of the beta-catenin gene. *Oncogene*, 20: 5972-5981.

Saburi, S., Hester, I., Fischer, E. (2008) Loss of Fat4 disrupts PCP signalling and orientated cell division and leads to cystic kidney disease. *Nat Genet.*, 40: 1010-1015.

Saharinen, P., Takaluoma, K., Silvennoinen, O. (2000) Regulation of the Jak2 tyrosine kinase by its pseudokinase domain. *Mol Cell Biol.*, 20: 3387-3395.

Sahoo, B., Handa, S., Kumar, B. (2000) Tuberous sclerosis with macrodactyly. *Pediatr Dermatol.*, 17: 463-465.

Saifudeen, Z., Dipp, S., El-Dahr, S. S. (2002) A role for p53 in terminal epithelial cell differentiation. *J Clin Invest.*, 109: 1021-1030.

Sampson, J. R., Scahill, S. J., Stephenson, J. B., Mann, L., Connor, J. M. (1989a) Genetic aspects of tuberous sclerosis in the west of Scotland. *J Med Genet.*, 26: 28-31.

Sampson, J. R., Yates, J. R. W., Pirrit, L. A., Fleury, P., Winship, I., Beighton, P., Connor, J. M. (1989) Evidence for genetic heterogeneity in tuberous sclerosis. *J Med Genet.*, 26: 511-516.

Sampson, J. R., Maheshwar, M. M., Aspinwall, R., Thompson, P., Cheadle, J. P., Ravine, D., Roy, S., Haan, E., Bernstein, J., Harris, P. C. (1997) Renal cystic disease in tuberous sclerosis: role of the polycystic kidney disease 1 gene. *Am J Hum Genet.*, 61: 843-851.

Sancak, O., Nellist, M., Goedbloed, M., Elfferich, P., Wouters, C., Maat-Kieviet, A., Zonnenberg, B., Verhoef, S., Halley, D., van den Ouweland, A. (2005) Mutational analysis of the *TSC1* and *TSC2* genes in a diagnostic setting: genotype-phenotype correlations and comparisons of diagnostic DNA techniques in tuberous sclerosis complex. *Eur J Hum Genet.*, 13: 731-741.

Sandford, R., Sgotto, B., Aparicio, S., Brenner, S., Vaudin, M., Wilson, R. K., Chisoe, S., Pepin, K., Bateman, A., Chothia, C. (1997) Comparative analysis of the polycystic kidney disease 1 gene reveals an integral membrane glycoprotein with multiple evolutionary conserved domains. *Hum Mol Genet.*, 6: 1483-1489.

Santarosa, M., Ashworth, A. (2004) Haploinsufficiency for tumour suppressor genes: when you don't need to go all the way. *Biochim Biophys Acta.*, 1654: 105-122.

Sarbassov, D. D., Ali, S. M., Kim, D. H., Guertin, D. A., Latek, R. R., Erdjument-Bromage, H., Tempest, P., Sabatini, D. M. (2004) Rictor, a novel binding partner of mTOR, defines a rapamycin-insensitive and raptor-independent pathway that regulates the cytoskeleton. *Curr Biol.*, 14: 1296-1302.

Sarbassov, D. D., Guertin, D. A., Ali, S. M., Sabatini, D. M. (2005) Phosphorylation and regulation of Akt/PKB by the rictor mTOR complex. *Science*, 307: 1098-1101.

Saucedo, L. J., Gao, X., Chiarelli, D. A., Li, L., Pan, D., Edgar, B. A. (2003) Rheb promotes cell growth as a component of the insulin/TOR signalling network. *Nat Cell Biol.*, 5: 566-571.

Sayyah, J., Sayeski, P. P. (2009) Jak2 inhibitors: rational and role as therapeutic agents in hematologic malignancies. *Curr Oncol Rep.*, 11: 117-124.

Schmidt, E. V. (1999) The role of c-myc in cellular growth control. *Oncogene*, 18: 2988-2996.

Seghal, S. N., Baker, H., Vzina, C. (1975) Rapamycin (AY-22, 989) a new antifungal antibiotic. II. Fermentation, isolation and characterization. *J Antibiot (Tokyo)*, 28: 727-732.

Segrelles, C., Moral, M. Lorz, C., Santos, M., Lu, J., Cascallana, J-L., Lara, M. F., Carbajal, S., Martínez-Cruz, A. B., García-Escudero, R., Beltran, L., Segovia, J. C., Bravo, A., DiGiovanni, J., Paramio, J. M. (2008) Constitutively active Akt induces ectodermal defects and impaired bone morphogenic protein signalling. *Mol Cell Biol.*, 19: 137-149.

Serra, A. L., Kistler, A. D., Poster, D., Strucker, M., Wuthrich, R. P., Weishaupt, D., Tschirch, F. (2007) Clinical proof of concept trial to assess the therapeutic effect of

Sirolimus in patients with autosomal dominant polycystic kidney disease: SUISE ADPKD study. *BMC Nephrol.*, 8: 13.

Shen, A., Iseman, M. D., Walden, J. A., King, T. E. (1987) Exacerbation of pulmonary lymphangioleiomyomatosis by exogenous estrogens. *Chest*, 91: 782-785.

Shen, Y., Schlessinger, K., Zhu, X., Meffre, E., Quimby, F., Levy, D. E., Darnell Jr., J. E. (2004) Essential role of STAT3 in postnatal survival and growth revealed by mice lacking STAT3 Serine 727 phosphorylation. *Mol Cell Biol.*, 24: 407-419.

Sherstha, R., McKinley, C., Russ, P., Scherzinger, A., Bronner, T., Showlater, R., Everson, G. T. (1997) Postmenopausal estrogen therapy selectively stimulates hepatic enlargement in women with autosomal dominant polycystic kidney disease. *Hepatology*, 26: 1282-1286.

Shillingford, J. M., Murcia, N. S., Larson, C. H., Low, S. H., Hedgepeth, R., Brown, N., Flask, C. A., Novick, A. C., Goldfarb, D. A., Kramer-Zucker, A. (2006) The mTOR pathway is regulated by polycystin-1, and its inhibition reverses renal cystogenesis in polycystic kidney disease. *Proc Nat Acad Sci USA*. 103: 5466-5471.

Shin K., Straight, S., Margolis, B. (2005) PATJ regulates tight junction formation and polarity in mammalian epithelial cells. *J Cell Biol.*, 168: 705-711.

Shneider, B. L., Magid, M. S. (2005) Liver disease in autosomal recessive polycystic kidney disease. *Pediatr Transplant*, 9: 634-639.

Simmers, R. N., Mulley, J. C., Hyland, V. J., Callen, D. F., Sutherland, G. R. (1987) Mapping the human alpha globin gene complex to 16p13.2-pter. *J Med Genet.*, 24: 761-766.

Simons, M., Gloy, J., Ganner, A., Bullerkotte, A., Bashkurov, M., Krönig, C., Schermer, B., Benzing, T., Cabello, O. A., Jenny, A. (2005) Inversin, the gene product mutated in nephronophthisis type II, functions as a molecular switch between Wnt signalling pathways. *Nat Genet.*, 37: 537-543.



Simons, M., Walz, G. (2006) Polycystic kidney disease: cell division without a clue? *Kidney Int.*, 70: 854-864.

Smalley, S. L., Tanguay, P. E., Smith, M., Gutierrez, G. (1992) Autism and tuberous sclerosis. *J Autism Dev Disord.*, 22: 339-355.

Smith, H. C., Watson, G. H., Patel, R. G., Super, M. (1989) Cardiac rhabdomyomata in tuberous sclerosis: their course and diagnostic value. *Arch Dis Child.*, 64: 196-200.

Sparagana, S. P., Wilkes, D. C., Thompson, C. E., Bowers, D. C. (2010) Optic nerve tumour in tuberous sclerosis is not responsive to Sirolimus. *Pediatr Neurol.*, 42: 443-446.

Sparling, J. D., Hong, C., Brahim, J. S., Moss, J., Darling, T. N. (2007) Oral findings in 58 adults with tuberous sclerosis complex. *J Am Acad Dermatol.*, 56: 786-790.

Spirli, C., Okolicsanyi, S., Fiorotto, R., Fabris, L., Cadamuro, M., Lecchi, S., Tian, X., Somlo, S., Strazzabosco, M. (2010) Mammalian target of rapamycin regulates vascular endothelial growth factor-dependent liver cyst growth in polycystin-2 defective mice. *Hepatology*, 51: 1778-1788.

Stambolic, V., MacPherson, D., Sas, D. (2001) Regulation of PTEN transcription by p53. *Mol Cell*, 8: 317-325.

Stillwell, T. J., Gomez, M. R., Kelalis, P. P. (1987) Renal lesions in tuberous sclerosis. *Urology*, 138: 477-481.

Stoyanova, R., Clapper, M. L., Bellacosa, A., Henske, E. P., Testa, J. R., Ross, E. A., Yeung, A. T., Nicolas, E., Tsiachlis, N., Li, Y. S., Linehan, W. M., Howard, S., Campbell, K. S., Godwin, A. K., Boman, B. M., Crowell, J. A., Kopelovich, L., Knudson, A. G. (2004) Altered gene expression in phenotypically normal renal cells

from carriers of tumour suppressor gene mutations. *Cancer Biol Ther.*, 12: 1313-1321.

Strater, J., Wedding, U., Barth, T. F., Koretz, K., Elsing, C., Moller, P. (1996) Rapid onset of apoptosis in vitro following disruption of beta 1-integrin/ matrix interactions in human colonic crypt cells. *Gastroenterol.*, 110: 1776-1784.

Strasser, A., Puthalakath, H., Bouillry, P., Huang, D. C., O'Connor L., O'Reilly, L. A., Cullen, L., Cory, S., Adams, J. M. (2000) The role of bim, a proapoptotic BH3-only family member of the Bcl2 family in cell death control. *Ann N Y Acad Sci.*, 917: 541-548.

Sutters, M., Germino, G. G. (2003) Autosomal dominant polycystic kidney disease: molecular genetics and pathophysiology. *J Lab Clin Med.*, 13: 91-101.

Takakura, A., Contrino, L., Beck, A. W., Zhou, J. (2008) *Pkd1* inactivation induced in adulthood produces focal cystic disease. *J Am Soc Nephrol.*, 19: 2351-2363.

Takayama, H., LaRochelle, W. J., Sabnis, S. G., Otsuka, T., Merlino, G. (1997) Renal tubular hyperplasia, polycystic disease and glomerulosclerosis in transgenic mice overexpressing hepatocyte growth factor/scatter factor. *Lab Invest.*, 77: 131-138.

Takeda, K., Noguchi, K., Shi, W. (1997) Targeted disruption of the mouse Stat3 gene leads to embryonic lethality. *Proc Nat Acad Sci USA.*, 94: 3801-3804.

Talbot, J. T., Shillingford, J. M., Vasanth, S., Doerr, N., Mukherjee, S., Kinter, M. T., Watnick, T., Weimbs, T. (2011) Polycystin-1 regulates STAT activity by a dual mechanism. *PNAS Early Edition*, 1-6.

Tang, L. H., Hui, P., Garcia-Tsao, G., Salem, R. R., Jain, D. (2002) Multiple angiomyolipomata of the liver: case report. *Mod Pathol.*, 15: 167-171.

Tao, Y., Kim, J., Schrier, R. W., Edelstein, C. L. (2005) Rapamycin markedly slows disease progression in a rat model of polycystic kidney disease. *J Am Soc Nephrol.*, 16: 46-51.

Tapon, N., Ito, N., Dickson, B. J., Treisman, J. E., Hariharan, I. K. (2001) The *Drosophila* tuberous sclerosis complex gene homologs restrict cell growth and cell proliferation. *Cell*, 105: 345-355.

Tavazoie, S. F., Alvarez, V. A., Ridenour, D. A., Kwiatkowski, D. J., Sabatini, B. L. (2005) Regulation of neuronal morphology and function by the tumour suppressors *Tsc1* and *Tsc2*. *Nat Neurosci.*, 8: 1727-1734.

Taylor, R. C., Cullen, S. P., Martin, S. J. (2008) Apoptosis: controlled demolition at the cellular level. *Mol Cell Biol.*, 9: 231-241.

Tee, A. R., Fingar, D. C., Manning, B. D., Kwiatkowski, D. J., Cantley, L. C., Blenis, J. (2002) Tuberous sclerosis complex-1 and -2 gene products function together to inhibit mammalian target of rapamycin (mTOR)- mediated downstream signalling. *Proc Natl Acad Sci USA.*, 99: 13571-13576.

Tee, A. R., Manning, B. D., Roux, P. P., Cantley, L. C. Blenis, J. (2003) Tuberous sclerosis complex gene products, tuberlin and hamartin, control mTOR signalling by acting as a GTPase-activating protein complex towards Rheb. *Curr Biol.*, 13: 1259-1268.

Tee, A. R., Blenis, J. (2005) mTOR, translational control and human disease. *Semin Cell Dev Biol.*, 16: 29-37.

Telenti, A., Torres, V. E., Gross, J. B., Van Scoy, R. E., Brown, M. L., Hattery, R. R. (1990) Hepatic cyst infection in autosomal dominant polycystic kidney disease. *Mayo Clin Proc.*, 65: 933-942.

Tello, R., Blickman, J. G., Buonomo, C., Herrind, J. (1998) Meta analysis of the relationship between tuberous sclerosis complex and renal cell carcinoma. *Eur J Radiol.*, 27: 131-138.

Tomasoni, R., Mondino, A. (2011) The tuberous sclerosis complex: balancing proliferation and survival. *Biochem Soc Trans.*, 39: 466-471.

Torra, R., Badenas, C., Darnell, A., Nicolau, C., Volpini, V., Revert, L., Estivill, X. (1996) Linkage, clinical features and prognosis of autosomal dominant polycystic kidney disease types 1 and 2. *J Am Soc Nephrol.*, 7: 2142-2151.

Torra, R., Badenas, C., San Millan, J. L., Perez-Oller, L., Estivill, X., Darnell, A. (1999) A loss of function model for cystogenesis in human autosomal dominant polycystic kidney disease type 2. *Am J Hum Genet.*, 65: 345-352.

Torres, V. E., Wilson, D. M., Burnett, J. C. J., Johnson, C. M., Offord, K. P. (1991) Effect of inhibition of converting enzyme on renal hemodynamics and sodium management in polycystic kidney disease. *Mayo Clin Proc.*, 66: 1010-1017.

Torres, V. E., Wilson, D. M., Hattery, R. R., Segura, J. W. (1993) Renal stone disease in autosomal dominant polycystic kidney disease. *Am J Kidney Dis.*, 22: 513-519.

Torres, V. E. Apoptosis in cystogenesis: hands on or hands off? *Kidney Int.*, 55: 334-335.

Torres, V. E., Harris, P. C. (2006) Mechanisms of disease: autosomal dominant and recessive polycystic kidney diseases. *Nat Clin Pract Nephrol.*, 2: 40-55.

Torres, V. E., Harris, P. C. (2007) Polycystic kidney disease: genes, proteins, animal models, disease mechanisms and therapeutic opportunities. *J Intern Med.*, 261., 17-31.

Torres, V. E., Harris, P. C., Pirson, Y. (2007) Autosomal dominant polycystic kidney disease. *Lancet*, 369: 1287-1301.

Trudel, M., Lanoix, J., Barisoni, L., Blouin, M-J., Desforges, M., L'Italien, C., D'Agati, V. (1997) C-MYC induced apoptosis in polycystic kidney disease is Bcl-2 and p53 independent. *J Exp Med.*, 11: 1873-1884.

Tsuchiya, H., Orimoto, K., Kobayashi, K., Hino, O. (1996) Presence of potent transcriptional activation domains in the predisposing tuberous sclerosis (Tsc2) gene product of the Eker rat model. *Cancer Res.*, 56: 429-433.

Tsujimoto, Y. (2001) Bcl2 family of proteins: Life or death switch in mitochondria. *Biosci Rep.*, 22: 47-58.

Turco, A. E., Clementi, M., Rossetti, S., Tenconi, R., Pignatti, P. F. (1996) An Italian family with autosomal dominant polycystic disease unlinked to either the *PKD1* or *PKD2* gene. *Am J Kidney Dis.*, 28: 759-761.

Turkson, J., Ryan, D., Kim, J. S., Zhang, Y., Chen, Z., Haura, E., Laudano, A., Sebt, S., Hamilton, A. D., Jove, R. (2001) Phosphotyrosyl peptides block Stat3-mediated DNA binding activity, gene regulation and cell transformation. *J Biol Chem.*, 276: 45443-45455.

Uhlmann, E. J., Apicelli, A. J., Baldwin, R. L., Burke, S. P., Bajenaru, M. L., Onda, H., Kwiatkowski, D. J., Gutmann, D. H. (2002) Heterozygosity for the tuberous sclerosis complex (TSC) gene products results in increased astrocyte numbers and decreased p27-Kip1 expression in TSC2+/- cells. *Oncogene*, 21: 4050-4059.

Umeoka. S., Koyama, T., Miki, Y., Akai, M., Tsutsui. K., Togashi, K. (2008) Pictorial review of tuberous sclerosis in various organs. *RadioGraphics*, 28: 32-61.

Uzzo, R. G., Libby, D. M., Vaughan, E. D., Levey, S. H. (1994) Coexisting lymphangiomyomatosis and bilateral angiomyolipomas in a patient with tuberous sclerosis. *J Urol.*, 151: 1612-1615.

Van Adelsberg, J., Chamberlain, S., D'Agati, V. (1997) Polycystin expression is temporally and spatially regulated during renal development. *Am J Physiol.*, 272: 602-609.

Van Baal, J. G., Smits, N. J., Keeman, J. N., Lindhout, D., Verhoef, S. (1994) The evolution of renal angiomyolipomas in patients with tuberous sclerosis. *J Urol.*, 152: 35-38.

Van Slegtenhorst, M., de Hooght, R., Hermans, C., Nellist, M., Janssen, B., Verhoef, S., Lindhout, D., van den Ouweland, A., Halley, D., Young, J. *et al.* (1997) Identification of the tuberous sclerosis gene *TSC1* on chromosome 9q34. *Science*, 277: 805-808.

Van Slegtenhorst, M., Nellist, M., Nagelkerken, B., Cheadle, J. P., Snell, R., van den Ouweland, A., Reuser, A., Sampson, J. R., Halley, D., van der Sluijs, P. (1998) Interaction between hamartin and tuberin, the *TSC1* and *TSC2* gene products. *Hum Mol Genet.*, 7: 1053-1057.

Van Slegtenhorst, M., Verhoef, S., Tempelaars, A., Bakker, L., Wang, Q., Wessels, M., Bakker, R., Nellist, M., Lindhout, D., Halley, D., Ouweland, A van den (1999) Mutational spectrum of the *TSC1* gene in a cohort of 225 tuberous sclerosis complex patients: no evidence for genotype-phenotype correlation. *J Med Genet.*, 36: 285-289.

Veeman, M. T., Axelrod, J. D., Moon, R. T. (2003) A second canon. Functions and mechanisms of beta-catenin-independent Wnt signalling. *Dev Cell*, 5: 367-377.

Veis, D. J., Sorenson, C. M., Shutter, J. R., Korsmeyer, S. J. (1995) Bcl2 deficient mice demonstrate fulminant lymphoid apoptosis, polycystic kidneys and hypopigmented hair. *Cell*, 75: 229-240.

Verghese, H., Weidenfeld, R., Bertram, J. F., Ricardo, S., Deane, J. A. (2008) Renal cilia display length alterations following tubule injury and are present early in epithelial repair. *Nephrol Dial Transplant*, 23: 834-841.

Vermeulen, K., Berneman, Z. N., van Bockstaele, D. R. (2003) Cell cycle and apoptosis. *Cell Prolif.*, 36: 165-175.

Vogt, H. (1908) Zur Pathologie und pathologischen Anatomie der verschiedenen idiotieform. *Monatsschr Psychiatr Neurol.*, 24: 106-150.

Vousden, K. H. (2000) p53: death star. *Cell*, 103: 691-694.

Wahl, P. R., Serra, A. L., Le Hir, M., Molle, K. D., Hall, M. N., Wuthrich, R. P. (2006) Inhibition of mTOR with Sirolimus slows disease progression in Han:SPRD rats with autosomal dominant polycystic kidney disease (ADPKD). *Nephrol Dial Transplant*, 21: 598-604.

Wallingford, J. B., Fraser, S. E., Harland, R. M. (2002) Convergent extension: the molecular control of polarised cell movement during embryonic development. *Dev Cell*, 2: 695-706.

Wallingford, J. B., Habas, R. (2005) The developmental biology of Dishevelled: an enigmatic protein governing cell fate and cell polarity. *Development*, 132: 4421-4436.

Walz, G. (2006) Therapeutic approaches in autosomal dominant polycystic kidney disease: Is there light at the end of the tunnel? *Nephrol Dial Transplant*, 21: 1752-1757.

Wan, X., Harkavy, B., Shen, N., Grohar, P., Helman, L. J. (2007) Rapamycin induces feedback activation of Akt signalling through an IGF-1R-dependant mechanism. *Oncogene*, 26: 1932-1940.

Ward, A. C. (2002) The JAK/STAT signalling pathway in haematopoiesis and disease. Kluwer academic / Plenum publishers.



Ward, C. J., Hogan, M. C., Rossetti, S., Walker, D., Sneddon, T., Wang, X., Kubly, V., Cunningham, J. M., Bacallao, R., Ishibashi, M. (2002) The gene mutated in autosomal recessive polycystic kidney disease encodes a large, receptor-like protein. *Nat Genet.*, 30: 259-269.

Ward, C. J., Yuan, D., Masyuk, T. V., Wang, X., Punyashthiti, R., Whelan, S., Bacallao, R., Torra, R., LaRusso, N. F., Torres, V. E. (2003) Cellular and subcellular localisation of the ARPKD protein: fibrocystin is expressed on primary cilia. *Hum Mol Genet.*, 12: 2703-2710.

Washecka, R. and Hanna, M. (1991) Malignant renal tumours in tuberous sclerosis. *Urology*, 37: 340-343.

Watnick, T. J., Torres, V. E., Gandolph, M. A., Qian, F., Onuchic, L. F., Klinger, K. W., Landes, G., Germino, G. G. (1998) Somatic mutation in individual liver cysts supports a two hit model of cystogenesis in autosomal dominant polycystic kidney disease. *Mol Cell*, 2: 247-251.

Watnick, T., Phakdeekitcharoen, B., Johnson, A., Gandolph, M., Wang, M., Briefel, G., Klinger, K. W., Kimberling, W., Gabow, P., Germino, G. G. (1999) Mutation detection of *PKD1* identifies a novel mutation common to three families with aneurysms and/or very early onset disease. *Am J Hum Genet.*, 65: 1561-1571.

Watnick, T., He, N., Wang, K., Liang, Y., Parfrey, P., Hefferton, D., St George-Hyslop, P., Germino, G. G., Pei, Y. (2000) Mutations of *PKD1* in ADPKD2 cysts suggests a pathogenic effect of trans-heterozygous mutations. *Nat Genet.*, 25: 143-144.

Watnick, T., Germino, G. G. (2003) From cilia to cyst. *Nat Genet.*, 34: 355-356.

Watson, M., Macnicol, A., Allan, P., Wright, A. (1992) Effects of angiotensin converting enzyme inhibition in adult polycystic kidney disease. *Kidney Int.*, 41: 206-210.

Webb, D. W., Thomas, R. D., Osborne, J. P. (1993) Cardiac rhabdomyomas and their association with tuberous sclerosis. *Arch Dis Child.*, 68: 367-370.

Weber, J. D., Zambetti, G. P. (2003) Renewing the debate over the p53 apoptotic response. *Cell Death Diff.*, 10: 409-412.

Weimbs, T. (2006) Regulation of mTOR by polycystin-1. *Cell Cycle*, 5: 2425-2429.

Weiner, D. M., Ewalt, D. H., Roach, S. E., Hensle, T. W. (1998) The tuberous sclerosis complex: a comprehensive review. *J Am Coll Surg.* 187: 548-561.

Weniger, M. A., Melzner, I., Menz, C. K., Wegener, S., Bucur, A. J., Dorsch, K., Mattfeldt, T., Barth, T. F., Möller, P. (2006) Mutations of the tumour suppressor gene SOCS1 in classical Hodgkin lymphoma are frequent and associated with nuclear phospho-STAT5 accumulation. *Oncogene*, 25: 2679-2684.

Weston, B. S., Bagneris, C., Price, R. G., Stirling, J. L. (2001) The polycystin 1 C-type lectin domain binds carbohydrate in a calcium dependent manner, and interacts with extracellular matrix proteins in vitro. *Biochem Biophys Acta.*, 1536: 161-176.

Weston, B. S., Malhas, A. N., Price, R. G. (2003) Structure function relationships of the extracellular domain of the autosomal dominant polycystic kidney disease related protein, polycystin-1. *FEBS Lett.*, 538: 8-13.

White, R., Hua, Y., Scheithauer, B., Lynch, D. R., Henske, E. P., Crino, P. B. (2001) Selective alterations in glutamate and GABA receptor subunit mRNA expression in dysplastic neurons and giant cells of cortical tubers. *Ann Neurol.*, 49: 67-78.

Wienecke, R., Konig, A., DeClue, J. E. (1995) Identification of tuberin, the tuberous sclerosis 2 gene product – tuberin possesses specific rap1GAP activity. *J Biol Chem.*, 270: 16409-16414.

Wienecke, R., Maize, J. C., Shoarinejad, F., Vass, W. C., Reed, J., Bonifacino, J. S., Resau, J. H., de Gunzburg, J., Yeung, R. S., DeClue, J. E. (1996) Co-localisation of the TSC2 product tuberlin with its target Rap1 in the Golgi apparatus. *Oncogene*, 13: 913-923.

Wilson, C., Idziaszczyk, S., Parry, L., Guy, C., Griffiths, D. F. R., Lazda, E., Bayne, R. A. L., Smith, A. J. H., Sampson, J. R., Cheadle, J. P. (2005) A mouse model of tuberous sclerosis 1 showing background specific early post-natal mortality and metastatic renal cell carcinoma. *Hum Mol Genet.*, 14: 1839-1850.

Wilson, C., Bonnet, C., Guy, C., Idziaszczyk, S., Colley, J., Humphreys, V., Maynard, J., Sampson, J. R. Cheadle, J. P. (2006) *Tsc1* haploinsufficiency without mammalian target of rapamycin activation is sufficient for renal cyst formation in *Tsc1*<sup>+/-</sup> mice. *Cancer Res.*, 66: 7934-7938.

Wilson, P. D., Sherwood, A. C., Palla, K., Du, J., Watson, R., Norman, J. T. (1991) Reverse polarity of Na<sup>+</sup>K<sup>+</sup>-ATPase: mislocation to apical plasma membranes in polycystic kidney disease epithelia. *Am J Physiol Renal Physiol.*, 260: 420-430.

Wilson, P. D. (2001) Polycystin: new aspects of structure, function and regulation. *J Am Soc Nephrol.*, 12: 834-845.

Winyard, P. J. D., Nauta, J., Lirenman, D. S., Hardman, P., Sams, V. R., Risdon, R. A., Woolf, A. S. (1996) Deregulation of cell survival in cystic and dysplastic renal development. *Kidney Int.*, 49: 135-146.

Witzgall, R. (2005) Polycystin 2 – an intracellular or plasma membrane channel. *Arch Pharmacol.*, 371: 342-347.

Woo, D. (1995) Apoptosis and loss of renal tissue in polycystic kidney diseases. *N Engl J Med.*, 333: 18-25.

Wu, K. L., Miao, H., Khan, S. (2007) JAK kinases promote invasiveness in VHL mediated renal cell carcinoma by a suppressor of cytokine signalling-regulated, HIF-independent mechanism. *Am J Physiol Renal Physiol.*, 293: 1836-1846.

Xiao, G. H., Jeffers, M., Bellacosa, A., Mitsuuchi, Y., Vande Woude, G. F., Testa, J. R. (2001) Anti-apoptotic signaling by hepatocyte growth factor/Met via the phosphatidylinositol 3-kinase/Akt and mitogen-activated protein kinase pathways. *Proc Nat Acad Sci USA.*, 98: 247-252.

Xu, X., Brodie, S. G., Yang, X., Im, Y. H., Parks, W. T., Chen, L., Zhou, Y. X., Weinstein, M., Kim, S. J., Deng, C. X. (2000) Haploid loss of the tumour suppressor Smad4/Dpc4 initiates gastric polyposis and cancer in mice. *Oncogene*, 19: 1868-1874.

Yamaguchi, T., Wallace, D. P., Magenheimer, B. S., Hempson, S. J., Grantham, J. J., Calvet, J. P. (2004) Calcium restriction allows cAMP activation of Braf/Erk pathway, switching cells to a cAMP dependent growth stimulated phenotype. *J Biol Chem.*, 40419-40430.

Yamaguchi, T., Hempson, S. J., Reif, G. A., Hedge, A. M., Wallace, D. P. (2006) Calcium restores a normal proliferation phenotype in human polycystic kidney disease epithelial cells. *J Am Soc Nephrol.*, 17: 178-187.

Yang, B., Chen, W-H., Shi, P-Z., Xiang, J-J., Xu, R-J., Liu, J-H. (2008) Coincidence of hepatocellular carcinoma and hepatic angiomyolipomas in tuberous sclerosis complex: a case report. *World J Gastro.*, 14: 812-814.

Ye, M., Grant, M., Shartha, M., Elzinga, L., Swan, S., Torres, V. E. (1992) Cyst fluid from human ADPKD promotes cyst formation by renal epithelial cells in vitro. *J Am Soc Nephrol.*, 3: 984-994.

Yeung, R., Xiao, G-H., Jin, F., Lee, W-C., Testa, J., Knudson, A. (1994) Predisposition to renal carcinoma in the Eker rat is determined by germ-line mutation of the tuberous sclerosis (TSC2) gene. *Proc Natl Acad Sci USA.*, 91: 11413-11416.

Yoder, B. K., Hou, X., Guay-Woodford, L. M. (2002) The polycystin proteins, polycystin-1, polycystin-2, polaris and cystin and co- localised in renal cilia. *J Am Soc Nephrol.*, 13: 2508-2516.

Yokogami, K., Wakisaka, S., Avruch, J., Reeves, S. A. (2000) Serine phosphorylation and maximal activation of STAT3 during CNTF signaling is mediated by the rapamycin target mTOR. *Curr Biol.*, 10: 47-50.

Yoshikawa, H., Matsubara, K., Qian, G. S., Jackson, P., Groopman, J. D., Manning, J. E., Harris, C. C., Herman, J. G. (2001) SOCS1, a negative regulator of the JAK/STAT pathway, is silenced by methylation in human hepatocellular carcinoma and shows growth-suppression activity. *Nature*, 28: 29-35.

Young, J. M., Burley, M. W., Jeremiah, S. J., Jeganathan, D., Ekong, R., Osborne, J. P., Povey, S. (1998) A mutation screen of the *TSC1* gene reveals 26 protein truncating mutations and 1 splice site mutation in a panel of 79 tuberous sclerosis patients. *Ann Hum Genet.*, 62: 203-213.

Yu, H., Jove, R. (2004) The STATs of cancer – new molecular targets come of age. *Cancer*, 4: 97-105.

Yu, H., Pardoll, D., Jove, R. (2009) STATs in cancer, inflammation and immunity: a leading role for STAT3. *Nat Rev Cancer*, 9: 798-809.

Zeng, L. H., Xu, L., Gutmann, D. H., Wong, M. (2008) Rapamycin prevents epilepsy in a mouse model of tuberous sclerosis complex. *Ann Neurol.*, 63: 415-417.

Zhan, M., Zhao, H., Han, Z. C. (2004) Signalling mechanisms of anoikis. *Histol Histopathol.*, 19: 973-983.

Zhang, J. G., Farley, A., Nicholson, S. E., Willson, T. A., Zugaro, L. M., Simpson, R. J., Moritz, R. L., Cary, D., Richardson, R., Hausman, G., Kile, B. J., Kent, S. B. H., Alexander, W. S., Metcalf, D., Hilton, D. J., Nicola N. A., Baca, M. (1999) The

conserved SOCS box motif in suppressors of cytokine binds to elongins B and C and may couple bound proteins to proteasomal degradation, *Proc Nat Acad Sci USA.*, 96: 2071–2076.

Zhang, H., Cicchetti, G., Onda, H., Koon, H. B., Asrican, K., Bajraszewski, N., Vazquez, F., Carpenter, C. L., Kwiatkowski, D. J. (2003) Loss of Tsc1/Tsc2 activates mTOR and disrupts PI3K-Akt signalling through downregulation of PDGFR. *J Clin Invest.*, 112: 1223-1233.

Zhang, Y-W., Graveel, C., Shinomiya, N., Vande Woude, G. F. (2004) Met decoys. *Cancer Cell.*, 6: 5-6.

Zhao, R., Xing, S. U., Li, Z. H., Fu, X., Li, Q. N., Krantz, S. B., Zhao, Z, J. (2005) Identification of an acquired JAK2 mutation in polycythemia vera. *J Biol Chem.*, 280: 22788-22792.

Zhong, H., Voll, R. E., Ghosh, S. (1998) Phosphorylation of NF- $\kappa$ B p65 by PKA stimulates transcriptional activity by promoting a novel bivalent interaction with the coactivator CBP/p300. *Mol Cell Biol.*, 5: 661-671.

Zhou, J., Pei, Y. (2008) Autosomal dominant polycystic kidney disease. In: Molecular and genetic basis of renal disease. Pp 85-117, Mount, D. B., Pollak, M. R. (eds.), Elsevier Saunders, Philadelphia, USA.

Zou, H., Yan, D., Mohi, G. (2011) Differential biological activity of disease associated JAK2 mutants. *FEBS.*, 585: 1007-1013.